



UNIVERSITY OF
LIVERPOOL

**IDENTIFICATION OF PROGENITOR CELL-RICH SITES
OF THE CONJUNCTIVA**

Thesis submitted in accordance with the requirements of the
University of Liverpool for the degree of Doctor of Philosophy

by

Rosalind M. K. Stewart

July 2013

To my parents

Abstract

The conjunctiva is a mucous membrane which forms the majority of the ocular surface, and plays a key role in ocular surface defence and maintenance of the tear film. *Ex vivo* expansion of conjunctival epithelial cells offers potential to reconstruct the ocular surface in cases of severe cicatrising disease; but in order to ensure long term success, conjunctival stem cells which produce both keratinocytes and goblet cells must be present. An initial biopsy rich in stem cells would aid this, however the distribution of human conjunctival stem cells has not been clearly elucidated. I hypothesised that human conjunctival progenitor cells reside in specific areas of the tissue.

A surgical method to retrieve whole human conjunctival tissue for research purposes is described. Expression of the stem cell marker ABCG2 and the transit amplifying cell marker p63 was assessed across 22 different regions of such fixed paraffin-embedded tissue, with significantly higher expression of ABCG2 demonstrated basally in the medial canthal and inferior medial/central forniceal areas. Tissue was also cultured *ex vivo*, and clonogenic ability assessed across 8 different regions. Significantly higher colony forming efficiency was demonstrated in the medial canthal and inferior forniceal areas. Similar significant patterns were demonstrated for the expression of the stem cell markers ABCG2, Δ Np63 and Hsp70 in these cultures, with highest expression of each in these same areas, and significant associations between each marker. Increasing donor age and longer post mortem retrieval times were associated with significantly lower ABCG2 expression in fixed tissue, colony forming efficiency, and stem cell marker expression in cell cultures. Preliminary propagation studies demonstrated that conjunctival epithelial cell growth is supported by fibronectin, collagen IV and laminin 1.

This is the first study to comprehensively assess the distribution of human conjunctival progenitor cells. Substantial evidence is here presented that progenitor cells are distributed basally throughout the human conjunctiva, but with highest levels in the medial canthal and inferior forniceal areas. This region may offer physical protection and niches which are rich in goblet cells, vasculature, melanocytes and immune cells. Biopsies from this area, from younger donors, and with short post mortem retrieval times offer the greatest potential to developing stem cell-rich epithelial constructs for transplantation.

Acknowledgements

I would like to thank my supervisors Dr. Carl M. Sheridan, Professor Stephen B. Kaye and Professor Paul S. Hiscott, for their wisdom, guidance and encouragement throughout these studies. I am forever indebted.

I gratefully acknowledge the generous funding from The Guide Dogs for the Blind Association and the donors and families, without whom this study would not have been possible. I thank Mr Paul Rooney and the Tissue Services nurses at NHS Blood and Transplant for providing research consent; and the mortuary staff at the Royal Liverpool University Hospital for assisting in obtaining tissue, often out-of-hours. I also thank Mr Simon Biddolph, Department of Pathology at the Royal Liverpool University Hospital for expert advice and assistance in sectioning tissues; Mr Sajjad Ahmad, Newcastle University for cell culture advice and the gift of the J23T3 cell line; and Dr Gabriela Czanner, Department of Eye and Vision Science for valuable statistical advice.

A special thank you to all the research staff and students in the Department of Eye and Vision Science, who have joined me on the many highs and lows, and endless cups of tea.

Finally, I would like to express my dear thanks to my family and friends, who have borne with me and encouraged me along the way. I look forwards to celebrating with you all!

Publications from this Study

Papers:

STEWART, R. M. K., HISCOTT, P. S., MURPHY, M.D., SHERIDAN, C.M., KAYE, S.B. 2012. A Surgical Technique for Retrieval of Whole Human Cadaveric Conjunctiva. *Acta Ophthalmologica*, 90,e415-416.

MASON, S. L.* , STEWART, R. M. K.*, KEARNS, V. R., WILLIAMS, R. L. & SHERIDAN, C. M. 2011. Ocular epithelial transplantation: Current uses and future potential. *Regenerative Medicine*, 6, 767-782. *Joint first authors.

Book Chapters:

AHMAD, S., STEWART, R., HALLAM, D., OSEI-BEMPONG, C., FOLEY, L. 2012. Ocular surface Reconstruction Using Cellular Therapies. In: BELGARIS, D. & SAVARESE, A., (eds.) *Cell Transplantation: New Research*. New York: Nova Science Publishers Inc.

KEARNS, V.* , STEWART, R.*, MASON, S., SHERIDAN, C. & WILLIAMS, R. 2012. Ophthalmic applications of biomaterials in regenerative medicine. In: RAMALINGHAM, M., RAMAKRISHNA, S. & BEST, S. (eds.) *Biomaterials and Stem Cells in Regenerative Medicine*. London: CRC Press. *Joint first authors.

Oral Presentations:

STEWART, R. M. K., KAYE, S.B., HISCOTT, P. S., SHERIDAN, C.M. September 2011. Localisation of Human Conjunctival Stem Cells. *UK Limbal Stem Cell Forum*.

STEWART, R. M. K. May 2011. Isolation and Propagation of Stem Cell-Rich Sites of the Conjunctiva. *The Royal College of Ophthalmologists Annual Congress*. (Invited speaker).

Published Abstracts:

STEWART, R. M. K., KAYE, S.B., HISCOTT, P. S., AHMAD, S., ROONEY, P., SHERIDAN, C.M. 2012. Human Conjunctival Stem Cells are Predominantly Located in the Medial Canthus and Inferior Fornix. *Investigative Ophthalmology and Visual Science* 2012;53:e-abstract 3973.

STEWART, R. M. K., KAYE, S.B., SHERIDAN, C.M., HISCOTT, P. S. 2011. A Surgical Technique for Retrieval of Whole Human Cadaveric Conjunctiva. *Investigative Ophthalmology and Visual Science* 2011;52:e-abstract 1926.

Table of Contents

ABSTRACT.....	i
ACKNOWLEDGEMENTS	ii
PUBLICATIONS FROM THIS STUDY	iii
TABLE OF CONTENTS.....	iv
LIST OF FIGURES.....	viii
LIST OF TABLES	xvii
GLOSSARY.....	xviii
ABBREVIATIONS	xxii
1. INTRODUCTION.....	1
1.1. THE HUMAN OCULAR SURFACE.....	1
1.1.1. <i>The Cornea and Limbus</i>	2
1.1.2. <i>The Conjunctiva</i>	5
1.1.3. <i>The Tear Film and Ocular Mucins</i>	9
1.2. DEVELOPMENT OF THE HUMAN OCULAR SURFACE	12
1.3. HUMAN CONJUNCTIVAL DISEASE	14
1.3.1. <i>Diseases Affecting the Conjunctiva</i>	14
1.3.2. <i>Management of Cicatrising Conjunctival Disease</i>	16
1.4. THE CELL CYCLE AND CELL DIVISION	18
1.4.1. <i>The Cell Cycle</i>	18
1.4.2. <i>Mitosis</i>	19
1.4.3. <i>Regulation of Cell Division and Growth</i>	20
1.5. STEM CELLS.....	21
1.5.1. <i>Adult Stem Cells</i>	22
1.5.2. <i>The Stem Cell Niche</i>	22
1.5.3. <i>Identification of Stem Cells</i>	23
1.5.4. <i>Human Stem Cell-Based Therapies</i>	25
1.6. OCULAR SURFACE STEM CELLS	25
1.6.1. <i>Limbal Stem Cells</i>	26
1.6.2. <i>Conjunctival Stem Cells</i>	27
1.6.3. <i>Ocular Surface Stem / Progenitor Cell Markers</i>	29
1.7. OCULAR SURFACE EPITHELIAL PROPAGATION EX VIVO	33
1.7.1. <i>Culture Conditions</i>	33
1.7.2. <i>Substrates</i>	35

1.8.	HUMAN OCULAR SURFACE REGENERATIVE THERAPIES	38
1.8.1.	<i>Limbal Stem Cell Transplantation</i>	39
1.8.2.	<i>Conjunctival Epithelial Transplantation</i>	39
1.9.	SUMMARY, HYPOTHESIS AND AIMS.....	41
1.9.1.	<i>Summary</i>	41
1.9.2.	<i>Hypothesis</i>	41
1.9.3.	<i>Aims</i>	41
2.	MATERIALS AND METHODS	42
2.1.	TISSUE RETRIEVAL.....	42
2.2.	TISSUE FIXATION, PARAFFIN EMBEDDING AND SECTIONING	42
2.2.1.	<i>Fixation and Embedding</i>	42
2.2.2.	<i>Sectioning</i>	43
2.2.3.	<i>Slides</i>	44
2.3.	HISTOLOGY.....	44
2.4.	IMMUNOHISTOCHEMICAL STUDIES	45
2.4.1.	<i>Antigen Retrieval</i>	45
2.4.2.	<i>Antibody Staining</i>	45
2.4.3.	<i>Tissue for Positive Controls</i>	47
2.4.4.	<i>Semi-Quantitative analysis</i>	47
2.4.5.	<i>Presentation of Results</i>	48
2.5.	CELL CULTURE.....	49
2.5.1.	<i>Cell Sources</i>	49
2.5.2.	<i>Conjunctival Epithelial Cell Harvesting and Culture</i>	49
2.5.3.	<i>Media Preparation</i>	51
2.5.4.	<i>Cell Growth</i>	52
2.5.5.	<i>Conjunctival Epithelial Growth</i>	54
2.6.	COLONY FORMING EFFICIENCY ASSAYS	56
2.6.1.	<i>Presentation of Results</i>	57
2.7.	IMMUNOCYTOCHEMICAL STUDIES	59
2.7.1.	<i>Cell Growth and Fixation</i>	59
2.7.2.	<i>Antibody Staining</i>	59
2.7.3.	<i>Quantitative analysis</i>	60
2.7.4.	<i>Presentation of Results</i>	60
2.8.	CONJUNCTIVAL CELL GROWTH ON EXTRACELLULAR MATRIX PROTEINS	61
2.8.1.	<i>Extracellular Matrix Protein Coatings</i>	61
2.8.2.	<i>Cell Seeding</i>	62
2.8.3.	<i>Assessment of Cell Growth</i>	62

2.9. STATISTICAL METHODS	62
3. RESULTS	64
3.1. CONJUNCTIVAL RETRIEVAL.....	64
3.1.1. <i>Surgical Retrieval Technique</i>	64
3.1.2. <i>Tissue Retrieved</i>	69
3.2. TISSUE HISTOLOGY.....	71
3.3. IMMUNOHISTOCHEMICAL STUDIES	73
3.3.1. <i>Antibody Optimisation</i>	73
3.3.2. <i>Grading of Immunohistochemical Staining</i>	75
3.3.3. <i>Cytokeratin 19 Staining</i>	77
3.3.4. <i>Further Immunohistochemical Staining</i>	77
3.3.5. <i>ABCG2 Staining</i>	77
3.3.6. <i>p63 Staining</i>	84
3.3.7. <i>Pan-Cytokeratin MNF116 Staining</i>	90
3.3.8. <i>Pan-Cytokeratin AE1/AE3 Staining</i>	90
3.3.9. <i>Immunohistochemical Staining and Donor age</i>	93
3.3.10. <i>Immunohistochemical Staining and Post Mortem Retrieval Time</i>	93
3.4. CELL CULTURE.....	95
3.4.1. <i>Conjunctival Cell Harvesting</i>	95
3.4.2. <i>Conjunctival Epithelial Cell Growth</i>	96
3.4.3. <i>Comparative Limbal Epithelial Cell Growth</i>	100
3.5. COLONY FORMING EFFICIENCY ASSAYS	101
3.5.1. <i>Cell Seeding Number and Colony Forming Efficiency</i>	101
3.5.2. <i>Colony Forming Efficiency across the Conjunctiva</i>	103
3.5.3. <i>Colony Forming Efficiency and Donor Age</i>	110
3.5.4. <i>Colony Forming Efficiency and Post Mortem Retrieval Time</i>	110
3.5.5. <i>Conjunctival versus Limbal Colony Forming Efficiency</i>	111
3.6. IMMUNOCYTOCHEMICAL STUDIES	113
3.6.1. <i>Antibody Optimisation</i>	113
3.6.2. <i>Grading of Immunocytochemical Staining</i>	114
3.6.3. <i>Cytokeratin 19 Staining</i>	115
3.6.4. <i>Further Immunocytochemical Staining</i>	115
3.6.5. <i>ABCG2 Staining</i>	116
3.6.6. <i>ΔNp63 Staining</i>	120
3.6.7. <i>Hsp70 Staining</i>	124
3.6.8. <i>Correlation between the Immunocytochemical Stains</i>	127
3.6.9. <i>Immunocytochemical Staining and Donor Age</i>	128

3.6.10.	<i>Immunocytochemical Staining and Post Mortem Retrieval Time</i>	128
3.7.	STEM CELL MARKER STAINING AND COLONY FORMING EFFICIENCY	131
3.8.	CONJUNCTIVAL CELL GROWTH ON EXTRACELLULAR MATRIX PROTEINS	132
3.9.	SUMMARY OF KEY FINDINGS.....	134
4.	DISCUSSION	136
5.	CONCLUSIONS	169
6.	FUTURE WORK	170
7.	REFERENCES	172

List of Figures

Figure 1: Schematic drawing of the human ocular surface, which comprises the cornea, limbus, conjunctiva and tear film. Adapted in part from Paulsen and Berry (Paulsen and Berry, 2006). ...	1
Figure 2: Photomicrograph of the normal human cornea demonstrating the 5 different layers, from the epithelium externally (forming part of the ocular surface), to the endothelium internally (H&E stain). Scale bar 50µm.	2
Figure 3: Photomicrograph of the normal human conjunctiva showing 4-5 layer polygonal cell epithelium with goblet cells. The epithelium rests on a basement membrane and an underlying loose connective tissue, the lamina propria (H&E stain). Scale bar 50µm.	6
Figure 4: Schematic diagram demonstrating the distribution of A) goblet cells (black) and Krause's accessory lacrimal glands (green) B) saccular and branched crypts (red) and C) intra-epithelial mucous crypts (blue) across the conjunctiva. These all predominantly reside within the fornices and/or medial canthal area. Dashed lines (----) represent the borders of the intra-palpebral bulbar conjunctiva, the fornices and the margins of the tarsal plates. Adapted from Kessing (Kessing, 1968).	7
Figure 5: Schematic drawing of the structure of the tear film on the ocular surface, demonstrating the epithelial surface glycocalyx, thick mucous/aqueous layer and thin superficial lipid layer. A variety of antimicrobial agents are enclosed within. Adapted from Gipson (Gipson, 2004).	10
Figure 6: Schematic drawing to demonstrate the development of the human ocular surface at the 7 th -8 th week of embryogenesis. Following invagination of the lens vesicle, surface ectodermal tissue differentiates to become the corneal, limbal and conjunctival epithelia. The latter folds in on itself as the underlying mesoderm proliferates, thus creating the conjunctival fornices and eyelids. Adapted from Wolosin et al. (Wolosin et al., 2004).	12
Figure 7: Clinical images of cicatrising conjunctival disease. A) Severe conjunctival scarring with symblepharon in ocular mucous membrane pemphigoid, B) conjunctival and corneal desiccation and scarring in chemical burn injury, C) acute conjunctival scarring in Stevens-Johnson Syndrome. Images courtesy of Professor S. B. Kaye.	15
Figure 8: Diagram to represent the phases of the cell cycle. The cell grows continuously in interphase (G1, S and G2), with DNA synthesis confined to S phase, and gaps at G1 and G2. The nucleus and cytoplasm divide (mitosis and cytokinesis) in M phase. Cells may exit the cycle into G0 either temporarily or indefinitely.	18
Figure 9: Schematic diagram to represent the turnover of stem cells to maintain self-renewal and produce transit amplifying and terminally differentiated cells.	21
Figure 10: Schematic diagram to represent the dissection of conjunctival tissue into specific areas for comparative immunohistochemical studies.	43

Figure 11: Schematic diagram of the whole human conjunctiva with fornices represented by dashed lines (-----), labelling the multiple areas assessed for immunohistochemical staining.	48
Figure 12: Schematic diagram to represent the dissection of conjunctival tissue into specific areas for cell culture comparative studies.	50
Figure 13: Schematic diagram representing the method of cell counting with a haemocytometer. View of one 1mm ² corner square. All cells including those touching the top and left border gridlines are counted (black) but not those touching the bottom or right gridlines (red).	53
Figure 14: Schematic diagram to demonstrate conjunctival epithelial cell seeding on a feeder layer.	55
Figure 15: Schematic diagram to represent CFE assay plate, showing number of viable conjunctival cells seeded into each 9.6cm ² well.	56
Figure 16: Schematic diagram of the whole human conjunctiva with fornices represented by dashed lines (-----), labelling the multiple areas assessed for colony forming efficiency assays and immunocytochemical staining.	58
Figure 17: Images of the surgical technique for retrieval of whole human cadaveric conjunctiva: A) a grey line eyelid split is made with a scalpel blade, B) the incision is extended posteriorly C) and deep to the fornices. D) The incision is adjoined to an equivalent lower eyelid incision at both canthi. E) A full 360° limbal peritomy is made with scissors and F) a deep blunt sub-Tenon's dissection is performed. G) The fatty tissue and Tenon's capsule posterior to the fornices is divided to enable H) whole conjunctival excision. I) Eye sockets are reconstructed with cotton wool and eye shields to produce J) good aesthetic reconstruction.	67
Figure 18: Schematic diagram to demonstrate the surgical technique for conjunctival retrieval in the sagittal plane. The eyelids are split anteriorly-posteriorly commencing at the grey line alongside the tarsal plates and deep past the fornices (— —), a 360° limbal peritomy is performed with full deep sub-Tenon's blunt dissection (-----), and the fatty tissue between the two surgical planes divided (.....).	67
Figure 19: Section of human conjunctival tissue from the upper eyelid demonstrating loss of tarsal conjunctiva due to instrument damage in retrieval process (H&E stain). Photomicrographs stitched together manually in Microsoft PowerPoint. Scale bar 1mm	68
Figure 20: Image of whole human cadaveric conjunctival specimen with eyelids everted such that the tarsal epithelium is visible. Scale bar 1cm.	68
Figure 21: Whole section of human conjunctival tissue from the upper eyelid demonstrating normal anatomy and intact conjunctival epithelium from the bulbar through forniceal area to tarsal conjunctiva (H&E stain). Photomicrographs stitched together manually in Microsoft PowerPoint. Scale bar 1mm.	72
Figure 22: Photomicrographs of immunohistochemical antibody optimisation for ABCG2 using placental tissue, varying times of citrate buffer antigen retrieval and varying antibody dilutions. Positive immunoreactivity in brown is observed throughout the cytoplasm (arrows), with haematoxylin counter-staining in blue. Scale bars 50µm. In this case, optimal staining balanced	

- against minimal tissue loss during antigen retrieval was achieved with 10 minutes of citrate buffer and 1:20 antibody dilution, and was used as a final protocol. 73
- Figure 23:** Figure to demonstrate the first immunoreactivity grading scale employed (the proportion of positively staining cells per image: 0 cells: -, $\leq 1/3$ cells: +, $1/3-2/3$ cells: ++, $\geq 2/3$ cells: +++). Photomicrographs showing positive ABCG2 immunoreactivity in brown, with haematoxylin counter staining in blue. Scale bars 50 μ m. 75
- Figure 24:** Photomicrographs of immunohistochemical staining for CK19. Positive immunoreactivity in brown is observed throughout the cytoplasm (arrows), with haematoxylin counter-staining in blue. A) Immunoreactivity is demonstrated throughout most layers of the conjunctival epithelium, B) tonsillar tissue positive control, C) negative control. Scale bars 50 μ m. 77
- Figure 25:** Photomicrographs of immunohistochemical staining for ABCG2 in the bulbar-forniceal conjunctival epithelium. Positive immunoreactivity in brown is observed both at the cell membrane (black arrows) and throughout the cytoplasm (dashed arrows), with haematoxylin counter-staining in blue. A) and B) Immunoreactivity is demonstrated to varying levels in the conjunctival epithelium, C) placental positive control and D) negative control. Scale bars 50 μ m. 78
- Figure 26:** Photomicrographs of immunohistochemical staining for ABCG2 across the conjunctiva. Positive immunoreactivity in brown is observed both at the cell membranes and throughout the cytoplasm (arrows), with haematoxylin counter-staining in blue. Mild immunoreactivity is observed in A) tarsal, intense staining in B) forniceal and moderate staining in C) bulbar areas. Scale bars 50 μ m. 79
- Figure 27:** Schematic diagram of the human conjunctiva (as labelled in Figure 11) with fornices represented by dashed lines (----), demonstrating photomicrographs of immunohistochemical staining for ABCG2 across all areas of the conjunctiva from one donor (tissue 26). Positive immunoreactivity in brown is observed both at the cell membranes and throughout the cytoplasm, predominantly in the basal layers of the epithelium. In this example, immunoreactivity is observed most intensely in the medial canthal and forniceal areas. Haematoxylin counter-staining in blue. A) Placental positive control, B) negative control. Scale bars 50 μ m. 80
- Figure 28:** Schematic diagram of the human conjunctiva (as labelled in Figure 11) with fornices represented by dashed lines (----), demonstrating average grades of immunohistochemical reactivity for ABCG2 using grading scale 1 (Figure 23) by proportion of immunoreactive cells, across all areas of the conjunctiva from all 10 donors. Highest grades of staining are observed in the medial canthal, inferior medial and inferior central forniceal areas (red) compared to other areas ($p < 0.01$). 81
- Figure 29:** Schematic diagram of the human conjunctiva (as labelled in Figure 11) with fornices represented by dashed lines (----), demonstrating average grades of immunohistochemical reactivity for ABCG2 using grading scale 2 (Table 6) by proportion and intensity of

immunoreactive cells, across all areas of the conjunctiva from all 10 donors. Highest grades of staining are observed in the medial canthal, inferior medial and inferior central forniceal areas (red) compared to other areas ($p < 0.01$). 82

Figure 30: Photomicrographs of immunohistochemical staining for ABCG2 in the conjunctiva in proximity to clusters of goblet cells (arrows). Positive immunoreactivity in brown varies from A) light to D) intense, with haematoxylin counter-staining in blue. A) Tarsal conjunctiva, B) tarsal-forniceal conjunctiva, C) medial canthal conjunctiva and D) forniceal conjunctiva. Scale bars 50µm. 83

Figure 31: Photomicrographs of immunohistochemical staining for p63 across the conjunctiva. Positive immunoreactivity in brown is observed in the nuclei (arrows), with haematoxylin counter-staining in blue. Mild immunoreactivity is observed in A) tarsal, intense staining in B) forniceal and moderate staining in C) bulbar areas, with D) limbal positive control and E) negative control. Scale bars 50µm. 84

Figure 32: Schematic diagram of the human conjunctiva (as labelled in Figure 11) with fornices represented by dashed lines (----), demonstrating photomicrographs of immunohistochemical staining for p63 across all areas of the conjunctiva from one donor (tissue 26). Positive immunoreactivity in brown is observed in the nuclei, predominantly in the basal layers of the epithelium. In this example, immunoreactivity is observed most intensely in the medial canthal and inferior forniceal areas. Haematoxylin counter-staining in blue. A) Limbal positive control, B) negative control. Scale bars 50µm. 86

Figure 33: Schematic diagram of the human conjunctiva (as labelled in Figure 11) with fornices represented by dashed lines (----), demonstrating average grades of immunohistochemical reactivity for p63 using grading scale 1 (Figure 23) by proportion of immunoreactive cells, across all areas of the conjunctiva from 2 donors. Significant variation of staining was observed across the tissue ($p = 0.02$), but although highest grades of staining were observed in the medial canthal, inferior medial and inferior central forniceal areas this was not significant ($p = 0.5$). 87

Figure 34: Schematic diagram of the human conjunctiva (as labelled in Figure 11) with fornices represented by dashed lines (----), demonstrating average grades of immunohistochemical reactivity for p63 using grading scale 2 (Table 6) by proportion and intensity of immunoreactive cells, across all areas of the conjunctiva from 2 donors. Significant variation of staining was observed across the tissue ($p = 0.02$), but although highest grades of staining were observed in the medial canthal, inferior medial and inferior central forniceal areas this was not significant ($p = 0.5$). 88

Figure 35: Photomicrographs of immunohistochemical staining for p63 in the conjunctiva in proximity to clusters of goblet cells (arrows). Positive immunoreactivity in brown varies from A) light to D) intense, with haematoxylin counter-staining in blue. A) Tarsal conjunctiva, B) - D) forniceal conjunctiva. Scale bars 50µm. 89

- Figure 36:** Photomicrographs of immunohistochemical staining for MNF116 across the conjunctiva. Positive immunoreactivity in brown is observed in the cytoplasm (arrows), with haematoxylin counter-staining in blue. Intense immunoreactivity is observed throughout all layers of A) tarsal, B) forniceal and C) bulbar conjunctiva. D) tonsil positive control, E) negative control. Scale bars 50µm. 90
- Figure 37:** Photomicrographs of immunohistochemical staining for AE1/AE3 across the conjunctiva. Positive immunoreactivity in brown is observed in the cytoplasm (arrows), with haematoxylin counter-staining in blue. Intense immunoreactivity is observed throughout all layers of A) tarsal, B) forniceal and C) bulbar conjunctiva. D) tonsil positive control, E) negative control. Scale bars 50µm. 91
- Figure 38:** Photomicrographs of immunohistochemical staining for AE1/AE3 in the forniceal conjunctiva. Positive immunoreactivity in brown is observed in the cytoplasm (arrows), with haematoxylin counter-staining in blue. A) intense immunoreactivity is observed throughout all layers of the forniceal conjunctiva, but a small collection of non-immunoreactive cells are demonstrated basally (arrow). B) Negative control. Scale bars 100µm. 91
- Figure 39:** Photomicrographs of immunohistochemical staining for Melan-A. Positive immunoreactivity is observed in the cytoplasm in brown with haematoxylin counter-staining in blue. A) Occasional immunoreactive cells (arrows) are observed in the conjunctival epithelium, B) melanoma positive control, C) negative control. Scale bars 50µm. 92
- Figure 40:** Photomicrographs of immunohistochemical staining for S-100. Positive immunoreactivity is observed in the cytoplasm in brown with haematoxylin counter-staining in blue. A) Occasional immunoreactive cells (arrows) are observed in the conjunctival epithelium and lamina propria, B) colonic positive control, C) negative control. Scale bars 50µm. 92
- Figure 41:** Line graph showing variance in average conjunctival ABCG2 immunohistochemical staining grade with donor age. A decrease in ABCG2 staining is demonstrated with increasing donor age ($p<0.01$)*. Error bars +/- 1SD, --- linear trend line. 93
- Figure 42:** Line graph showing variance in average conjunctival ABCG2 immunohistochemical staining grade with PMRT. A decrease in ABCG2 staining is demonstrated with increasing PMRT ($p<0.01$)*. Error bars +/- 1SD, --- linear trend line. 94
- Figure 43:** Section of human conjunctival tissue demonstrating complete loss of epithelium following cell harvesting attempts with cloning rings (H&E stain). Photomicrographs stitched together manually in Microsoft PowerPoint. Scale bar 1mm. 95
- Figure 44:** Phase contrast micrographs of conjunctival epithelial cell culture at day 7 on A) tissue culture plastic, B) Matrigel™ basement membrane matrix and C) 3T3 feeder layer. Conjunctival epithelial cell colonies (arrow) are only observed growing on the feeder layer. Scale bars 100µm. 96

Figure 45: Phase contrast micrographs of conjunctival epithelial explants (arrows) at day 7 on A) tissue culture plate, B) Matrigel™ basement membrane matrix and C) 3T3 feeder layer. No cell growth was observed on any extracellular matrix. Scale bars 100µm. 97

Figure 46: Phase contrast micrographs of conjunctival epithelial cell cultures from one donor (tissue 23), demonstrating differing size of colony formations (arrows) in culture from different conjunctival areas. Largest colonies are demonstrated in the medial canthal and inferior forniceal areas in this donor at day 7. Scale bars 100µm. 98

Figure 47: Phase contrast micrographs of conjunctival epithelial cells demonstrating that epithelial cells become increasingly more differentiated in appearance with increasing passage (p). Scale bars 100µm. 99

Figure 48: Phase contrast micrographs of passage 0 limbal and conjunctival epithelial cells in culture demonstrating similar epithelial cell morphology but higher growth rates in culture of limbal epithelial cells. Limbal cells are observed to reach confluence at day 7, compared to conjunctival cells which are near confluency at day 10. Scale bars 100µm. 100

Figure 49: Colony forming efficiency (CFE) assay plate demonstrating conjunctival epithelial cell colonies stained with 1% Rhodamine B. Wells plated with A) 0, B) 500, C) 1000, D) 2000, E) 5000 and F) 10000 cells per 9.6cm² well. Scale bar 1cm. 101

Figure 50: Line graph showing the effect of cell seeding number on number of colonies cultured. A linear association is observed at lower concentrations, but the number of colonies cultured reaches a plateau at 5000 cells per well. Error bars +/- 1SD. 102

Figure 51: Line graph showing the effect of cell seeding number on CFE value. No difference in CFE is observed at seeding densities less than 2000 cells per well (p=0.94), but significantly lower CFE is observed at both 5000 (p<0.01)* and 10000 cells per well (p<0.01)*. Error bars +/- 1SD. 103

Figure 52: Schematic diagram of the human conjunctiva (as labelled in Figure 16) with fornices represented by dashed lines (----), demonstrating varying colony growth on CFE analysis as stained with Rhodamine B, from each comparative tissue area from one donor (tissue 31). In this example, greater number of colonies are observed in the medial canthal, inferior forniceal and inferior bulbar areas. 104

Figure 53: Histogram demonstrating the CFE values across 8 different areas of the conjunctiva from all 8 donors (each represented in different shade of blue). For each highest CFE was observed in the medial canthal and inferior forniceal areas. Error bars +/- 1SD. 105

Figure 54: Histogram demonstrating the mean overall CFE values across 8 different areas of the conjunctiva from all 8 donors. The highest CFE was observed in the medial canthal area alone (p<0.01)*, and medial canthal and inferior forniceal areas combined (p<0.01)*. Error bars +/- 1SD. 105

Figure 55: Histogram demonstrating the CFE values across 8 different areas of the conjunctiva from one donor (tissue 17). Highest CFE was observed in the medial canthal and inferior forniceal areas. Error bars +/- 1SD. 106

Figure 56: Histogram demonstrating the CFE values across 8 different areas of the conjunctiva from one donor (tissue 19). Highest CFE was observed in the medial canthal, inferior forniceal and inferior bulbar areas. Error bars +/- 1SD.	106
Figure 57: Histogram demonstrating the CFE values across 8 different areas of the conjunctiva from one donor (tissue 23). Highest CFE was observed in the medial canthal and inferior forniceal areas. Error bars +/- 1SD.	107
Figure 58: Histogram demonstrating the CFE values across 8 different areas of the conjunctiva from one donor (tissue 25). Highest CFE was not observed in the medial canthal area. Error bars +/- 1SD.....	107
Figure 59: Histogram demonstrating the CFE values across 8 different areas of the conjunctiva from one donor (tissue 27). Highest CFE was observed in the medial canthal, inferior bulbar and inferior forniceal areas. Error bars +/- 1SD.....	108
Figure 60: Histogram demonstrating the CFE values across 8 different areas of the conjunctiva from one donor (tissue 31). Highest CFE was observed in the medial canthal and inferior forniceal areas. Error bars +/- 1SD.	108
Figure 61: Histogram demonstrating the CFE values across 8 different areas of the conjunctiva from one donor (tissue 33). Highest CFE was observed in the medial canthal, inferior forniceal and inferior bulbar areas. Error bars +/- 1SD.	109
Figure 62: Histogram demonstrating the CFE values across 8 different areas of the conjunctiva from one donor (tissue 35). Highest CFE was observed in the medial canthal and inferior forniceal areas. Error bars +/- 1SD.	109
Figure 63: Line graph showing the variance in whole conjunctival CFE with donor age. A decrease in CFE value was demonstrated with increasing donor age ($p < 0.01$)*. Error bars +/-1SD, --- linear trend line.	110
Figure 64: Line graph showing the variance in whole conjunctival CFE with PMRT. A decrease in CFE value was demonstrated with increasing PMRT ($p < 0.01$)*. Error bars +/-1SD, --- linear trend line.	111
Figure 65: Histogram showing comparative CFE across the whole conjunctiva, medial canthal conjunctiva alone and limbus, with representative CFE images below each. Highest CFE is demonstrated in the limbus than either the whole conjunctiva or medial canthal area alone (insufficient data for statistical analysis). Error bars +/- 1SD.	112
Figure 66: Photomicrographs of immunocytochemical antibody optimisation for ABCG2 using MCF7 cells and antibodies from both Chemicon and Abcam at both 1:20 and 1:50 antibody dilutions. Positive immunoreactivity in green is observed in the cytoplasm (arrows), with PI nuclear counter-staining in red. Scale bars 25 μ m. In this case, optimal staining was achieved with the Chemicon antibody at 1:20 dilution, and was used as a final protocol.	113
Figure 67: Examples of photomicrographs of immunocytochemical staining for Hsp70 to demonstrate the immunoreactivity grading scale employed (the number of positively staining cells per	

average of 5 x20 fields of view: 0 cells: -, <5 cells: +/-, 5-10 cells: +, 10-15 cells: ++, 15-20 cells: +++, >20 cells: ++++). Positive immunoreactivity is observed in green (arrows) with PI nuclear counter-staining in red. Scale bars 50µm. 114

Figure 68: Photomicrographs of immunocytochemical staining for CK19. Positive immunoreactivity is observed throughout the cytoplasm in green (arrows), with PI nuclear counter-staining in red. A) Intense staining of conjunctival epithelial cells, B) MCF7 positive control and C) negative control. Scale bars 50µm. 115

Figure 69: Photomicrographs of immunocytochemical staining for ABCG2. Positive immunoreactivity is observed throughout the cytoplasm in green (arrows), with PI nuclear counter-staining in red. A) A collection of positively staining conjunctival epithelial cells, B) MCF7 positive control and C) negative control. Scale bars 50µm. 116

Figure 70: Schematic diagram of the human conjunctiva (as labelled in Figure 16) with fornices represented by dashed lines (----), demonstrating photomicrographs of immunocytochemical staining for ABCG2 across 8 areas of the conjunctiva from one donor (tissue 19). Positive immunoreactivity is observed at the cell membranes and within the cytoplasm in clusters of cells in green, with PI nuclear counter-staining in red. In this example, larger clusters of positively staining cells are observed in the medial canthal and inferior forniceal areas. A) MCF7 positive control, B) negative control. Scale bars 50µm. 117

Figure 71: Schematic diagram of the human conjunctiva (as labelled in Figure 16) with fornices represented by dashed lines (----), demonstrating average grades of immunocytochemical reactivity for ABCG2 in cell cultures from 8 areas of the conjunctiva from 8 separate donors. Highest grades of staining were observed in the medial canthal ($p<0.01$) (red) and together with inferior forniceal ($p<0.01$) (red) and inferior bulbar areas compared to other areas. 118

Figure 72: Histogram demonstrating the overall level of ABCG2 staining in cell cultures from 8 different areas of the conjunctiva from 8 separate donors. Highest grades of staining were observed in the medial canthal ($p<0.01$)* together with inferior forniceal areas ($p<0.01$)*. Error bars +/- 1SD. 119

Figure 73: Photomicrographs of immunocytochemical staining for ΔNp63. Positive immunoreactivity is observed in the nuclei in green (arrows). A) A collection of positively staining conjunctival epithelial cells, B) limbal positive control and C) negative control. Scale bars 50µm. 120

Figure 74: Schematic diagram of the human conjunctiva (as labelled in Figure 16) with fornices represented by dashed lines (----), demonstrating photomicrographs of immunocytochemical staining for ΔNp63 across 8 areas of the conjunctiva from one donor (tissue 19). Positive immunoreactivity is observed in the nuclei of clusters of cells in green. In this example, the largest clusters of positively staining cells are observed in the medial canthal area. A) Limbal positive control, B) negative control. Scale bars 50µm. 121

Figure 75: Schematic diagram of the human conjunctiva (as labelled in Figure 16) with fornices represented by dashed lines (----), demonstrating average grades of immunocytochemical

reactivity for Δ Np63 in cell cultures from 8 areas of the conjunctiva from 8 separate donors. Highest grades of staining were observed in the medial canthal ($p < 0.01$) (red) and together with inferior forniceal ($p < 0.01$) (red) and inferior bulbar areas compared to other areas. 122

Figure 76: Histogram demonstrating the overall level of Δ Np63 staining in cell cultures from 8 different areas of the conjunctiva from 8 separate donors. Highest grades of staining were observed in the medial canthal ($p < 0.01$)* together with inferior forniceal areas ($p < 0.01$)*. Error bars +/- 1SD. 123

Figure 77: Photomicrographs of immunocytochemical staining for Hsp70. Positive immunoreactivity is observed throughout the cytoplasm in green (arrows), with PI nuclear counter-staining in red. A) A collection of positively staining conjunctival epithelial cells, B) limbal positive control and C) negative control. Scale bars 50 μ m. 124

Figure 78: Schematic diagram of the human conjunctiva (as labelled in Figure 16) with fornices represented by dashed lines (----), demonstrating photomicrographs of immunocytochemical staining for Hsp70 across 8 areas of the conjunctiva from one donor (tissue 19). Positive immunoreactivity is observed throughout the cytoplasm in clusters of cells in green, with PI nuclear counter-staining in red. In this example, large clusters of positively staining cells are observed throughout all areas of the conjunctiva but less so in the tarsal areas. A) Limbal positive control, B) negative control. Scale bars 50 μ m. 125

Figure 79: Schematic diagram of the human conjunctiva (as labelled in Figure 16) with fornices represented by dashed lines (----), demonstrating average grades of immunocytochemical reactivity for Hsp70 in cell cultures from 8 areas of the conjunctiva from 8 separate donors. Highest grades of staining were observed in the medial canthal ($p < 0.01$) (red) and together with inferior forniceal areas ($p < 0.01$) (red), compared to other areas. 126

Figure 80: Histogram demonstrating the overall level of Hsp70 staining in cell cultures from 8 different areas of the conjunctiva from 8 separate donors. Highest grades of staining were observed in the medial canthal ($p < 0.01$)* together with inferior forniceal areas ($p < 0.01$)*. Error bars +/- 1SD. 127

Figure 81: Line graphs showing the variance in conjunctival cell culture staining for A) ABCG2, B) Δ Np63 and C) Hsp70 with donor age. A reduction in both ABCG2 and Hsp70 staining is observed with increasing donor age ($p < 0.01$ for each)*, but no relationship was evident between Δ Np63 staining and donor age. Error bars +/-1SD, ---- linear trend lines. 129

Figure 82: Line graphs showing the variance in conjunctival cell culture staining for A) ABCG2, B) Δ Np63 and C) Hsp70 with PMRT. A reduction in ABCG2 staining is observed with increasing PMRT ($p < 0.01$)*, but no relationship was evident between Δ Np63 or Hsp70 staining and PMRT. Error bars +/-1SD, ---- linear trend lines. 130

Figure 83: Phase contrast micrographs of conjunctival epithelial cell growth on A) collagen IV, B) fibronectin, C) laminin 1 and D) 3T3 feeder layer at day 10. Similar cell morphology is observed

on each extracellular matrix protein but with greater number of cells evident on B) fibronectin.
Scale bars 100µm. 132

Figure 84: Line graph showing conjunctival epithelial cell growth curves on various extracellular matrix protein coatings. Highest growth rates were observed on fibronectin, with significant differences seen at day 7 ($p < 0.01$)*, but there was no significant difference between growth on any extracellular matrix protein by day 10. Error bars +/- 1 SD. 133

Figure 85: Overall graph showing both CFE and expression of the SC markers ABCG2, ΔNp63 and Hsp70 in cell cultures from 8 donors across 8 different areas of the human conjunctiva. Error bars +/- 1SD. 134

List of Tables

Table 1: Table of antibodies used for immunohistochemical studies with clone and source.....	46
Table 2: Table to quantify immunohistochemical staining grading scale 2 by proportion of and intensity of positively staining cells in an area. N/A = not applicable.	47
Table 3: Table of antibodies used for immunocytochemical studies with clone and source.....	60
Table 4: Table showing donor demographics, cause of death and PMRTs of conjunctival tissue retrieved. (CVA = Cerebrovascular Accident).....	71
Table 5: Table of optimised immunohistochemical protocols for different antibodies used. *Secondary antibody is HRP anti-mouse or anti-rabbit.....	74
Table 6: Table to demonstrate the second immunohistochemical immunoreactivity grading scale by both proportion of and intensity of positively staining cells in an area. Photomicrographs demonstrating positive ABCG2 immunoreactivity in brown, with haematoxylin counter-staining in blue. Scale bars 50µm. N/A = not applicable.	76
Table 7: Table of optimised immunocytochemical protocols for different antibodies used. *Secondary antibody is alexafluor 488 goat anti-mouse or -rabbit.....	114

Glossary

Adult Stem Cell Multipotent cells resident in fetal or adult tissue that are responsible for tissue replenishment and repair.

Airlifting Cultivation of epithelial cells at the air-liquid interface to induce stratification.

Amniotic Membrane The innermost layer of the placenta, consisting of a thick basement membrane and avascular stroma.

Ankyloblepharon Adhesion of the superior and inferior eyelids.

Basement Membrane A sheet of supporting and anchoring tissue which underlies epithelia.

Bulbar Conjunctiva The portion of the conjunctiva which covers the surface of the eye, from the limbus to the fornices.

Caruncle An ovoid body of modified skin at the medial canthus, adjacent to the plica semilunaris.

Cell Cycle An orderly series of events within a cell that lead to its replication.

Cicatrising Conjunctivitis Severe inflammation and scarring of the conjunctiva.

Collagen A group of naturally occurring proteins which are the main components of connective tissue.

Conjunctiva A mucous membrane that forms the majority of the ocular surface and plays a key role in ocular surface defence and maintenance of the tear film.

Cornea The transparent refractive window at the front of the eye.

Differentiation The process by which a less specialised cell becomes a more specialised cell type.

Ectoderm One of the three primary germ cell layers in the early embryo, which differentiates to form amongst other tissues, the nervous system, epidermis, and parts of the eye.

Entropion In-turning of the eyelid towards the eye.

Epithelium A tissue that lines the cavities and surfaces of structures the body and many glands.

Extracellular Matrix Extracellular tissue which provides structural and proliferative support to cells.

Feeder Layer A layer of cells used to condition the media and support the growth of other cells in culture.

Fibronectin A high-molecular weight glycoprotein, which is widely distributed in the extracellular matrix and plasma.

Forniceal Conjunctiva The portion of the conjunctiva which lines the fornix, adjoining the bulbar and palpebral conjunctiva.

Fornix A deep arch of tissue, such as that formed between the eye and eyelid.

Goblet Cell Large glandular simple columnar epithelial cells which secrete mucin.

Induced Pluripotent Stem Cell Pluripotent stem cells derived by artificial genetic reprogramming of non-pluripotent cells.

J23T3 Cells A mouse fibroblast cell line widely used to support the culture of keratinocytes.

Keratinocyte The predominant cell type of epithelia.

Label-Retention The cellular retention of DNA markers, a marker of slow-cycling and/or asymmetric division.

Lacrimal Gland A gland in the superior lateral aspect of the orbit which secretes the aqueous portion of the tear film.

Lagophthalmos The inability to completely close the eyelids.

Laminin A group of naturally occurring proteins which are major components of basement membranes.

Lateral Canthus The lateral junction of the superior and inferior eyelids.

Limbus The border of the cornea with the conjunctiva and sclera.

MCF7 A breast cancer cell line.

Mesoderm One of the three primary germ cell layers in the early embryo, which differentiates to form amongst other tissues, connective tissue, muscles, and parts of the eye.

Medial Canthus The medial junction of the superior and inferior eyelids.

Meibomian Gland Sebaceous glands within the tarsal plate of the eyelid which secrete lipids which form the superficial lipid layer of the tear film.

Mitosis A complex series of events by which a cell separates previously replicated chromosomes - the process by which cells divide to produce daughter cells genetically identical to the parent cell.

Mucin Heavily glycosylated, high molecular weight glycoproteins which form gels. They are key components of secretions on all moist epithelia.

Mucocutaneous Junction The transitional zone where mucosal epithelium and epidermis adjoin, such as at the eyelid margin.

Multipotency The ability of a cell to differentiate into a number of closely related cell lineages.

Ocular Surface The cornea, limbus, conjunctiva and tear film.

Palpebral Conjunctiva The portion of the conjunctiva which covers the inner aspect of the eyelid, from the mucocutaneous junction to the fornices.

Passage Sub-culturing of cells *in vitro* to maintain growth and/or expand the number of cells.

Plasticity The ability of adult stem cells to broaden their potency upon exposure to a novel environment.

Plica Semilunaris A narrow crescentic fold of medial bulbar conjunctiva, adjacent to the caruncle.

Pluripotency The ability of a cell to differentiate into all adult cell lineages - a feature of embryonic stem cells.

Potency The ability of a cell to differentiate into different cell types.

Progenitor Cell Any dividing cell with the capacity to differentiate, including putative stem cells in which self-renewal has not been demonstrated.

Self-renewal Cellular division that generates at least one daughter cell equivalent to the mother cell with latent capacity for differentiation - the defining property of stem cells.

Stem Cell A cell that that can give rise to multiple differentiated cell types, and has the ability to self-renew and resist progression along the line of specialisation.

Stem Cell Niche The cellular microenvironment that provides support and stimuli, enabling stem cells to remain quiescent and maintain self-renewal.

Stemness An unproven notion that common genes and mechanisms regulate different stem cells.

Symblepharon Adhesion of the bulbar and palpebral conjunctiva.

Tarsal Conjunctiva The portion of the conjunctiva which covers the inner aspect of the tarsal plate of the eyelid, thus forming the majority of the palpebral conjunctiva.

Tear Film A complex layer of aqueous, mucin and lipid which coats the surface of the eye.

Terminally Differentiated Cell A cell which no longer maintains the capacity to divide.

Totipotency The ability of a cell to differentiate into all fetal and adult cells - a feature of zygotic stem cells.

Transit Amplifying Cell The progeny of stem cells, which have low proliferative capacity and initially may retain self-renewal, but ultimately are fated for differentiation.

Trichiasis Abnormally positioned eyelashes which are mis-directed towards the eye.

Abbreviations

ABCG2	ATP-Binding Cassette Protein G2
APES	3-aminopropyltriethoxysilane
BrdU	Bromodeoxyuridine
BSA	Bovine Serum Albumin
CDK	Cyclin-Dependent Kinase
CFE	Colony Forming Efficiency
CK	Cytokeratin
DMEM	Dulbecco's Modified Eagle's Media
DMSO	Dimethyl Sulphoxide
DNA	Deoxyribonucleic Acid
EDTA	Ethylenediaminetetraacetic Acid
EGF	Epidermal Growth Factor
FCS	Fetal Calf Serum
H&E	Haematoxylin and Eosin
HEPES	4-(2-hydroxyethyl)-1-piperazineethanesulfonic Acid
HRP	Horseradish Peroxidase
Hsp70	Heat Shock Protein 70
MEM	Eagles Minimal Essential Media
mRNA	Messenger Ribonucleic Acid
NBF	Neutral Buffered Formaldehyde
NHSBT	National Health Service, Blood and Transplant
PAS	Periodic Acid Schiff
PBS	Phosphate Buffered Saline
PC	Progenitor Cell
PCNA	Proliferating Cell Nuclear Antigen
PCR	Polymerase Chain Reaction
PI	Propidium Iodide
PMRT	Post Mortem Retrieval Time
PS	Penicillin-Streptomycin solution
SC	Stem Cell
SD	Standard Deviation
TAC	Transit Amplifying Cells

TGF-β	Transforming Growth Factor- β
[³H]TdR	Tritiated Thymidine
3T3	J23T3 murine fibroblast cell line

1. Introduction

1.1. The Human Ocular Surface

The ocular surface comprises the cornea, limbus, conjunctiva and tear film (Figure 1); all aspects of which are essential for ocular functions. The cornea is the transparent refractive window of the eye, the clarity of which is essential for vision. The health of the cornea and thus maintenance of vision depends on the ocular surface as a whole. The border of the cornea with the conjunctiva/sclera is termed the limbus and is where the corneal epithelial stem cells (SC) reside. The conjunctiva comprises the majority of the ocular surface. It plays a key role in its immunological defence; provides a barrier to protect the underlying tissues; and as a mucous membrane, it is critical for maintaining the tear film, thus preventing desiccation and preserving homeostasis of the ocular surface.

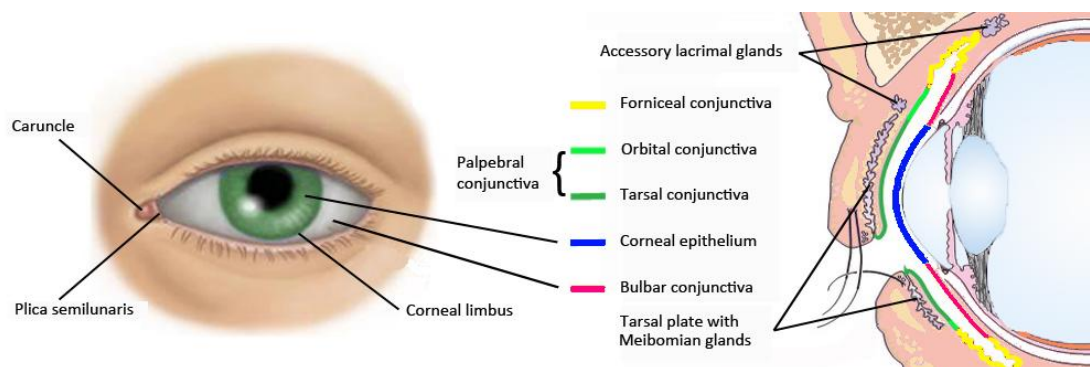


Figure 1: Schematic drawing of the human ocular surface, which comprises the cornea, limbus, conjunctiva and tear film. Adapted in part from Paulsen and Berry (Paulsen and Berry, 2006).

The ocular surface is in turn protected by the superior and inferior eyelids. The form and shape of the eyelids are maintained by a dense fibrous tissue termed the tarsal plates, which contain the lipid-secreting meibomian glands. Blinking, which protects the eye from trauma and foreign bodies and helps to redistribute the tear film, is achieved by the levator palpebrae superioris and orbicularis oculi muscles. Rows of eyelashes on each eyelid further increase protection from foreign debris.

The eyelids fuse medially and laterally at the medial and lateral canthi respectively (Bron *et al.*, 1997).

1.1.1. The Cornea and Limbus

The cornea lies within the outer protective fibrous structure of the eye, otherwise formed by the sclera. It is 540-700 μm in thickness (Dawson *et al.*, 2011) and comprised of five layers as shown in Figure 2. The superficial epithelium is continuous with the limbal and then conjunctival epithelia peripherally. These epithelia bear many resemblances, but differ significantly in that the corneal and limbal epithelia do not possess goblet cells.

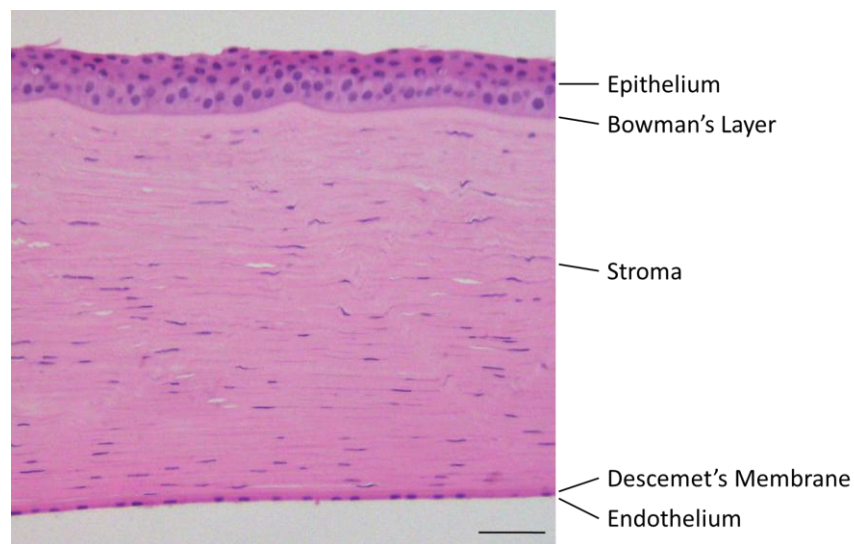


Figure 2: Photomicrograph of the normal human cornea demonstrating the 5 different layers, from the epithelium externally (forming part of the ocular surface), to the endothelium internally (H&E stain). Scale bar 50 μm .

The corneal epithelium is a stratified squamous non-keratinised non-secretory epithelium of 5-6 layers of cells in depth. The basal cells are columnar, the intermediate cells are polyhedral, and the superficial cells become increasingly wider and flattened to create a smooth surface (Bron *et al.*, 1997). The superficial cells have numerous microvillae and express membrane-associated mucins which form a dense glycocalyx at the epithelium-tear film interface. The overlying tear

film is protective both immunologically and in preventing epithelial desiccation (see Section 1.1.3). The cells are connected by numerous desmosomes, which reduce shear and enable them to provide a barrier to control the hydration of the underlying stroma. Although dendritic cells are present in the peripheral epithelium in the adult, the central corneal epithelium is effectively devoid of immunocompetent cells or melanocytes (Bron *et al.*, 1997).

The basement membrane of the corneal epithelium is primarily composed of collagens IV and VII, and is also rich in laminins -332 and γ 2, fibronectin and other glycoproteins including fibrillin, nidogen, clusterin and perlecan (Schlötzer-Schrehardt *et al.*, 2007). This anchors the epithelium to a modified acellular region of the stroma, known as Bowman's layer. This latter structure is 8-14 μ m thick and terminates peripherally at the summits of the marginal corneal capillary arcades (Bron *et al.*, 1997).

The epithelium is the most densely innervated tissue in the body, with primarily sensory but also sympathetic fibres, which respond to mechanical, chemical and temperature stimuli (Dawson *et al.*, 2011). These are supplied by the anterior ciliary nerves and those of the surrounding conjunctiva (Bron *et al.*, 1997).

The corneal epithelium responds rapidly to disruptions in its integrity by initial amoeboid sliding of cells at the wound margin, followed by cell replication. SCs, that are cells which can give rise to multiple differentiated cell types, have the ability to self-renew and resist progression along the line of specialization (Potten and Loeffler, 1990, Mikkers and Frisén, 2005) (see Section 1.5) reside in basal crypts of the limbal epithelium. They are responsible for renewing and maintaining the corneal epithelium by superficial and centripetal migration of their differentiating progeny (see Section 1.6.1). In comparison to that of the cornea, the limbal epithelium is approximately 10 cells in depth and features radial papillae (the limbal palisades of Vogt). The basement membrane bears many similarities to that of the cornea but is richer in collagen IV α 2, laminin α 1, β 1 and γ 1, and contains lower levels of clusterin and fibrillins (Schlötzer-Schrehardt *et al.*, 2007). The underlying

stroma is equally innervated, but additionally densely vascularised (Li *et al.*, 2007). The cells within this region also act as a barrier preventing encroachment of the conjunctival epithelium with its blood vessels which would otherwise impair corneal transparency (Chen and Tseng, 1991).

The stroma is a dense connective tissue formed of 200-250 lamellae of thick (30nm) flattened parallel collagen fibres which stretch from limbus to limbus. The fibres are predominantly collagen type I, with lesser amounts of type V and VI. Regular spacing of the fibres at 42-44nm apart is maintained by the surrounding proteoglycans, which are predominantly composed of chondroitin sulphate and keratan sulphate glycosaminoglycans. This organised structure ensures that the stroma scatters less than 10% of normal incident light. Modified fibroblasts named keratocytes are scattered throughout the stroma, which secrete and maintain the stromal extracellular matrix. Immunocompetent cells are also dispersed throughout, with dendritic cells distributed more anteriorly and macrophages posteriorly (Dawson *et al.*, 2011).

The posterior surface of the cornea is lined by the corneal endothelium, which rests upon a modified 10-15µm thick basement membrane (Descemet's membrane). This is composed of collagen IV, laminin and fibronectin and increases in thickness throughout life. The endothelium is a barrier monolayer of hexagonal cuboidal cells which are interconnected by numerous tight junctions and gap junctions. The tight junctions are however significantly more permeable than those of the corneal epithelium; thus the endothelium actively controls fluid and electrolyte transport across the posterior surface of the cornea by a 'pump-leak' model (Noske *et al.*, 1994). As such it has a critical role in maintaining corneal hydration and hence transparency (Bron *et al.*, 1997).

Other than the marginal corneal arcades, the cornea is an avascular structure, and is dependent upon the tear film and aqueous as sources of oxygen and other nutrients (Bron *et al.*, 1997, Dartt, 2011). The transparency of the cornea may be attributable to a number of factors: the regularity and smoothness of the surface

epithelium, the regular spacing arrangement of collagen fibres within the stroma, and its avascularity (Bron *et al.*, 1997). Disturbance to any of these properties may reduce visual acuity. The regular spacing of collagen fibres within the stroma may be disrupted by either increased corneal hydration or scarring secondary to any form of injury (Dawson *et al.*, 2011).

1.1.2. The Conjunctiva

The conjunctiva is a thin transparent mucous membrane which connects the eye to the eyelids. It covers the inner surface of the eyelids from the mucocutaneous junction posterior to the openings of the meibomian glands at the eyelid margin, to the fornices, and across the surface of the eye to the limbus, where it is continuous with the limbal and corneal epithelia. It is thus a relatively large tissue, with an estimated total surface area of 12cm². Although it is a continuous tissue it is described in distinct areas: the palpebral (that covering the inner aspect of the eyelids); the bulbar (that covering the sclera of the eye); and the forniceal conjunctiva (the area comprising the annular sac adjoining the two). The palpebral conjunctiva is mostly comprised of the tarsal (that overlying the tarsal plates) with a small region of marginal (that adjacent to the mucocutaneous junction) and the remainder termed orbital conjunctiva, as shown in Figure 1 (Bron *et al.*, 1997). The superior fornix lies approximately 8-10mm and the inferior fornix approximately 8mm from the limbus. Medially the fornix is replaced by the caruncle and plica semilunaris (Figure 1), whereas laterally the fornix is deep at approximately 14mm from the limbus (Pepperl, 2007). The conjunctiva is strongly adherent to the tarsal plates, to the globe adjacent to the limbus, and to connective tissue deep in the fornices in order to maintain their depth. In other areas it is loose and flexible, a property conveyed by elastic fibrils within the lamina propria, thus allowing free movement of the eye and eyelids (Bron *et al.*, 1997). The conjunctiva is thus dynamic in shape, and the delineation of the zones of the conjunctiva is therefore not precise.

The conjunctiva is a highly specialised tissue, composed of a stratified non-keratinized epithelium containing goblet cells, which rests on a basement membrane and an underlying vascular lamina propria (Figure 3). It is thin and translucent. The epithelium comprises mostly cuboidal and polyhedral cells, and varies from 2-9 layers of cells in depth. It is deepest at the marginal zone where the basal layers feature papillae, whilst the remaining tarsal conjunctiva comprises 2-5 layers of cuboidal cells. Additional intermediate layers of polyhedral cells are found in the forniceal and canthal regions. As the bulbar conjunctiva approaches and is continuous with the limbal conjunctiva, the cells of the deeper layers become taller and the superficial cells become flattened (Bron *et al.*, 1997). Similar to the corneal epithelium, the superficial cells have numerous microvillae and express membrane-associated mucins which form a dense glycocalyx at the epithelium-tear film interface (see Section 1.1.3).

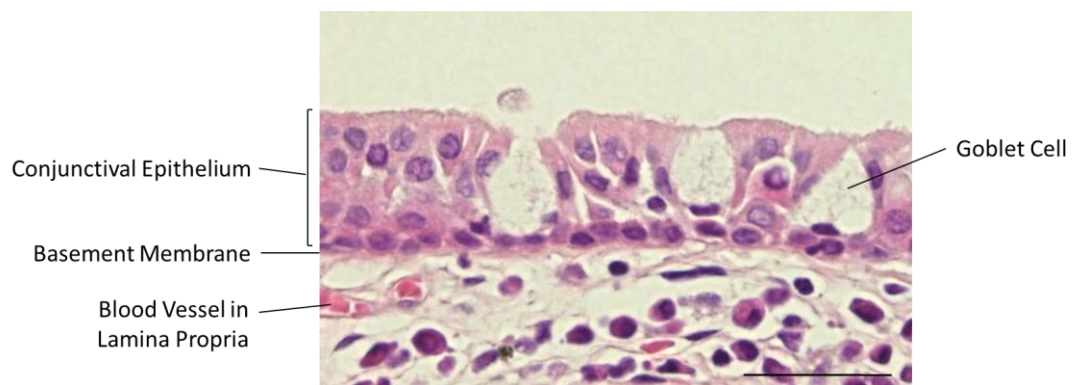


Figure 3: Photomicrograph of the normal human conjunctiva showing 4-5 layer polygonal cell epithelium with goblet cells. The epithelium rests on a basement membrane and an underlying loose connective tissue, the lamina propria (H&E stain). Scale bar 50 μ m.

Large round or oval goblet cells are scattered throughout the epithelium, with the exception of the marginal zone. They span the entire depth of the epithelium, with a slender basal portion and broad apical portion distended by their secretory products. They appear either singly or in clusters, the latter often within intra-epithelial crypts. They are most dense nasally, especially in the plica semilunaris, and in the inferior fornix (Kessing, 1968) (Figure 4). These cells are packed with copious large secretory granules, releasing the gel-forming mucin MUC5AC, which

forms the bulk of the mucin component of the tear film (Inatomi *et al.*, 1996, McKenzie *et al.*, 2000), and an array of antimicrobial factors (see Section 1.1.3). Goblet cell mucin production appears to be controlled by activation of the sympathetic and parasympathetic nerve supply, and also stimulated by growth factors such as epidermal growth factor (EGF), and purinergic agonists. The latter may be released from nerves, platelets, damaged cells or bacteria (Dartt, 2004).

Additional glandular tissue is also located in the conjunctival fornices. Krause's accessory lacrimal glands which are adjunctive to the lacrimal gland in secreting the aqueous component of the tear film (see Section 1.1.3), are located predominantly in the superior and inferior fornices. Saccular and branched crypts, which have been considered rudimentary accessory lacrimal glands, but also contain goblet cells, are located in the inferior and superior fornices (Kessing, 1968) (Figure 4).

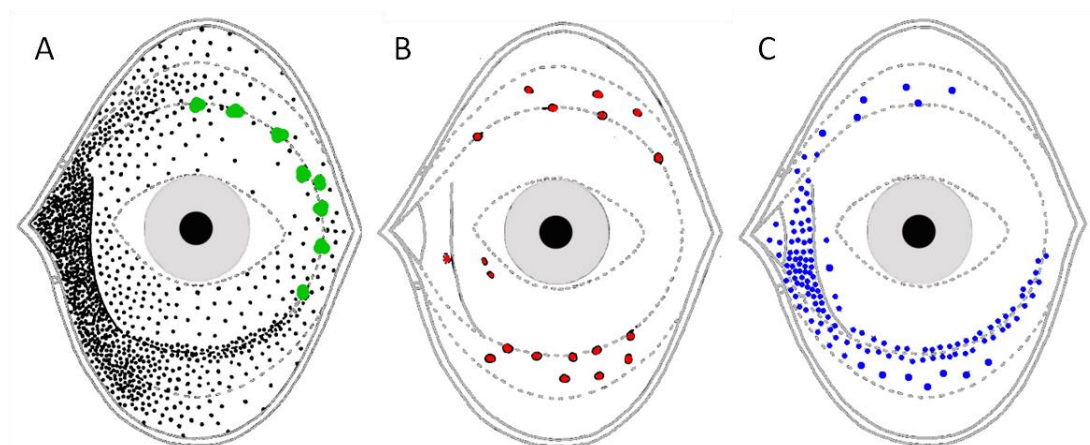


Figure 4: Schematic diagram demonstrating the distribution of A) goblet cells (black) and Krause's accessory lacrimal glands (green) B) saccular and branched crypts (red) and C) intra-epithelial mucous crypts (blue) across the conjunctiva. These all predominantly reside within the fornices and/or medial canthal area. Dashed lines (----) represent the borders of the intra-palpebral bulbar conjunctiva, the fornices and the margins of the tarsal plates. Adapted from Kessing (Kessing, 1968).

The conjunctival epithelium is also populated by scattered melanocytes and a wealth of immune cells. The latter provide both innate and adaptive effector mechanisms to destruct invading pathogens. Lymphocytes (predominantly T cells), dendritic cells and neutrophils reside within the epithelium; whilst lymphocytes

(often forming lymphoid aggregations), neutrophils, plasma cells and mast cells are found in the underlying lamina propria (Bron *et al.*, 1997). In addition, the goblet cells secrete a wealth of antimicrobial factors into the tear film (see Section 1.1.3). Together this forms the eye-associated lymphoid tissue (EALT), a component of the mucosal immune system. This system one of the few sites that confers immune privilege, by immunological ignorance and tolerance, based on different-reactivity and anti-inflammatory responses distinct from the central immune system (Knop and Knop, 2007).

The medial canthal area contains a narrow crescentic fold of bulbar conjunctiva known as the plica semilunaris (Figure 1); this enables full ocular abduction despite the shallow medial fornix. Being highly vascular, hence pink in colour, and especially rich in goblet cells, melanocytes, and both specific and non-specific immune cells; it has been proposed that the plica semilunaris is a specialised organ of ocular defence (Arends and Schramm, 2004). Medial to the plica semilunaris lies the caruncle, an area of modified skin with a stratified squamous epithelium rich in goblet cells, modified lacrimal glands, melanocytes, specific and non-specific immune cells, hairs and sebaceous glands (Bron *et al.*, 1997, Arends and Schramm, 2004).

The conjunctival epithelium has an immense regenerative capacity and wound-healing response (Dartt, 2004), with both the keratinocytes and goblet cells being capable of proliferation (Wei *et al.*, 1995, Pellegrini *et al.*, 1999, Shatos *et al.*, 2003). The distribution of conjunctival SCs has not however been clearly elucidated (see Section 1.6.2).

The conjunctival basement membrane is similar but subtly different to that of the limbal and corneal epithelia. It is again comprised primarily of collagens IV and VII, laminins -332, α 3, γ 1, γ 2 and 5, integrin- β 4, nidogen, clusterin, perlecan and fibronectin. Similar to the limbal basement membrane it is rich in collagen IV α 2, laminin γ 1 and nidogens; whereas in common with the corneal epithelial basement membrane it is rich in clusterin (Tuori *et al.*, 1996, Schlötzer-Schrehardt *et al.*, 2007,

Messmer *et al.*, 2012). These components may be altered in the presence of disease (Messmer *et al.*, 2012). Unlike the corneal epithelium, the conjunctival epithelium rests on an underlying lamina propria comprised of highly vascularised loose connective tissue, which is also rich in immune cells as described above.

The rich vascular supply to the conjunctiva is provided from the palpebral branches of the ophthalmic and lacrimal arteries, and from the anterior conjunctival branches of the anterior ciliary artery. Together these form anastomoses of marginal and peripheral tarsal arcades and a pericorneal plexus. The conjunctival veins accompany and outnumber the arteries, draining into the post-tarsal venous plexus or the superior or inferior ophthalmic vein. In addition, there is an irregular network of lymphatics (Bron *et al.*, 1997).

The conjunctiva is supplied by sensory, sympathetic and parasympathetic nerves, but not as richly as the cornea. These derive from the infra- and supratrochlear, infra- and supraorbital and lacrimal nerves, which are branches of the ophthalmic division of the trigeminal nerve (cranial nerve V), and the sympathetic plexus (Bron *et al.*, 1997).

1.1.3. The Tear Film and Ocular Mucins

The pre-ocular tear film is a complex layer consisting of aqueous, mucin and lipid components, the depth of which remains debated, with reports varying widely from 3-45µm depending on the analytical method employed (Paulsen and Berry, 2006). These three components are hypothesised to form a multifaceted structure as shown in Figure 5.

The aqueous component of the tear film is primarily produced by the lacrimal gland, and accessory lacrimal glands. The former resides in the superior lateral aspect of the orbit, within the lacrimal fossa. The conjunctival keratinocytes and goblet cells, and to a small extent the corneal keratinocytes also appear to secrete water and electrolytes (Dartt, 2011). The lacrimal gland fluid is isotonic, which is of

key significance in preventing aqueous deficiency dry eye. In addition, the lacrimal glands and accessory lacrimal glands secrete MUC7, and a range of antimicrobial proteins including lactoferrin, lysozyme and IgA (Dartt, 2011).

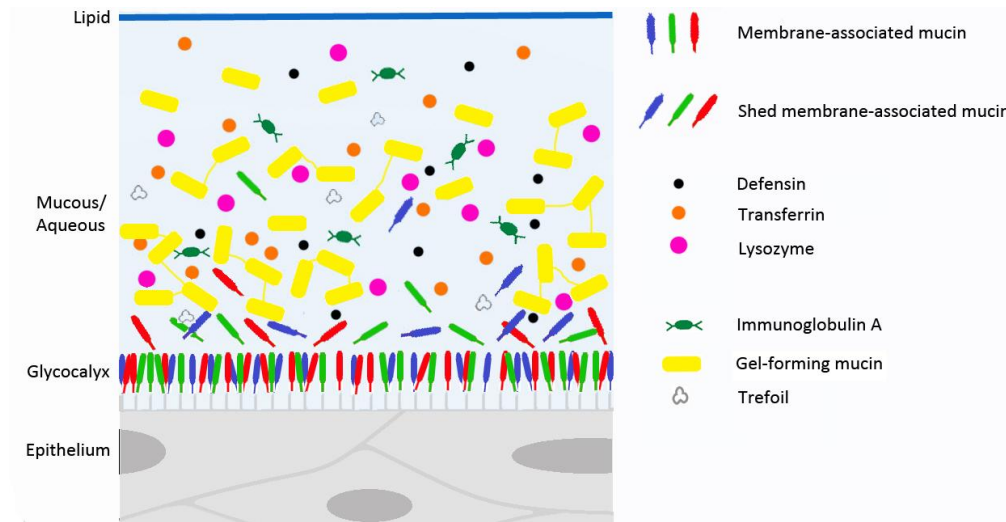


Figure 5: Schematic drawing of the structure of the tear film on the ocular surface, demonstrating the epithelial surface glycocalyx, thick mucous/aqueous layer and thin superficial lipid layer. A variety of antimicrobial agents are enclosed within. Adapted from Gipson (Gipson, 2004).

The other main constituent of the tear film is mucin. These are heavily glycosylated, high molecular weight glycoproteins with tandem repeats of amino acids rich in serine and threonine in their backbone, that serve as sites for O-glycosylation (Gipson, 2004). They are present on all moist epithelia, and are characterised by their hydrophilicity and ability to form gels. Numerous mucins have been characterised which are either gel-forming/secretory or membrane-associated. The superficial cells of the corneal and conjunctival epithelia express a range of membrane-associated mucins on their microvillae including MUC1, MUC4 and MUC16 (Inatomi *et al.*, 1995, Pflugfelder *et al.*, 2000, Argüeso *et al.*, 2003a); these contribute to a dense glycocalyx barrier at the epithelial-tear film interface. The large gel-forming mucin MUC5AC is secreted from conjunctival goblet cells (Inatomi *et al.*, 1996, McKenzie *et al.*, 2000), which forms the scaffolding of the tear film, together with the small soluble mucin MUC7 produced by the lacrimal gland, and soluble forms of the membrane-associated mucins (Dartt, 2004, Gipson, 2004,

Paulsen and Berry, 2006). In addition, the goblet cells also secrete trefoil proteins which interact with mucins, transferrin and antimicrobial factors such as peroxidase and defensins (Iwata *et al.*, 1976, Langer *et al.*, 1999, Haynes *et al.*, 1999, McNamara *et al.*, 1999).

The superficial lipid component, a product of the meibomian glands of the eyelids is a complex of polar and non-polar lipids, including free fatty acids, triacylglycerols and wax and sterol esters. There is increasing evidence that the polar lipids interact with the major proteins of the tear film (lactoferrin, lysozyme, lipocalin and IgA), thus creating a stable inner lipid-aqueous interface beneath the outer non-polar lipid-air interface. This complex layer varies from 13-100nm in depth, and plays a key role in preventing aqueous evaporation, thus preserving the integrity of the whole tear film complex (Butovich *et al.*, 2008).

The unique composition of the tear film confers many critical functions. The gel-like consistency of the mucous/aqueous layer lubricates and prevents desiccation of the ocular surface epithelia. The glycocalyx provides a deep barrier which prevents pathogen penetrance and anchors the mucous/aqueous layer (Gipson, 2004, Kesimer *et al.*, 2013). In addition to the plethora of secreted antimicrobial factors, mucins also bind and trap bacteria (Mantelli and Argüeso, 2008), recruit leucocytes (Aknin *et al.*, 2003) and activate neutrophils (Aknin *et al.*, 2004). Bacteria together with cellular debris and foreign bodies are then removed with tear film movement during blinking, to be cleared down the nasolacrimal drainage system (Dartt, 2011). Finally, the smooth surface that is created by the tear film is optimal for light refraction (Paulsen and Berry, 2006).

The conjunctiva plays a key role in maintaining a healthy tear film. The presence of goblet cells and its large surface area result in it having a substantially greater capacity to produce mucins than the lacrimal gland or corneal epithelium. Ocular surface mucin production is tightly regulated, both by its synthesis and secretion and by the proliferation of ocular surface cells (Dartt, 2004). This is critical, as either mucin under- or overproduction may cause ocular surface disease (Lemp and

Marquardt, 1992). Conversely, ocular surface disease (see Section 1.3.1) itself is associated with both goblet cell depletion (Tseng *et al.*, 1984, Doughty, 2012); and alterations in the expression, distribution and/or glycosylation of mucins, resulting in severe dry eye (Argüeso *et al.*, 2003b). Normal mucin glycosylation is important for neutrophil activation (Aknin *et al.*, 2004).

1.2. Development of the Human Ocular Surface

The eye develops from week 4 of embryogenesis, from invaginations of both neural and surface ectoderm, together with consolidation of some of the surrounding mesoderm. The details of the future ocular surface are apparent from the 7th to 8th week of embryogenesis, when surface ectoderm consolidates centrally to form the future cornea, and folds in on itself superiorly and inferiorly to form the future conjunctiva (Duke-Elder and Cook, 1963) (Figure 6).

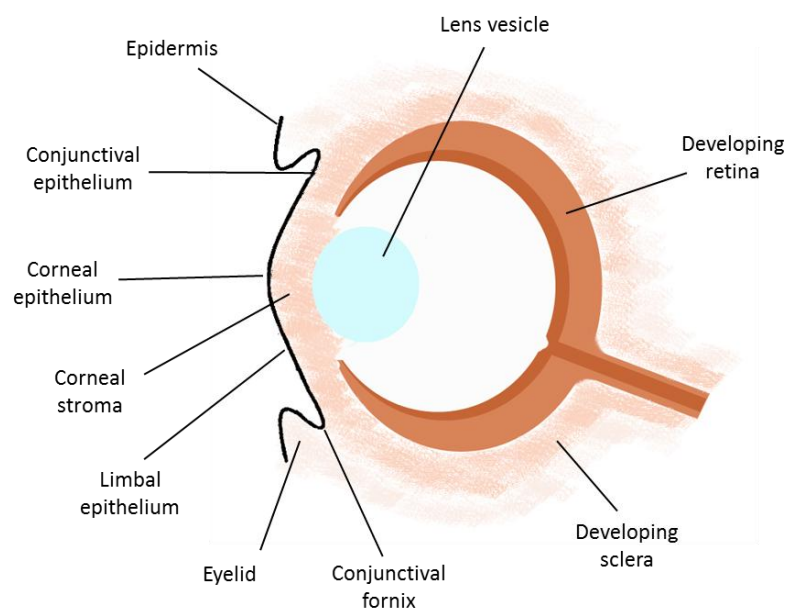


Figure 6: Schematic drawing to demonstrate the development of the human ocular surface at the 7th-8th week of embryogenesis. Following invagination of the lens vesicle, surface ectodermal tissue differentiates to become the corneal, limbal and conjunctival epithelia. The latter folds in on itself as the underlying mesoderm proliferates, thus creating the conjunctival fornices and eyelids. Adapted from Wolosin *et al.* (Wolosin *et al.*, 2004).

Once the lens vesicle separates from the invaginating surface ectoderm, a remaining few Pax-6 positive surface ectodermal cells begin to differentiate (Nishina *et al.*, 1999). Initial epithelial differentiation involves a switch from the universal stratified epithelial cytokeratins CK5 and CK14, to the tissue specific cytokeratins CK3 and CK12 for the cornea, and CK4 for the conjunctiva. The phenotypic characteristics of the two epithelia then develop; the control of which appears to be underpinned by large subsets of genes only present in each tissue (Turner *et al.*, 2007).

At week 8, a two-three layered epithelium with junctional complexes resting on a thin basal lamina is detectable. The cells are flat and rich in glycogen granules (Sellheyer and Spitznas, 1988). At the same time, the mesoderm underlying the future conjunctiva proliferates to create eyelid folds (Figure 6). These advance towards each other and elongate laterally to become the eyelids, and thus generate the fornices (Duke-Elder and Cook, 1963).

At the 9th week of embryogenesis the epithelia fuse along the eyelid margin, such that the future cornea and conjunctiva then develop in a protected cavity (Duke-Elder and Cook, 1963). The conjunctival epithelium is well differentiated by this stage; with larger cells possessing microplacae; and with goblet cells detectable in the forniceal conjunctival area, and shortly afterwards extending towards the palpebral and bulbar conjunctival regions (Sellheyer and Spitznas, 1988, Miyashita *et al.*, 1992). The tight structural integrity of the epithelia which is created by hemidesmosomes, desmosomes and tonofilaments, does not however form until the 4th month. It has been proposed, that it is for this reason that the tissue is protected by eyelid fusion in the early months (Sellheyer and Spitznas, 1988).

Vascularisation develops from the 12th week, but only to the limbal and conjunctival epithelia. The mesoderm lying immediately underneath develops centrally into the corneal stroma, and elsewhere, into the sub-conjunctival connective tissue (Tenon's capsule), extra-ocular and eyelid muscles, sclera, and within the developing eyelids forms the tarsal plates (Duke-Elder and Cook, 1963).

The plica semilunaris and caruncle develop from the 3rd month. It is not clear whether the plica semilunaris originates from the superior and inferior forniceal tissue and merges, or whether its origin is more nasal (Arends and Schramm, 2004). It develops at a different rate to the surrounding tissues, and consequently is relatively large at stages. Although ultimately it has the highest concentrations of goblet cells, they are not detectable here until the 4th month. At this same time, a dense infiltration of leucocytes is noted in both the epithelium and underlying connective tissue. Its rich vascular network develops by the 5th month (Arends and Schramm, 2004).

The eyelids remain adherent until the 5th to 7th month; with separation beginning nasally (Duke-Elder and Cook, 1963, Andersen *et al.*, 1965). The fully formed ocular surface is then revealed.

1.3. Human Conjunctival Disease

1.3.1. Diseases Affecting the Conjunctiva

The conjunctiva is subject to a wide variety of insults including: trauma (chemical, mechanical and thermal), infection (including trachoma), neoplasms, oculocutaneous disease (including ocular mucous membrane pemphigoid, linear IgA disease, Stevens-Johnson syndrome and atopic keratoconjunctivitis), other systemic diseases (such as Sjögren's syndrome and graft-versus-host disease), drug-induced, and topical therapy (such as the use of anti-glaucoma medication). In the most severe forms, many of these processes may trigger limited or chronic inflammation, fibrosis, keratinisation and scarring (cicatrisation) (Bernauer *et al.*, 1997).

Such fibrosis and scarring leads to numerous sequelae including: forniceal shortening, symblepharon, ankyloblepharon, entropion, trichiasis, lagophthalmos, predisposition to ocular surface infection, and severe dry eye secondary to goblet cell and mucin deficiency. These diseases are characterised by unremitting ocular

pain, and the secondary tear film deficiency and resulting limbal SC failure lead to corneal desiccation, conjunctivalisation, vascularisation and ulceration, with loss of sight (Figure 7). Scarring may be so aggressive that in end-stage disease the fornices may be totally obliterated and the cornea becomes opaque (Bernauer *et al.*, 1997).

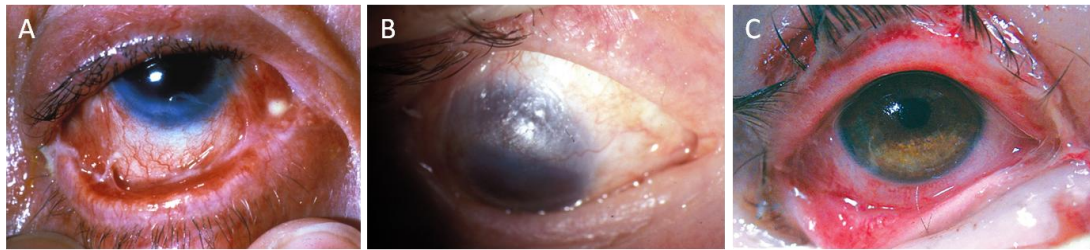


Figure 7: Clinical images of cicatrising conjunctival disease. A) Severe conjunctival scarring with symblepharon in ocular mucous membrane pemphigoid, B) conjunctival and corneal desiccation and scarring in chemical burn injury, C) acute conjunctival scarring in Stevens-Johnson Syndrome. Images courtesy of Professor S. B. Kaye.

The reported incidence and morbidity of these conditions varies greatly. Trachoma is endemic in more than 50 countries, with highest prevalence in sub-Saharan and East Africa, the Middle East, the Indian sub-Continent and Southeast Asia; but is rarely seen in the Western world. It is estimated that 1.3 million people are blind from the disease (Burton and Mabey, 2009). In developed countries, chemical and thermal burns represent 7-18% of ocular injuries seen in emergency departments (Merle *et al.*, 2008) and 17.3% of battlefield injuries (Ari, 2006); 33% of which experience visual disability and 15% blindness (Kuckelkorn *et al.*, 2002). The annual incidence of ocular mucous membrane pemphigoid has been reported as 1.16 per million, with ocular involvement in 60-95% (Chan *et al.*, 2002); and of Stevens-Johnson syndrome is 2-3 per million, with ocular involvement in 43-81%, and permanent visual disability in 35% (Fritsch, 2008). Yet the overall annual incidence of all cicatrising conjunctivitis in the UK has recently been reported as 1.3 per million, but this is thought to be an underestimation (Radford *et al.*, 2012).

Although *Chlamydia trachomatis* infection is treatable with oral antibiotics, lack of access to healthcare and repeated infections mean that severe ocular surface cicatrization is widespread. At this end-stage, like the other conditions above there is a lack of an effective treatment (see Section 1.3.2). Given the chronic pain and visual disability which ensue, these conditions represent a significant burden to individuals, healthcare systems and wider societies.

1.3.2. Management of Cicatrizing Conjunctival Disease

Cicatrizing conjunctival disease is one of the most challenging conditions for ophthalmologists to treat. Early diagnosis and management are essential for any prospect of obtaining a favourable outcome (Williams *et al.*, 2011). Sadly, trachoma is often untreated/recurrent and thus progresses to end-stage cicatrization, and chemical and thermal injuries often progress to severe disease despite immediate treatment. Many of the other diseases are often only recognised at late stages due to their rarity (Radford *et al.*, 2012).

Organised trachoma control programs using widespread antibiotic therapy has had variable success (Burton and Mabey, 2009). Treatment options for other diseases are limited and usually aimed at preventing disease progression and symptom control. Early aggressive intervention in the acute stages of chemical or thermal injuries and Stevens-Johnson syndrome may help prevent blinding sequelae. Chemical injuries should be managed with immediate copious irrigation. Intensive topical tear supplements, steroids, antibiotics, ascorbate and citrate have all been advocated for these acute conditions; together with the early use of amniotic membrane transplantation, which reduces inflammation and scarring, and promotes epithelisation (Fish and Davidson, 2010, Liu *et al.*, 2012b, Ciralsky *et al.*, 2013).

Long term management of chronic cicatrization aims to control inflammation with systemic steroids or immunosuppressive agents; and to eliminate correctable factors which may exacerbate ocular disease. These latter measures encompass

artificial tear supplements (including autologous serum tears), punctual occlusion, surgical correction of trichiasis or entropion, and prevention and/or treatment of secondary bacterial infection (Bernauer *et al.*, 1997). Side effects of immunosuppressive agents may however be significant, and despite control of inflammation, progressive symblepharon formation often still occurs (Radford *et al.*, 2012).

Endeavours to surgically reconstruct the ocular surface with excision of scar tissue and application of a tissue substitute have resulted in limited success. Conjunctival autografts were first used to cover small conjunctival defects with success (Thoft, 1977, Vastine *et al.*, 1982), but are insufficient in size to replace areas of widespread disease or to reconstruct the fornices. Thus oral mucosa (Shore *et al.*, 1992), nasal turbinate mucosa (Wenkel *et al.*, 2000) and amniotic membrane (Honavar *et al.*, 2000, Barabino and Rolando, 2003) have all been proposed. As many of these diseases affect other body sites, alternative mucous membranes may also be involved in the original disease process. Their use is also not without morbidity to the donor site, and furthermore they are prone to shrinkage and often give cosmetically poor results (Shore *et al.*, 1992, Schrader *et al.*, 2009b). Although amniotic membrane has been demonstrated to enhance conjunctival regeneration (Barabino and Rolando, 2003); it is prone to recurrent shrinkage in the presence of uncontrolled inflammation, with recurrent symblepharon formation in 10-44% and progressive loss of approximately half of the fornix depth originally obtained within 4 months of surgery (Honavar *et al.*, 2000, Barabino and Rolando, 2003). Attempted limbal SC or corneal transplantation to improve vision is prone to failure in the presence of such significant conjunctival disease (Tseng *et al.*, 2005, Shortt and Tuft, 2011).

There is evidently a great need to establish alternative methods to regenerate or reconstruct a healthy ocular surface in these patients. Transplantation of a cultured conjunctival epithelial equivalent containing SCs and their progeny offers one such approach; replenishing a deficient ocular surface and leading to restoration of function (Holland, 1996). Conjunctival replacement therapy would also assist

ocular surface reconstruction in many cases of conjunctival loss, such as post-surgical excision of neoplastic lesions and pterygia, and in glaucoma surgery.

1.4. The Cell Cycle and Cell Division

Two distinct types of cell division take place in eukaryotes: that producing daughter cells which are genetically identical to the parent cell (mitosis), and that producing haploid gametes (meiosis). Mitosis is responsible for tissue replenishment and repair, which occurs within the framework of the cell cycle.

1.4.1. The Cell Cycle

The cell cycle is an orderly series of events which takes place within the cell, leading to its division and duplication (replication). It consists of four distinct phases as shown in Figure 8.

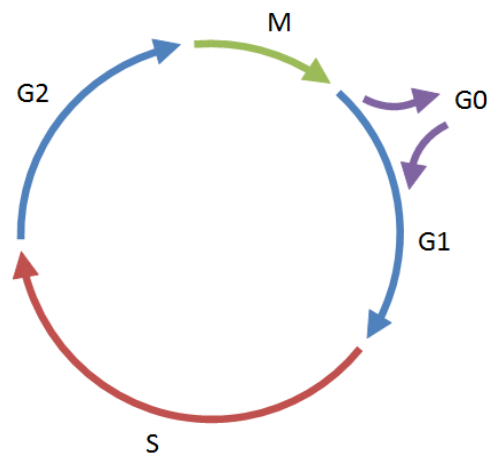


Figure 8: Diagram to represent the phases of the cell cycle. The cell grows continuously in interphase (G1, S and G2), with DNA synthesis confined to S phase, and gaps at G1 and G2. The nucleus and cytoplasm divide (mitosis and cytokinesis) in M phase. Cells may exit the cycle into G0 either temporarily or indefinitely.

DNA synthesis and chromosomal replication occurs during S phase (synthesis), a process which requires 10-12 hours. Chromosomal segregation (mitosis (see Section 1.4.2)) and cytoplasmic division (cytokinesis) occur as a rapid (less than 1 hour) series of events in M phase (mitosis). These stages are separated by gap

phases (G1 and G2), which enable protein and organelle synthesis, permit monitoring of the internal and external environments and control checkpoints before committing to the active S or M phases. G1, S and G2 phases are together termed interphase. Completion of the whole cycle takes approximately 24 hours (Alberts *et al.*, 2008).

Quiescent or senescent cells enter the G0 state, where they may remain for long periods of time or indefinitely. Senescence may occur as a result of detected DNA damage or degradation. Terminally differentiated cells (see Section 1.5) permanently exit the cell cycle at G0 with no possibility of re-entry (Zieske *et al.*, 2004).

1.4.2. Mitosis

Mitosis is itself a complex series of events which result in separation of the previously replicated chromosomes. It may be segregated into five distinct phases:

- *Prophase* - nuclear material condenses from loosely coiled chromatin into discrete chromosomes, with each replicated sister chromatid being bound centrally at the centromere.
- *Prometaphase* - the nuclear membrane disintegrates and the centromeres attach to a complex of microtubules which form the mitotic spindle.
- *Metaphase* - the chromosomes align at the equator of the mitotic spindle, poised for segregation.
- *Anaphase* - the sister chromatids separate and the chromosomes are drawn to opposite poles of the spindle / ends of the cell.
- *Telophase* - the chromosomes decondense and the nuclear membranes reform (Alberts *et al.*, 2008).

Cytokinesis then ensues to complete cellular division and the M phase of the cell cycle (see Section 1.4.1).

1.4.3. Regulation of Cell Division and Growth

Regulation of the cell cycle is governed by a complex network of regulatory proteins, known as the cell-cycle control system. This not only controls the proliferation of cells, but is crucial to cell survival: both by detection of DNA damage (enabling its repair or apoptosis of the cell), and in prevention of uncontrolled cell division (Alberts *et al.*, 2008). The key regulatory molecules of the cell cycle are the cyclin-dependent kinases (CDKs). At least 9 have been identified in mammalian systems, each regulating specific control points within the cell cycle. CDKs are in turn regulated both positively by cyclins, and negatively by cyclin-dependent kinase inhibitors.

The decision to proliferate is made in G1 phase of the cycle. Both intracellular and extracellular signals ensure that cell growth and division is regulated in response to local requirements. The primary positive signals for which are provided by various extracellular growth factors, such as EGF and keratocyte growth factor. These induce formation of the CDK4(6)/cyclin D complex. Inhibitory signals are provided by cell contact inhibition, cAMP and transforming growth factor- β (TGF- β). Both of these mitotic and anti-mitotic CDK/cyclin signalling pathways focus on a single protein pRb. A critical mass of cyclin D and E must be reached to enable phosphorylation of Rb, which triggers the MAP kinase pathway and the expression of cell proliferation genes, permitting the cell to enter S phase. This checkpoint is known as the restriction point, beyond which cells are no longer dependent on extracellular proliferation stimulants to proceed through the remainder of the cycle. (Zieske *et al.*, 2004, Alberts *et al.*, 2008).

There are two other main checkpoints of the cell cycle: the DNA replication checkpoint, and the spindle checkpoint. The first occurs at the end of G2 phase. The presence of unreplicated DNA initiates negative signals to block the action of CDK1/cyclin B complex (also known as maturing promoting factor) until DNA replication is complete. The cell is then permitted to enter M phase. The second occurs in metaphase. Improper attachment of the replicated chromosomes to the

mitotic spindle initiates negative signals to block the anaphase promoting complex, until correct chromosomal alignment is achieved (Alberts *et al.*, 2008).

It has been suggested that SCs (see Section 1.5) are arrested in the G1 phase of the cell cycle rather than G0, and are actively inhibited from proliferating in their resting state (Joyce *et al.*, 1996).

1.5. Stem Cells

SCs are present in all multicellular organisms, and can be defined as cells that can give rise to multiple differentiated cell types, that is multipotency, have the ability to self-renew, and resist progression along the line of specialization (Potten and Loeffler, 1990, Mikkers and Frisén, 2005). Thus they can theoretically generate and maintain a tissue for a lifetime. Transit amplifying cells (TAC) arise from these, have a low proliferative capacity and represent the largest group of dividing cells. These generate terminally differentiated cells which no longer have the capacity to divide (Lajtha and Holtzer, 1979, Barrandon, 1993) (Figure 9). The purest SCs are zygotic SCs, in that they are unlimited in their self-renewal and can differentiate into all fetal and adult cells (totipotency) (Smith, 2006).

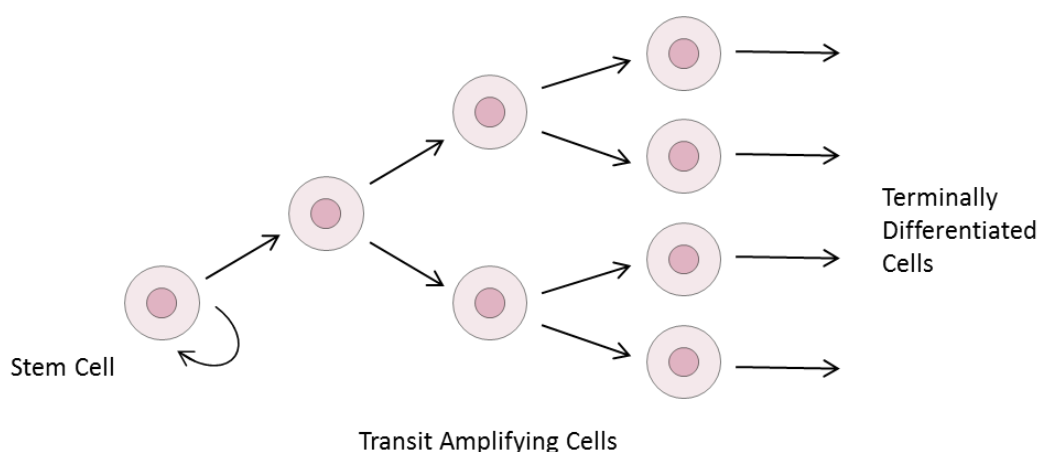


Figure 9: Schematic diagram to represent the turnover of stem cells to maintain self-renewal and produce transit amplifying and terminally differentiated cells.

The term progenitor cell (PC) is attributed to any dividing cell with the capacity to differentiate. It is often used within research to recognise putative SCs in which self-renewal has not yet been demonstrated (Smith, 2006).

The manner in which SCs maintain both self-renewal and the production of daughter cells with more restrictive properties is not clear. It is widely accepted that SCs are able to divide both symmetrically (generating increased numbers of SCs) during embryonic development or injury, and asymmetrically (maintaining the number of SCs, whilst generating daughter TACs) (Snippert and Clevers, 2011). Regulation of this is proposed to be attributable to distinctive gene expression patterns, in combination with unique epigenetic mechanisms including DNA methylation, histone modifications, and non-coding RNA-mediated regulatory events (Wu and Yi, 2006).

Although specific SC genes have been identified, various transcriptome analyses suggest that SCs do not have a unique transcriptional profile (Ivanova *et al.*, 2002, Ramalho-Santos *et al.*, 2002); but rather their common feature may be a large accessible chromatin thus enabling expression of a large number of genes (Mikkers and Frisén, 2005).

1.5.1. Adult Stem Cells

In the adult state, SCs are responsible for tissue replenishment and repair, and the maintenance of all regenerative tissues such as epithelia (Fuchs and Chen, 2013). Although adult SCs are only multipotent, they often possess greater functional versatility than expected; with the ability to cross lineage barriers and adopt expression profiles and functional phenotypes of cells unique to other tissues upon exposure to a novel environment - an ability termed plasticity (Smith, 2006).

1.5.2. The Stem Cell Niche

The immediate environment of SCs and their interaction with it has been termed the 'stem cell niche' (Spradling *et al.*, 2001). This highly regulated microenvironment plays a key feature in their function; the ability of a SC to self-

renew and remain in a quiescent state is governed not only by the intrinsic proteins it expresses, but also by the extrinsic signals it receives from its niche microenvironment (Fuchs and Chen, 2013). The niche provides protection from differentiation and apoptotic stimuli and safeguarding from excessive SC production which may lead to cancer. It must also balance the requirements for SC quiescence and activity (Moore and Lemischka, 2006). Although there is diversity of SC niches and some of their signalling pathways, both positive and negative signalling are integrated, and some key molecules and pathways such as the Wnt signalling pathway appear to be consistent across niches from all tissues and organs (Mitsiadis *et al.*, 2007).

Niches may be simple (containing a single SC), complex (containing two or more SCs), or a quiescent storage niche. Loss of SCs and SC niches *in vivo* may induce tissue construction of new simple niches. It has been proposed that any tissue that is dependent on SCs and capable of growth is likely to have the capacity to produce new niches (Ohlstein *et al.*, 2004).

Adult SC niches have been characterised in many tissues including the bone marrow, incisor, epidermal hair follicles and intestinal epithelium (Moore and Lemischka, 2006, Mitsiadis *et al.*, 2007). Typically epithelial SC niches occur in basal clusters throughout the tissue, a key exception to this being corneal epithelial SCs which reside in the limbus (Dua *et al.*, 2005, Shortt *et al.*, 2007a, Shanmuganathan *et al.*, 2007).

1.5.3. Identification of Stem Cells

Whilst a single unambiguous indicator of a SC in any organism remains elusive, SCs may be characterised by a number of indirect properties which include: expression of specific molecular markers, slow cycling (label-retention), a high level of dye efflux activity (side population) or clonogenicity. However, none of these criteria is specific (Barrandon, 2007).

Stem Cell Marker Expression

SCs may be identified by their possession of distinctive molecular markers. The expression of these markers may be assessed by immunohistochemical or immunocytochemical techniques, or the levels of their mRNA expression detected by molecular techniques such as real time polymerase chain reaction (rtPCR). The purity of many of these markers as true SC markers is however controversial and their expression may be altered in *in vitro* culture conditions (Vascotto and Griffith, 2006).

Label Retention

The slow-cycling nature and/or asymmetric division of SCs may be measurable *in vivo* or *in vitro* by either tritiated thymidine ($[^3\text{H}]\text{TdR}$)- or bromodeoxyuridine (BrdU)-label retention (Cotsarelis *et al.*, 1990, Tumber *et al.*, 2004). These *in vivo* studies are however restricted to use in laboratory animal models which may not accurately represent the anatomical or pathophysiological state of the human being, and slow-cycling nature does not necessarily indicate the proliferative potential of a cell (Pellegrini *et al.*, 1999, Snippert and Clevers, 2011). Indeed, the basis of label retention as a marker of SCs has been questioned (Kiel *et al.*, 2007, Snippert and Clevers, 2011).

Dye Efflux Activity

The DNA dye Hoechst 33342 can be used *ex vivo* to identify a side population of SCs which demonstrate very low fluorescent emission intensities and a reduced bathochromic shift, due to their ability to actively efflux Hoechst (Challen and Little, 2006). This characteristic is mediated by the SC marker ATP-binding cassette protein G2 (ABCG2) (Zhou *et al.*, 2001) (see Section 1.6.3).

Clonogenic Ability

SCs demonstrate the highest clonogenic ability of all cells *in vitro*, with single cells producing large rapidly growing colonies (holoclones), in contrast to the limited growth (paraclones and meroclones) produced by TACs (Barrandon and Green, 1987). This must however, be assessed by colony forming efficiency (CFE) assays *ex*

vivo, thus perhaps not representing the true potential of the SC within its natural niche. Self-renewal is considered the ultimate indicator of stemness. It is best demonstrated by the clonal analysis of a single isolated cell, followed by serial transplantation (of it or its progeny) and long-term reconstitution of a tissue (Barrandon, 2007). Thus without first isolating individual cells, CFE is correctly a measure of PCs rather than SCs.

1.5.4. Human Stem Cell-Based Therapies

Recognition of the role of SCs in tissue repair and regeneration, and their unique ability to treat a wide spectrum of diseases that are ineffectively treated by traditional approaches, has led to much interest in SC-based therapies; either in the possibility of manipulating SCs *in situ* using drugs, or expanding them *ex vivo*. The use of haematopoietic SCs in bone marrow transplantation and autologous epidermal keratinocyte SC therapy for the management of severe burns, has paved the way for other tissue-specific therapies. Although few SC therapies have yet reached clinical use, there is a plethora of research activity in the field. Research is required to both further characterise the biology of SCs and to further develop therapeutic strategies (Mayhall *et al.*, 2004). Due to the ethical issues surrounding the use of embryonic SCs, much research has focused on the use of adult SCs and induced pluripotent SCs.

1.6. Ocular Surface Stem Cells

Like all epithelia, the corneal and conjunctival epithelia are renewed constantly, a process for which they rely on the presence of SCs. Although the two are closely related, both being demonstrated to arise from a few surface Pax-6 positive ectodermal cells in animals and humans (Koroma *et al.*, 1997, Nishina *et al.*, 1999) (see Section 1.2), they are of distinct cell lineages. Each produce their own phenotype when rabbit cells are injected into athymic mice (Wei *et al.*, 1996) or human cells are cultured *in vitro* (Pellegrini *et al.*, 1999); and limbal but not

conjunctival cells can restore the human corneal epithelium *in vivo* (reviewed in (Lavker *et al.*, 2004).

1.6.1. Limbal Stem Cells

Much evidence including pigment migration studies (Davanger and Evensen, 1971), label-retaining studies (Cotsarelis *et al.*, 1989), proliferative capacity (Ebato *et al.*, 1988, Lindberg *et al.*, 1993) and the expression of progenitor markers (Pellegrini *et al.*, 2001, Di Iorio *et al.*, 2005, Budak *et al.*, 2005, Dua *et al.*, 2005, Kawasaki *et al.*, 2006) suggests that animal and human corneal epithelial SCs reside in the basal layers of the limbal epithelium; hence they are termed limbal SCs. Indeed, conjunctivalisation of the rabbit cornea is demonstrated post limbal epithelial removal (Kruse *et al.*, 1990, Chen and Tseng, 1991, Huang and Tseng, 1991), and human corneal epithelial regeneration has been demonstrated following limbal grafting (Kenyon and Tseng, 1989). The complementary XYZ model for corneal epithelial maintenance, whereby basal TACs and their differentiated progeny migrate both superficially and centripetally, before being shed (Thoft and Friend, 1983) is widely accepted. By this process the entire human epithelium is renewed every seven days (Hanna *et al.*, 1961). The human limbal SC niche resides in limbal epithelial crypts between the palisades of Vogt (Dua *et al.*, 2005, Shortt *et al.*, 2007a, Shanmuganathan *et al.*, 2007), and is characterised by the presence of melanocytes, Langerhans cells and T lymphocytes (Li *et al.*, 2007), rich vascularisation (Goldberg and Bron, 1982), and a unique expression of extracellular matrix components (Schlötzer-Schrehardt *et al.*, 2007) (see Section 1.1.1).

Limbal SC deficiency in humans may develop in a variety of conditions including those causing cicatrising conjunctival disease (see Section 1.3.1) and hereditary disorders such as aniridia. It is characterised by encroachment of the conjunctival epithelium with its blood vessels over the corneal surface. This not only results in visual impairment, but the new epithelium is prone to constant erosion and breakdown, causing chronic pain and photophobia (Shapiro *et al.*, 1981, Tseng, 1996).

1.6.2. Conjunctival Stem Cells

Animal Studies

Studies in animal models have generated much conflicting evidence as to the location of conjunctival SCs. These have predominantly been label-retention studies. Using [³H]TdR, one research group identified label-retaining cells throughout the mouse conjunctiva, but predominantly in the fornix (Wei *et al.*, 1995), and subsequently demonstrated that the forniceal epithelia also shows a significantly greater proliferative response to both acute and chronic chemical stimulation (Lavker *et al.*, 1998). A similar study to the latter, but using BrdU in rats again demonstrated label-retaining cells throughout the conjunctiva, but conversely with greatest proliferative response in the limbal and palpebral regions (Chen *et al.*, 2003). Other studies have documented movement of labelled conjunctival cells. Pe'er *et al.* studied rat conjunctiva following a single dose of [³H]TdR. Over a 28 day period labelled cells became more abundant in the fornix and declined in the limbal and palpebral areas. They concluded that SCs are present in the limbus and mucocutaneous junction and stream towards the fornix (Pe'er *et al.*, 1996). These findings were in part confirmed by both Wirtschafter *et al.* and Su *et al.*, using BrdU in rabbits. They both additionally noted long-term label retention at the mucocutaneous junction and concluded that this was the source of conjunctival SCs (Wirtschafter *et al.*, 1997, Wirtschafter *et al.*, 1999, Su *et al.*, 2011). A subsequent study of the movement of mouse bulbar conjunctival cells by BrdU pulse-chase, in contrast concluded that they are uniformly distributed and generally immobile (Nagasaki and Zhao, 2005). Aside from the inherent presumption that the anatomical distribution of SCs should be constant across species, the accuracy of label retention studies in isolating SCs has also been questioned (Kiel *et al.*, 2007, Snippert and Clevers, 2011). These factors may explain the conflicting results that these studies demonstrate.

Two recent studies have compared the clonogenic ability of conjunctival epithelial cells across the whole tissue in animal models. Su *et al.* demonstrated both higher CFE and proliferating cell nuclear antigen (PCNA) expression in the palpebral region, than in the forniceal, than bulbar regions of the rabbit conjunctiva (Su *et al.*, 2011).

The highest level of PCNA expression has however previously been noted in the mucocutaneous junction of the rabbit conjunctiva (Wirtshafter *et al.* 1999). Eidet *et al.* also demonstrated clonogenic ability throughout the rat conjunctival epithelium, but conversely with highest CFE levels in the forniceal epithelium, especially superiorly (Eidet *et al.*, 2012a). Indeed, a previous study has also demonstrated greater growth of rabbit forniceal cells in culture than either palpebral or bulbar cells (Wei *et al.*, 1993).

Human Studies

There are very few studies concerning the location of SCs in human conjunctiva. An *in vitro* study analysing the clonogenic properties of the ocular surface epithelia indicated that SCs are uniformly distributed in small biopsies of bulbar and forniceal conjunctiva from one donor (Pellegrini *et al.*, 1999). Expression of the SC marker ABCG2 (see Section 1.6.3) has been demonstrated immunohistochemically in basal clusters of conjunctival epithelium, with highest levels in the palpebral-forniceal zone, but it is not clear whether the whole conjunctival tissue was assessed, nor from how many donors (Budak *et al.*, 2005). A further immunohistochemical assessment of a number of SC markers including Δ Np63 and ABCG2 (see Section 1.6.3) concluded the presence of rare scattered bulbar conjunctival SCs, but did not assess other areas of the conjunctiva, and the number of tissues included in this study is not clear (Vascotto and Griffith, 2006). More recent studies (published during the conduction of this study) have not provided much greater clarification on the overall distribution of conjunctival SCs. Qi *et al.* confirmed the findings of Vascotto and Griffin in the bulbar conjunctiva using tissue from four donors and additional SC markers, but did not assess other areas (Qi *et al.*, 2010). Two further studies have assessed expression of a host of pluripotency genes by real-time PCR. Pauklin *et al.* assessed bulbar and forniceal tissue from four donors, demonstrating similar levels of pluripotent markers throughout, but higher levels of ABCG2 gene expression in the fornices (Pauklin *et al.*, 2011). Harun *et al.* assessed biopsies of tissue from inferior bulbar, forniceal and tarsal conjunctiva of three donors, reporting highest levels of pluripotency genes in the fornices (Harun *et al.*, 2013). A recent immunohistochemical study using several SC markers has also proposed that

the ductal epithelium of the meibomian glands and the bulge region of the eyelid hair follicle may represent sites for human conjunctival SCs (Tektaş *et al.*, 2012). Clearly further investigation is thus required to clarify the location of human conjunctival SCs.

Conjunctival keratinocytes and goblet cells are derived from a common bipotent progenitor which may be a TAC (Wei *et al.*, 1997, Pellegrini *et al.*, 1999). The drive to differentiate into goblet cells appears to be time-dependent at specific cell doubling intervals (Pellegrini *et al.*, 1999). Goblet cells themselves may also retain some proliferative potential (Wei *et al.*, 1995, Shatos *et al.*, 2003, Pellegrini *et al.*, 1999).

Wherever the richest sources of conjunctival SCs lie, it can be presumed that widespread or total severe conjunctival disease (see Section 1.3.1) results in, or is at least characterised by conjunctival SC loss. Goblet cell deficiency alone is certainly implicated in many disabling conjunctival diseases (Doughty, 2012, Tseng *et al.*, 1984).

1.6.3. Ocular Surface Stem / Progenitor Cell Markers

Although there are no definitive markers of ocular surface SCs a number of putative markers are recognised, some of which are widely renowned SC markers detectable in other tissues. They include an array of structural and regulatory proteins, transporters, enzymes and growth factors. Most putative conjunctival SC markers are recognised limbal SC markers (Budak *et al.*, 2005, Vascotto and Griffith, 2006, Qi *et al.*, 2010, Pauklin *et al.*, 2011), although there are some distinct differences, particularly in cytokeratin (CK) expression (Kasper *et al.*, 1988, Elder *et al.*, 1997, Qi *et al.*, 2010). Many markers do not discriminate true stemness but rather may also detect a fraction of TACs which retain a stem-like phenotype (Vascotto and Griffith, 2006), and hence should correctly be termed PC markers. ABCG2 and $\Delta Np63\alpha$ are considered to be the most reliable ocular surface SC markers (Vascotto and Griffith,

2006), although some evidence even questions their validity (Chen *et al.*, 2004, Watanabe *et al.*, 2004, Kawasaki *et al.*, 2006).

ABCG2

ATP-binding cassette protein (ABCG2) is a lipid membrane ATP-dependent transport protein that is expressed in many adult SCs and has been proposed as a universal SC marker (Zhou *et al.*, 2001). Although its precise physiological role remains unclear, it may protect cells by exporting a wide variety of endogenous and exogenous compounds out of cells, and promote maintenance and proliferation of the SC phenotype (Ding *et al.*, 2010). It has been detected in the basal cells of the limbus and bulbar conjunctiva, but not in the suprabasal cells of these tissues or in any layers of the cornea (Chen *et al.*, 2004, Watanabe *et al.*, 2004, Budak *et al.*, 2005, Vascotto and Griffith, 2006). Indeed the efflux of Hoechst 33342 by side population cells (see Section 1.5.3) is mediated by ABCG2 (Zhou *et al.*, 2001); and these cells comprising <1% of ocular surface cells exhibit many features of stemness (Budak *et al.*, 2005).

Δ Np63 α

p63 is a transcription factor involved in morphogenesis and is critical for maintaining SC populations. p63-null mice lack stratified squamous epithelia (Yang *et al.*, 1999), and heterozygous humans develop ectodermal dysplasias (Rinne *et al.*, 2006). The p63 gene generates TAp63 and Δ Np63 isoforms, each having α , β and γ isotypes (Yang and McKeon, 2000). Δ Np63 sustains the proliferative potential of keratinocytes (Parsa *et al.*, 1999), and specifically Δ Np63 α is the major transcript expressed by ectodermal SCs, including ocular surface SCs (Di Iorio *et al.*, 2005, Kawasaki *et al.*, 2006). Δ Np63 α acts as a transcriptional repressor at select p53 growth regulatory gene promoters, and loss of Δ Np63 α facilitates the growth arrest associated with differentiation (Westfall *et al.*, 2003). The antibody to the Δ Np63 α isotype is not however widely available for immunochemical techniques, hence most studies have employed antibodies to Δ Np63 (Chen *et al.*, 2004, Vascotto and Griffith, 2006). Identification of all p63 isoforms (by the common 4A4 clone of antibody) is considered a marker of TACs (Parsa *et al.*, 1999).

Cytokeratins

Keratins form the predominant cytoskeletal component of epithelial cells, maintaining cell morphology, intracellular signal transduction, mobility and proliferation (Fenteany and Glogauer, 2004). They have long been proposed as markers of conjunctival differentiation (Krenzer and Freddo, 1994). They were divided by Moll *et al.* into smaller acidic type I (CK9-20) and larger, neutral-basic type II (CK1-8); and are obligate heteropolymers combining a type I with type II subunit (Moll *et al.*, 1982). CK8, 15 and 19 are reported as putative limbal SC markers (Merjava *et al.*, 2011a, Yoshida *et al.*, 2006, Kasper *et al.*, 1988, Barnard *et al.*, 2001, Chen *et al.*, 2004); and CK5, 8 and 15 have been noted in basal layers of the conjunctival epithelium (Pitz and Moll, 2002, Qi *et al.*, 2010, Merjava *et al.*, 2011b). Conversely, CK19 has long been recognised as marker of conjunctival epithelial phenotype, being expressed throughout all layers of the epithelium (Kasper *et al.*, 1988, Elder *et al.*, 1997). Similarly, CK3 has been proposed as a negative limbal SC marker (being expressed in the suprabasal and superficial layers of the limbal epithelium and throughout the central corneal epithelium); but conversely is not expressed in any layers of the bulbar conjunctiva (Merjava *et al.*, 2011b). Clearly further studies are required to clarify CK expression and validity as SC markers across the ocular surface.

$\alpha 9\beta 1$ Integrin

Integrins are transmembrane glycoproteins, composed of an α and β chain, that mediate cell-cell and cell-matrix attachments (Belkin and Stepp, 2000). $\alpha 9\beta 1$ integrin has been demonstrated in basal limbal epithelial cells (Stepp *et al.*, 1995); and limbal cells adhering to the $\beta 1$ integrin ligand collagen IV, possess SC properties (Li *et al.*, 2005). However widespread expression of the $\beta 1$ subunit has also been detected across the corneal epithelium; thus bringing into question its validity as an SC marker (Vascotto and Griffith, 2006).

Hsp70

Heat shock proteins (Hsp) act as molecular protein chaperones to preserve epithelial cell integrity, and are thus upregulated in response to various

environmental stresses (Garrido *et al.*, 2001). Hsp70 has been implicated in corneal epithelial proliferation, differentiation and migration during wound healing (Mushtaq *et al.*, 2007), and is reported to be up regulated by Δ Np63 α (Wu *et al.*, 2005). It is highly abundant in the basal layers of the limbal and bulbar conjunctival epithelia (Lyngholm *et al.*, 2008) and its expression is correlated with Δ Np63 α expression (Ma *et al.*, 2012). It has however also been reported to a minor extent in the central corneal epithelium (Lyngholm *et al.*, 2008) and is thus perhaps better considered a PC or TAC marker.

N-Cadherin

Cadherins are transmembrane proteins which form desmosome junctions. It has been suggested that N-Cadherin is involved in the maintenance of haematopoietic SCs (Zhang *et al.*, 2003, Calvi *et al.*, 2003). N-Cadherin has also been detected in limbal SCs (Hayashi *et al.*, 2007), and shown to play a key role in their maintenance *in vitro* (Higa *et al.*, 2009).

CD168

Cluster of differentiation 168 (CD168), otherwise known as Hyaluronan-mediated motility receptor (HMMR/RHAMM) is a receptor for hyaluronan, an important component of the extracellular matrix (Turley *et al.*, 2002) and has been implicated in mobilisation of haematopoietic SCs (Pilarski *et al.*, 1999). It has been proposed as a negative limbal SC marker (Ahmad *et al.*, 2008).

Other markers

There are a wealth of additional reported putative limbal SC markers which may also represent conjunctival SC markers. These include EGF (Zieske and Wasson, 1993), nerve growth factor and its receptor TrkA (Qi *et al.*, 2008) and pluripotency genes such as OCT4 and NANOG (Pauklin *et al.*, 2011), and the negative expression of connexin 43 (Wolosin *et al.*, 2000). Some of these markers have recently been demonstrated in the basal layers of the conjunctival epithelium, and thus are also proposed as putative conjunctival SC markers (Vascotto and Griffith, 2006, Qi *et al.*, 2010, Pauklin *et al.*, 2011).

1.7. Ocular Surface Epithelial Propagation *Ex Vivo*

The discovery by Rheinwald and Green that a feeder layer of inactivated J23T3 murine fibroblasts (3T3) permitted the clonal growth of keratinocytes (Rheinwald and Green, 1975a, Rheinwald and Green, 1975b), paved the way for animal and human *in vitro* epithelial culture studies. Methods for isolating and expanding epithelial SCs *ex vivo* were subsequently established (Barrandon and Green, 1987). More recent years have led to an increasing interest in the isolation and *ex vivo* expansion of human corneal and conjunctival SCs (Lindberg *et al.*, 1993, Pellegrini *et al.*, 1999, Ramaesh and Dhillon, 2003, Papini *et al.*, 2005, Ahmad *et al.*, 2006).

1.7.1. Culture Conditions

Animal or human cells may be harvested by enzymatic digestion or used in explant culture. Cultures have traditionally been performed using co-culture with an inactivated 3T3 feeder layer (Lindberg *et al.*, 1993, Pellegrini *et al.*, 1997), which is thought to act as a surrogate SC niche environment. Although culture systems have been described where there is no contact with the feeder layer or no feeder layer present (Ang *et al.*, 2004b), there is no definitive evidence that these actually support SCs. Culture on amniotic membrane alone (Tsai *et al.*, 2000, Grueterich *et al.*, 2003) or in combination with 3T3 feeder layers (Koizumi *et al.*, 2001) has also been employed; however, it appears that a feeder layer is required to maintain SC phenotype in culture (Balasubramanian *et al.*, 2008). The addition of hydrocortisone, fetal calf serum (FCS), EGF and insulin to the media, amongst other factors, improves cell morphology, proliferation and stratification (Rheinwald and Green, 1975b, Hayashi *et al.*, 1978, Lindberg *et al.*, 1993, Pellegrini *et al.*, 1999). Airlifting may then be employed to promote stratification and differentiation of the epithelial culture (Meller and Tseng, 1999).

Given the aim of generating human epithelial constructs for clinical transplantation, and the increasing concerns regarding the risk of transmission of xenobiotic infective agents, advances have been made to negate the requirement of both murine feeder cells and FCS in the culture conditions. Amniotic membrane (Ang *et*

et al., 2004a, Chen *et al.*, 2007, Shahdadfar *et al.*, 2012) or alternative feeder layers (Omoto *et al.*, 2009, Schrader *et al.*, 2010, Sharma *et al.*, 2012, Schrader *et al.*, 2012) have been employed, and FCS has been replaced with autologous or cord blood serum (Ang *et al.*, 2005b, Nakamura *et al.*, 2006, Kolli *et al.*, 2010, Shahdadfar *et al.*, 2012, Ang *et al.*, 2011, Schrader *et al.*, 2012). Though, to date there is no firm evidence that human epithelial SCs are maintained in such environments.

Whilst significant advances have been made in generating human limbal SC containing epithelial constructs *in vitro* (Ahmad *et al.*, 2006, Mariappan *et al.*, 2010, Osei-Bempong *et al.*, 2009); there remains much discrepancy amongst research groups regarding optimal culture conditions, and uncertainty to the true SC content of such constructs.

Development of a conjunctival SC containing epithelial equivalent is even more complex, due to the additional need to also support the growth of goblet cells. Whilst both goblet cells and mucins have been demonstrated in human conjunctival cultures (Corfield *et al.*, 1991, Frescura *et al.*, 1993, Diebold and Calonge, 1997, Pellegrini *et al.*, 1999, Risse Marsh *et al.*, 2002, Shatos *et al.*, 2003, Berry and Radburn-Smith, 2005), there has generally been a notable absence in stratified constructs (Tanioka *et al.*, 2006). Goblet cells require stringent culture conditions; being supported by RPMI-1640 media (Shatos *et al.*, 2003), rather than Dulbecco's modified eagle's media (DMEM) and Ham's F12 media commonly used in other studies. There is a quandary for example, in the addition of hydrocortisone to media, which although improves epithelial cell morphology and proliferation (Rheinwald and Green, 1975b), has been shown to inhibit differentiation of goblet cells in chick embryo duodenal explants (Black and Moog, 1977). Other studies have however demonstrated that hydrocortisone appears to increase the production of mucins in human conjunctival cultures (Diebold *et al.*, 1999, Gipson *et al.*, 2003). Similarly, although rabbit and human conjunctival epithelial PCs capable of generating goblet cell phenotypes have been cultured *in vitro* on amniotic membrane (Meller *et al.*, 2002, Budak *et al.*, 2005), it is noted that non-goblet cell

differentiation is either preferentially promoted or results in potential loss of PCs (Meller *et al.*, 2002).

However, studies employing keratinocyte growth media (Lonza, USA) have demonstrated positivity for MUC5AC mRNA in stratified human epithelial equivalents (Ang *et al.*, 2004b, Ang *et al.*, 2004a). On tissue culture plastic alone, these constructs showed equivalent CFE to cells cultured with serum and a 3T3 feeder layer; and on amniotic membrane they showed higher CFE than cells cultured with serum (Ang *et al.*, 2004a). Notably, the use of human serum in conjunctival cultures has been demonstrated to additionally negate the requirement for bovine pituitary extract, and produce constructs with both comparable CFE and clusters of goblet cells (Ang *et al.*, 2005b). Significantly, human conjunctival PCs and goblet cells have recently been noted to be preserved in a serum-free system co-cultured with mitotically active subconjunctival fibroblasts (Schrader *et al.*, 2010). The use of umbilical cord blood serum has also demonstrated higher proliferative capacity (Ang *et al.*, 2011). A completely xenobiotic-free culture system for human conjunctival epithelial PCs using human serum and a MRC-5 human fetal lung fibroblast feeder layer has been reported, but supports lower CFE and SC marker expression (Schrader *et al.*, 2012).

1.7.2. Substrates

Epithelial cells require a basement membrane or matrix to support their adhesion and growth; indeed the nature of the matrix determines the cell growth pattern and differentiation (Ma, 2008). Substrates for *ex vivo* expansion must therefore be tailored to mimic the native extracellular matrix of a specific cell type; and with regard to transplantation, to be amenable to surgical manipulation, integrate with the host tissue and modulate the wound healing response.

In order to preserve optical clarity and hence vision, the development of substrates to support corneal and/or limbal epithelial growth is dictated largely by the need for transparency. Substrates for conjunctival reconstruction are in contrast not

restricted in this manner, but must be flexible and elastic materials, able to accommodate eye movement; yet strong enough to act as a mechanical barrier to prevent re-scarring and symblepharon formation in forniceal reconstruction (Kearns *et al.*, 2012). In addition, they must provide sufficient cellular attachment to prevent sloughing off of the epithelium by mechanical shearing forces in both surgical transplantation and postoperative movement of the eye and eyelids (Ang *et al.*, 2004a). Specifically, they must also promote the regenerative capacity of SCs and goblet cells.

Human amniotic membrane has long been the favoured substrate for ocular surface reconstruction as its thick basement membrane and avascular stroma has similar constituents to the human limbal and conjunctival basement membranes (Fukuda *et al.*, 1999). It is thin and elastic, relatively transparent, promotes rapid epithelialisation, and has anti-inflammatory, anti-scarring, anti-angiogenic and analgesic properties (Liu *et al.*, 2010). Indeed it has been demonstrated to enhance corneal and conjunctival regeneration when used as a protective onlay or for human fornix reconstruction in a variety of disease processes (Barabino and Rolando, 2003, Honavar *et al.*, 2000, Solomon *et al.*, 2003). It may be processed and preserved by a variety of methods (Shortt *et al.*, 2009), including decellularisation to reduce the risk of disease transmission (Wilshaw *et al.*, 2006). Decellularised amniotic membrane has been shown to enhance cell attachment and support a more mature human limbal tissue construct (Grueterich *et al.*, 2002, Koizumi *et al.*, 2007), but the process may remove the high levels of growth factors present in the intact membrane which maintain SCs in culture (Hernandez Galindo *et al.*, 2003). The ideal preparation remains debated (Osei-Bempong *et al.*, 2009, Chen *et al.*, 2010).

In either form, amniotic membrane remains the most widely used substrate for the successful transplantation of human limbal SC epithelial equivalents (Baylis *et al.*, 2011). It has also been demonstrated to support the growth of rabbit conjunctival PCs and goblet cells (Meller *et al.*, 2002), and stratified human conjunctival epithelial constructs (Ang *et al.*, 2004a, Martínez-Osorio *et al.*, 2009). It has been

used as a substrate for transplantation of small areas of *ex vivo* expanded human conjunctival epithelium (Tan *et al.*, 2004, Ang *et al.*, 2005a, Ang and Tan, 2005). However, amniotic membrane is variable in quality (Liu *et al.*, 2010), liable to shrinkage (Barabino and Rolando, 2003, Honavar *et al.*, 2000), and its *in vivo* degradation rate is very unpredictable: with reports varying from less than 3 weeks to greater than 24 weeks on the human ocular surface (Vyas and Rathi, 2009).

Fibrin, a fibrous non-globular protein, used in the form of both films and gel matrices, offers better mechanical properties and transparency (Liu *et al.*, 2012a), and have been demonstrated to maintain rabbit and human holoclones and limbal SCs in culture (Han *et al.*, 2002, Liu *et al.*, 2012a), but there are no reports of their use to support conjunctival cells. They have been successfully employed in human limbal SC transplantation for over 10 years (Rama *et al.*, 2010). However, even following additional crosslinking, fibrin degrades within a few days (Han *et al.*, 2002), which is unlikely to offer sufficient time for the cells to lay down a new replacement basement membrane, and thus it is improbable that it would offer benefit in forniceal reconstruction.

Use of other biological substrates such as collagen and laminin have been reported. Collagens are triple helix proteins which self-assemble into scaffolds providing structural integrity. Collagen IV is the major component of basement membranes. In addition to providing a structural scaffold, it interacts with the cells it supports and promotes cell adhesion, migration, growth and differentiation (Khoshnoodi *et al.*, 2008). It has been demonstrated to support the growth of limbal SCs (Chakraborty *et al.*, 2013). Collagen I gels have been successfully used to culture both human limbal epithelial constructs (Levis *et al.*, 2010, Mi *et al.*, 2010) with evidence to support the presence of limbal SCs (Levis *et al.*, 2010), and stratified human conjunctival epithelium constructs (Berry and Radburn-Smith, 2005).

Other constituents of basement membranes which may also be considered include laminins and fibronectin. Laminins are heterotrimeric glycoproteins composed of differing combinations of alpha, beta and gamma subunits. Laminin 1 is an $\alpha 1 \beta 1$

γ 1 trimer, and is the other major structural constituent of basement membranes. It also promotes cell adhesion, migration, growth, and differentiation (Malinda and Kleinman, 1996); and has been reported to maintain a conjunctival epithelial cell line (Lin *et al.*, 2000) and undifferentiated pluripotent SCs (Hoffman *et al.*, 1998). Fibronectin is a high-molecular weight glycoprotein which is a product of most epithelial cells, and is widely distributed in both the extracellular matrix and the plasma. It aids cellular migration during wound healing and development, and regulates cell growth and differentiation (Pankov and Yamada, 2002). Used as a substrate, it sustains human embryonic cells in an undifferentiated phenotype (Kalaskar *et al.*, 2013). Biological substrates are however often inconsistent in quality and carry the risk of disease transmission and allograft rejection (Liu *et al.*, 2010).

Synthetic substrates offer a reliable disease free alternative. Ultrathin Poly(ϵ -Caprolactone), a bio-resorbable polymer which is elastic and mechanically strong has been demonstrated to support the growth of stratified human conjunctival epithelial sheets with equivalent levels of goblet cells as seen on amniotic membrane (Ang *et al.*, 2006). In order to maintain long-term reconstruction of the fornices in severe ocular surface disease, a synthetic non-degradable scaffold which maintains forniceal depth may be more likely to offer greater success.

1.8. Human Ocular Surface Regenerative Therapies

The development of SC-based therapies has offered a significant breakthrough in the management of many diseases. Therapies for the ocular surface offer a cure for many otherwise unmanageable chronically painful and blinding eye conditions. The ocular surface is unique in that it easily accessible, not only conferring benefit for initial surgical intervention, but also for long-term follow-up of the acceptance of such grafts into the host environment. Whilst there has been significant progress in the development of limbal SC therapies, such that they are now recognised

treatments; much remains to be achieved in the development of conjunctival SC therapies for severe conjunctival disease.

1.8.1. Limbal Stem Cell Transplantation

Traditionally limbal autografts and allografts were performed (Herman *et al.*, 1983, Kenyon and Tseng, 1989, Thoft, 1984) with variable degrees of success. The advances in cell culture techniques and preparation of cohesive sheets of stratified epithelia detailed above have since enabled transplantation of *ex vivo* expanded limbal epithelium taken from a small biopsy (Pellegrini *et al.*, 1997). This has overcome the risk of inducing limbal SC deficiency in the healthy donor eye and often the need for systemic immunosuppression. Significant clinical improvements in corneal clarity and ocular surface stability have been achieved with these methods (Schwab, 1999, Tsai *et al.*, 2000, Grueterich *et al.*, 2002, Di Iorio *et al.*, 2010, Rama *et al.*, 2010). Reported success rates range from 0-100%, with a mean of 76-77% (Shortt *et al.*, 2007b, Baylis *et al.*, 2011).

The long-term outcomes and fate of the transplanted SCs are not however clear. Although a few studies describe post-operative follow-up up to 10 years (Tsai *et al.*, 2000, Rama *et al.*, 2010), the mean follow-up times are generally less than 3 years, with failures normally occurring within the first 1-2 years (Sangwan *et al.*, 2006, Pauklin *et al.*, 2010, Rama *et al.*, 2010). The absence of detectable donor DNA beyond 9 months (Daya *et al.*, 2005) raises questions as to whether viable SCs have been transplanted, or whether restoration of the limbal SC niche revives host SCs. Transplantation of TACs alone may give the impression of success but result in early failure (Holland, 1996). There are clearly still many improvements to be made and questions to be answered.

1.8.2. Conjunctival Epithelial Transplantation

Conjunctival epithelial transplantation was first described by Thoft in the form of multiple autografts for monocular chemical burns (Thoft, 1977), however, this or equivalent allografts cause considerable co-morbidity to the donor eye. In light of

the apparent success of transplantation of limbal cultivated epithelial equivalents, interest in conjunctival epithelial expansion developed. There are a number of reports of the limited clinical success of transplantation of autologous cultivated conjunctival epithelial equivalents on amniotic membrane. These were performed to replace focal areas of conjunctival loss in cases with limited deficiencies, such as post excision of pterygia or viral papillomas (Tan *et al.*, 2004, Ang *et al.*, 2005a, Ang and Tan, 2005). Patients were followed up for up to 25 months and success defined as persistent epithelialisation and absence of significant complications. Histologic examination of the transplanted tissue in each case showed a 4-5 layer deep, stratified squamous epithelial sheet. Interestingly there was no mention of the presence of SCs or goblet cells or assessment of the mucin expression within these cultured epithelial equivalents; and equally no attempts were made to postoperatively define the grafted conjunctival epithelium by either impression cytology or confocal analysis (Tan *et al.*, 2004, Ang *et al.*, 2005a, Ang and Tan, 2005). Thus it is plausible that these constructs were relatively sparse or even absent of SCs, goblet cells or mucins.

Given that these reports are in conditions with relatively localised conjunctival disease, it may be that there are sufficient SCs, goblet cells and mucin production from the remaining healthy conjunctiva to maintain the tissue and a healthy tear film in these cases. However, in conditions with extensive conjunctival destruction, with widespread SC and goblet cell loss, and where large grafts would be required, this is unlikely to hold true. Long-term success rates may also depend upon these factors.

The ideal transplanted *ex vivo* expanded conjunctival tissue would be fully functioning with normal mucin production, and contain an adequate number of SCs (Holland, 1996, De Luca *et al.*, 2006). Additionally, it would be supported by a substrate which supports these cells, is flexible, elastic, inert and maintains a reconstructed fornix. An initial greater concentration of SCs can only aid both SC and goblet cell levels, and mucin production from the transplanted tissue. This

could be achieved by further research into the location of conjunctival SCs to aid choice of initial biopsy site.

1.9. Summary, Hypothesis and Aims

1.9.1. Summary

The conjunctiva is a mucous membrane which forms the majority of the ocular surface, and plays a key role in ocular surface defence and maintenance of the tear film. *Ex vivo* expansion of conjunctival epithelial cells offers potential to reconstruct the ocular surface in cases of severe cicatrising disease; but in order to ensure long term success, conjunctival stem cells which produce both keratinocytes and goblet cells must be present. An initial biopsy rich in stem cells would aid this, however the distribution of human conjunctival stem cells has not been clearly elucidated.

1.9.2. Hypothesis

I hypothesise that PCs are located in specific areas of the human conjunctiva, and can be identified using CFE assays and the immunochemical detection of putative SC markers.

1.9.3. Aims

- 1) To develop a technique to retrieve whole human cadaveric conjunctiva.
- 2) To identify and locate the PC-rich areas within the retrieved whole conjunctiva by CFE assays and immunochemical staining.
- 3) To assess the effect of donor age and post mortem retrieval time (PMRT) on markers of PCs.
- 4) To culture conjunctival cells *in vitro* on suitable substrates into stratified sheets of conjunctival epithelium.

2. Materials and Methods

2.1. Tissue Retrieval

Ethical approval was obtained from Trent Research Ethics Committee (REC reference 07/MRE04/31) to retrieve human conjunctival tissue from patients who had died and whose next-of-kin had given consent for eye and eye tissue donation for transplantation and research. In addition to the standard exclusion criteria for ocular tissue donation (UK Blood Transfusion and Tissue Transplantation Services, 2013), an additional exclusion of those who had undergone previous eyelid surgery was applied. Consent was obtained by the Tissue Services nurses at National Health Service, Blood and Transplant (NHSBT) and was fully compliant with the relevant legislation that is, The Human Tissue Act (Human Tissue Act, 2004), the European Union Tissues and Cells Directive (Tissues and Cells Directive, 2004) and the Data Protection Act (Data Protection Act, 1998).

A surgical technique was developed to retrieve whole conjunctival tissue. This conformed to the standards for eye retrieval for transplantation and research (The Royal College of Ophthalmologists, 2008). Conjunctival tissue from both eyes was retrieved from each donor within 28 hours of death. A single surgeon (R. Stewart) retrieved all tissues. Tissue was numbered consecutively 01, 02 etc. Each right conjunctiva (01, 03, 05...) was processed for cell culture studies and the left (02, 04, 06...) fixed and paraffin-embedded for immunohistochemical staining. Data on donor age, sex, cause of death and PMRT was recorded for comparative analysis.

2.2. Tissue Fixation, Paraffin Embedding and Sectioning

2.2.1. Fixation and Embedding

Whole conjunctival specimens were rinsed in phosphate buffered saline (PBS) (Oxoid Ltd) and surgically divided into sections as demonstrated in Figure 10. The

lateral, central and medial eyelid sections encompassed complete tissue from the bulbar conjunctiva adjacent to the limbus to that at the eyelid margin. The other sections comprised the closely connected bulbar, forniceal and tarsal tissue immediately adjacent to the medial and lateral canthi, and were hence termed canthal areas for ease of nomenclature. Each section was pinned onto cork board and fixed with 3.7% neutral buffered formaldehyde (NBF) (Bios Europe Limited) for 24 hours. The specimens were then processed through ethanol (Dept. Chemistry, University of Liverpool), xylene (Fisher Scientific) and paraffin (Surgipath) wax washes overnight using a tissue processor (Shandon) and embedded in Formula R paraffin wax (Surgipath) using an embedding unit (Shandon).

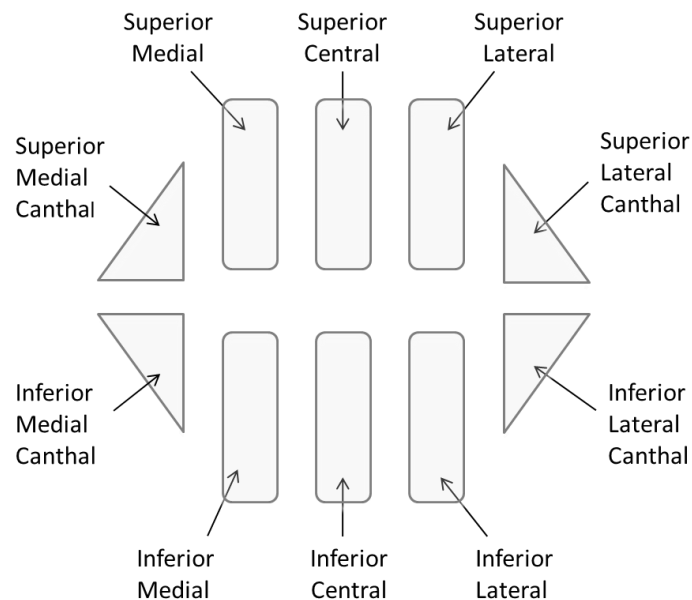


Figure 10: Schematic diagram to represent the dissection of conjunctival tissue into specific areas for comparative immunohistochemical studies.

2.2.2. Sectioning

A microtome (Shandon) was used to cut sections of the paraffin embedded conjunctival specimens. The paraffin blocks were trimmed back using 30 μ m sections with the microtome until tissue from the whole specimen was present on a section. Consecutive 4 μ m sections were then cut, wet mounted onto glass slides

and labelled serially. Sections were cut in the axial plane from the canthal specimens and in the sagittal plane from all other specimens.

2.2.3. Slides

Tissue sections were wet mounted onto either superfrost glass slides (Thermo Scientific) which were precoated with 3-aminopropyltriethoxysilane (APES) (Sigma), or onto X-tra adhesive slides (Surgipath).

APES Coating

Superfrost glass slides were immersed in 3% APES/acetone (Sigma) solution for 30 seconds at room temperature and then rinsed in acetone followed by deionised water before being left to dry overnight in a chemical fume hood. The process was repeated the following day to “double APES coat” the slides before use.

2.3. Histology

To define the anatomy of the tissue specimens a section of each was stained with haematoxylin and eosin (H&E). The slides were firstly de-paraffinised with a series of 5 minute xylene and 100% then 70% ethanol washes. They were then stained with Haematoxylin solution Gills III (Surgipath) for 3-5 minutes at room temperature, rinsed in running tap water, briefly in 1% acid-alcohol (Surgipath) and again in running tap water, before staining with alcoholic Eosin (Surgipath) for 5 minutes at room temperature. Following a further brief rinse in running tap water the slides were dehydrated with 70%, 90% and 100% ethanol for 30 seconds each in turn before being returned to xylene for 2 minutes and mounted with pertex (Surgipath) and glass cover slips (Surgipath). Multiple images were taken along the length of each specimen with an Olympus BX60 microscope and merged manually in Microsoft PowerPoint 2007.

2.4. Immunohistochemical Studies

Slides were deparaffinised through xylene and ethanol washes as in Section 2.3 and then placed into PBS. Antigen retrieval (see Section 2.4.1) was performed in most cases prior to antibody staining.

2.4.1. Antigen Retrieval

Various antigen retrieval techniques were used depending on the primary antibody: incubation with trypsin (Sigma) at 37°C for 30 minutes; microwaving in 0.01M citrate (BDH) buffer pH6 for 5-20 minutes before allowing to cool for 10 minutes at room temperature; incubating with Envision Target Retrieval pH9 (Dako) for 10 minutes at 95°C; and microwaving in 0.001M ethylenediaminetetraacetic acid (EDTA) (Sigma) buffer pH8 for 5 minutes.

2.4.2. Antibody Staining

Specific antibodies for epithelial (CK), SC and differentiation markers, and markers of other cell lineages namely melanocyte and neural cells were used as shown in Table 1. The p63 antibodies identify differing isotypes of the transcription factor, and are subsequently referred to as simply ΔNp63 (clone ΔN, Biolegend) and p63 (clone 4A4, Dako). The pan-CK antibodies each recognise an array of but not all CKs, thus using multiple pan-CK antibodies detected overlapping spectra.

Slides were rinsed in 0.05% PBS tween (Sigma), before and after blocking of endogenous peroxidases with 0.03% hydrogen peroxide (Envision™ kit, Dako) for 10 minutes at room temperature. Blocking of non-specific antibody binding was then performed with 20% goat serum (Dako) for 30 minutes at room temperature, before incubating with the primary antibodies for 2 hours (30 minutes for CK19) at room temperature, at varying dilutions in 1% goat serum. Slides were then rinsed three times with 1% goat serum before adding the secondary antibody, horseradish peroxidase (HRP) anti-mouse (Envision™ kit) or HRP anti-rabbit (Envision™ kit) as appropriate for 30 minutes at room temperature. 3-amino-9-ethylcarbazole (AEC)

chromagen was allowed to develop for 5-15 minutes, and after counterstaining with haematoxylin for 30 seconds, the slides were mounted with Aquatex aqueous mountant (Merck) and glass cover slips (Surgipath) and imaged on an Olympus BX60 microscope. A representative image was taken from the central area of each tarsal, forniceal and bulbar zone, along each superior and inferior specimen, and from the central area of each canthal specimen.

Antibody	Clone	Source
CK19	RCK108	Dako
ABCG2 (anti-BRCP)	21	Chemicon
p63	Δ N	Biolegend
p63	4A4	Dako
CD168	2D6	Abcam
Pan-CK	MNF116	Dako
Pan-CK	AE1/AE3	Dako
Pan-CK	Lu5	Abcam
Melan-A	A103	Dako
S-100	polyclonal	Dako

Table 1: Table of antibodies used for immunohistochemical studies with clone and source.

Limbal, placental, tonsillar, melanoma and colonic tissue were used as positive controls (see Section 2.4.3) and 1% goat serum alone was used as a negative control. Protocols were optimised using various antibody concentrations and antigen retrieval methods.

Due to constraints of large numbers of slides to process, it was not possible to run all samples for each antibody together. Thus samples representing all areas of 2 donor tissues were processed together with positive and negative controls as a

single experiment. Positive and negative controls from each experiment were then compared across experiments to ensure equivalent staining.

2.4.3. Tissue for Positive Controls

Limbal tissue that had been consented for both transplant and research purposes was obtained as corneo-scleral rings remaining after corneal graft procedures from Organ Donation and Transplantation (NHSBT). This was similarly fixed with 3.7% NBF for 24 hours before being processed and paraffin-embedded, and 4 μ m sections cut with a microtome as in Section 2.2. Pre-prepared slides of placental, tonsil, melanoma and colonic tissue, as control tissue for ABCG2, pan-cytokeratins, Melan-A and S-100 staining respectively were a kind gift from Mr S. Biddolph, Department of Pathology, Royal Liverpool University Hospital.

2.4.4. Semi-Quantitative analysis

Expression of immunohistochemical markers in tissue sections was analysed using two semi-quantitative grading scales. The first represented the proportion of positively staining epithelial cells throughout the epithelium: 0 cells: -, $\leq 1/3$ cells: +, $1/3-2/3$ cells: ++, and $\geq 2/3$ cells: +++. The second scale also took into account intensity of positive staining as described in Table 2. Distribution and localisation of marker expression were also qualitatively assessed.

Proportion of positively staining cells	Staining Intensity			
	None	Mild	Moderate	Intense
0	-	N/A	N/A	N/A
$\leq 1/3$	N/A	+/-	+	++
$1/3 - 2/3$	N/A	+	++	+++
$\geq 2/3$	N/A	++	+++	++++

Table 2: Table to quantify immunohistochemical staining grading scale 2 by proportion of and intensity of positively staining cells in an area. N/A = not applicable.

2.4.5. Presentation of Results

Images and grading scales from all areas were compared and presented on a schematic diagram of the whole conjunctiva as labelled in Figure 11.

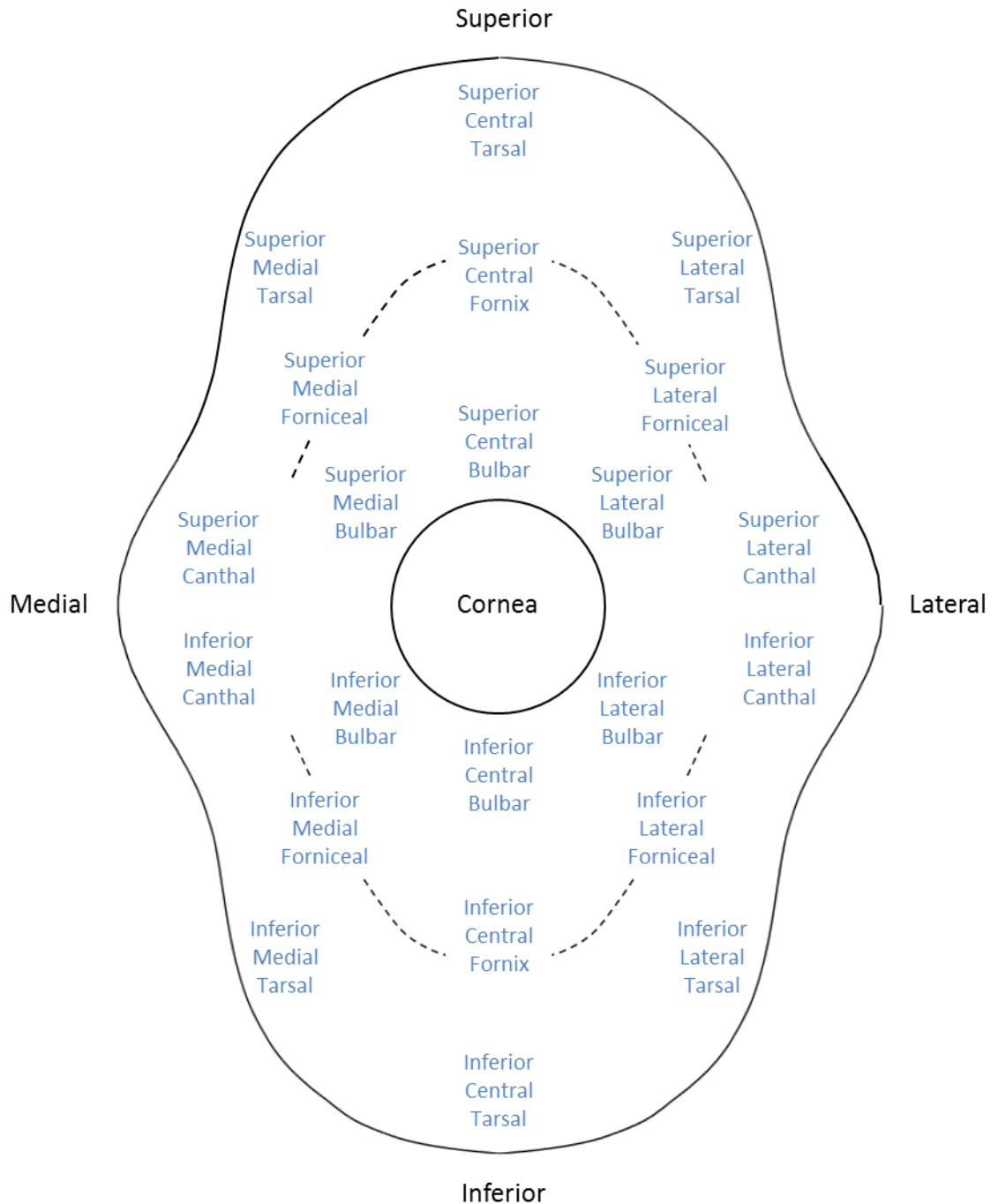


Figure 11: Schematic diagram of the whole human conjunctiva with fornices represented by dashed lines (-----), labelling the multiple areas assessed for immunohistochemical staining.

2.5. Cell Culture

All work was undertaken using an aseptic technique in a class II microbiological safety cabinet (Walker) cleaned with virkon (DuPont) and 70% ethanol. Cells were cultured in an incubator (New Brunswick) at 37°C with 5% carbon dioxide (CO₂).

2.5.1. Cell Sources

Human conjunctival epithelial cells were obtained from donors within 28 hours of death and the cells harvested (see Section 2.5.2) within 48 hours of death. Limbal tissue was obtained as outlined in Section 2.4.3. A J23T3 mouse fibroblast cell line (3T3) was kindly received from Dr. S. Ahmad (Newcastle University). The MCF7 breast carcinoma cell line was obtained from frozen supplies in the Institute of Ageing and Chronic Disease, University of Liverpool.

2.5.2. Conjunctival Epithelial Cell Harvesting and Culture

Tissue Dissection

Tissue dissecting and processing was carried out under aseptic conditions in a laminar air flow hood. Whole conjunctival specimens were washed in PBS containing 2% penicillin-streptomycin (PS) (Sigma) and 2% fungizone (Sigma) for one hour at room temperature with gentle agitation. If the cells were to be harvested the following day the tissue was then stored in CO₂ independent media (see Section 2.5.3) at +4°C overnight.

The tissue was rinsed in PBS, the underlying fat and connective tissue was carefully removed using sterile Moorfields dissecting forceps and Westcott scissors (Malosa Medical), taking care not to damage the conjunctival epithelium. The conjunctival epithelium was surgically divided using Westcott scissors into 8 approximately equal areas representing the tarsal, forniceal and bulbar areas of both superior and inferior conjunctiva, and the medial and lateral canthal areas, as shown in Figure 12. The medial and lateral canthal areas similarly comprised the closely connected bulbar, forniceal and tarsal tissue immediately adjacent to the canthi as those in

Figure 10, and were hence also termed canthal for ease of nomenclature. Various methods were then employed to harvest and culture the epithelial cells as described below.

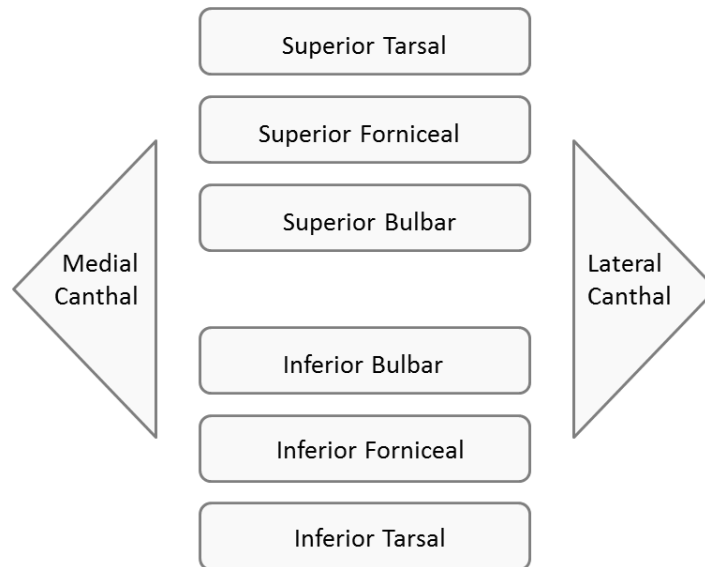


Figure 12: Schematic diagram to represent the dissection of conjunctival tissue into specific areas for cell culture comparative studies.

Trypsinisation in cloning rings

Sterile 8mm cloning rings (Millipore) were placed either directly, or with sterile high vacuum grease (Dow Corning) onto the epithelial surface of each area of the conjunctiva. 60µl of 1x trypsin EDTA (trypsin) (Sigma) was added and the tissue incubated for a selection of time periods: 1, 3, 5, 10, 15 and 20 minutes, at 37°C. The trypsin-cell solution was gently agitated by drawing and discarding with a 200µl micropipette (Thermo Scientific) and transferred into 1ml of media and centrifuged at 1000rpm/180g for 5 minutes. The supernatant was discarded and the cell pellet re-suspended, counted and seeded as per Sections 2.5.4 and 2.5.5. Remaining tissue was assessed for residual epithelial cells by fixation, paraffin embedding, sectioning and H&E staining as in Sections 2.2 and 2.3 above.

Trypsinisation of chopped whole tissue

Each area of conjunctiva was finely chopped with sterile scissors, placed in a 15ml centrifuge tube with 1ml of trypsin and incubated at 37°C for 20 minutes with gentle agitation. The trypsin-cell solution was removed and neutralised in 10ml of fresh conjunctival media. This cycle was repeated a further 3 times with fresh trypsin added to the tissue each time. The cell suspensions were pipetted up and down 50 times to disperse the cell clumps, passed through a 70µm pore cell strainer (BD Biosciences) and then centrifuged at 1000rpm/180g for 5 minutes. The supernatant was discarded and the cell pellet re-suspended, counted and seeded as per Sections 2.5.4 and 2.5.5.

Explant Culture

2 x 2mm specimens of each conjunctival area were surgically dissected and these explants were placed epithelial side up in tissue culture plates (Greiner Bio One). Sufficient media to barely cover the explants only was used for the first 3 days to encourage the explants to attach to the plates.

Explants or cell suspensions were plated onto tissue culture plates with and without an inactivated 3T3 feeder layer or Matrigel™ basement membrane matrix (BD Biosciences) (see Section 2.5.5).

2.5.3. Media Preparation

CO₂ Independent Media

CO₂ Independent Media (Invitrogen) with 1g/l glucose, 10% FCS (Biosera), 2% PS and 2% fungizone was used to store conjunctival tissue at +4°C overnight prior to cell harvesting and culture. This contains a unique phosphate-based buffering system.

Conjunctival/Limbal Epithelial Cell Media

3 parts low glucose (1g/L) DMEM with pyruvate and glutaMAX (Invitrogen) and 1 part Ham's F12 media (Invitrogen), was mixed with 10% FCS, 1% PS, 1% fungizone,

and 4-(2-hydroxyethyl)-1-piperazineethanesulfonic acid (HEPES) (Sigma) and sodium hydrogen carbonate (NaHCO_3) (BDH) to final concentrations of 20mM and 26mM respectively. Complete media for final use was made by adding transferrin (5 $\mu\text{g}/\text{ml}$) (Sigma), insulin (5 $\mu\text{g}/\text{ml}$) (Sigma), triiodothyronine (1.4ng/ml) (Sigma), adenine (12 $\mu\text{g}/\text{ml}$) (Sigma), hydrocortisone (0.4 $\mu\text{g}/\text{ml}$) (Sigma) and EGF (0.1 $\mu\text{g}/\text{ml}$) (Sigma). Complete media was used within 1 week of preparation.

J23T3 Cell Media

High glucose (4.5g/L) DMEM with glutaMAX (Invitrogen) with 10% FCS, 1% PS and 1% fungizone was used when growing 3T3 cells alone. When acting as a feeder layer with conjunctival cells, complete conjunctival media was used.

MCF7 Cell Media

Eagle's minimal essential media (MEM) with glutaMAX (Invitrogen), with 10% FCS, 1% non-essential amino acids (Invitrogen), 1% PS and 1% fungizone was used.

2.5.4. Cell Growth

Feeding

Cells were fed every 2-3 days by removing 70% of the existing media and replacing it with fresh media pre-warmed to 37°C. Some media was purposefully left as it may contain growth factors secreted by the cells. Cells were frequently inspected under a Nikon Diaphot microscope to monitor growth and detect any infection.

3T3 and MCF7 Cell Passage

When cells reached 90% confluency they were split (passaged). 3T3 and MCF7 cells were split 1:20 and 1:3 respectively. The media was removed and discarded into bleach solution; cells were washed twice with PBS and then incubated at 37°C with trypsin for 5 minutes. Having ensured the cells had detached from the tissue culture flasks by viewing under the microscope the trypsin was neutralised with 10x volume of media and the suspension centrifuged at 1000rpm/180g for 5 minutes. The supernatant was discarded and the cell pellet re-suspended in 1ml fresh media

by drawing and dispensing with a micropipette. This was diluted with an appropriate volume of media (see Section 2.5.3) into a fresh culture flask.

Cell Counting

In order to plate at specific concentrations, cell solutions were evenly suspended by repeated drawing and dispensing with a micropipette and 10 μ l pipetted onto a haemocytometer. This was viewed under the microscope and all cells counted in each of the four 1mm² corner squares of the grid. Cells touching the top and left border gridlines, but not the bottom or right borders were counted as shown in Figure 13. The average number of cells per 1mm² grid represents the number of cells x10⁴/ml.

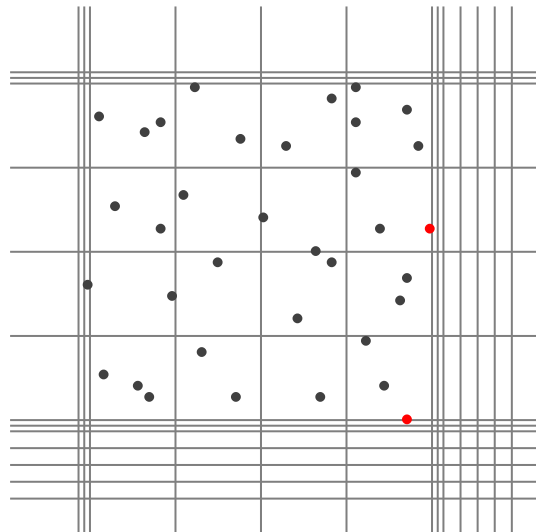


Figure 13: Schematic diagram representing the method of cell counting with a haemocytometer. View of one 1mm² corner square. All cells including those touching the top and left border gridlines are counted (black) but not those touching the bottom or right gridlines (red).

Viable cell counts were performed by gently but evenly mixing 10 μ l of cell suspension with an equal volume of 0.4% trypan blue (Sigma), allowing to stand for 2 minutes and then similarly counting the unstained (viable) rather than stained (dead) cells.

Cryopreservation

Surplus cells were kept in liquid nitrogen as stock. Following trypsinisation cells were re-suspended in media as above. 900µl of each cell suspension was transferred into a 1ml cryovial on ice and 100µl of dimethyl sulphoxide (DMSO) (Sigma) was gradually added with continuous swirling of the tube to ensure even dispersal. Cryovials were placed in an isopropanol container (Nunc) at room temperature and subjected to gradual temperature loss at a rate of approximately -1°C /minute to reach -80°C, before long-term storage in liquid nitrogen.

Cell Recovery

As viable cells must be protected from DMSO, the cryovials were thawed in a +37°C water bath and the contents immediately transferred into 20ml of warmed media. This was centrifuged at 1000rpm/180g for 5 minutes and the supernatant discarded. The cell pellet was re-suspended in fresh media and transferred into a culture flask.

2.5.5. Conjunctival Epithelial Growth

Primary conjunctival epithelial explants or cells were seeded onto tissue culture plates alone or plates pre-seeded with a 3T3 feeder layer or basement membrane matrix. Primary cells at passage zero were seeded at 15000 cells/cm². Cultures were maintained with conjunctival epithelial cell media (see Section 2.5.3).

Feeder Layer

3T3 cells were grown in 175cm² tissue culture flasks. When near confluent they were removed with trypsin (see Section 2.5.4), and re-suspended to 1x10⁷ cells/ml. In order to inactivate the cells, 50µl mitomycin C (Sigma) was added per ml of cell suspension to give a final concentration of 20µg/ml, and the suspension carefully re-suspended to ensure effective mixing. Following incubation at 37°C for 1hr with gentle agitation, the suspension was centrifuged at 1000rpm/180g for 5 minutes and the supernatant discarded. The cell pellet was washed four times with 10ml

media, and the cells seeded as a feeder layer at 1×10^5 cells/cm² as shown in Figure 14.

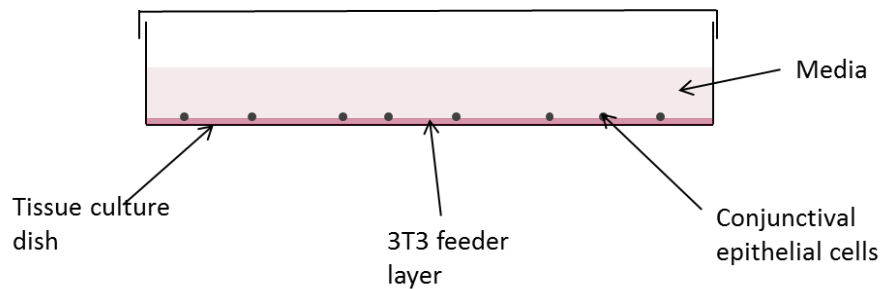


Figure 14: Schematic diagram to demonstrate conjunctival epithelial cell seeding on a feeder layer.

Matrigel™ basement membrane matrix

Tissue culture plates were coated with Matrigel™ basement membrane matrix using the thin gel method for cell growth on the surface of the gel. The matrix was thawed and mixed to homogeneity with a cooled micropipette. $50 \mu\text{l}/\text{cm}^2$ was pipetted onto culture plates on ice, and the plates incubated at 37°C for 30 minutes prior to seeding of conjunctival cells.

Conjunctival Cell Passage

Prior to confluency of the epithelial colonies, the cells were passaged. The media was removed and the cells washed with PBS before incubation with 0.02% EDTA solution (Sigma) for 30 seconds. Following vigorous pipetting over the base of the well to ensure removal of all the feeder cells the EDTA was discarded and the remaining epithelial cells incubated with trypsin for 10 minutes at 37°C . Conjunctival media was added to neutralise the trypsin and the suspension centrifuged at 1000rpm/180g for 5 minutes. The supernatant was discarded and conjunctival cells reseeded onto fresh 3T3 feeder layers at 6000 cells/cm².

Morphological Assessment

Cells were imaged regularly in phase contrast with a Nikon Diaphot microscope to qualitatively assess morphology and growth.

Limbal Epithelial Cell Growth

Limbal cells were isolated from corneo-scleral discs (see Sections 2.5.1 and 2.5.2) and cultured in the same manner to conjunctival epithelial cells (see Sections 2.5.3 and 2.5.4), for comparative CFE assays and use as immunocytochemical positive controls.

2.6. Colony Forming Efficiency Assays

In order to determine the efficiency of conjunctival cells to make colonies, CFE assays were performed at the first conjunctival cell passage.

A 6 well tissue culture plate was taken for each area of the conjunctiva and pre-seeded with a 3T3 feeder layer as above (see Section 2.5.5). Having removed the primary conjunctival cells as detailed above (see Section 2.5.5) a viable cell count was performed using trypan blue (see Section 2.5.4). Viable conjunctival cells were seeded at varying concentrations per 9.6cm^2 well of a 6 well plate (Greiner) as shown in Figure 15.

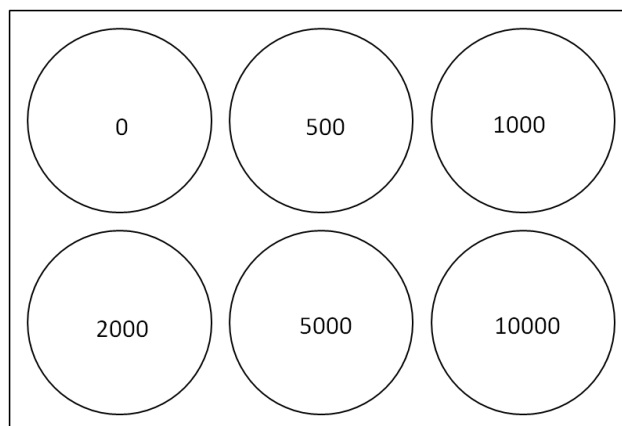


Figure 15: Schematic diagram to represent CFE assay plate, showing number of viable conjunctival cells seeded into each 9.6cm^2 well.

The cultures were treated as all others above and on the 16th day of culture, following removal the media, the cells were washed with PBS and fixed with 3.7%

NBF (Bios Europe Limited) for 10 minutes at room temperature. The NBF was discarded, and after a further wash with PBS, the cell colonies were stained with 1% Rhodamine B (Sigma) in methanol (Fisher Scientific) for 10 minutes at room temperature. Colonies were counted and the CFE calculated using the formula:
Number of colonies formed / number of cells plated x 100.

CFE assays were similarly performed on limbal epithelial cells at the first passage for comparative analysis.

2.6.1. Presentation of Results

Images and grading scales from all areas were compared and presented on a schematic diagram of the whole conjunctiva as labelled in Figure 16.

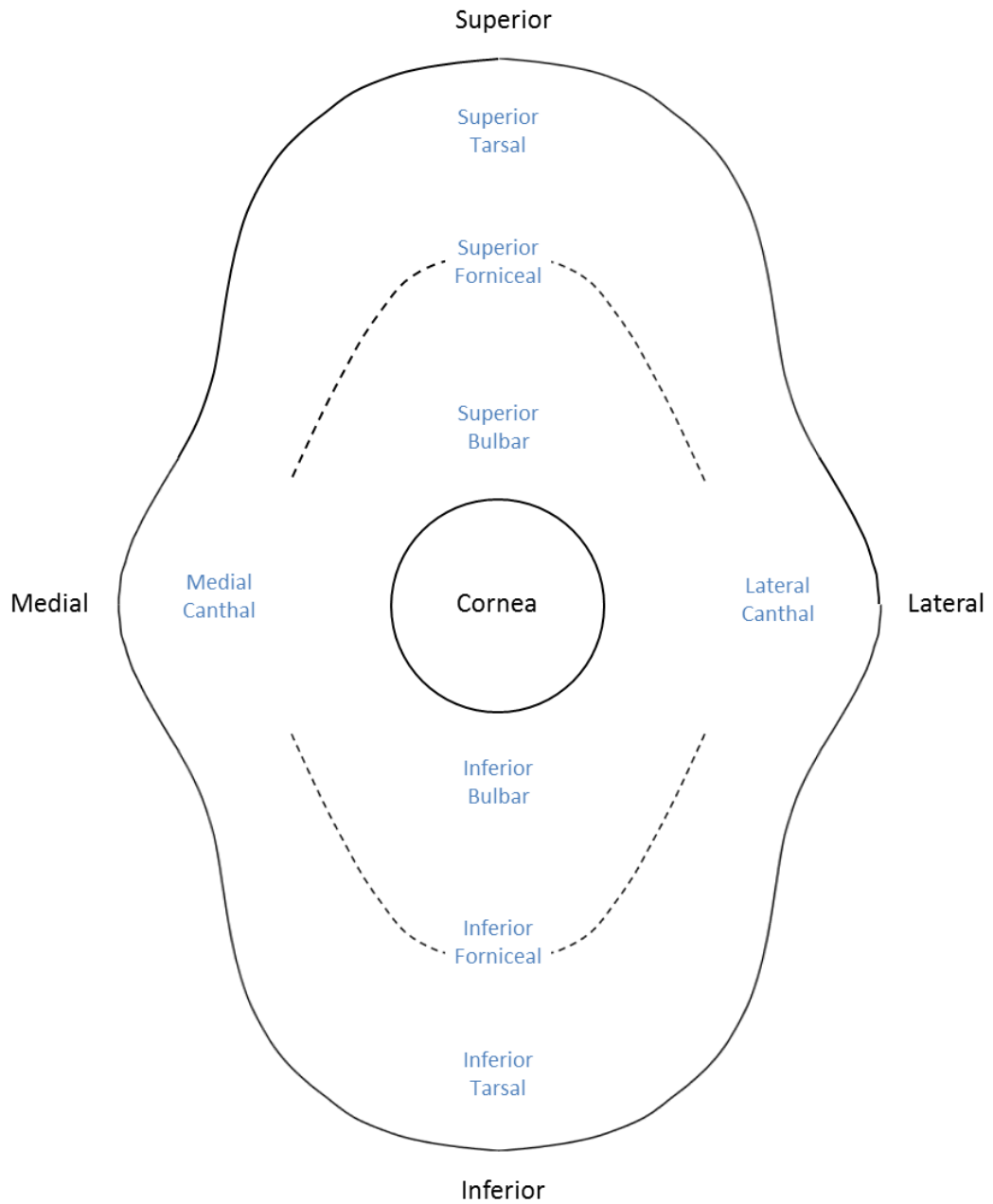


Figure 16: Schematic diagram of the whole human conjunctiva with fornices represented by dashed lines (----), labelling the multiple areas assessed for colony forming efficiency assays and immunocytochemical staining.

2.7. Immunocytochemical Studies

2.7.1. Cell Growth and Fixation

Conjunctival epithelial cells were equivalently also cultured in 8 well permanox™ plastic labteks (VWR) at passage 1 to enable immunocytochemical staining for SC markers. MCF7 and limbal cells were similarly cultured for antibody optimisation and positive controls, and 3T3 cells alone as negative controls.

At day 9, upon near confluency cells were washed twice with PBS and fixed with 100% methanol at -20°C for 10 minutes, air dried and stored at -80°C.

2.7.2. Antibody Staining

Antibodies shown in Table 3 were optimised. In addition to the SC and TAC markers assessed in fixed tissue (Table 1) an additional antibody to ABCG2 was assessed in an attempt to seek more optimal staining, as well as antibodies to N-Cadherin and Hsp70. Time constraints prevented assessment of the latter two antibodies in fixed tissue.

Cells were permeabilised and blocked together with 0.1% tween (Sigma), 1% Bovine Serum Albumin (BSA) (Sigma), and 10% goat serum for 1 hour at room temperature. They were then incubated with the primary antibodies at varying concentrations in 1% goat serum for 1 hour at room temperature. Following 3 washes with PBS they were incubated with the secondary antibody Alexafluor 488 goat-anti-mouse (Invitrogen) or Alexafluor 488 goat-anti-rabbit (Invitrogen) as appropriate, 1:250 in PBS for 1 hour at room temperature. Further PBS washes were undertaken before and after secondary staining for 10 minutes with 1% propidium iodide (PI) (Sigma) in 10% RNase (Sigma). The gasket was removed, slides mounted with aqueous fluorescent mountant (Dako) and imaged on a Polyvar microscope (Reichert Jung).

MCF7 or limbal cells were used as a positive controls, and conjunctival cells with 1% goat serum alone in place of the primary antibody as a negative control.

Antibody	Clone	Source
CK19	RCK108	Dako
ABCG2 (anti-BRCP)	21	Chemicon
ABCG2 (anti-BRCP)	MM0047-2J39	Abcam
p63	Δ N	Biolegend
p63	4A4	Dako
N-Cadherin	3B9	Life Technologies
Hsp70	BRM-22	Abcam
CD168	2D6	Abcam

Table 3: Table of antibodies used for immunocytochemical studies with clone and source.

2.7.3. Quantitative analysis

Expression of immunocytochemical markers was graded quantitatively by the number of positively staining cells per average of 5 x20 random fields of view with a grading scale of 0 cells: -, <5 cells: +/-, 5-10 cells: +, 10-15 cells: ++, 15-20 cells: +++, and >20 cells: ++++.

2.7.4. Presentation of Results

Images and grading scales from all areas were compared and presented on a schematic diagram of the whole conjunctiva as labelled in Figure 16.

2.8. Conjunctival Cell Growth on Extracellular Matrix Proteins

In order to optimise conjunctival epithelial cell adhesion and growth the effect of pre-coating tissue culture plastic with laminin 1, collagen IV or fibronectin was established.

2.8.1. Extracellular Matrix Protein Coatings

Extracellular matrix proteins were defrosted at +4°C for 15 minutes, diluted appropriately and coated on to pre-chilled 24 well tissue culture plastic plates.

Collagen IV

Mouse collagen IV (R&D Systems) was diluted in cold sterile deionised water to a concentration of 5µg/ml. 150µl per cm² was spread completely over the base of each well and allowed to absorb for 2 hours at room temperature. The excess protein solution was then aspirated, PBS added and the plates stored for up to one week at +4°C prior to use.

Fibronectin

Bovine fibronectin (R&D Systems) was diluted in cold serum-free DMEM to a concentration of 5µg/ml. Great care was taken not to aspirate or swirl the solution. 150µl per cm² was spread completely over the base of each well and allowed to absorb overnight at +4°C before the excess solution was removed. The wells were rinsed with PBS before storing airtight at +4°C for up to 1 week.

Laminin 1

Mouse laminin 1 (R&D Systems) was diluted in cold serum-free DMEM to a concentration of 10µg/ml. 150µl per cm² was spread completely over the base of each well and allowed to absorb for 1 hour at 37°C before the excess solution was removed and the plates allowed to air dry at room temperature. Plates were stored airtight at -20°C for up to 1 week.

All coated plates were rinsed with sterile culture media immediately prior to use.

2.8.2. Cell Seeding

Primary conjunctival cells were seeded on the coated plates at 15000 cells/cm² and maintained in the standard manner as above (see Section 2.5.4). Cells were similarly seeded at the same concentrations onto a 3T3 feeder layer in the standard manner as a control. Experiments were carried out in triplicate for each matrix protein / control at each time point.

2.8.3. Assessment of Cell Growth

Cell Morphology

Cell morphology on each coating / control was assessed qualitatively by phase contrast imaging on a Nikon Diaphot microscope at day 2, 4, 7, 10 and 14.

Cell Adhesion and Growth

At the same time points cells were fixed with 3.7% NBF as in Section 2.7.1 and stained for 10 minutes with 1% PI in 10% RNase. The control plates cultured on 3T3 feeder layers were additionally stained with CK19 as per Section 2.7.2. The cells were viewed on a Nikon Diaphot fluorescent microscope and 3 images taken (one centrally and two randomly placed) of each well at x10 magnification. Nuclei were counted and averaged for each well. Only nuclei of cells staining positive for CK19 were counted in the control plates. Growth curves for each coating were then determined.

2.9. Statistical Methods

Microsoft Excel 2007 (Microsoft) and SPSS Statistics 20 (SPSS) programs were used for statistical analysis. For all statistical tests $p < 0.05$ was considered significant ($\alpha = 5\%$).

As the variability of immunohistochemical staining, CFE and immunocytochemical staining across different areas of all conjunctival specimens and cell cultures could not be assumed to be of normal distribution, non-parametric statistical tests were

employed. Given the dependency of results across each tissue to each other, analysis was performed with a Friedman test, and *post-hoc* analysis with a Wilcoxon signed rank test, both of which take these factors into account. Bonferroni corrections were made to account for multiple tests.

The correlation between immunocytochemical staining for different markers and between these, CFE and immunohistochemical staining were each assessed with a Kendall's Tau correlation coefficient. This is a measure of rank correlation between two measured quantities.

The effect and interaction of donor age and PMRT on immunohistochemical staining, CFE and immunocytochemical staining was assessed with a generalised linear mixed model. This model is a flexible generalisation of ordinary linear regression that allows for response variables with non-parametric error distribution and both fixed and random linear prediction.

In contrast, the effect of cell seeding number on CFE measurements and the comparison of conjunctival epithelial cell growth on different extracellular matrix proteins could be assumed to be parametric and independent data. These were therefore analysed using a one-way analysis of variance (one-way ANOVA) test. This technique compares the mean of multiple samples, and is considered robust given normal data distribution and independency. *Post-hoc* analysis of cell growth on extracellular matrix proteins was analysed using a Student's paired *t*-test, which compares the sample and hypothesised means in parametric data.

3. Results

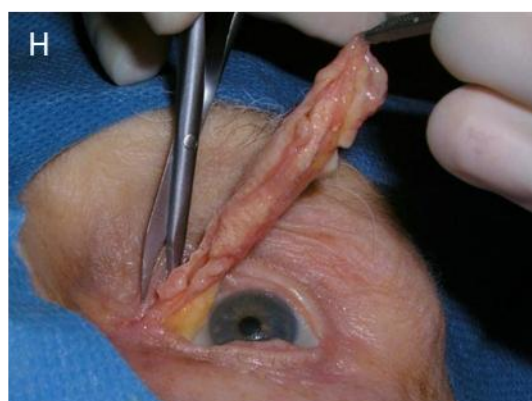
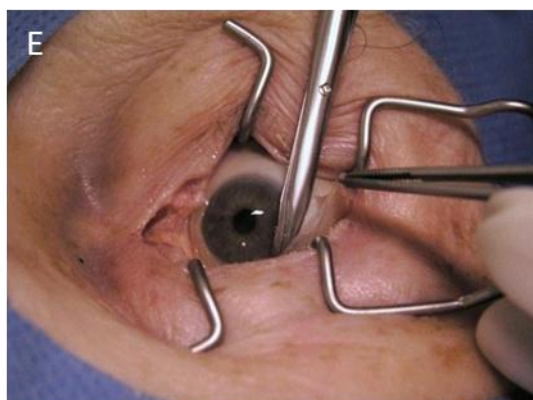
3.1. Conjunctival Retrieval

3.1.1. Surgical Retrieval Technique

A technique was developed to successfully excise whole human cadaveric conjunctiva. This was performed within 28 hours of death. The eyes and surrounding tissue were cleaned with sterile water followed by a 5% (w/v) solution of povidone iodine (Moorfields Pharmaceuticals). The surgical technique is demonstrated in Figure 17 and Figure 18. Using an aseptic technique, both eyelids were split medially to laterally along the grey line using a number 15 scalpel blade (Swann Morton) and Moorfields forceps (Malosa Medical). The dissection was continued back along this surgical plane until beyond the level of the fornices (Figure 17A-C, Figure 18). Great care was taken not to touch or handle the conjunctiva with any instruments as histological analysis of initial samples revealed corresponding tarsal epithelial loss as shown in Figure 19. Traction sutures and adhesive strips were employed to assist dissection at this stage but not found to be of benefit. The medial and lateral canthal areas were similarly dissected to adjoin the upper and lower eyelid dissections (Figure 17D). A speculum (Malosa Medical) was used to maintain the eyelids in an open position and a 360° limbal peritomy was then performed with Westcott scissors (Malosa Medical) as close to the limbus as possible, followed by a full blunt dissection below Tenon's capsule in the episcleral space around the surface of the globe. This dissection was similarly continued until past the level of the fornices (Figure 17E-F, Figure 18). These two natural surgical planes do not meet, and thus the fatty tissue and Tenon's capsule behind the conjunctiva was then divided until the anterior and posterior planes met, as demonstrated in Figure 18. It was found that it was easier to perform this dissection from the anterior plane using scissors to cut down onto the globe taking care to do so beyond the fornices so as not to breach the conjunctiva (Figure 17G). This was completed circumferentially allowing the conjunctiva to be excised as a

whole specimen as shown in Figure 17H and Figure 20. Tissue was placed in sterile media for transportation. Single-use disposable instruments were used throughout the procedure in accordance with the standards for eye retrieval for transplantation and research (The Royal College of Ophthalmologists, 2008, UK Blood Transfusion and Tissue Transplantation Services, 2013).

Following retrieval of the conjunctiva, the eyes were then retrieved for transplantation and/or research purposes in the standard manner (The Royal College of Ophthalmologists, 2008, UK Blood Transfusion and Tissue Transplantation Services, 2013). No trauma to any eyes was noted. Eye sockets were reconstructed using wet cotton wool and plastic eye shields (Figure 17I) which hold the eyelids in a closed position in accordance with the guidance standards of The Royal College of Ophthalmologists (The Royal College of Ophthalmologists, 2008) producing good aesthetic results (Figure 17J).



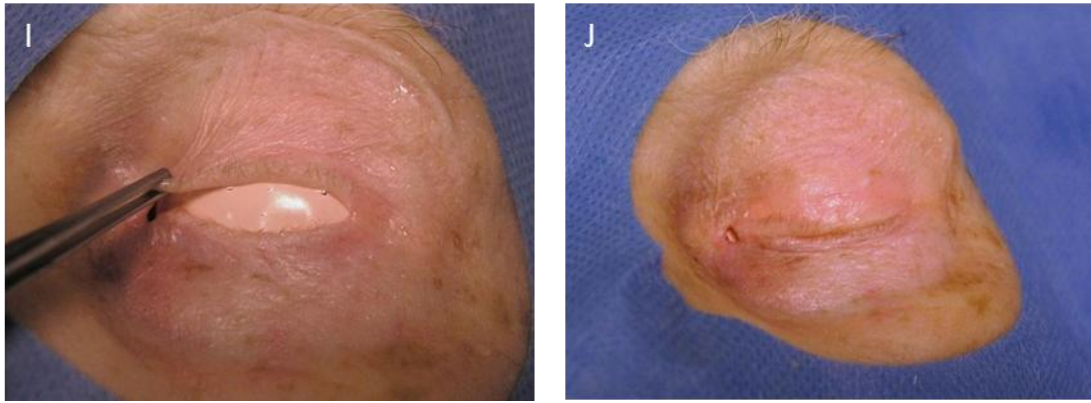


Figure 17: Images of the surgical technique for retrieval of whole human cadaveric conjunctiva: A) a grey line eyelid split is made with a scalpel blade, B) the incision is extended posteriorly C) and deep to the fornices. D) The incision is adjoined to an equivalent lower eyelid incision at both canthi. E) A full 360° limbal peritomy is made with scissors and F) a deep blunt sub-Tenon's dissection is performed. G) The fatty tissue and Tenon's capsule posterior to the fornices is divided to enable H) whole conjunctival excision. I) Eye sockets are reconstructed with cotton wool and eye shields to produce J) good aesthetic reconstruction.

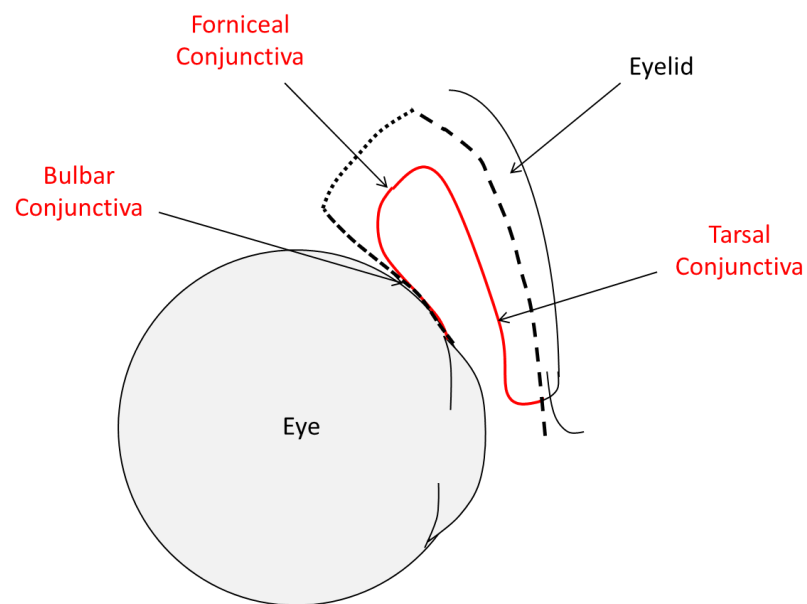


Figure 18: Schematic diagram to demonstrate the surgical technique for conjunctival retrieval in the sagittal plane. The eyelids are split anteriorly-posteriorly commencing at the grey line alongside the tarsal plates and deep past the fornices (---), a 360° limbal peritomy is performed with full deep sub-Tenon's blunt dissection (.....), and the fatty tissue between the two surgical planes divided (-·-·-).

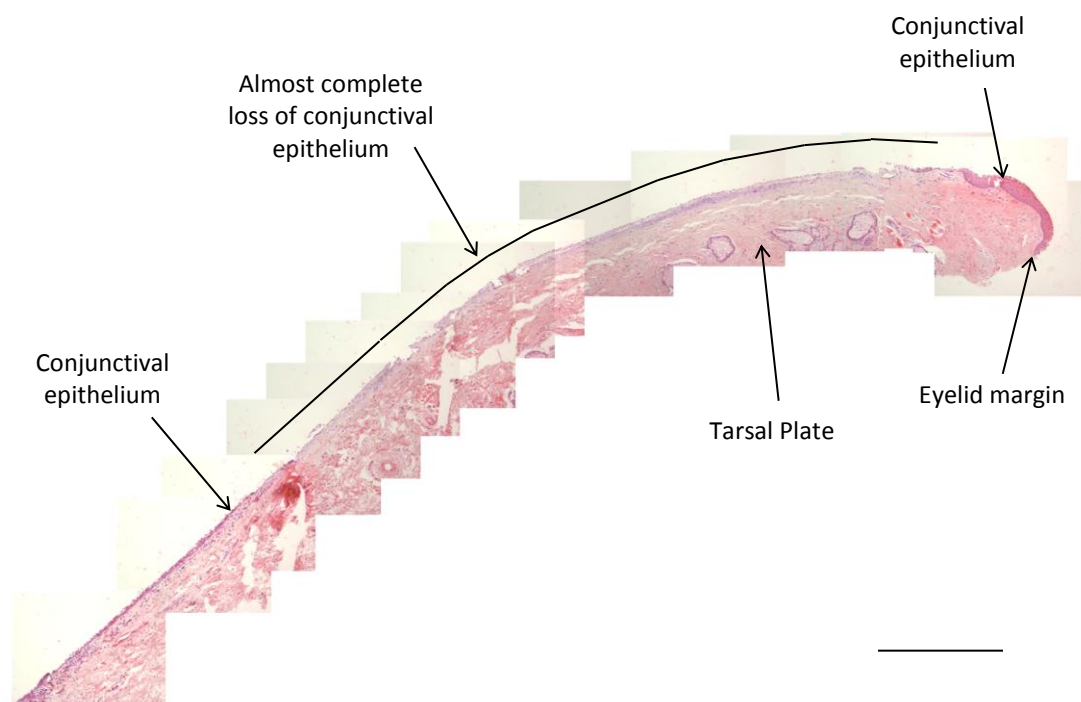


Figure 19: Section of human conjunctival tissue from the upper eyelid demonstrating loss of tarsal conjunctiva due to instrument damage in retrieval process (H&E stain). Photomicrographs stitched together manually in Microsoft PowerPoint. Scale bar 1mm

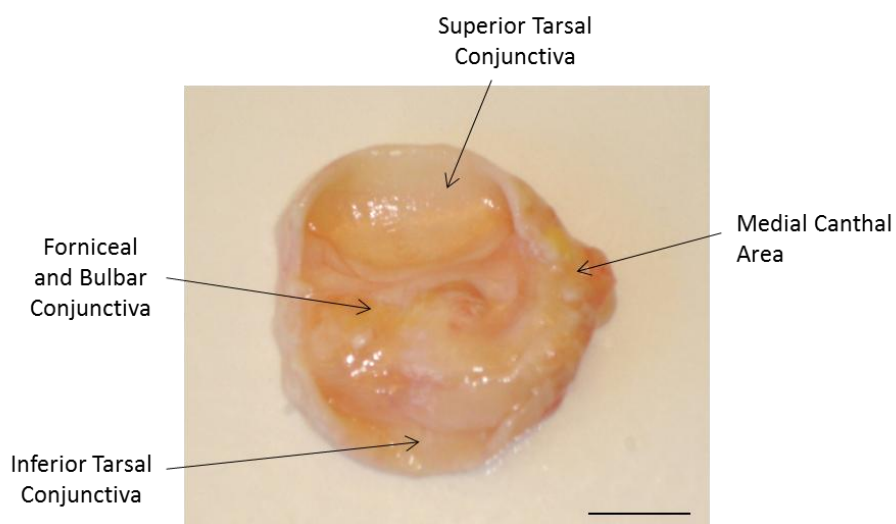


Figure 20: Image of whole human cadaveric conjunctival specimen with eyelids everted such that the tarsal epithelium is visible. Scale bar 1cm.

3.1.2. Tissue Retrieved

Conjunctiva was retrieved from 18 donors in total, giving 36 whole conjunctival specimens. These included 5 male and 13 female donors, aged 22-93 (mean 75.4, median 80.5) years; all of which were Caucasian. The PMRTs varied from 8.5-27.5 (mean 20.9, median 22) hours. The donor demographics, causes of death and PMRTs are detailed in as detailed in Table 4. Initial specimens were used to develop and optimise tissue retrieval, tissue fixation and embedding, and cell harvesting and culture techniques.

Limbal tissue was obtained from 3 Caucasian donors: 2 male and 1 female, aged 57-74 (mean 63.3, median 68) years.

Donor Age (Years)	Donor Sex	Cause of Death	Tissue Number	Post mortem Retrieval Time (Hours)
70	Male	Pneumonia	01	19.5
			02	20.5
65	Male	CVA	03	23.5
			04	25.0
79	Female	CVA	05	22.0
			06	23.5
62	Female	Multi-organ failure	07	25.5
			08	26.0
93	Female	CVA	09	18.5
			10	19.0
57	Female	Pneumonia	11	27.5
			12	28.0
85	Female	Renal failure	13	26.0
			14	26.5
92	Female	Gastroenteritis	15	17.0
			16	17.5
76	Female	Cardiac failure	17	18.0
			18	18.5
85	Male	Myocardial infarction	19	9.0
			20	8.5
82	Female	Bowel ischaemia	21	25.0
			22	25.5
22	Male	Multi-organ failure	23	24.0
			24	24.5
84	Female	Pneumonia	25	21.5
			26	22.0
90	Female	Renal failure	27	15.75
			28	16.25

68	Female	Gastric haemorrhage	29	24.0
			30	24.5
89	Female	Gastroenteritis	31	23.5
			32	24.0
82	Male	Pneumonia	33	16.5
			34	16.5
76	Female	Carcinomatosis	35	15.5
			36	16.0

Table 4: Table showing donor demographics, cause of death and PMRTs of conjunctival tissue retrieved. (CVA = Cerebrovascular Accident).

3.2. Tissue Histology

H&E staining of superior and inferior specimens demonstrated continuous sections of conjunctival tissue extending from bulbar through forniceal to tarsal conjunctiva. An example of which is demonstrated in Figure 21. Similar sections of canthal tissue demonstrated complete sections of conjunctival tissue.

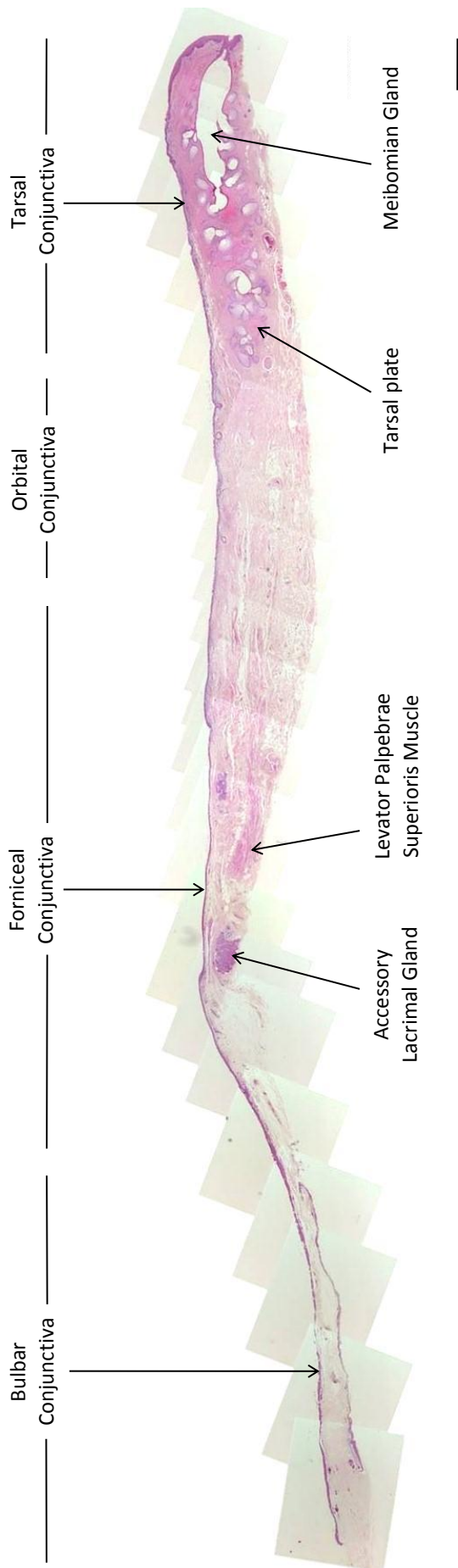


Figure 21: Whole section of human conjunctival tissue from the upper eyelid demonstrating normal anatomy and intact conjunctival epithelium from the bulbar through forniceal area to tarsal conjunctiva (H&E stain). Photomicrographs stitched together manually in Microsoft PowerPoint. Scale bar 1mm.

3.3. Immunohistochemical Studies

3.3.1. Antibody Optimisation

Antibodies for immunohistochemical studies were optimised by comparing both different antigen retrieval techniques and different antibody dilutions using positive control tissue. Optimal staining was assessed taking into account both staining intensity, minimal background staining and in the case of heat-induced antigen retrieval, significant loss of tissue from the slides with increasing antigen retrieval time. An example of antibody optimisation results for ABCG2 is shown in Figure 22. The final protocols used for each antibody are shown in Table 5.

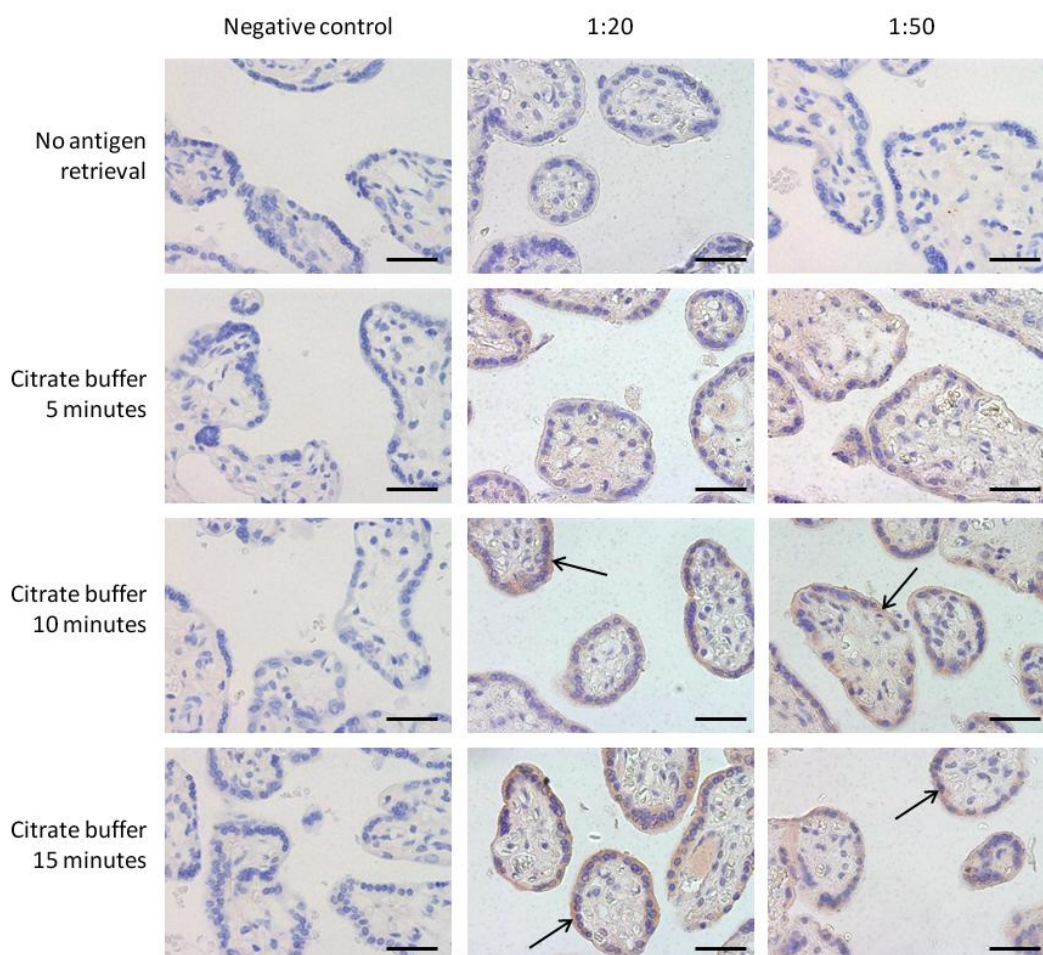


Figure 22: Photomicrographs of immunohistochemical antibody optimisation for ABCG2 using placental tissue, varying times of citrate buffer antigen retrieval and varying antibody dilutions. Positive immunoreactivity in brown is observed throughout the cytoplasm (arrows), with haematoxylin counter-staining in blue. Scale bars 50 μ m. In this case, optimal staining balanced against minimal tissue loss during antigen retrieval was achieved with 10 minutes of citrate buffer and 1:20 antibody dilution, and was used as a final protocol.

Antibody	Clone	Source	Antigen Retrieval	Antibody Dilution	Secondary Antibody*
CK19	RCK108	Dako	Target Retrieval	1:100	Anti-mouse
ABCG2	21	Chemicon	Citrate 10m 100°C	1:20	Anti-mouse
p63	4A4	Dako	None	1:50	Anti-mouse
Pan-CK	MNF116	Dako	None	1:100	Anti-mouse
Pan-CK	AE1/AE3	Dako	Trypsin 30m 37°C	1:200	Anti-mouse
Melan-A	A103	Dako	Target Retrieval	1:100	Anti-mouse
S-100	polyclonal	Dako	Citrate 10m 100°C	1:1000	Anti-rabbit

Table 5: Table of optimised immunohistochemical protocols for different antibodies used.
*Secondary antibody is HRP anti-mouse or anti-rabbit.

Despite numerous attempts at optimisation on limbal positive control samples no clear positive immunohistochemical staining was obtained with pan-CK Lu5, Δ Np63 or CD168 antibodies. These antibodies were therefore not used in any further immunohistochemical analyses.

3.3.2. Grading of Immunohistochemical Staining

Immunohistochemical staining was graded semi-qualitatively as described in Section 2.4.4. Examples of staining images for each grading system are demonstrated in Figure 23 and Table 6.

Equivalent staining was demonstrated across all positive and negative control samples from different experiment runs for each antibody; thus enabling direct comparisons to be made across samples from all tissues.

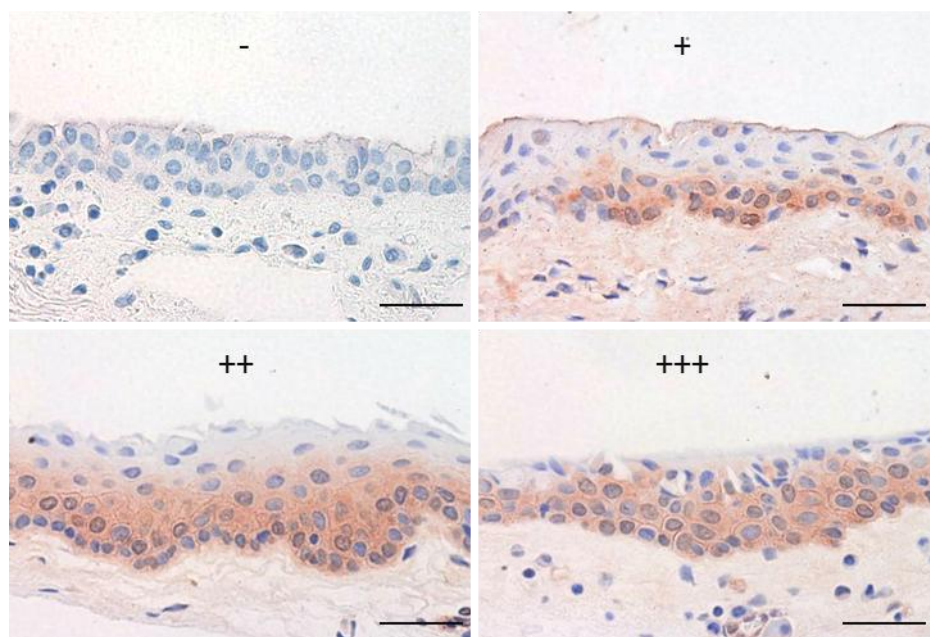


Figure 23: Figure to demonstrate the first immunoreactivity grading scale employed (the proportion of positively staining cells per image: 0 cells: -, $\leq 1/3$ cells: +, $1/3-2/3$ cells: ++, $\geq 2/3$ cells: +++). Photomicrographs showing positive ABCG2 immunoreactivity in brown, with haematoxylin counter staining in blue. Scale bars 50 μ m.

Proportion of positively staining cells	Staining Intensity			
	None	Mild	Moderate	Intense
0	N/A	N/A	N/A	N/A
≤ 1/3	N/A	+/-	+	++
1/3 – 2/3	N/A	+	++	+++
≥ 2/3	N/A	++	+++	++++

Table 6: Table to demonstrate the second immunohistochemical immunoreactivity grading scale by both proportion of and intensity of positively staining cells in an area. Photomicrographs demonstrating positive ABCG2 immunoreactivity in brown, with haematoxylin counter-staining in blue. Scale bars 50µm. N/A = not applicable.

3.3.3. Cytokeratin 19 Staining

Immunohistochemical staining for CK19 confirmed the presence of conjunctival epithelium in all samples. An example of which is shown in Figure 24. CK19 expression would not be expected in goblet cells, but it was not possible to accurately exclude this in these studies as the goblet cell bodies underlying the large secretory component of the cells are usually not easily detectable.

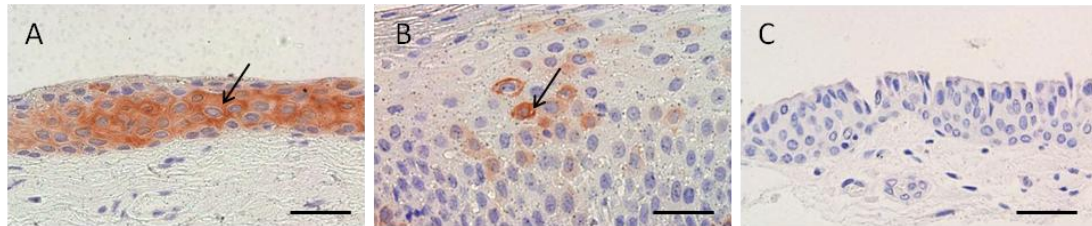


Figure 24: Photomicrographs of immunohistochemical staining for CK19. Positive immunoreactivity in brown is observed throughout the cytoplasm (arrows), with haematoxylin counter-staining in blue. A) Immunoreactivity is demonstrated throughout most layers of the conjunctival epithelium, B) tonsillar tissue positive control, C) negative control. Scale bars 50µm.

3.3.4. Further Immunohistochemical Staining

Further immunohistochemical staining for ABCG2, p63 and pan-CK MNF116 and AE1/AE3 antibodies were assessed across all tissue sections as described in Figure 10. This enabled analysis of the multiple comparison sites labelled in Figure 11. Data for each of these is presented in Section 3.3.5 to Section 3.3.8, with sample images from one donor tissue (tissue 26) presented on a schematic diagram of the conjunctiva for both ABCG2 and p63.

3.3.5. ABCG2 Staining

ABCG2 staining was demonstrated across the conjunctiva in the basal epithelium. Staining was noted not only at the cell membranes but also frequently throughout the cytoplasm as shown in Figure 25. ABCG2 expression would not be expected in goblet cells, but as noted above it was not possible to accurately exclude this in these studies as the goblet cell bodies underlying the large secretory component of the cells are usually not easily detectable (**Figure 26**).

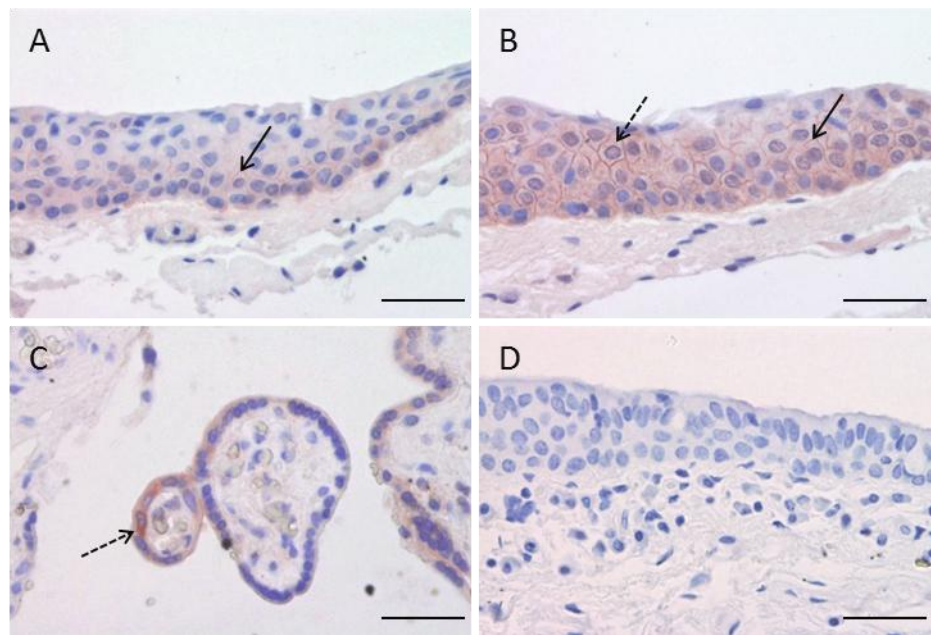


Figure 25: Photomicrographs of immunohistochemical staining for ABCG2 in the bulbar-forniceal conjunctival epithelium. Positive immunoreactivity in brown is observed both at the cell membrane (black arrows) and throughout the cytoplasm (dashed arrows), with haematoxylin counter-staining in blue. A) and B) Immunoreactivity is demonstrated to varying levels in the conjunctival epithelium, C) placental positive control and D) negative control. Scale bars 50µm.

Staining across sections from 10 donors was compared. Highest levels of staining were seen in the medial canthal and forniceal areas, especially inferiorly. In these areas staining was demonstrated in the majority of epithelial cells, but most intense basally, with often only the superficial epithelial layers spared. Lowest levels of staining were demonstrated in the tarsal conjunctival epithelium, hence a pattern of more intense staining in the forniceal than bulbar than tarsal areas was noted, as shown in Figure 26.

These patterns were consistently demonstrated across each donor tissue. An example of the pattern of staining across the whole conjunctiva from one donor is demonstrated in Figure 27. The overall gradings averaged from all donors are demonstrated on schematic diagrams using both grading scales (see Section 2.4.4). Gradings from scale 1 are shown in **Figure 28**, and from scale 2 in **Figure 29**. The overview of comparative sites compared in these diagrams is labelled in Figure 11.

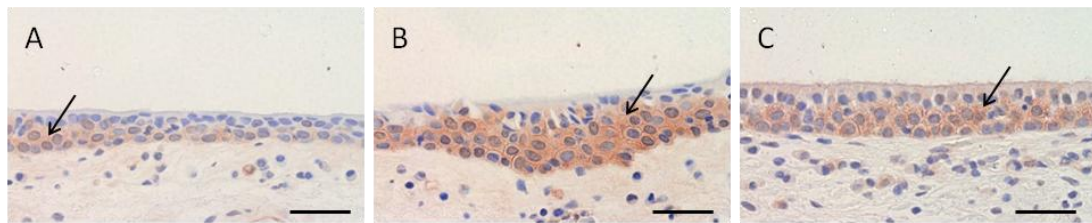


Figure 26: Photomicrographs of immunohistochemical staining for ABCG2 across the conjunctiva. Positive immunoreactivity in brown is observed both at the cell membranes and throughout the cytoplasm (arrows), with haematoxylin counter-staining in blue. Mild immunoreactivity is observed in A) tarsal, intense staining in B) forniceal and moderate staining in C) bulbar areas. Scale bars 50 μ m.

Although similar patterns of grading were demonstrated from each grading scale (**Figure 28** and **Figure 29**); scale 2 (**Figure 29**), in also taking into account the intensity of staining, revealed greater variation across the tissue as a whole. Non-parametric Friedman tests were employed demonstrating significant variation in staining across the whole tissue using either grading scale ($p < 0.01$ for each). The areas with overall highest staining grades (+++) using scale 2 (**Figure 29**) were located in a region comprising the medial canthal area and inferior medial and inferior central fornix. *Post-hoc* analysis of data using either grading scale confirmed significant increased staining in this region compared to the rest of the tissue using a Wilcoxon signed ranks test ($p < 0.01$ for each). Greater staining was also shown in the fornices than bulbar than tarsal areas, and this pattern was replicated in both superior and inferior conjunctiva, with greater staining in inferior compared to superior areas.

Given that intensity of marker expression cannot necessarily be assumed to have a linear correlation to the level of antigen present, immunohistochemical grading scale 1 (taking into account solely the proportion of positively staining cells) was used for further ABCG2 analysis from hereon.

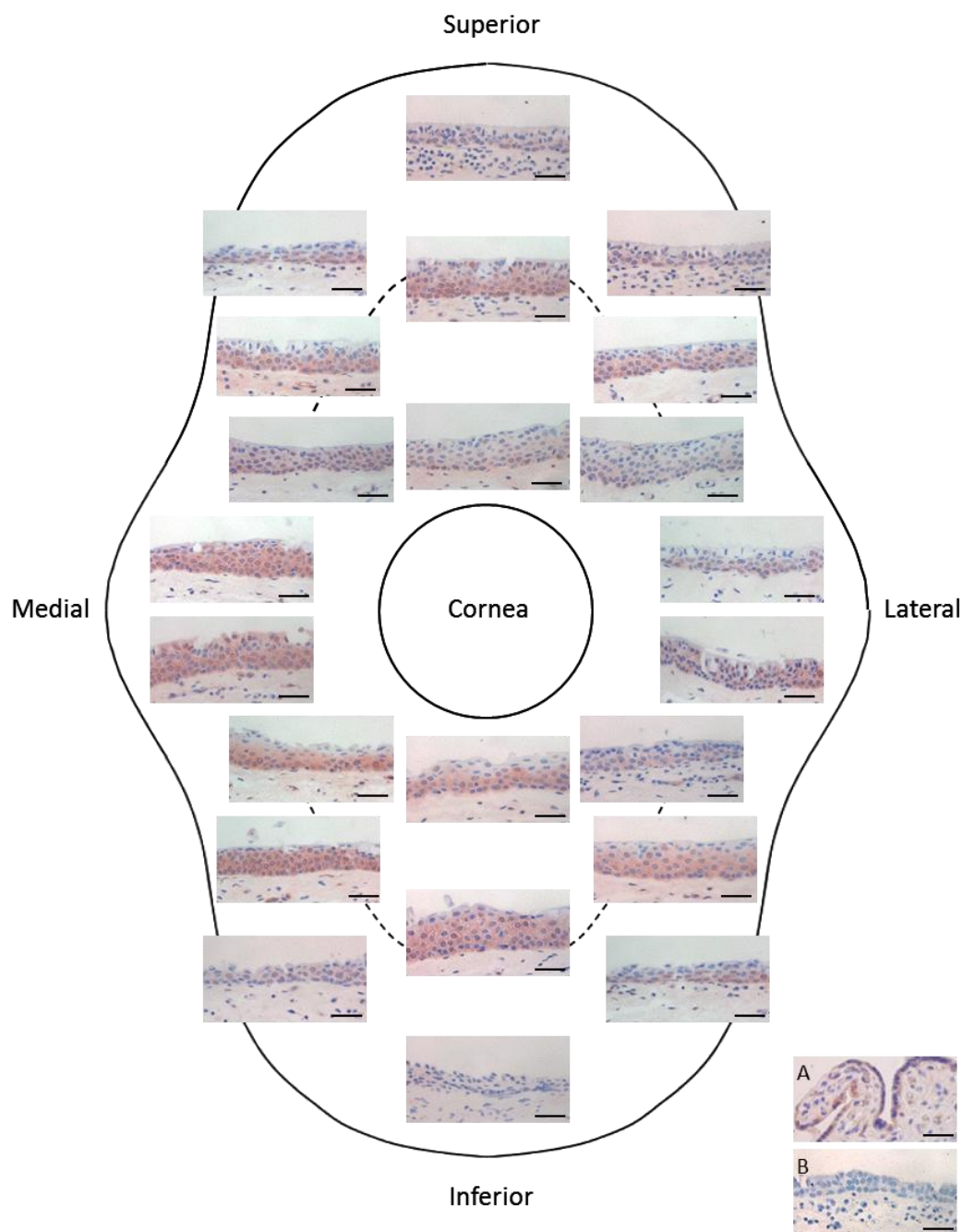


Figure 27: Schematic diagram of the human conjunctiva (as labelled in Figure 11) with fornices represented by dashed lines (----), demonstrating photomicrographs of immunohistochemical staining for ABCG2 across all areas of the conjunctiva from one donor (tissue 26). Positive immunoreactivity in brown is observed both at the cell membranes and throughout the cytoplasm, predominantly in the basal layers of the epithelium. In this example, immunoreactivity is observed most intensely in the medial canthal and forniceal areas. Haematoxylin counter-staining in blue. A) Placental positive control, B) negative control. Scale bars 50µm.

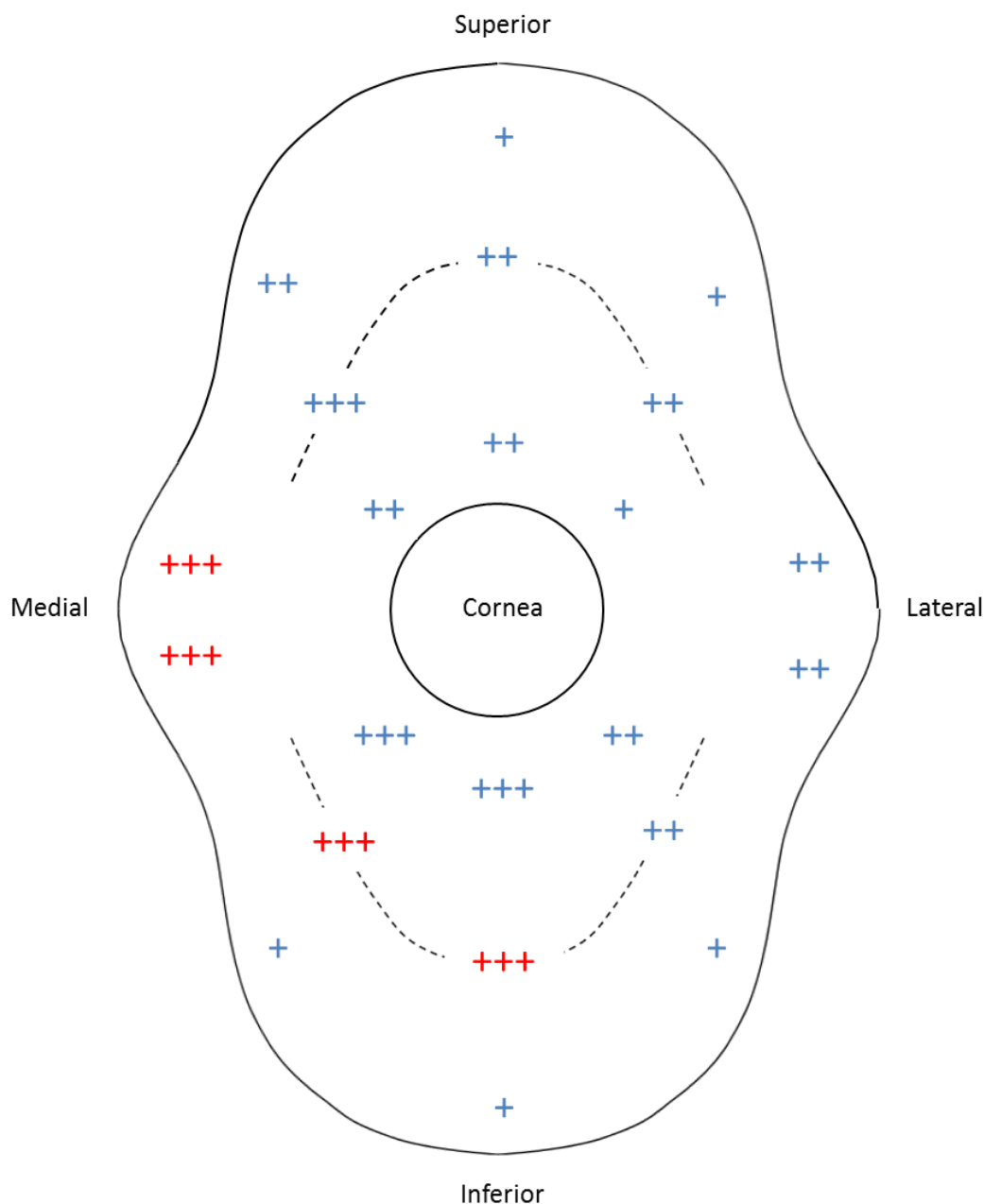


Figure 28: Schematic diagram of the human conjunctiva (as labelled in Figure 11) with fornices represented by dashed lines (-----), demonstrating average grades of immunohistochemical reactivity for ABCG2 using grading scale 1 (Figure 23) by proportion of immunoreactive cells, across all areas of the conjunctiva from all 10 donors. Highest grades of staining are observed in the medial canthal, inferior medial and inferior central forniceal areas (red) compared to other areas ($p < 0.01$).

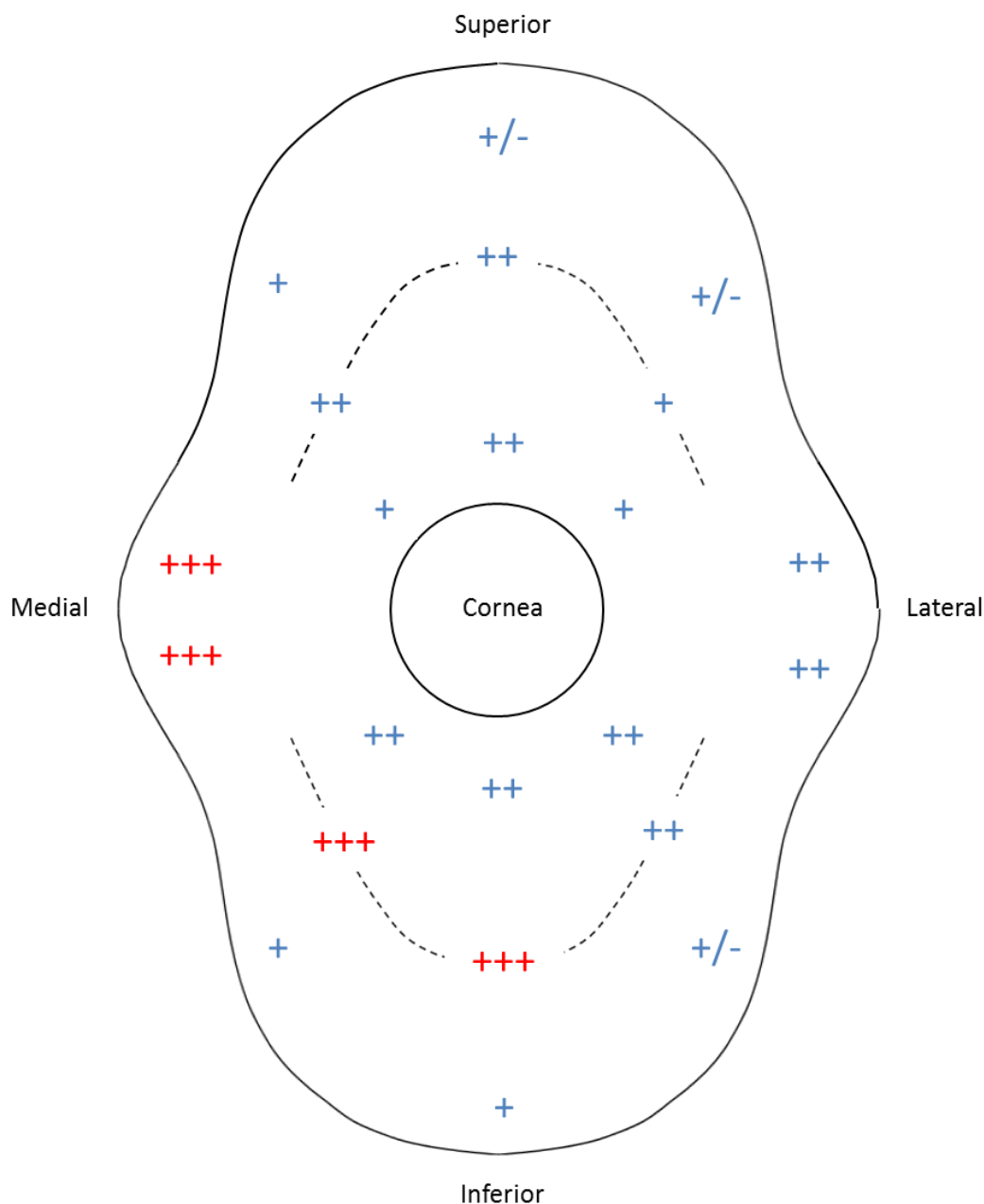


Figure 29: Schematic diagram of the human conjunctiva (as labelled in Figure 11) with fornices represented by dashed lines (-----), demonstrating average grades of immunohistochemical reactivity for ABCG2 using grading scale 2 (Table 6) by proportion and intensity of immunoreactive cells, across all areas of the conjunctiva from all 10 donors. Highest grades of staining are observed in the medial canthal, inferior medial and inferior central forniceal areas (red) compared to other areas ($p < 0.01$).

Although the areas of most intense ABCG2 staining within the conjunctival epithelium are also rich in goblet cells (Kessing, 1968), no correlation was noted between direct proximity of ABCG2 positively staining cells to goblet cells. Indeed varying intensity of ABCG2 staining was observed in close proximity to clusters of multiple goblet cells, with no clear pattern to different areas of the tissue as shown in Figure 30.

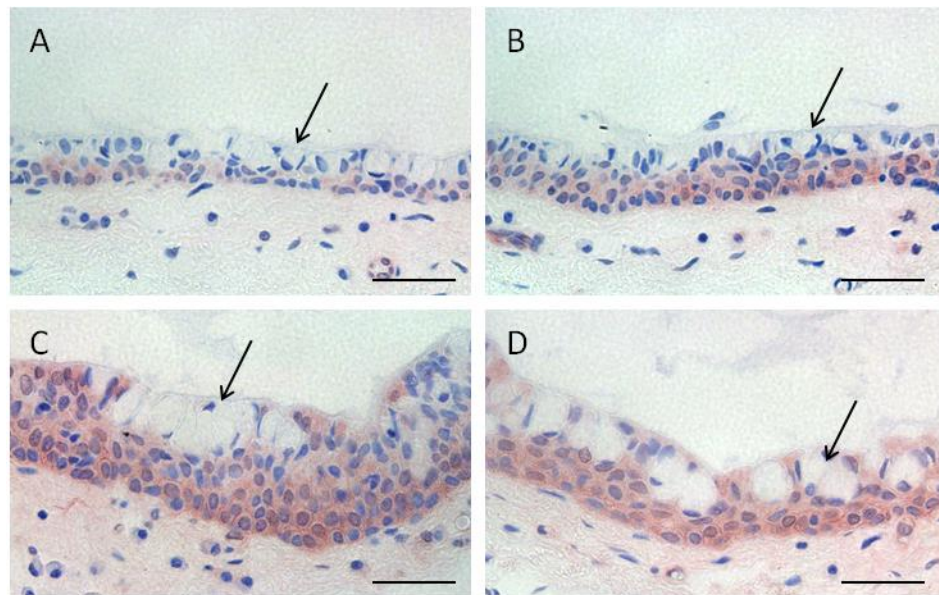


Figure 30: Photomicrographs of immunohistochemical staining for ABCG2 in the conjunctiva in proximity to clusters of goblet cells (arrows). Positive immunoreactivity in brown varies from A) light to D) intense, with haematoxylin counter-staining in blue. A) Tarsal conjunctiva, B) tarsal-forniceal conjunctiva, C) medial canthal conjunctiva and D) forniceal conjunctiva. Scale bars 50 μ m.

3.3.6. p63 Staining

p63 staining was similarly demonstrated across the conjunctiva in the basal layers of the epithelium (**Figure 31**). Staining across sections from only 2 donors was compared due to the manufacturers discontinuing the antibody and no suitable substitute being traced. Staining was solely nuclear, but the distribution across the tissue demonstrated similar patterns to that seen for ABCG2 (Figure 27, **Figure 28** and Figure 29), with highest levels of staining seen in the medial canthal and forniceal areas, especially inferiorly. In these areas there was both a greater proportion of positively staining epithelial cells, thus incorporating the intermediate epithelial layers, and a greater staining intensity. Lowest levels of staining were again demonstrated in the tarsal conjunctival epithelium, producing the same pattern of more intense staining in the forniceal than bulbar than tarsal areas, as shown in Figure 31. Again, although p63 expression would not be expected in goblet cells, it was not possible to accurately exclude this in these studies as the goblet cell bodies underlying the large secretory component of the cells are usually not easily detectable.

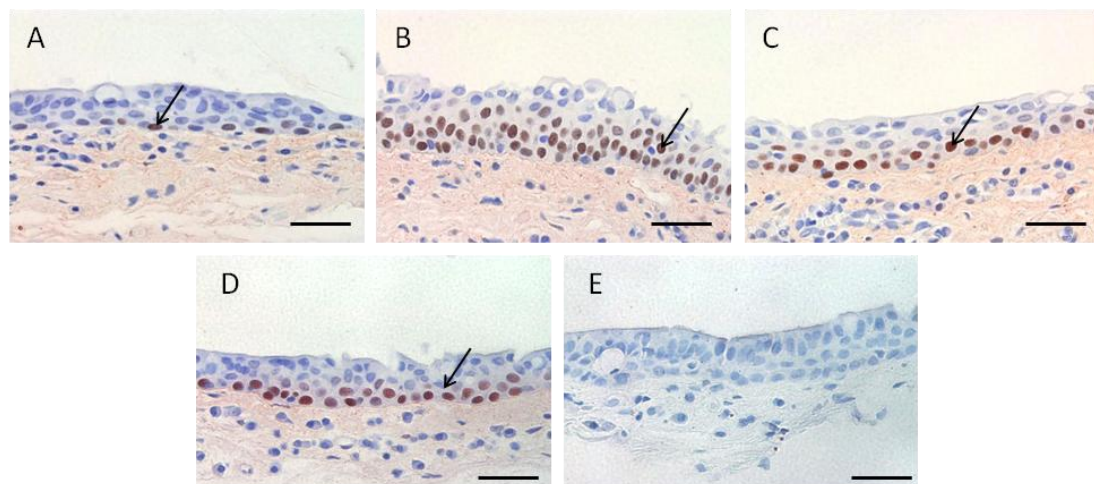


Figure 31: Photomicrographs of immunohistochemical staining for p63 across the conjunctiva. Positive immunoreactivity in brown is observed in the nuclei (arrows), with haematoxylin counterstaining in blue. Mild immunoreactivity is observed in A) tarsal, intense staining in B) forniceal and moderate staining in C) bulbar areas, with D) limbal positive control and E) negative control. Scale bars 50 μ m.

These patterns were demonstrated across both donor tissues. An example of the pattern of staining across the whole conjunctiva from one donor is demonstrated in Figure 32 and the overall gradings averaged from both donors using grading scale 1 (**Figure 33**) and grading scale 2 (Figure 34). The overview of comparative sites compared in these diagrams is labelled in Figure 11.

Friedman tests again confirmed significant variation of staining across the tissue using either grading scale ($p=0.02$ for each). Overall highest staining grades (+++) using grading scale 2 (taking into account the intensity of staining), were noted in the same region as those with highest staining for ABCG2, namely that comprising the medial canthal area and inferior medial and inferior central fornix, but this was not statistically significant compared to the rest of the conjunctiva on *post-hoc* analysis using either grading scale with a Wilcoxon test ($p=0.5$ for each). The pattern of greater staining in the fornices than bulbar than tarsal areas, and greater staining in the superior than inferior conjunctiva was also replicated. There was insufficient data from p63 immunohistochemical staining to enable a statistical correlation analysis between this and ABCG2 immunohistochemical staining.

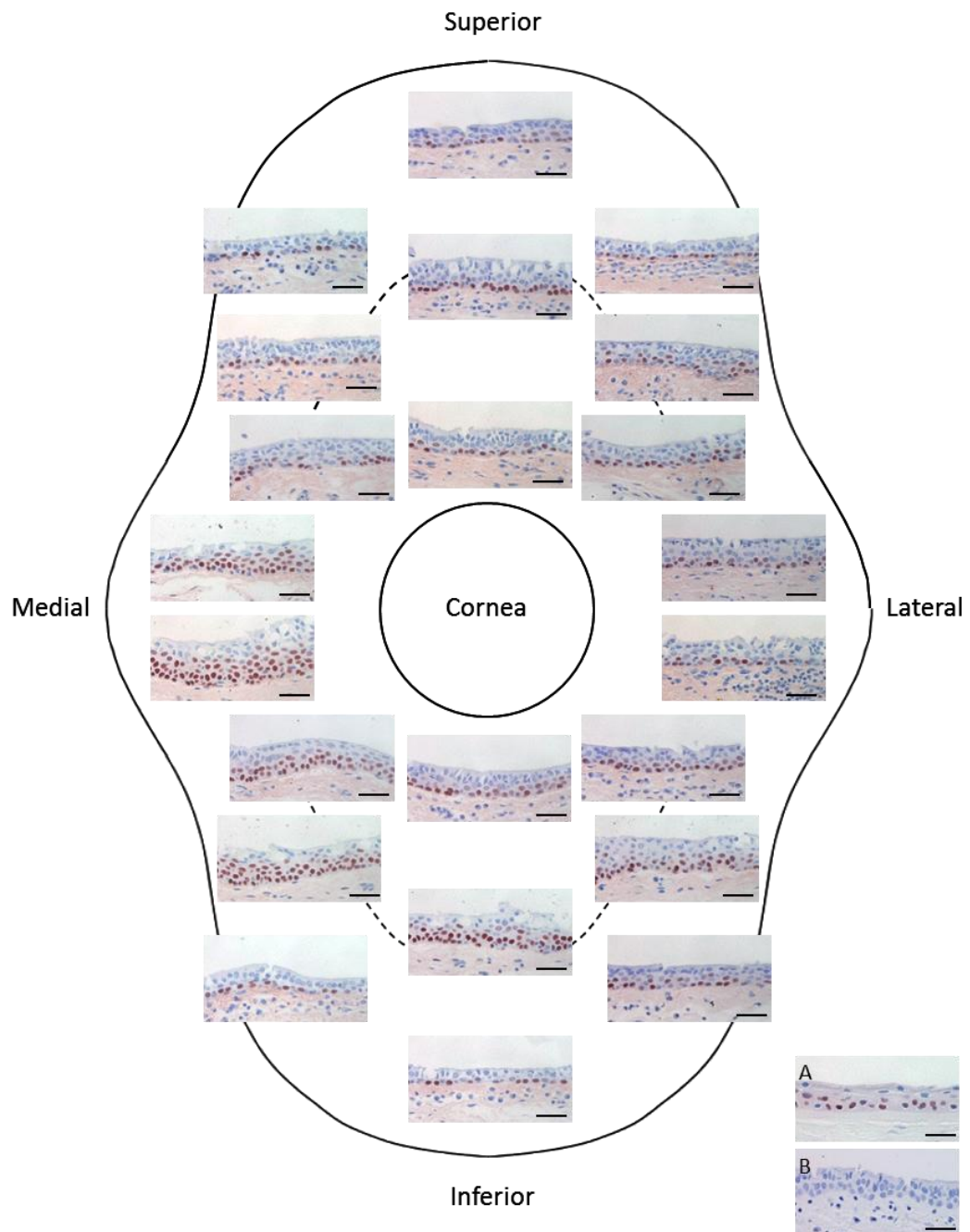


Figure 32: Schematic diagram of the human conjunctiva (as labelled in Figure 11) with fornices represented by dashed lines (----), demonstrating photomicrographs of immunohistochemical staining for p63 across all areas of the conjunctiva from one donor (tissue 26). Positive immunoreactivity in brown is observed in the nuclei, predominantly in the basal layers of the epithelium. In this example, immunoreactivity is observed most intensely in the medial canthal and inferior forniceal areas. Haematoxylin counter-staining in blue. A) Limbal positive control, B) negative control. Scale bars 50 μ m.

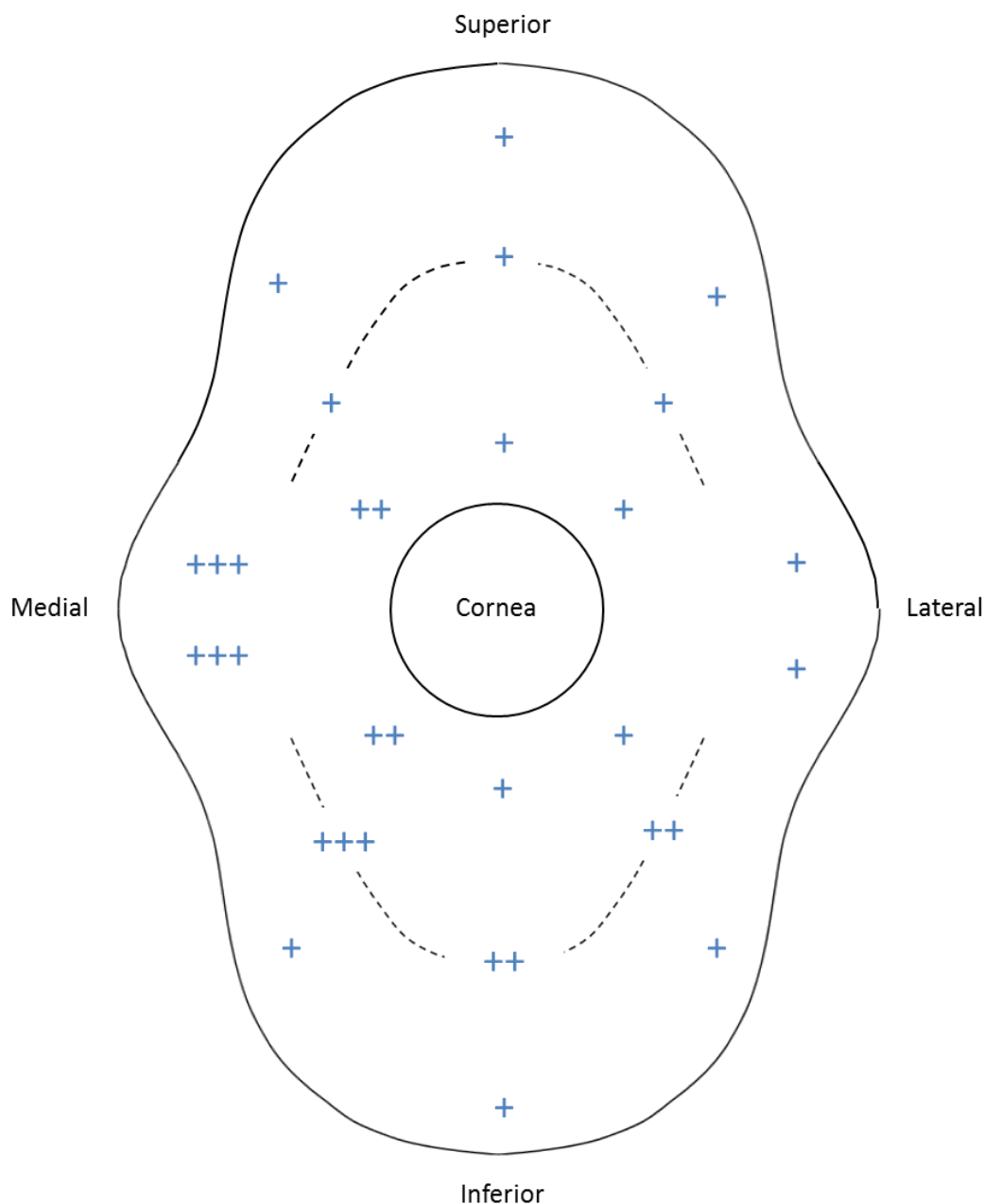


Figure 33: Schematic diagram of the human conjunctiva (as labelled in Figure 11) with fornices represented by dashed lines (-----), demonstrating average grades of immunohistochemical reactivity for p63 using grading scale 1 (Figure 23) by proportion of immunoreactive cells, across all areas of the conjunctiva from 2 donors. Significant variation of staining was observed across the tissue ($p=0.02$), but although highest grades of staining were observed in the medial canthal, inferior medial and inferior central forniceal areas this was not significant ($p=0.5$).

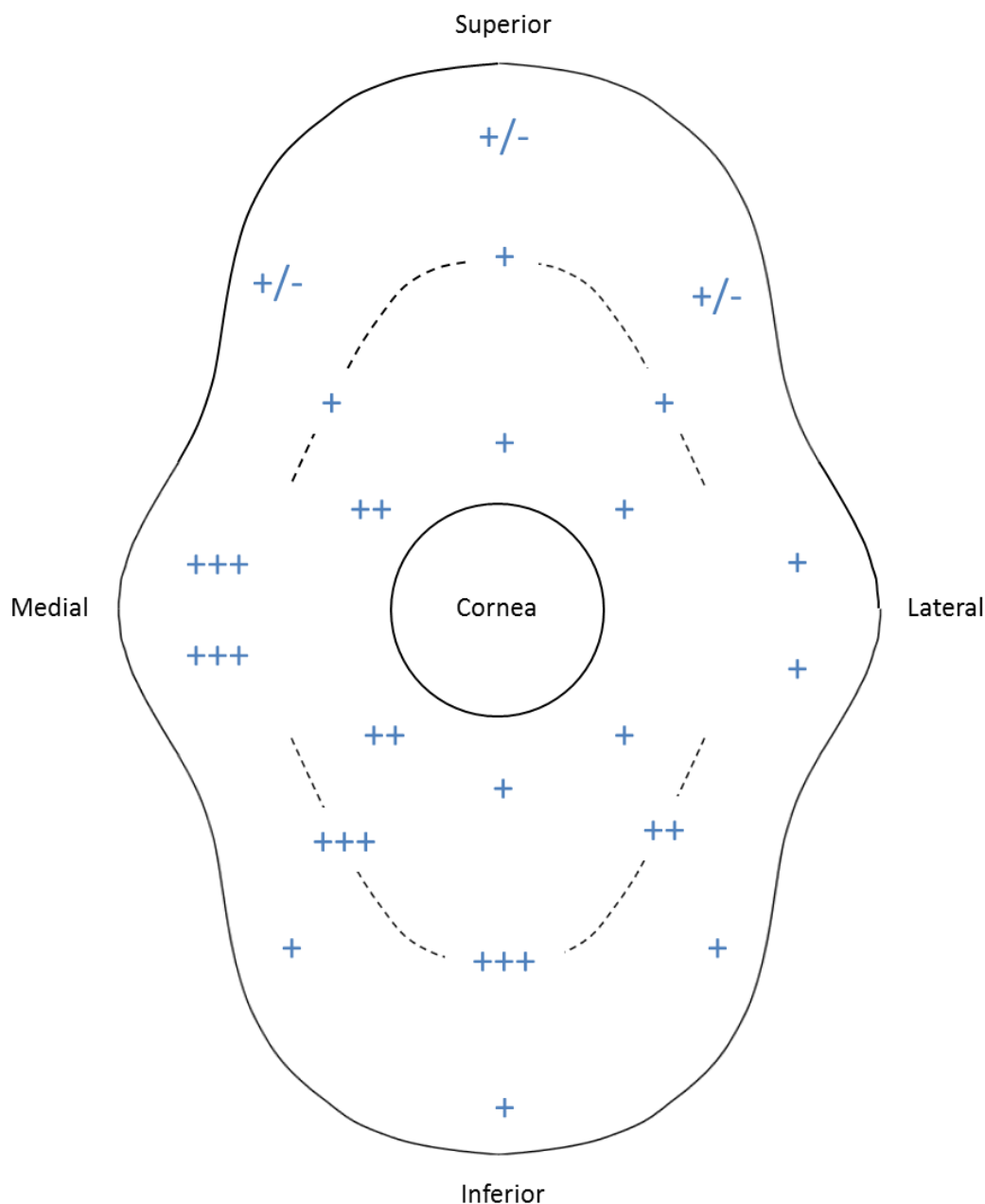


Figure 34: Schematic diagram of the human conjunctiva (as labelled in Figure 11) with fornices represented by dashed lines (----), demonstrating average grades of immunohistochemical reactivity for p63 using grading scale 2 (Table 6) by proportion and intensity of immunoreactive cells, across all areas of the conjunctiva from 2 donors. Significant variation of staining was observed across the tissue ($p=0.02$), but although highest grades of staining were observed in the medial canthal, inferior medial and inferior central forniceal areas this was not significant ($p=0.5$).

In a similar manner to the pattern of ABCG2 staining, no correlation of intensity of p63 positively staining cells was noted to the immediate proximity of goblet cells. Similarly, varying intensity of p63 staining was observed in close proximity to clusters of multiple goblet cells with no clear pattern to different areas of the tissue as shown in Figure 35.

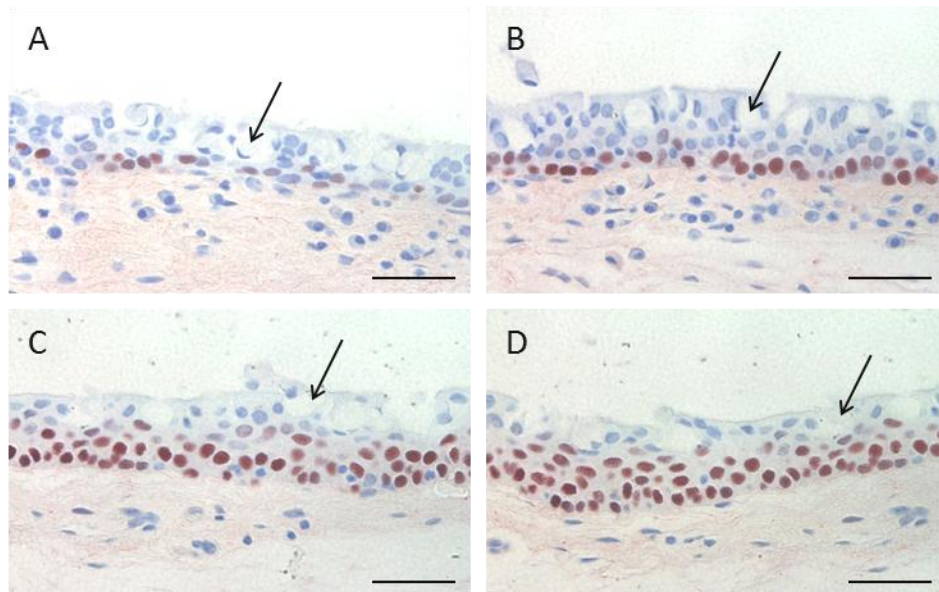


Figure 35: Photomicrographs of immunohistochemical staining for p63 in the conjunctiva in proximity to clusters of goblet cells (arrows). Positive immunoreactivity in brown varies from A) light to D) intense, with haematoxylin counter-staining in blue. A) Tarsal conjunctiva, B) - D) forniceal conjunctiva. Scale bars 50 μ m.

3.3.7. Pan-Cytokeratin MNF116 Staining

Pan-CK MNF116 staining was demonstrated throughout the conjunctival epithelium. Staining intensity varied to some degree amongst adjacent cells but overall the staining amongst epithelial cells was intense with the vast majority of cells staining strongly, giving a universal grading of +++ or ++++ across the tissue as a whole depending on the grading scale employed. The apical secretory portion of the goblet cells did not stain positively for MNF116, the slender nature of the basal bodies meant true positive or negative staining here could not be precisely elucidated. No pockets of non-staining basal cells were noted, suggestive of SCs. The staining across the tissue is summarised with representative images from the tarsal, forniceal and bulbar areas shown in Figure 36.

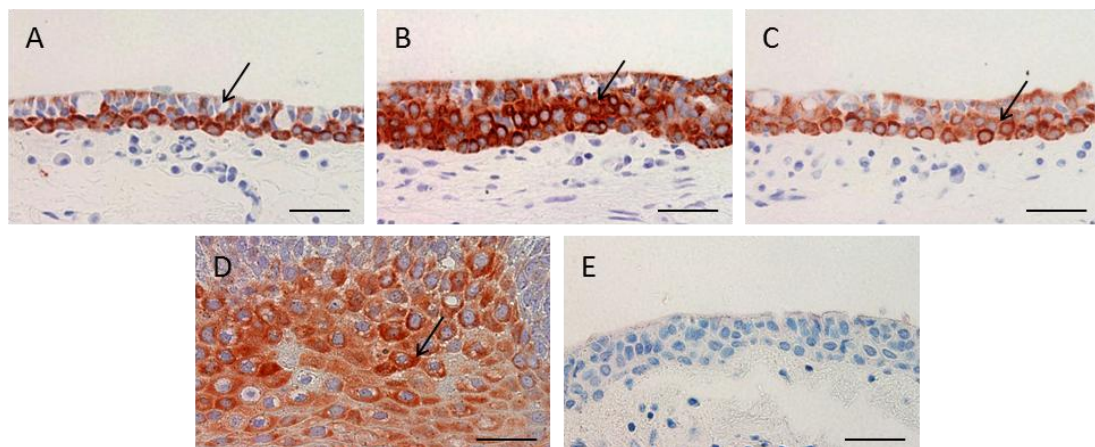


Figure 36: Photomicrographs of immunohistochemical staining for MNF116 across the conjunctiva. Positive immunoreactivity in brown is observed in the cytoplasm (arrows), with haematoxylin counter-staining in blue. Intense immunoreactivity is observed throughout all layers of A) tarsal, B) forniceal and C) bulbar conjunctiva. D) tonsil positive control, E) negative control. Scale bars 50µm.

3.3.8. Pan-Cytokeratin AE1/AE3 Staining

Pan-CK AE1/AE3 staining was similarly demonstrated throughout the conjunctival epithelium. Staining intensity was intense throughout with little variation between cells. Again the apical secretory portion of goblet cells did not stain positively, and true positive or negative staining of their slender basal bodies could not be precisely ascertained. A universal grading of +++ or ++++ across the tissue as a

whole depending on the grading scale employed was similarly demonstrated. This is summarised with representative images from the tarsal, forniceal and bulbar areas in Figure 37.

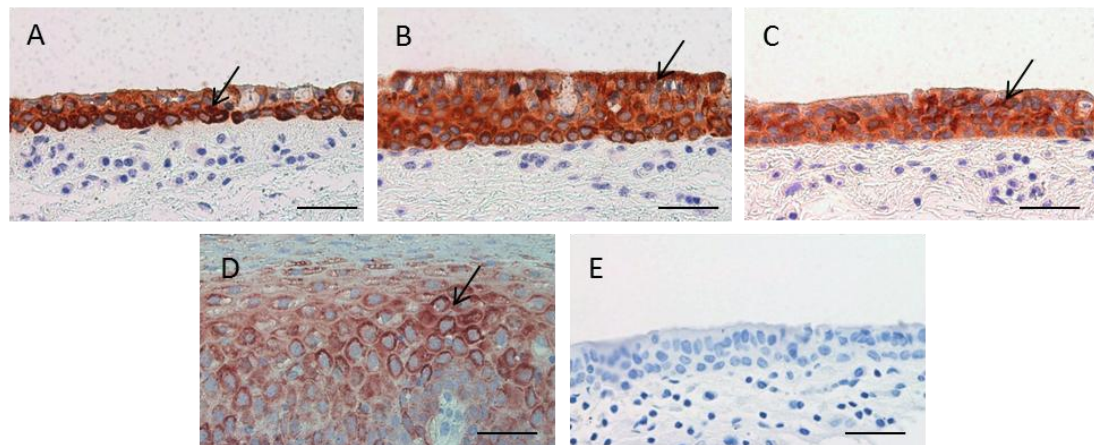


Figure 37: Photomicrographs of immunohistochemical staining for AE1/AE3 across the conjunctiva. Positive immunoreactivity in brown is observed in the cytoplasm (arrows), with haematoxylin counter-staining in blue. Intense immunoreactivity is observed throughout all layers of A) tarsal, B) forniceal and C) bulbar conjunctiva. D) tonsil positive control, E) negative control. Scale bars 50µm.

One small collection of basal non-staining cells was noted in the forniceal region of one sample as shown in Figure 38.

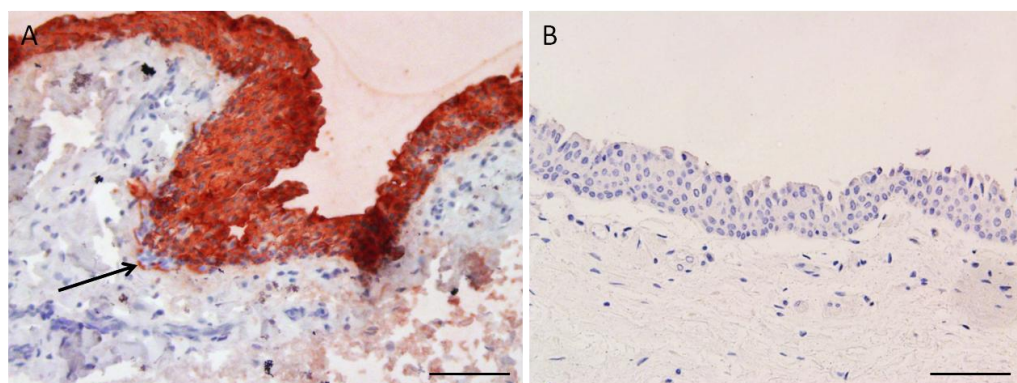


Figure 38: Photomicrographs of immunohistochemical staining for AE1/AE3 in the forniceal conjunctiva. Positive immunoreactivity in brown is observed in the cytoplasm (arrows), with haematoxylin counter-staining in blue. A) intense immunoreactivity is observed throughout all layers of the forniceal conjunctiva, but a small collection of non-immunoreactive cells are demonstrated basally (arrow). B) Negative control. Scale bars 100µm.

In order to further investigate the nature of this cluster of cells, Melan-A and S-100 stains were employed to exclude melanocytic or immunological origin respectively. Both of these cell types were demonstrated in the conjunctival epithelium as shown in Figure 39 and Figure 40, but unfortunately the adjacent histological section to that used in Figure 38 had already been used in a previous experiment and thus further characterisation of this non-AE1/AE3 staining cluster of cells was not possible. No further non-immunoreactive clusters of cells were observed.

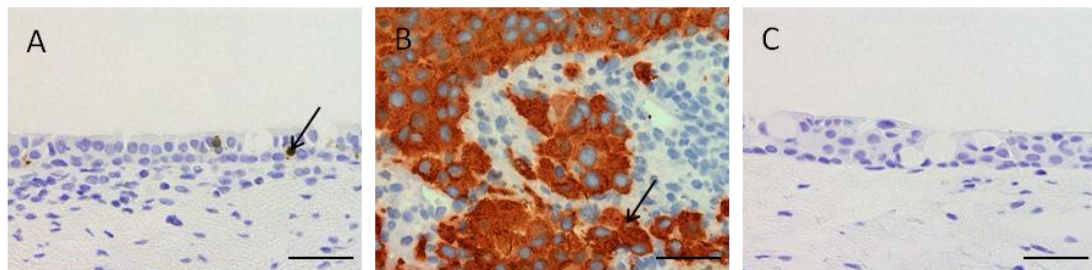


Figure 39: Photomicrographs of immunohistochemical staining for Melan-A. Positive immunoreactivity is observed in the cytoplasm in brown with haematoxylin counter-staining in blue. A) Occasional immunoreactive cells (arrows) are observed in the conjunctival epithelium, B) melanoma positive control, C) negative control. Scale bars 50µm.

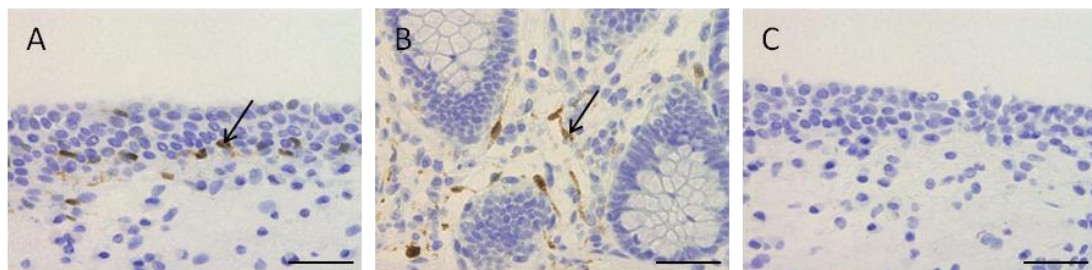


Figure 40: Photomicrographs of immunohistochemical staining for S-100. Positive immunoreactivity is observed in the cytoplasm in brown with haematoxylin counter-staining in blue. A) Occasional immunoreactive cells (arrows) are observed in the conjunctival epithelium and lamina propria, B) colonic positive control, C) negative control. Scale bars 50µm.

3.3.9. Immunohistochemical Staining and Donor age

Immunohistochemical staining (using grading scale 1) across all areas of the conjunctiva for each donor tissue was averaged and compared to donor age. There were greater numbers of older donors, but despite this, a significant association of reduced ABCG2 staining with increasing donor age was established using a generalised linear mixed model ($p < 0.01$). This data is shown in Figure 41. Although the linear trend line does not appear to demonstrate a clear relationship, this data includes the pattern from all areas across the tissue for each donor. In taking this into account the statistical analysis shows a significant correlation. There was insufficient data to analyse this association for p63 staining.

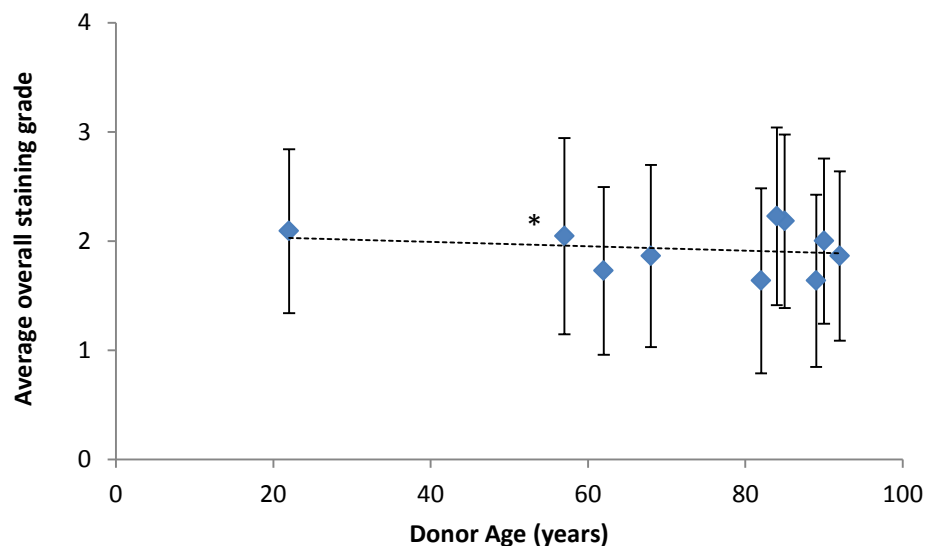


Figure 41: Line graph showing variance in average conjunctival ABCG2 immunohistochemical staining grade with donor age. A decrease in ABCG2 staining is demonstrated with increasing donor age ($p < 0.01$)*. Error bars +/- 1SD, ---- linear trend line.

3.3.10. Immunohistochemical Staining and Post Mortem Retrieval Time

Immunohistochemical staining (using grading scale 1) across all areas of the conjunctiva for each donor tissue was averaged and similarly compared to PMRT. Times varied from 8.5-28 hours. Longer PMRTs were associated with significantly lower ABCG2 staining by analysis with a generalised linear mixed model ($p < 0.01$).

This data is shown in Figure 42. Similarly, although the linear trend line does not appear to demonstrate a clear relationship, by taking into account the pattern of data from all areas across the tissue as a whole the statistical analysis shows a clear significant correlation. Again there was insufficient data to analyse this association for p63 staining.

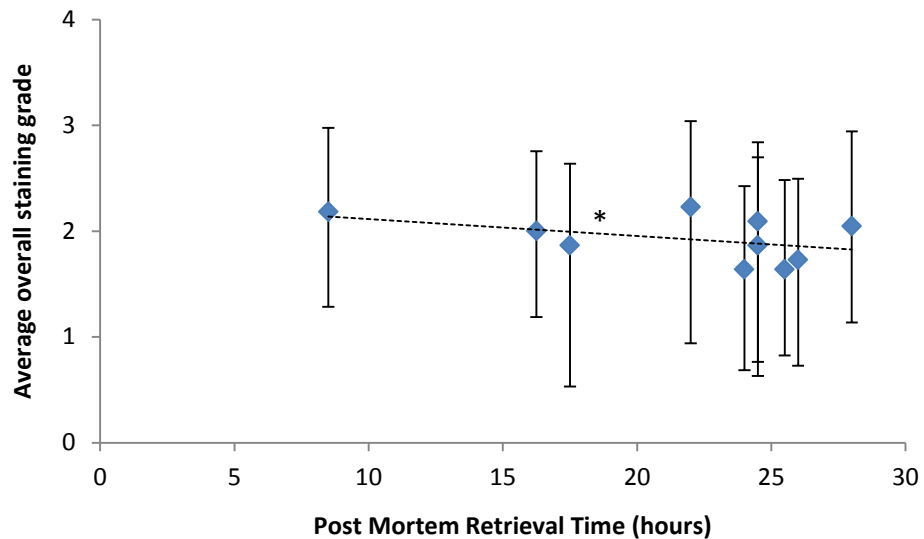


Figure 42: Line graph showing variance in average conjunctival ABCG2 immunohistochemical staining grade with PMRT. A decrease in ABCG2 staining is demonstrated with increasing PMRT ($p < 0.01$)*. Error bars +/- 1SD, ---- linear trend line.

3.4. Cell Culture

Conjunctiva from 17 eyes (from 17 donors) was processed for cell culture. Initial tissue was used to develop techniques and optimise methods for cell harvesting and culture.

3.4.1. Conjunctival Cell Harvesting

Experiments were undertaken to ascertain the optimal methods for conjunctival epithelial cell harvesting

Trypsinisation in cloning rings

8mm cloning rings placed on the conjunctival tissue were used to hold trypsin inside for varying time periods, but proved unsuccessful. Due to the irregular conjunctival surface, the trypsin often leaked out, and the addition of high-vacuum grease only enabled the rings to slide off the mucous membrane. Very few cells (<6000) were counted in the trypsin cell supernatant obtained from each cloning ring by this method, thus seeding concentrations were very low. No cell growth was observed from these samples in culture. In order to ascertain the depth of epithelium removed with different trypsin incubation time periods, the remaining tissue was NBF fixed and wax embedded, but sections revealed loss of epithelium not only within the area inside the cloning rings, but completely across the whole specimens, as shown in Figure 43.

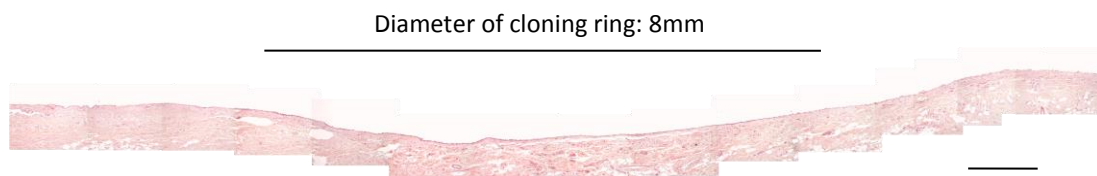


Figure 43: Section of human conjunctival tissue demonstrating complete loss of epithelium following cell harvesting attempts with cloning rings (H&E stain). Photomicrographs stitched together manually in Microsoft PowerPoint. Scale bar 1mm.

Trypsinisation of chopped tissue

Total cell counts of $347\text{-}1479 \times 10^4$ (mean 878×10^4) per whole conjunctiva were obtained after trypsinisation of whole chopped tissue. These were successfully grown in culture on 3T3 feeder layers as detailed below.

3.4.2. Conjunctival Epithelial Cell Growth

No growth of cells obtained following trypsinisation of chopped whole tissue was observed in culture on tissue culture plastic alone or on Matrigel™ basement membrane matrix. Discrete colonies of closely apposed polygonal cells with a high nuclear:cytoplasmic ratio were observed on the 3T3 feeder layer by day 7 (Figure 44).

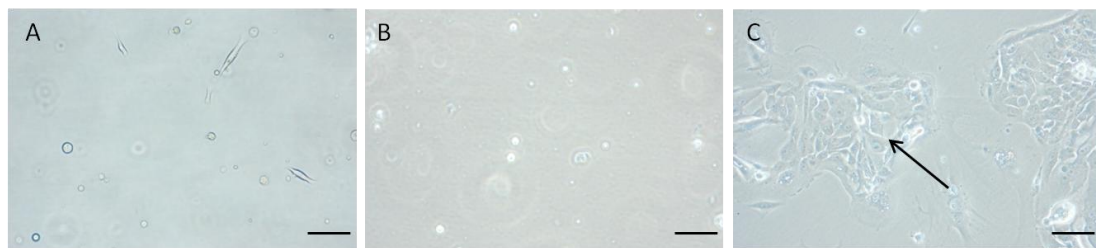


Figure 44: Phase contrast micrographs of conjunctival epithelial cell culture at day 7 on A) tissue culture plastic, B) Matrigel™ basement membrane matrix and C) 3T3 feeder layer. Conjunctival epithelial cell colonies (arrow) are only observed growing on the feeder layer. Scale bars 100µm.

Conjunctival explants were similarly plated on tissue culture plastic alone, on Matrigel™ basement membrane, and on the 3T3 feeder layer. No growth was observed from any explants cultured up to day 21 (Figure 45), however this experiment was only repeated on two occasions. Closer inspection of the latter revealed a very sparse feeder layer beside the explants and dense 3T3 cells around the periphery of the wells. This was a consistent finding, likely due to mechanical disruption of the feeder layer whilst placing the explants.



Figure 45: Phase contrast micrographs of conjunctival epithelial explants (arrows) at day 7 on A) tissue culture plate, B) Matrigel™ basement membrane matrix and C) 3T3 feeder layer. No cell growth was observed on any extracellular matrix. Scale bars 100µm.

All further studies were therefore employed following cell harvesting by trypsinisation of whole chopped tissue and seeding on a 3T3 feeder layer. Using this technique conjunctival epithelial growth was established from all 8 areas of the conjunctiva described in Figure 12. Colonies were first observed from day 4 to 7 and gradually enlarged and fused, such that the cells became 70-80% confluent as a uniform population of densely packed polygonal cells with cobblestone appearance by day 10-14. Colonies were consistently observed earlier in the medial canthal and forniceal areas, and to a lesser extent inferior bulbar and lateral canthal areas. Larger colonies were observed in these areas than in other areas at equivalent time points. An example of comparative growth images from one donor is shown in Figure 46.

Conjunctival epithelial cell culture was maintained up to passage 3. At passage 1 the cells were enlarged but remained polygonal in shape. With additional passages cells became increasingly elongated and more differentiated in appearance with a lower nuclear:cytoplasmic ratio, as shown in Figure 47. All cultures reached senescence by passage 4.

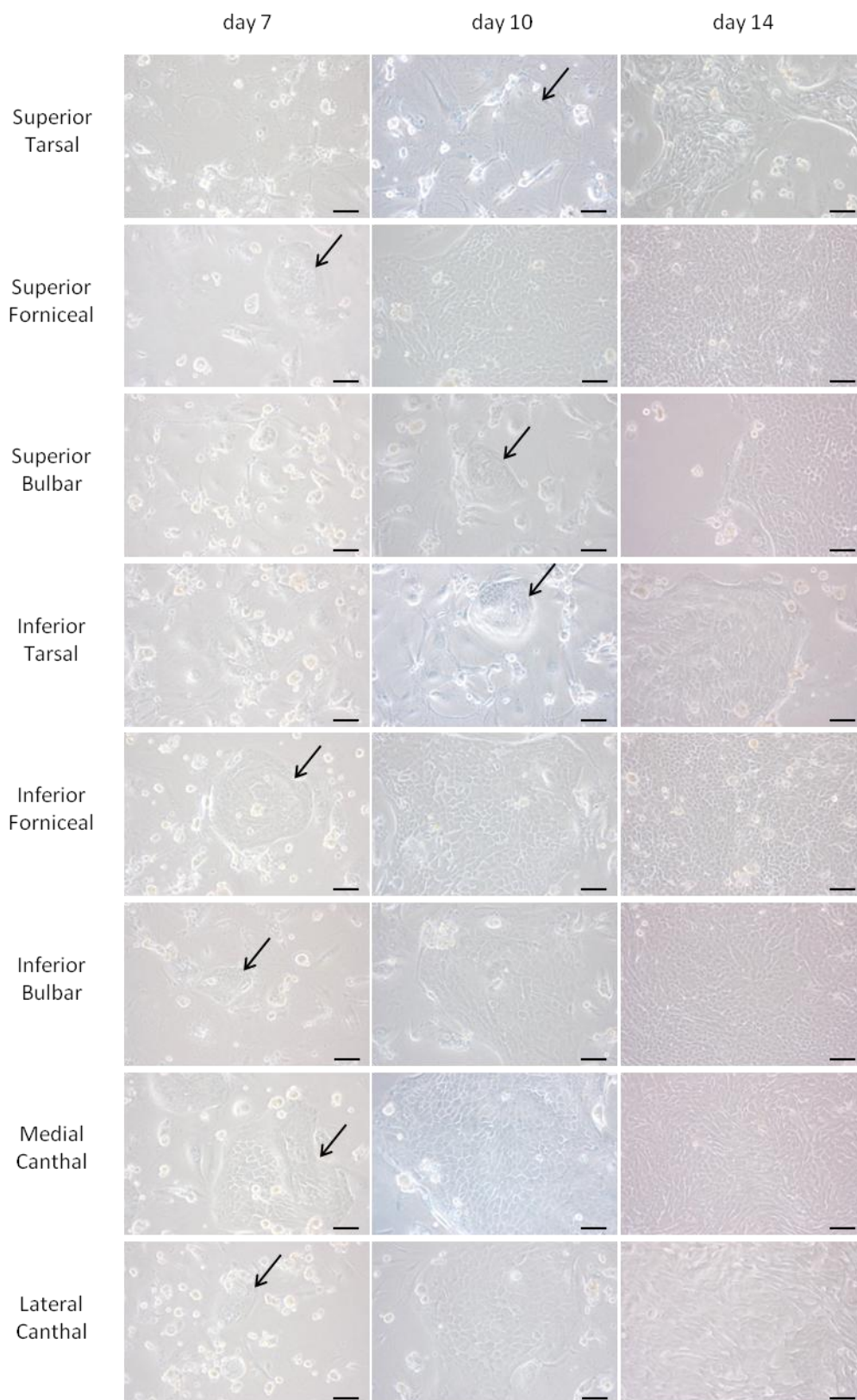


Figure 46: Phase contrast micrographs of conjunctival epithelial cell cultures from one donor (tissue 23), demonstrating differing size of colony formations (arrows) in culture from different conjunctival areas. Largest colonies are demonstrated in the medial canthal and inferior forniceal areas in this donor at day 7. Scale bars 100 μ m.

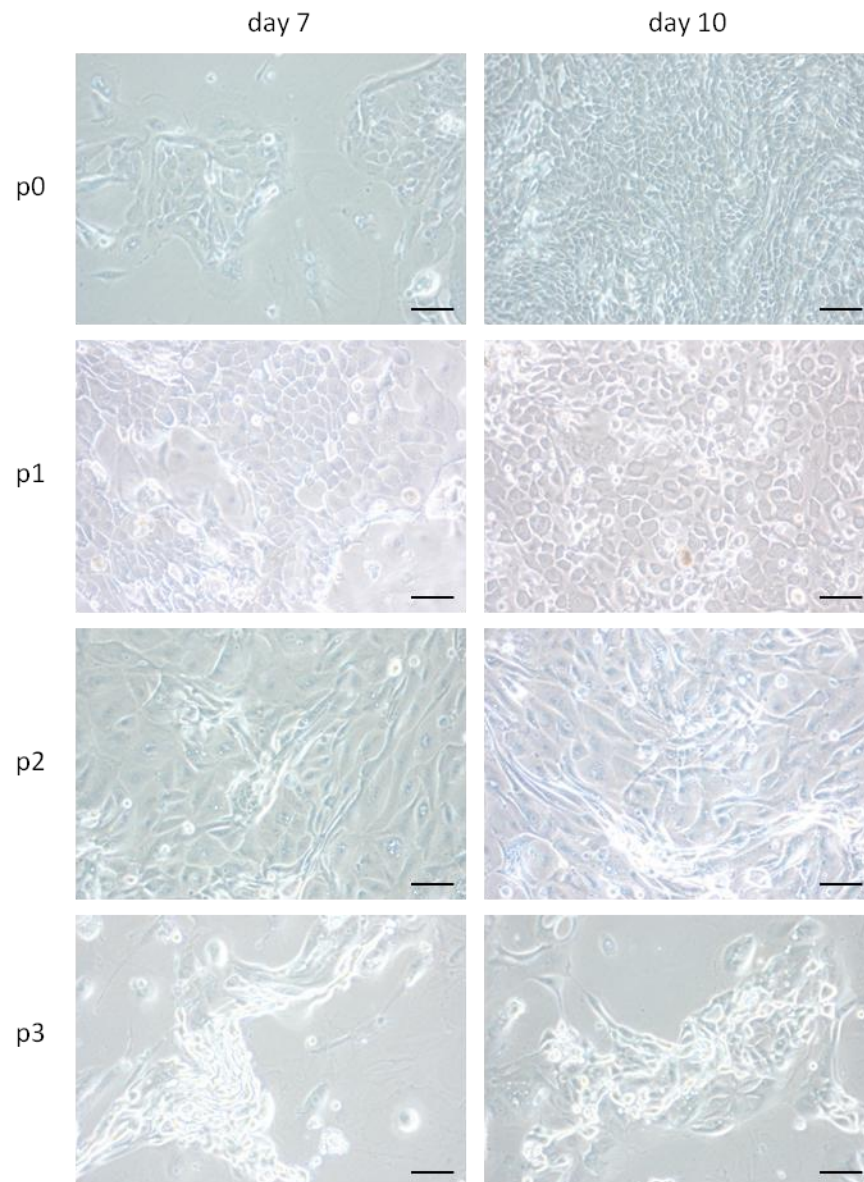


Figure 47: Phase contrast micrographs of conjunctival epithelial cells demonstrating that epithelial cells become increasingly more differentiated in appearance with increasing passage (p). Scale bars 100 μ m.

Cultures from two early specimens became infected (tissue 05, bacterial infection, and tissue 11, fungal infection). No association was observed between infection and donor age, cause of death or PMRT from these 6 initial cultures; there was insufficient data for statistical analysis. The additional step of washing out the donor fornices with povidone iodine before tissue retrieval was then introduced, following which no further infections were encountered.

Tissues 15, 21 and 29 failed to produce cell colonies in culture despite using previously successful techniques. One of these may be attributable to a drop in the incubator temperature, but there were no apparent reasons to account for the other two (tissues 15 and 21). Whilst these latter two were from elderly donors with relatively long PMRTs (92 years / 17 hours, and 82 years / 25 hours respectively), cultures were successfully generated from other tissues with similar donor characteristics (tissues 25, 27 and 31).

3.4.3. Comparative Limbal Epithelial Cell Growth

Limbal epithelial cells were harvested from corneo-scleral discs using the same technique as per successful conjunctival cell harvesting and culture (see Section 3.4.2). These cells demonstrated similar regular polygonal morphological features, but with faster growth rates, reaching confluence by day 7 (Figure 48), as compared to day 10-14 for conjunctival epithelial cultures.

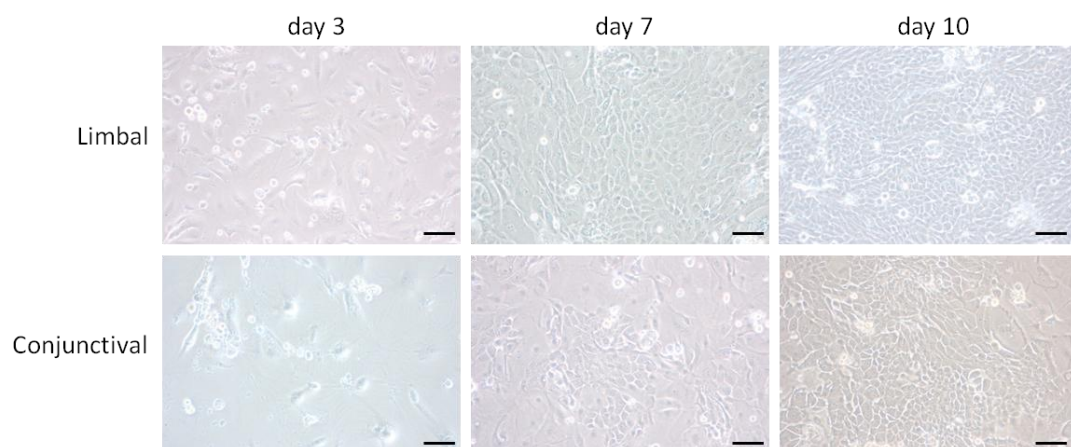


Figure 48: Phase contrast micrographs of passage 0 limbal and conjunctival epithelial cells in culture demonstrating similar epithelial cell morphology but higher growth rates in culture of limbal epithelial cells. Limbal cells are observed to reach confluence at day 7, compared to conjunctival cells which are near confluency at day 10. Scale bars 100 μ m

3.5. Colony Forming Efficiency Assays

CFE assays were performed on conjunctival and limbal epithelial cells from 8 and 3 donors respectively. A single plate of 6 wells was assessed for each area of the conjunctiva, an example of which is shown in Figure 49.

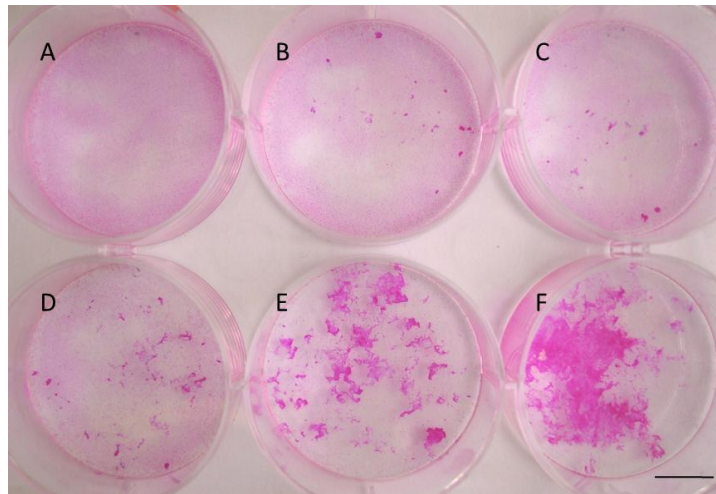


Figure 49: Colony forming efficiency (CFE) assay plate demonstrating conjunctival epithelial cell colonies stained with 1% Rhodamine B. Wells plated with A) 0, B) 500, C) 1000, D) 2000, E) 5000 and F) 10000 cells per 9.6cm^2 well. Scale bar 1cm.

Higher number of colonies growing in the well seeded with 10000 cells ($1 \times 10^4 / 9.6\text{cm}^2$) led to colony overcrowding by the time of fixation thus it was often not possible to obtain an accurate count from this well as shown in Figure 49, and this data was therefore incomplete.

3.5.1. Cell Seeding Number and Colony Forming Efficiency

In order to accurately interpret the CFE data the relationship between the number of cells seeded per well, and both the number of colonies cultured and CFE was firstly determined.

Although a linear association in number of cells seeded per well to number of colonies cultured was demonstrated at lower seeding densities, no proportionate

increase in number of colonies cultured was demonstrated at the highest seeding density of 10000 cells per well, as shown in Figure 50.

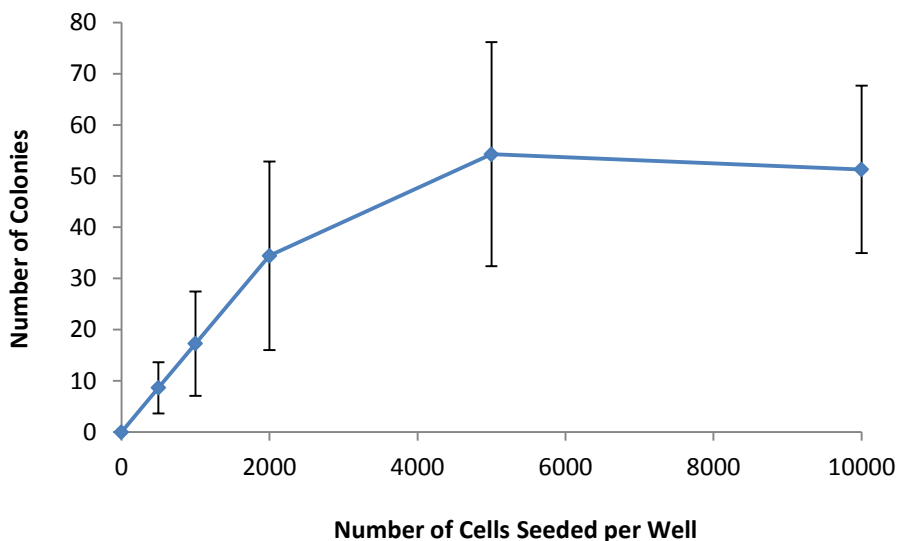


Figure 50: Line graph showing the effect of cell seeding number on number of colonies cultured. A linear association is observed at lower concentrations, but the number of colonies cultured reaches a plateau at 5000 cells per well. Error bars +/- 1SD.

Similarly, although there was significant variation in the CFE data at lower seeding densities, represented by the relatively large error bars in Figure 51; no significant difference was demonstrated between CFE values generated from these wells seeded with 500, 1000 and 2000 cells as assessed using a one-way ANOVA test ($p=0.94$). Significantly lower CFEs were generated from both the wells seeded with 5000 cells ($p<0.01$) and 10000 cells ($p<0.01$), as also assessed using a one-way ANOVA test.

For these reasons, together with the colony overcrowding and difficulty obtaining an accurate count described in Section 3.5 above, and hence a significant level of missing data, readings from both the wells seeded with 5000 and 10000 cells/well were excluded from all further calculations and analysis. Thus the CFE for each plate was determined as the mean CFE value from wells seeded with 500, 1000 and 2000 cells only.

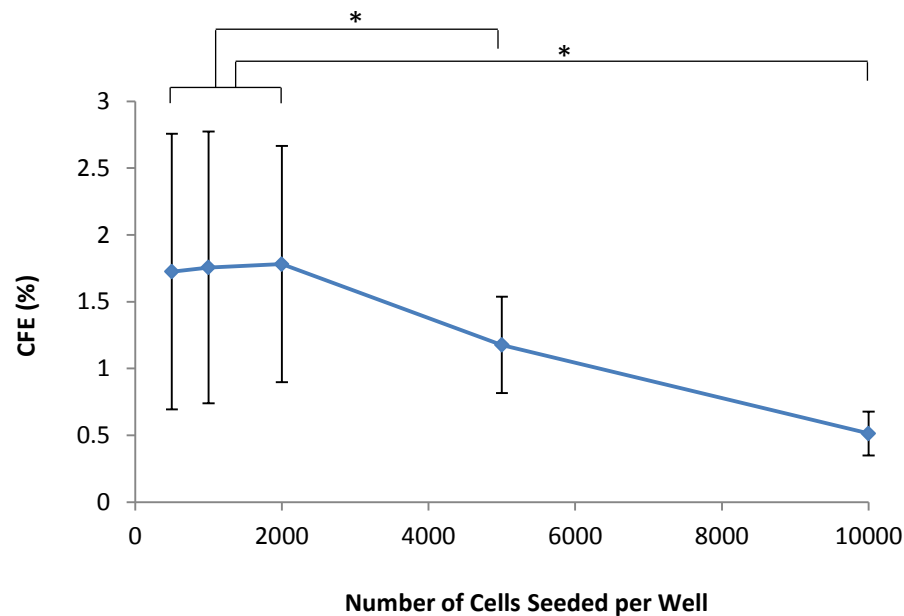


Figure 51: Line graph showing the effect of cell seeding number on CFE value. No difference in CFE is observed at seeding densities less than 2000 cells per well ($p=0.94$), but significantly lower CFE is observed at both 5000 ($p<0.01$)* and 10000 cells per well ($p<0.01$)*. Error bars +/- 1SD.

3.5.2. Colony Forming Efficiency across the Conjunctiva

CFE assays from different regions across the conjunctiva as shown in Figure 16, demonstrated varying clonogenic ability across the tissue as a whole, with a consistent pattern shown in all 8 separate donors. A non-parametric Friedman test confirmed significant overall variation across the tissue in all donors ($p<0.01$).

Overall highest CFE levels were consistently noted in the medial canthal, usually followed by the inferior forniceal areas. *Post-hoc* analysis with a Wilcoxon test showed statistically significantly higher CFE in the medial canthal area alone ($p<0.01$) and in the medial canthal and inferior forniceal areas together ($p<0.01$) compared to all other areas. Higher CFE was shown in the fornices than bulbar than tarsal areas, and this pattern was replicated in both superior and inferior conjunctiva, with higher CFE in inferior compared to superior areas. Using the schematic diagram of the whole conjunctiva labelled in Figure 16, an example of CFE images from one donor (tissue 31) is shown in Figure 52. Data from all 8 donors is demonstrated in a comparative histogram in **Figure 53**, and as overall

mean values in **Figure 54**. Data from each of the 8 donors individually is shown in Figure 55 to Figure 62. In order to further investigate the variation in CFE values between donors further analysis including donor age (Section 3.5.3) and PMRT (Section 3.5.4) was performed.

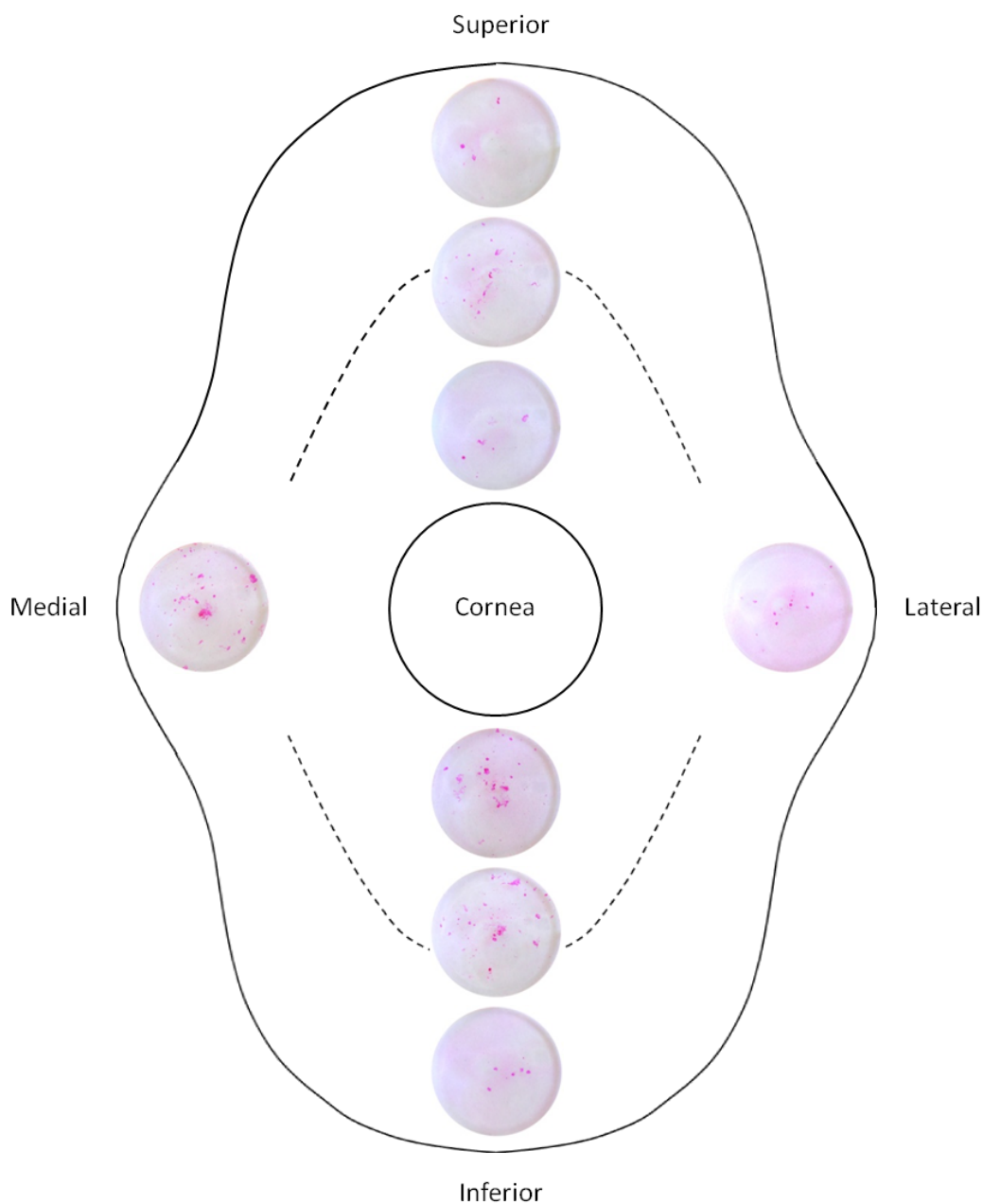


Figure 52: Schematic diagram of the human conjunctiva (as labelled in Figure 16) with fornices represented by dashed lines (-----), demonstrating varying colony growth on CFE analysis as stained with Rhodamine B, from each comparative tissue area from one donor (tissue 31). In this example, greater number of colonies are observed in the medial canthal, inferior forniceal and inferior bulbar areas.

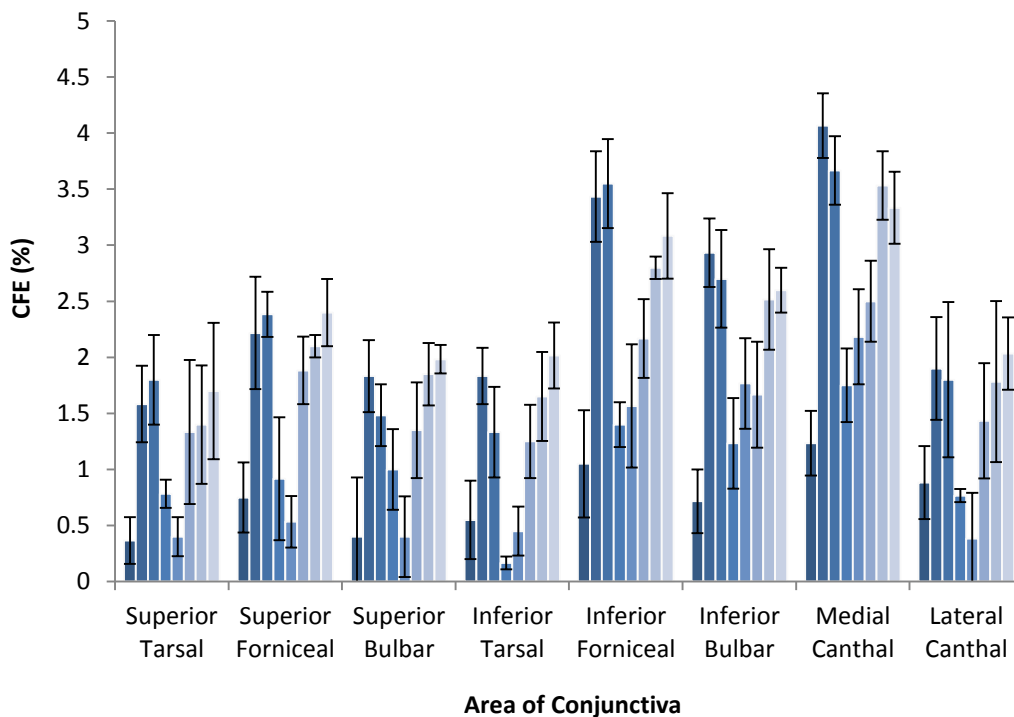


Figure 53: Histogram demonstrating the CFE values across 8 different areas of the conjunctiva from all 8 donors (each represented in different shade of blue). For each highest CFE was observed in the medial canthal and inferior forniceal areas. Error bars +/- 1SD.

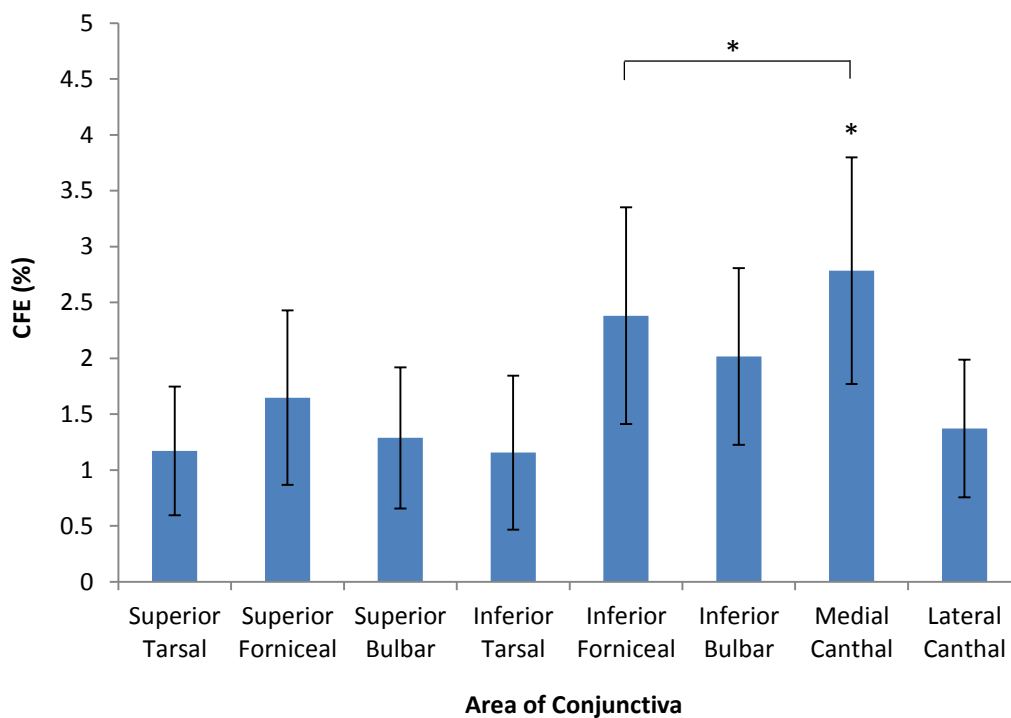


Figure 54: Histogram demonstrating the mean overall CFE values across 8 different areas of the conjunctiva from all 8 donors. The highest CFE was observed in the medial canthal area alone ($p < 0.01$)*, and medial canthal and inferior forniceal areas combined ($p < 0.01$)*. Error bars +/- 1SD.

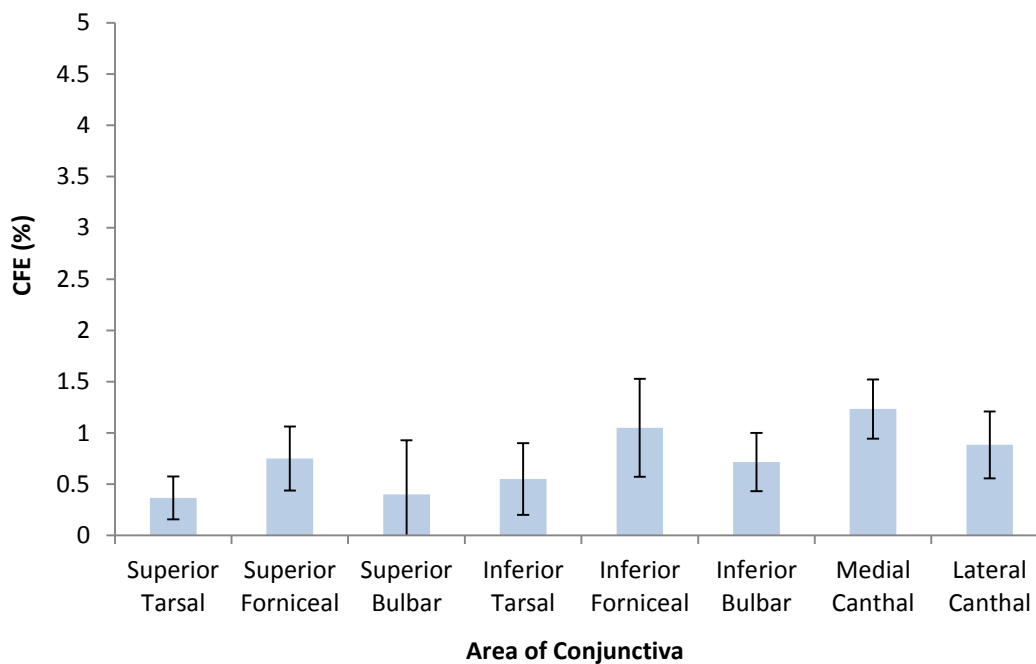


Figure 55: Histogram demonstrating the CFE values across 8 different areas of the conjunctiva from one donor (tissue 17). Highest CFE was observed in the medial canthal and inferior forniceal areas. Error bars +/- 1SD.

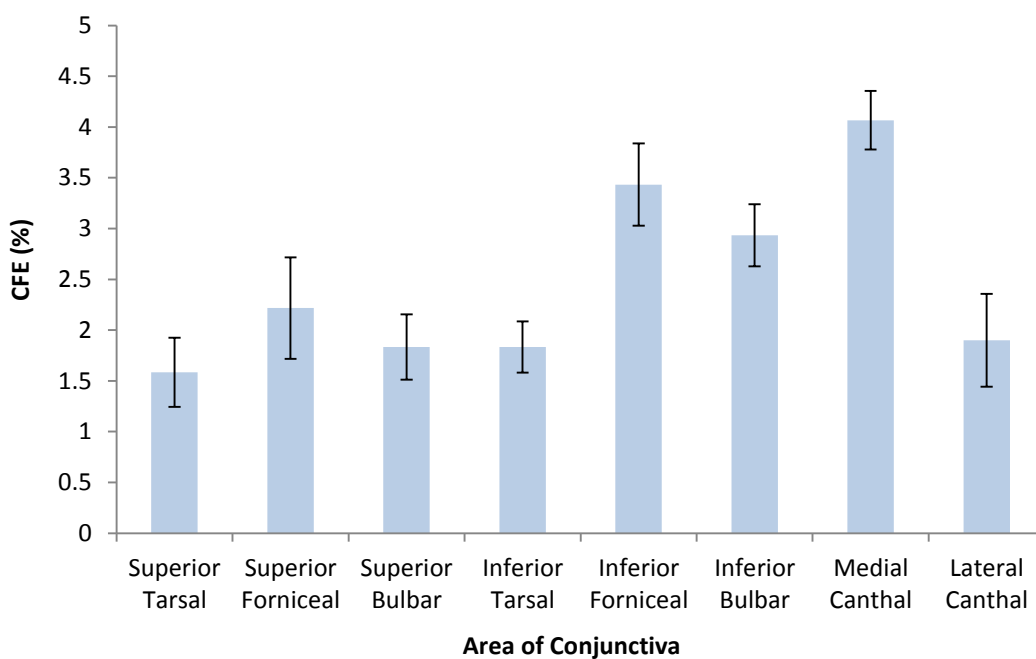


Figure 56: Histogram demonstrating the CFE values across 8 different areas of the conjunctiva from one donor (tissue 19). Highest CFE was observed in the medial canthal, inferior forniceal and inferior bulbar areas. Error bars +/- 1SD.

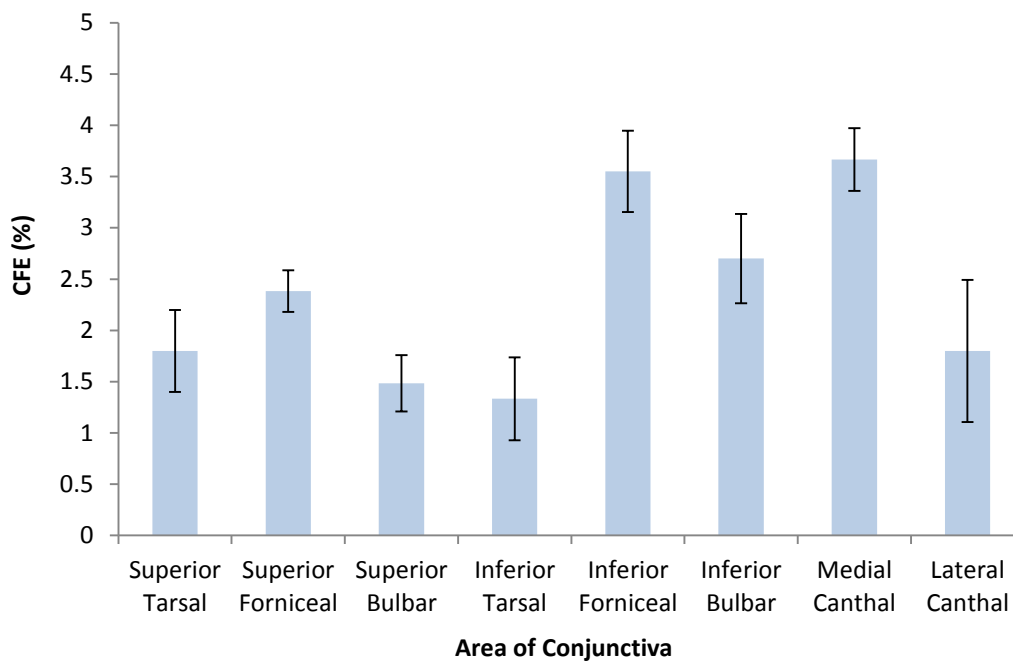


Figure 57: Histogram demonstrating the CFE values across 8 different areas of the conjunctiva from one donor (tissue 23). Highest CFE was observed in the medial canthal and inferior forniceal areas. Error bars +/- 1SD.

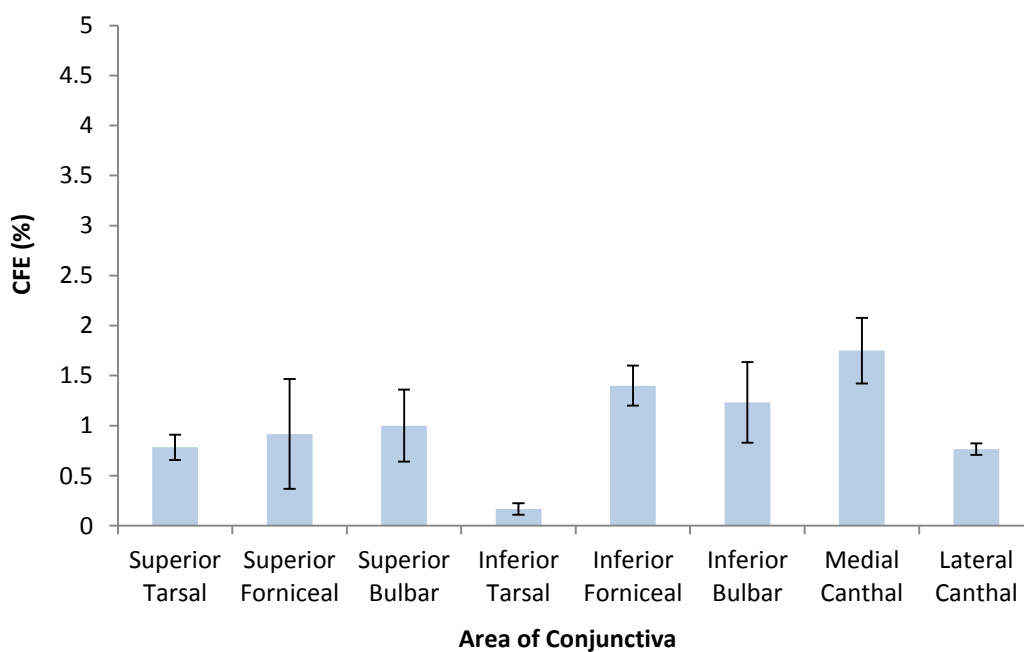


Figure 58: Histogram demonstrating the CFE values across 8 different areas of the conjunctiva from one donor (tissue 25). Highest CFE was not observed in the medial canthal area. Error bars +/- 1SD.

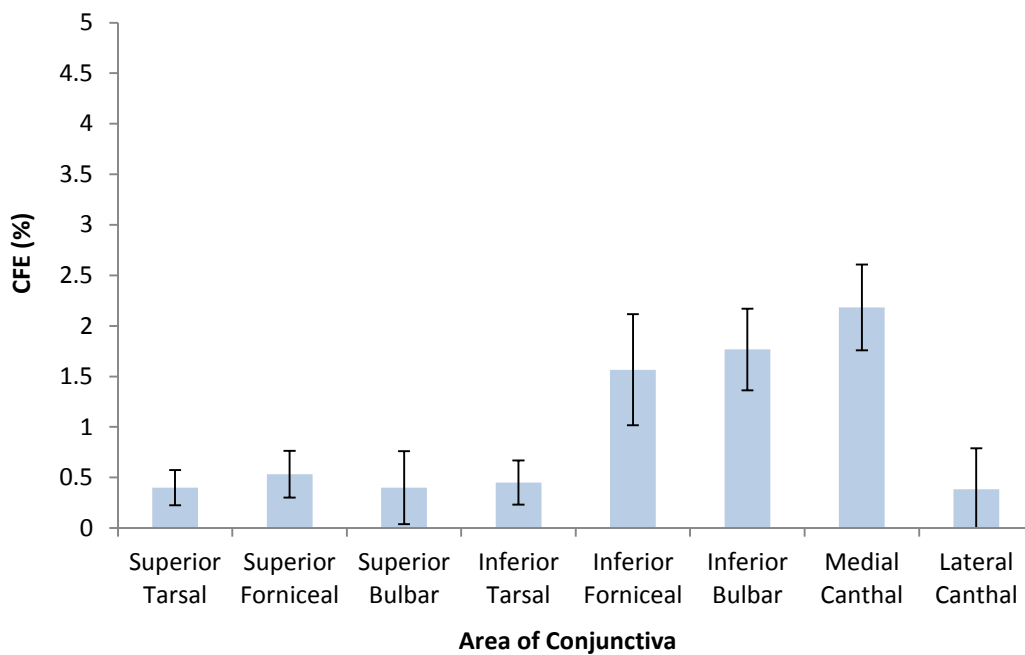


Figure 59: Histogram demonstrating the CFE values across 8 different areas of the conjunctiva from one donor (tissue 27). Highest CFE was observed in the medial canthal, inferior bulbar and inferior forniceal areas. Error bars +/- 1SD.

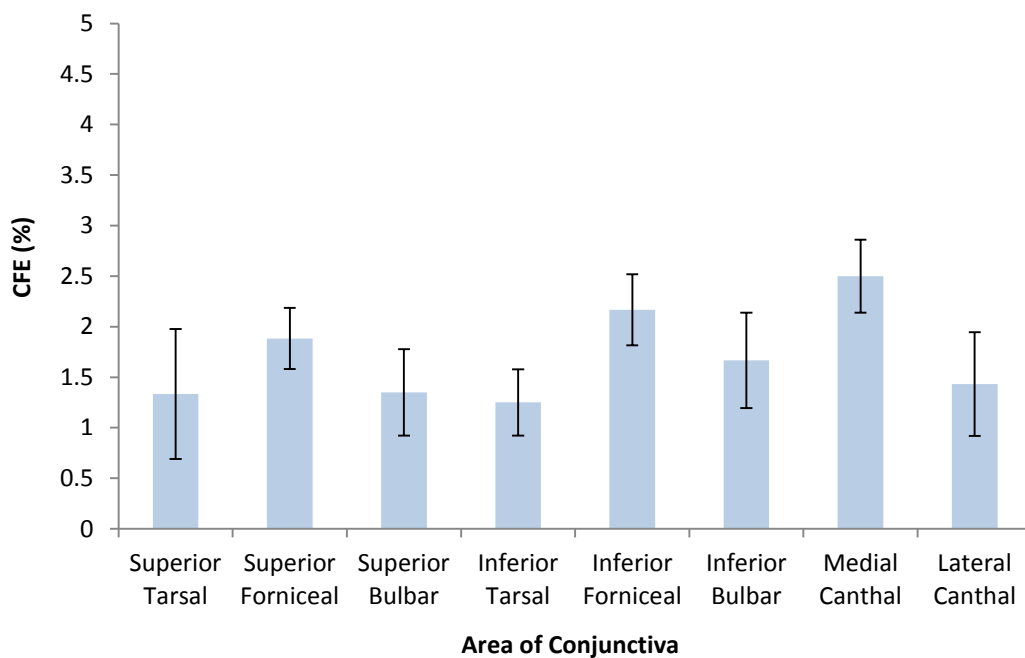


Figure 60: Histogram demonstrating the CFE values across 8 different areas of the conjunctiva from one donor (tissue 31). Highest CFE was observed in the medial canthal and inferior forniceal areas. Error bars +/- 1SD.

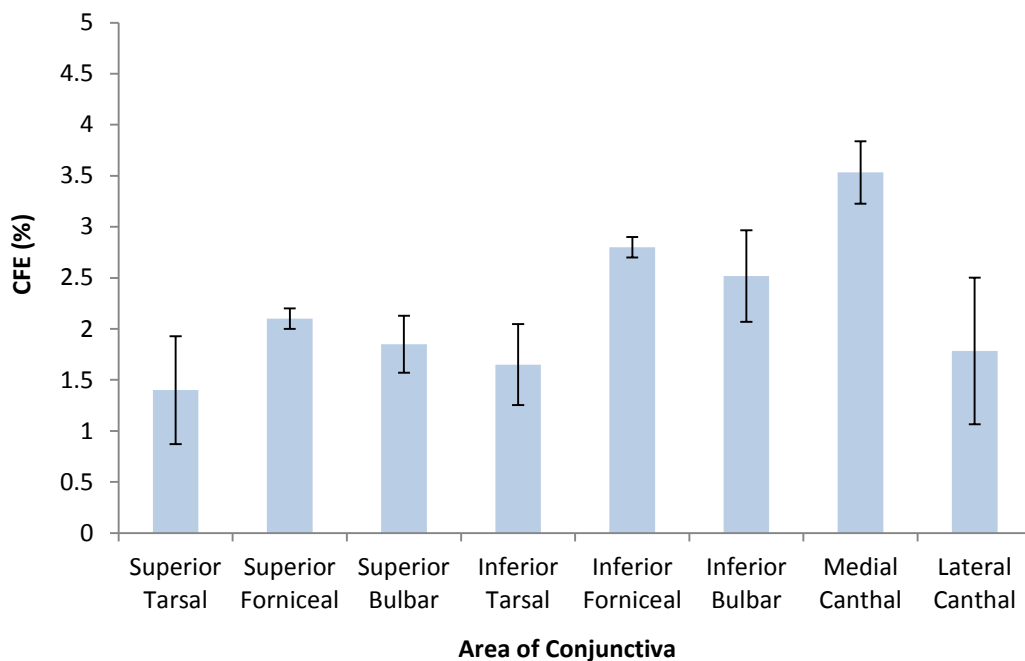


Figure 61: Histogram demonstrating the CFE values across 8 different areas of the conjunctiva from one donor (tissue 33). Highest CFE was observed in the medial canthal, inferior forniceal and inferior bulbar areas. Error bars +/- 1SD.

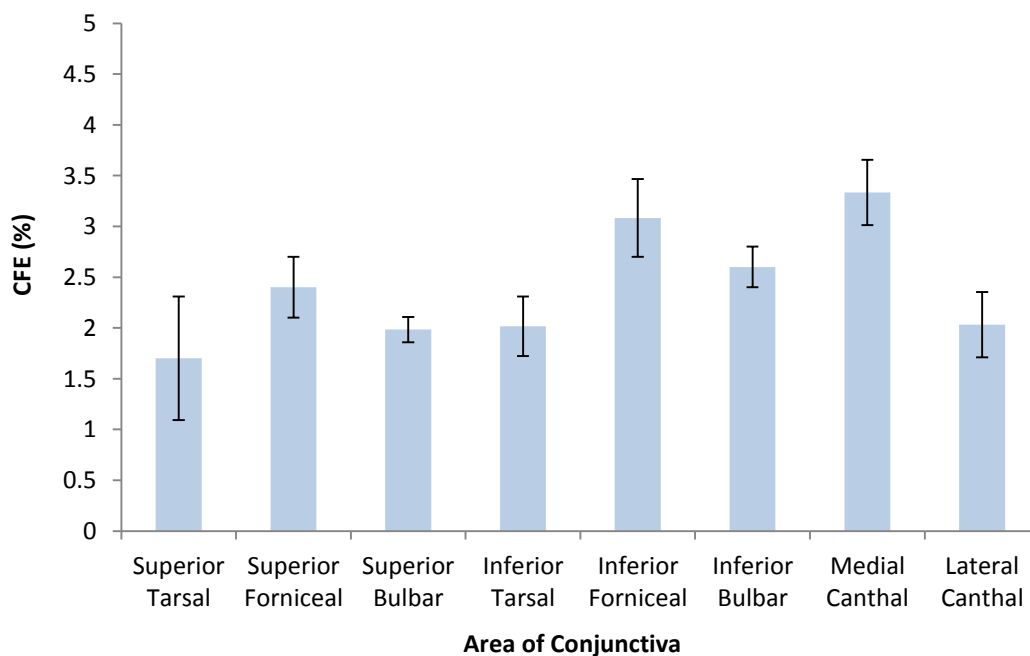


Figure 62: Histogram demonstrating the CFE values across 8 different areas of the conjunctiva from one donor (tissue 35). Highest CFE was observed in the medial canthal and inferior forniceal areas. Error bars +/- 1SD.

3.5.3. Colony Forming Efficiency and Donor Age

Whole conjunctival CFE was determined as the average CFE reading from all 8 individual areas for each donor and was compared to donor age. There was a significant clustering of older donors. CFE significantly reduced with age as established using a generalised linear mixed model ($p < 0.01$). This model takes into account the pattern of data across all areas of the conjunctivas which is averaged when the data is demonstrated in Figure 63.

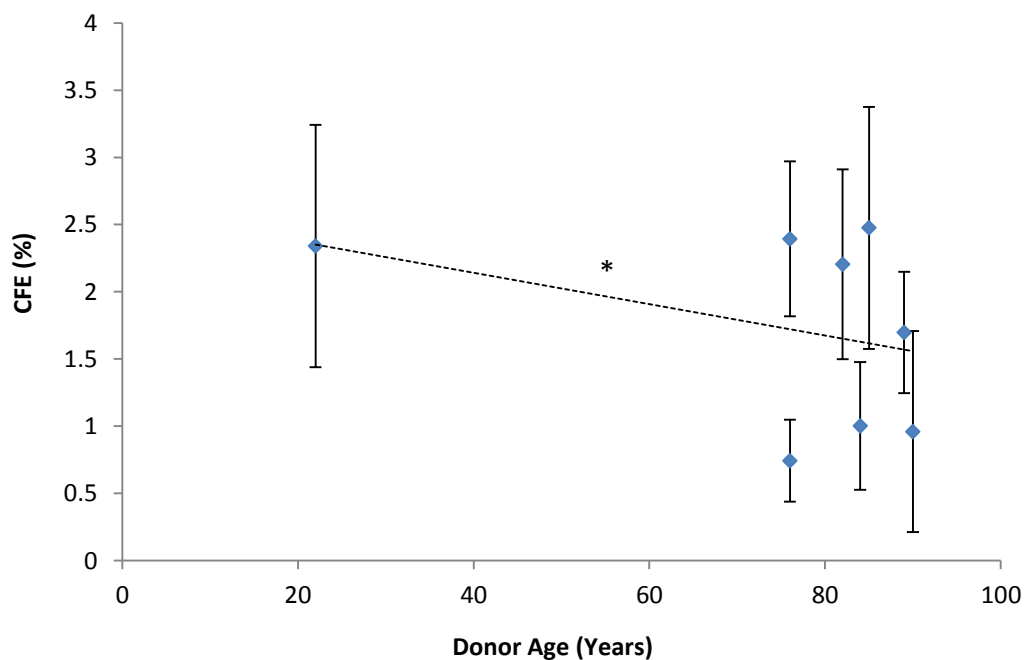


Figure 63: Line graph showing the variance in whole conjunctival CFE with donor age. A decrease in CFE value was demonstrated with increasing donor age ($p < 0.01$)*. Error bars +/-1SD, ---- linear trend line.

3.5.4. Colony Forming Efficiency and Post Mortem Retrieval Time

Whole conjunctival CFE was similarly compared to PMRT. All this tissue was retrieved within 24 hours of death with a range from 9-24 hours. Longer PMRTs were associated with significantly lower CFE values in culture by analysis with a generalised linear mixed model ($p < 0.01$). Again this model takes into account the pattern of data across all areas of the conjunctiva which is averaged when the data is shown in Figure 64.

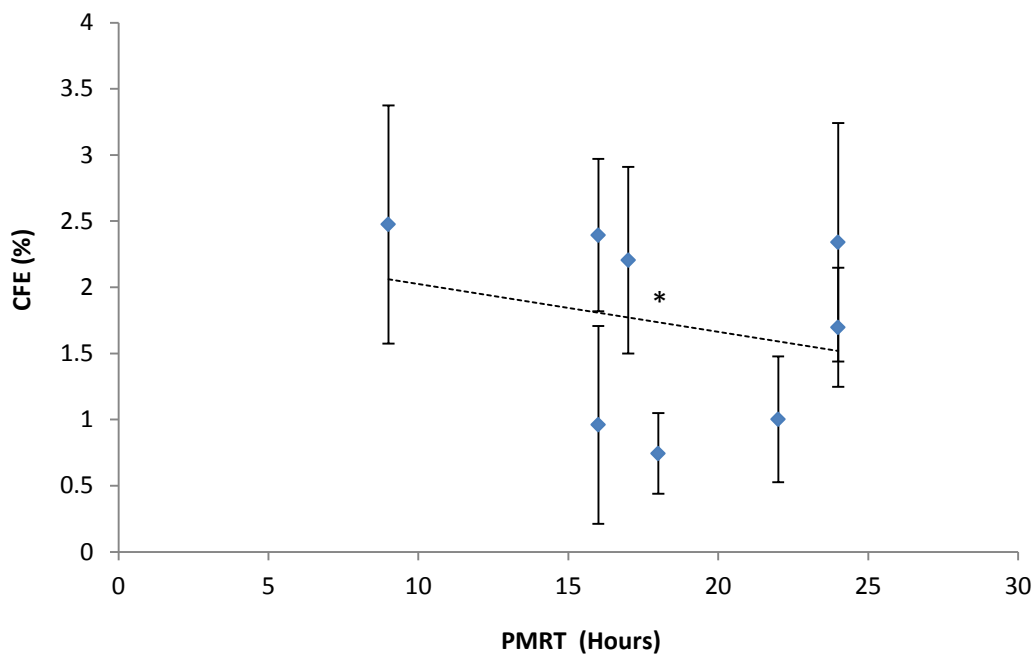


Figure 64: Line graph showing the variance in whole conjunctival CFE with PMRT. A decrease in CFE value was demonstrated with increasing PMRT ($p < 0.01$)*. Error bars $\pm 1SD$, ---- linear trend line.

3.5.5. Conjunctival versus Limbal Colony Forming Efficiency

Higher CFE was observed from limbal epithelial cell cultures than that from conjunctival epithelial cell cultures. No statistical analysis was possible due to insufficient limbal CFE values, but the trend was observed in both comparisons to overall conjunctival CFE and to conjunctival CFE from the medial canthal area alone. This data is demonstrated in Figure 65.

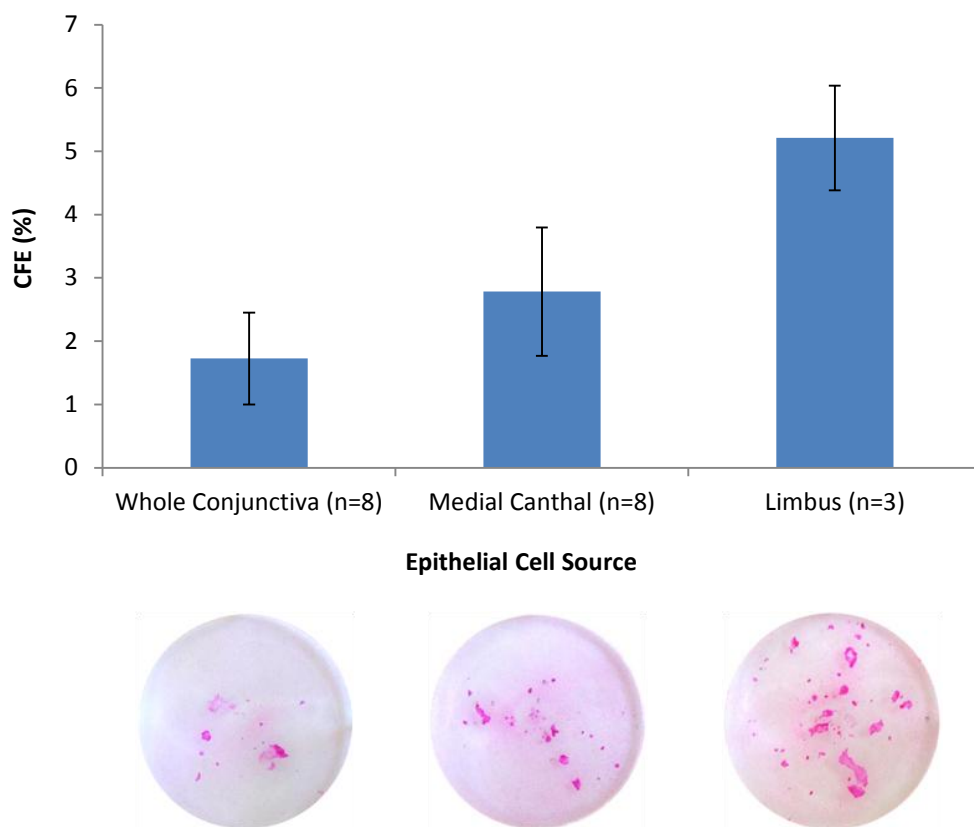


Figure 65: Histogram showing comparative CFE across the whole conjunctiva, medial canthal conjunctiva alone and limbus, with representative CFE images below each. Highest CFE is demonstrated in the limbus than either the whole conjunctiva or medial canthal area alone (insufficient data for statistical analysis). Error bars +/- 1SD.

3.6. Immunocytochemical Studies

Immunocytochemical studies were performed on cultures from the same 8 donors on which CFE assays were assessed, enabling direct comparisons.

3.6.1. Antibody Optimisation

Antibodies for immunocytochemical studies were optimised by comparing both different antibodies (in the case of ABCG2) and different antibody dilutions, using positive control cells. Optimal staining was assessed taking into account both staining intensity and minimal background staining. An example of antibody optimisation results for ABCG2 on MCF7 cells are shown in Figure 66. The final protocols used for each antibody are shown in Table 7.

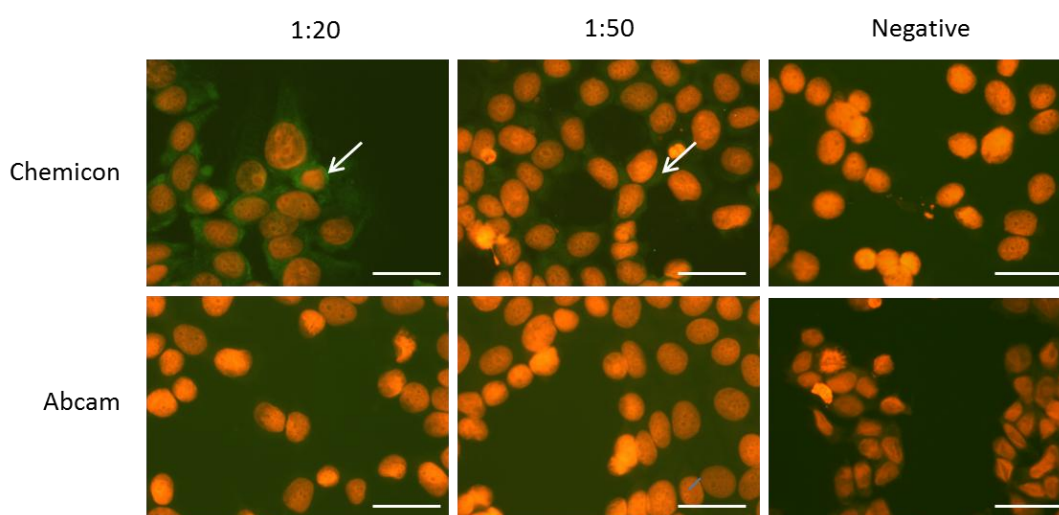


Figure 66: Photomicrographs of immunocytochemical antibody optimisation for ABCG2 using MCF7 cells and antibodies from both Chemicon and Abcam at both 1:20 and 1:50 antibody dilutions. Positive immunoreactivity in green is observed in the cytoplasm (arrows), with PI nuclear counterstaining in red. Scale bars 25 μ m. In this case, optimal staining was achieved with the Chemicon antibody at 1:20 dilution, and was used as a final protocol.

The ABCG2 antibody supplied by Chemicon was used in preference to that supplied by Abcam. Despite numerous attempts at optimisation on positive control samples no clear positive immunocytochemical staining was obtained with p63 (clone 4A4), N-Cadherin or CD168 antibodies. These antibodies were therefore not used in any further analyses.

Antibody	Clone	Source	Antibody Dilution	Secondary Antibody*
CK19	RCK108	Dako	1:50	Anti-mouse
ABCG2	21	Chemicon	1:20	Anti-mouse
p63	Δ N	Biolegend	1:100	Anti-rabbit
Hsp70	BRM-22	Abcam	1:1000	Anti-mouse

Table 7: Table of optimised immunocytochemical protocols for different antibodies used. *Secondary antibody is alexafluor 488 goat anti-mouse or -rabbit

3.6.2. Grading of Immunocytochemical Staining

Immunocytochemical staining was graded qualitatively as described in Section 2.7.3. An example of staining images for each grade is demonstrated Figure 67.

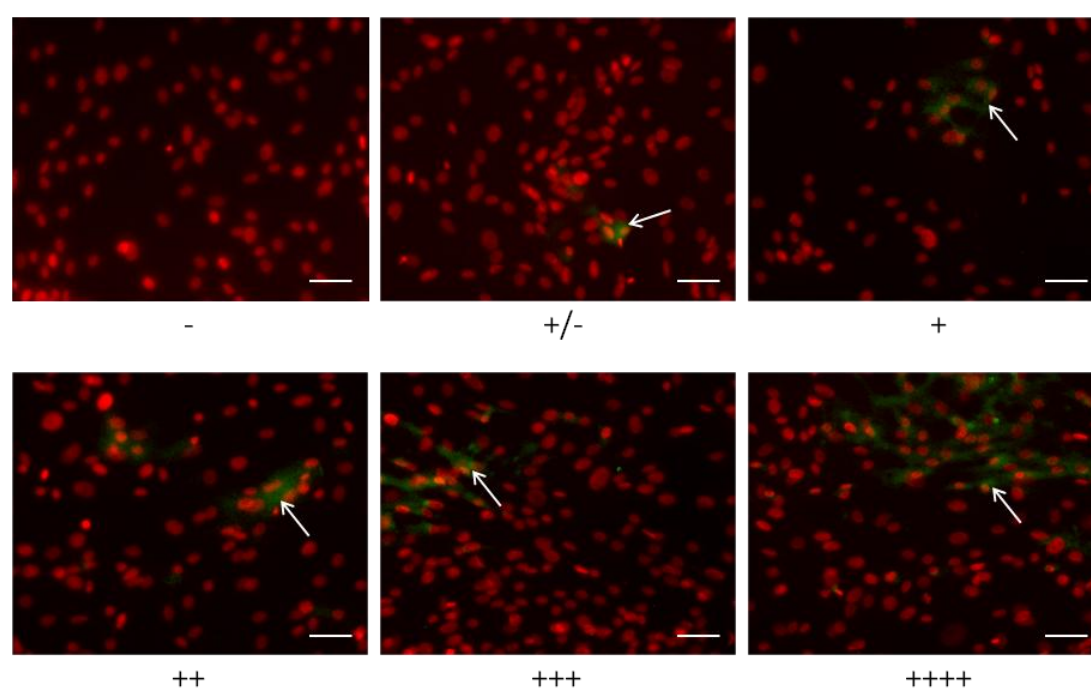


Figure 67: Examples of photomicrographs of immunocytochemical staining for Hsp70 to demonstrate the immunoreactivity grading scale employed (the number of positively staining cells per average of 5 x20 fields of view: 0 cells: -, <5 cells: +/-, 5-10 cells: +, 10-15 cells: ++, 15-20 cells: +++, >20 cells: +++++). Positive immunoreactivity is observed in green (arrows) with PI nuclear counter-staining in red. Scale bars 50 μ m.

3.6.3. Cytokeratin 19 Staining

Intense CK19 staining was demonstrated consistently across all cultures used for immunocytochemical staining, confirming the presence of conjunctival epithelial cells in culture. This is shown in Figure 68.

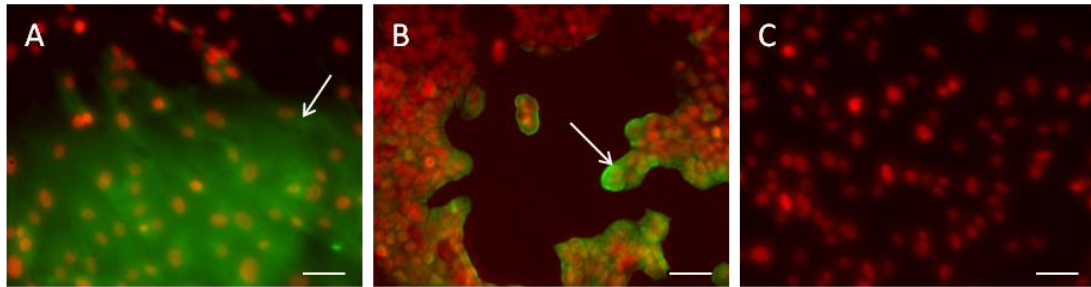


Figure 68: Photomicrographs of immunocytochemical staining for CK19. Positive immunoreactivity is observed throughout the cytoplasm in green (arrows), with PI nuclear counter-staining in red. A) Intense staining of conjunctival epithelial cells, B) MCF7 positive control and C) negative control. Scale bars 50 μ m.

3.6.4. Further Immunocytochemical Staining

Immunocytochemical staining with ABCG2, Δ Np63, and Hsp70 antibodies were assessed on passage 1 cultures from all 8 regions of the conjunctiva as described in Figure 12, and from the same 8 donor tissues which were used for CFE analysis. This enabled comparative data across the conjunctival tissue as a whole to be obtained and correlations to be made with proliferative potential in culture.

Data for each of these markers is presented in Sections 3.6.5 to 3.6.7 with sample images from one donor (tissue 19) presented on a schematic diagram of the conjunctiva. The overview of comparative sites compared on the schematic diagrams is labelled in Figure 16.

3.6.5. ABCG2 Staining

ABCG2 staining was demonstrated in a proportion of cells cultured from all regions across the conjunctiva. Staining was not noted to be predominantly at the cell membrane, but rather also consistently within the cytoplasm. Clusters of positively staining cells were usually found in close proximity. An example is shown in Figure 69.

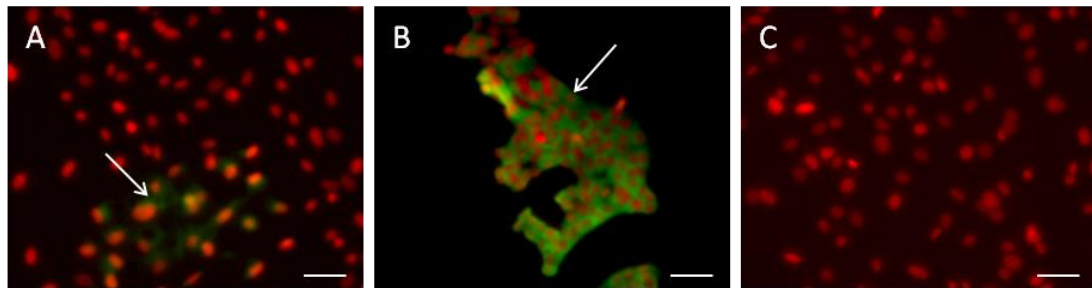


Figure 69: Photomicrographs of immunocytochemical staining for ABCG2. Positive immunoreactivity is observed throughout the cytoplasm in green (arrows), with PI nuclear counter-staining in red. A) A collection of positively staining conjunctival epithelial cells, B) MCF7 positive control and C) negative control. Scale bars 50 μ m.

Staining patterns were consistently demonstrated across the different anatomical areas for each donor tissue, with significant variation across the tissue as a whole as assessed by a Friedman test ($p < 0.01$). Highest levels of staining were demonstrated in the medial canthal and forniceal areas, especially inferiorly. Statistically significance was noted to both the higher level of staining in the medial canthal area alone ($p < 0.01$), and in the medial canthal and inferior forniceal areas grouped together ($p < 0.01$), as assessed by a Wilcoxon signed rank test. Lowest levels of staining were demonstrated in the tarsal conjunctival epithelium, hence the pattern of increased staining in the forniceal than bulbar than tarsal areas was again apparent. An example of the pattern of staining across the whole conjunctiva from one donor is demonstrated in Figure 70 and the overall gradings averaged from all 8 donors in Figure 71 and Figure 72.

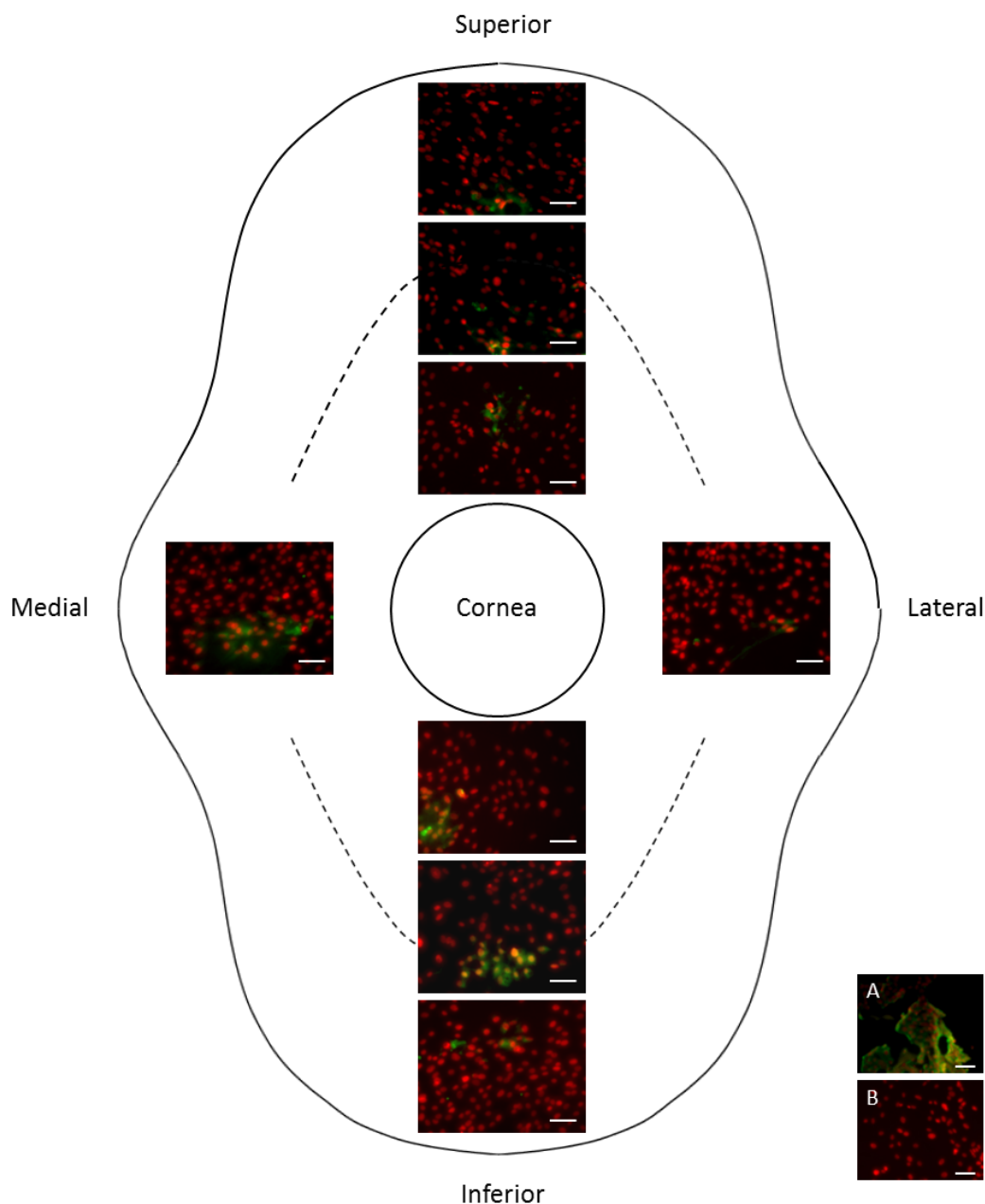


Figure 70: Schematic diagram of the human conjunctiva (as labelled in Figure 16) with fornices represented by dashed lines (----), demonstrating photomicrographs of immunocytochemical staining for ABCG2 across 8 areas of the conjunctiva from one donor (tissue 19). Positive immunoreactivity is observed at the cell membranes and within the cytoplasm in clusters of cells in green, with PI nuclear counter-staining in red. In this example, larger clusters of positively staining cells are observed in the medial canthal and inferior forniceal areas. A) MCF7 positive control, B) negative control. Scale bars 50 μ m.

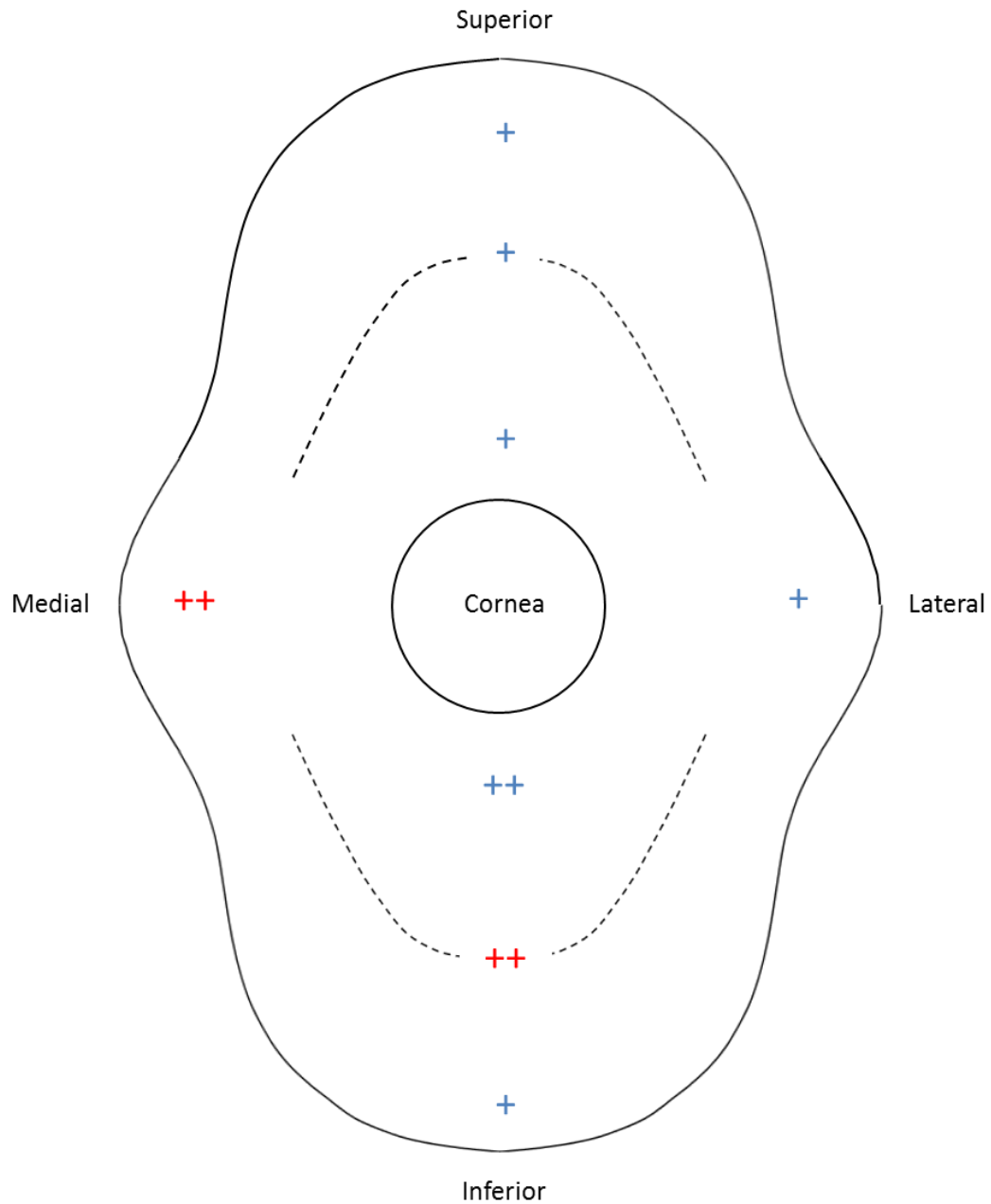


Figure 71: Schematic diagram of the human conjunctiva (as labelled in Figure 16) with fornices represented by dashed lines (-----), demonstrating average grades of immunocytochemical reactivity for ABCG2 in cell cultures from 8 areas of the conjunctiva from 8 separate donors. Highest grades of staining were observed in the medial canthal ($p < 0.01$) (red) and together with inferior forniceal ($p < 0.01$) (red) and inferior bulbar areas compared to other areas.

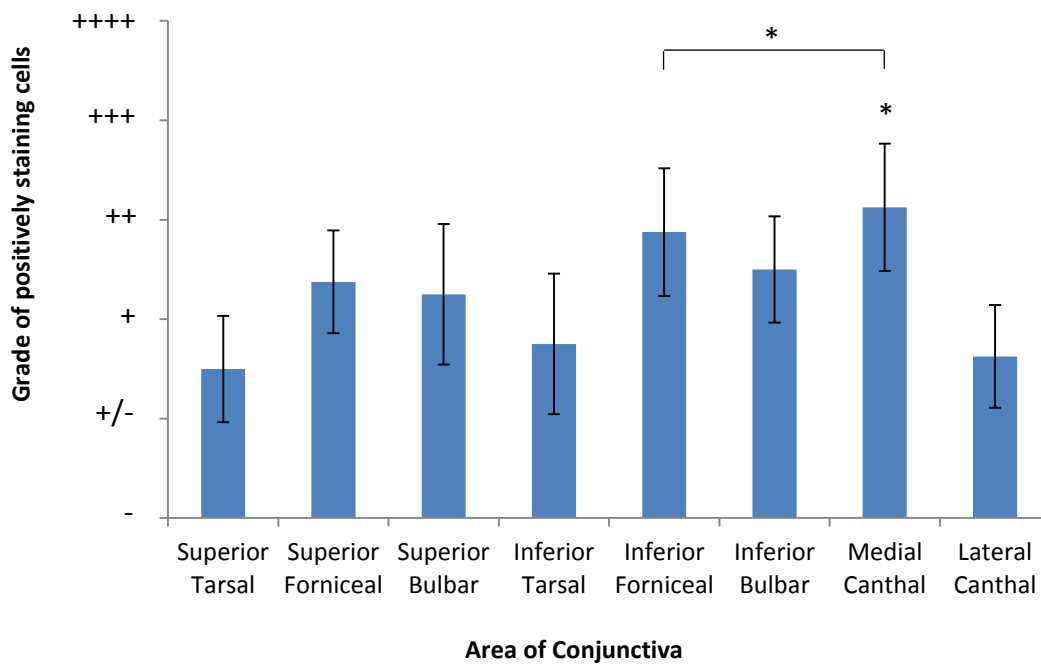


Figure 72: Histogram demonstrating the overall level of ABCG2 staining in cell cultures from 8 different areas of the conjunctiva from 8 separate donors. Highest grades of staining were observed in the medial canthal ($p < 0.01$)* together with inferior forniceal areas ($p < 0.01$)*. Error bars +/- 1SD.

3.6.6. Δ Np63 Staining

Δ Np63 staining was similarly demonstrated in a proportion of cells cultured from all regions across the conjunctiva. Staining was entirely nuclear, hence no secondary PI nuclear stain was employed. Fewer cells were noted to stain for Δ Np63 than for ABCG2. They were demonstrated both in clusters and in isolation. An example is shown in Figure 73.

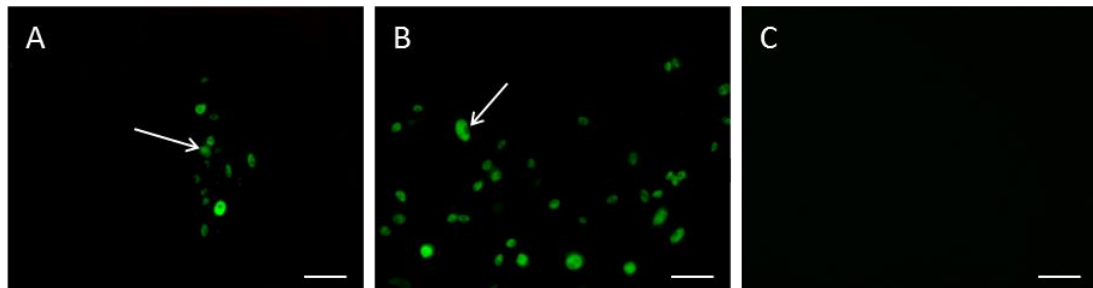


Figure 73: Photomicrographs of immunocytochemical staining for Δ Np63. Positive immunoreactivity is observed in the nuclei in green (arrows). A) A collection of positively staining conjunctival epithelial cells, B) limbal positive control and C) negative control. Scale bars 50 μ m.

Patterns were similarly consistently demonstrated across each donor tissue, with significant variation across the tissue as a whole as assessed by a Friedman test ($p < 0.01$). Highest levels of staining were again demonstrated in the medial canthal and forniceal areas, especially inferiorly. Statistically significant higher levels of staining were noted in the medial canthal area alone ($p < 0.01$), and the medial canthal and inferior forniceal areas grouped together ($p < 0.01$), as assessed by a Wilcoxon signed rank test. The same patterns of higher staining in the forniceal than bulbar than tarsal areas was again apparent. An example of the pattern of staining across the whole conjunctiva from one donor is demonstrated in Figure 74 and the overall gradings averaged from all 8 donors in Figure 75 and Figure 76.

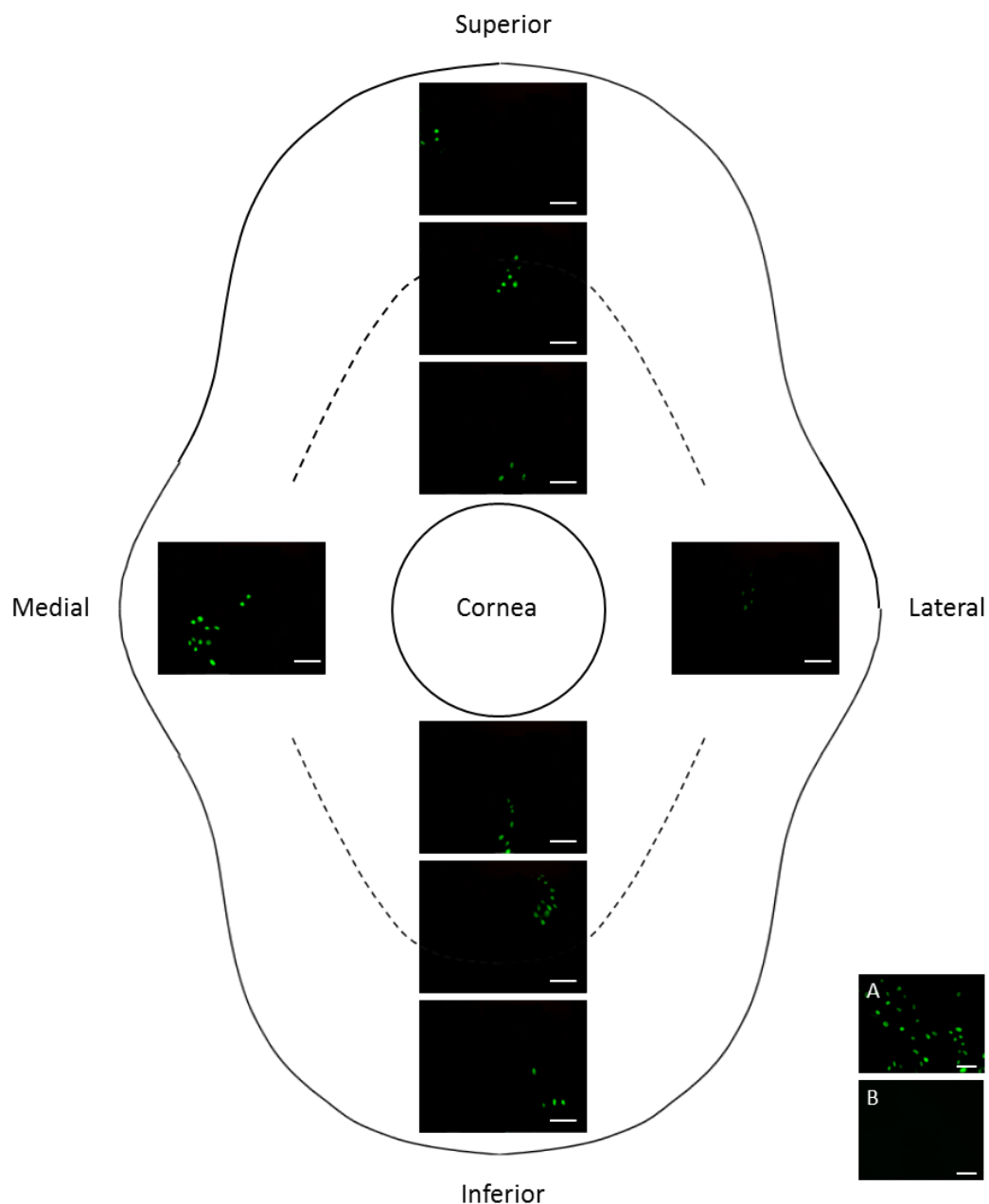


Figure 74: Schematic diagram of the human conjunctiva (as labelled in Figure 16) with fornices represented by dashed lines (----), demonstrating photomicrographs of immunocytochemical staining for $\Delta Np63$ across 8 areas of the conjunctiva from one donor (tissue 19). Positive immunoreactivity is observed in the nuclei of clusters of cells in green. In this example, the largest clusters of positively staining cells are observed in the medial canthal area. A) Limbal positive control, B) negative control. Scale bars $50\mu\text{m}$.

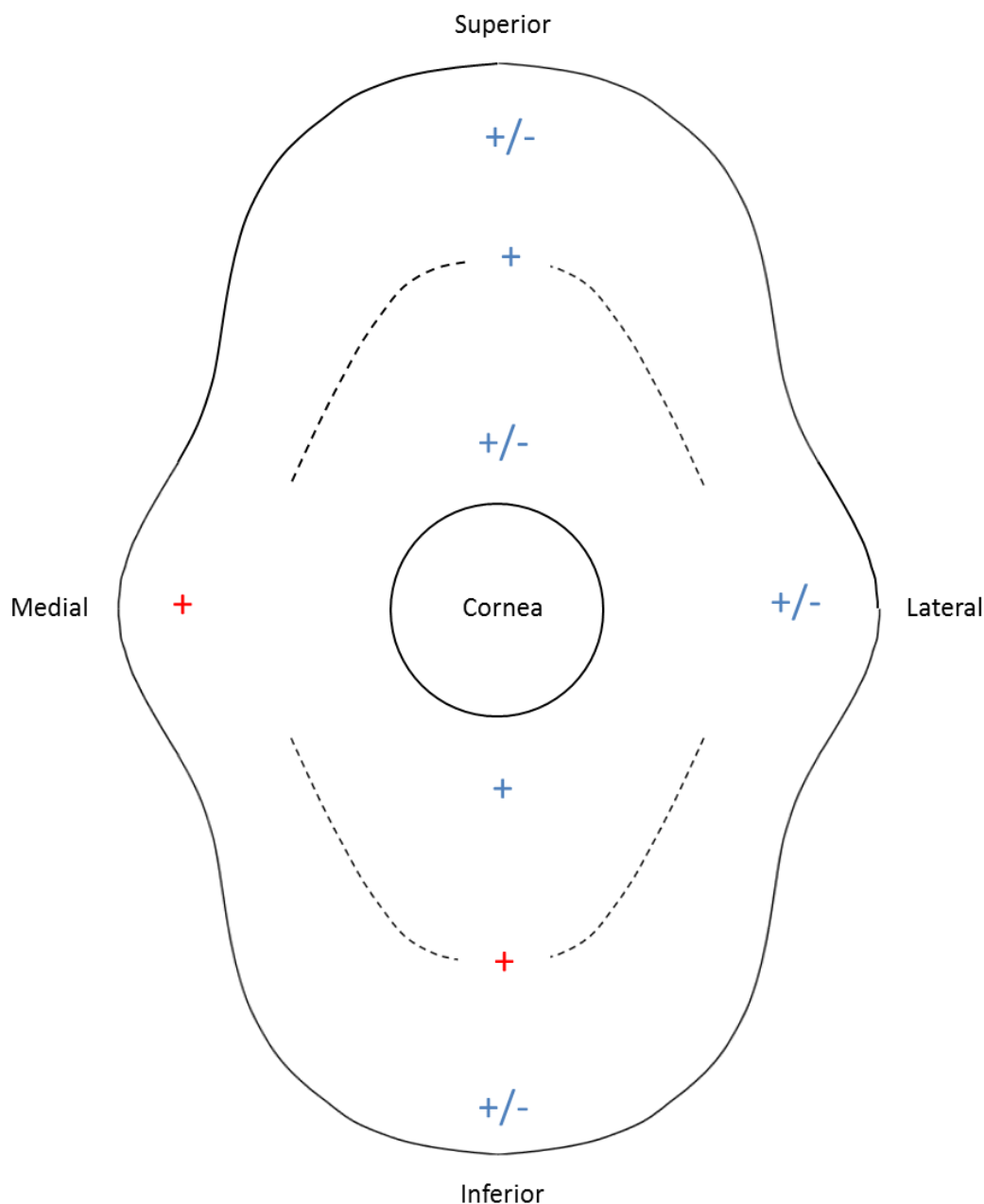


Figure 75: Schematic diagram of the human conjunctiva (as labelled in Figure 16) with fornices represented by dashed lines (-----), demonstrating average grades of immunocytochemical reactivity for $\Delta Np63$ in cell cultures from 8 areas of the conjunctiva from 8 separate donors. Highest grades of staining were observed in the medial canthal ($p < 0.01$) (red) and together with inferior forniceal ($p < 0.01$) (red) and inferior bulbar areas compared to other areas.

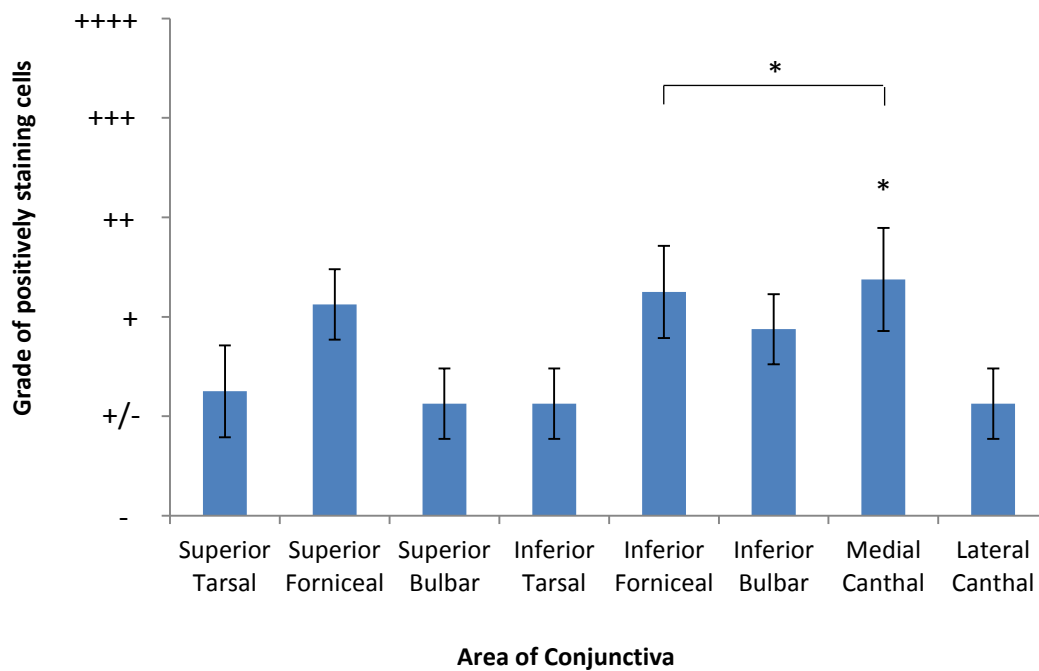


Figure 76: Histogram demonstrating the overall level of Δ Np63 staining in cell cultures from 8 different areas of the conjunctiva from 8 separate donors. Highest grades of staining were observed in the medial canthal ($p < 0.01$)* together with inferior forniceal areas ($p < 0.01$)*. Error bars +/- 1SD.

3.6.7. Hsp70 Staining

Cells staining positively for Hsp70 were similarly demonstrated in a proportion of cells cultured from all regions across the conjunctiva. Staining was uniformly cytoplasmic, usually in clusters of cells together. Proportionately greater number of cells were noted to stain positively for Hsp70 than either Δ Np63 or ABCG2. An example is shown in Figure 77.

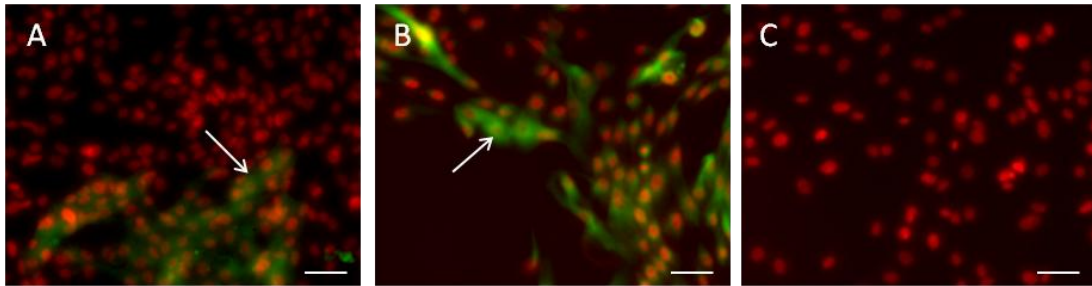


Figure 77: Photomicrographs of immunocytochemical staining for Hsp70. Positive immunoreactivity is observed throughout the cytoplasm in green (arrows), with PI nuclear counter-staining in red. A) A collection of positively staining conjunctival epithelial cells, B) limbal positive control and C) negative control. Scale bars 50 μ m.

Again staining patterns were consistently demonstrated across each donor tissue, with significant variation across the tissue as a whole as assessed by a Friedman test ($p < 0.01$), with highest levels of staining in the medial canthal area alone ($p < 0.01$) and the medial canthal with inferior forniceal areas ($p < 0.01$) as assessed by a Wilcoxon signed rank test, and lowest levels in the tarsal areas. The pattern of forniceal staining greater than bulbar than tarsal areas was again replicated. An example of the pattern of staining across the whole conjunctiva from one donor is demonstrated in Figure 78 and the overall gradings averaged from all 8 donors in Figure 79 and Figure 80.

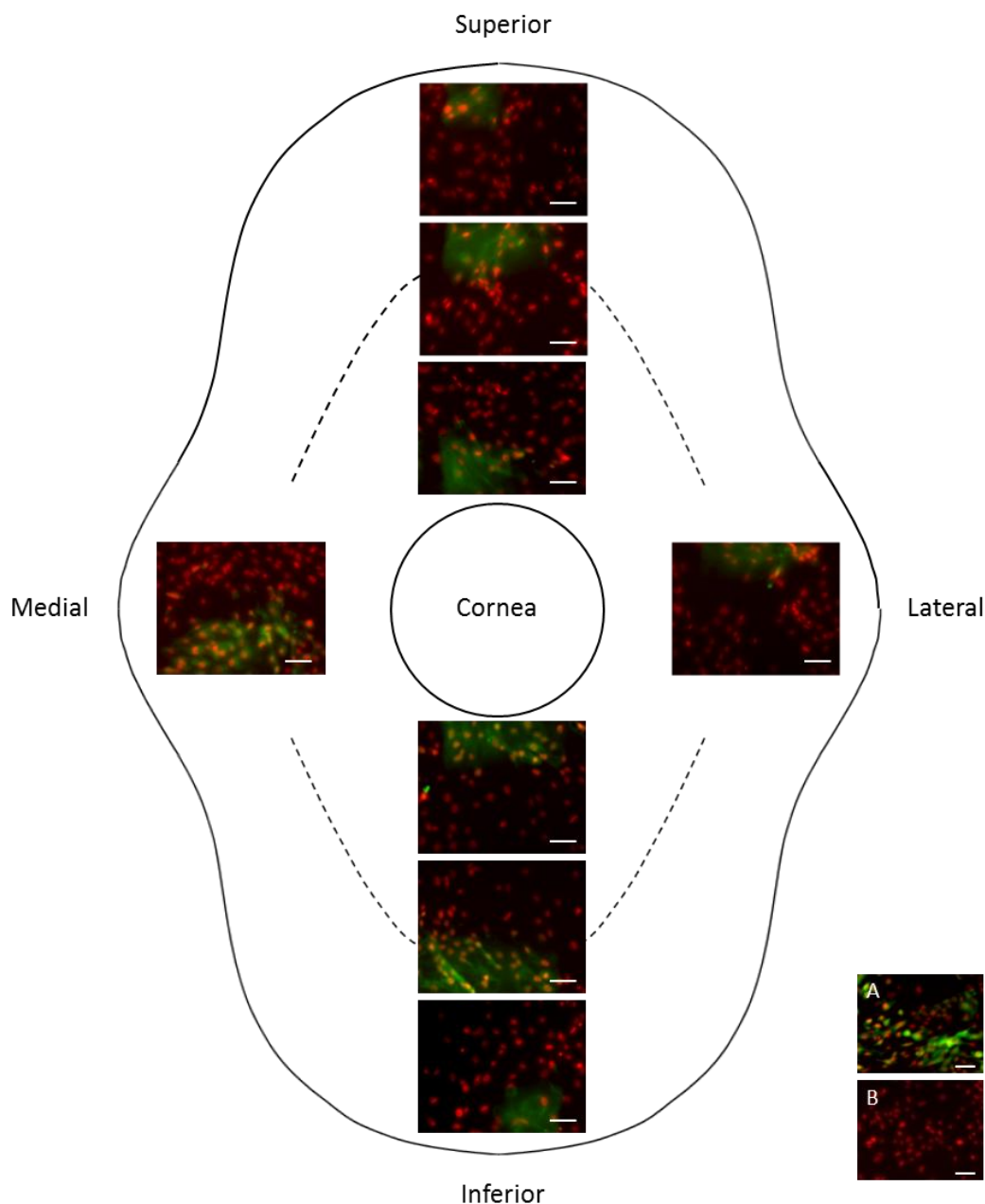


Figure 78: Schematic diagram of the human conjunctiva (as labelled in Figure 16) with fornices represented by dashed lines (----), demonstrating photomicrographs of immunocytochemical staining for Hsp70 across 8 areas of the conjunctiva from one donor (tissue 19). Positive immunoreactivity is observed throughout the cytoplasm in clusters of cells in green, with PI nuclear counter-staining in red. In this example, large clusters of positively staining cells are observed throughout all areas of the conjunctiva but less so in the tarsal areas. A) Limbal positive control, B) negative control. Scale bars 50 μ m.

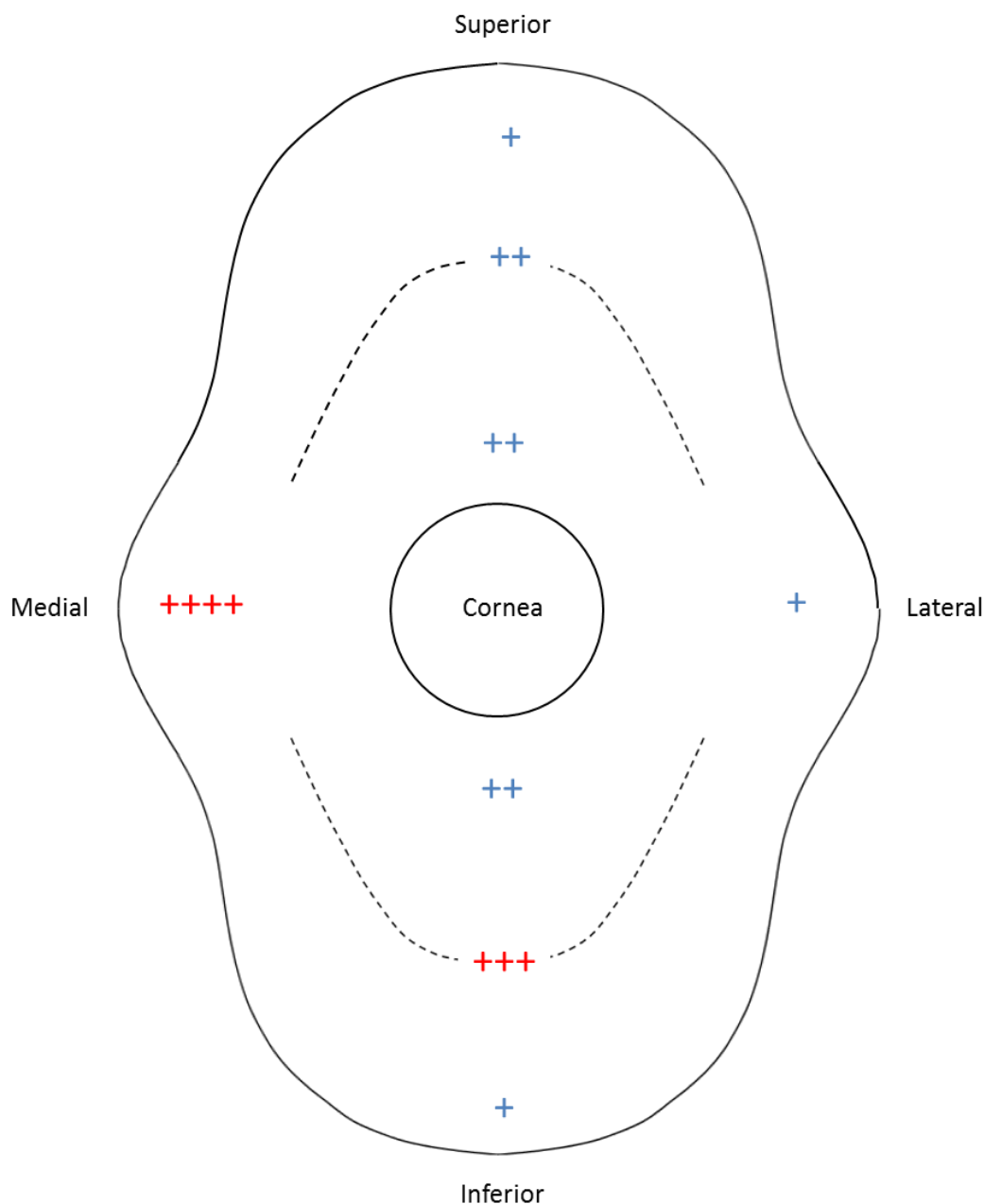


Figure 79: Schematic diagram of the human conjunctiva (as labelled in Figure 16) with fornices represented by dashed lines (-----), demonstrating average grades of immunocytochemical reactivity for Hsp70 in cell cultures from 8 areas of the conjunctiva from 8 separate donors. Highest grades of staining were observed in the medial canthal ($p < 0.01$) (red) and together with inferior forniceal areas ($p < 0.01$) (red), compared to other areas.

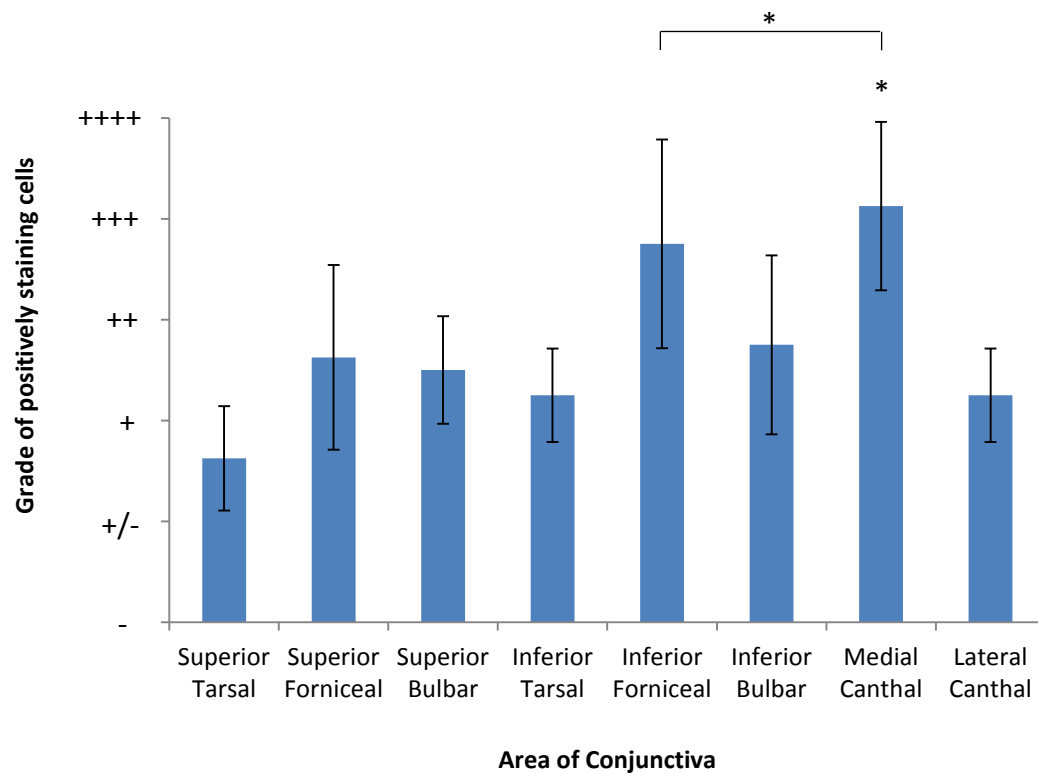


Figure 80: Histogram demonstrating the overall level of Hsp70 staining in cell cultures from 8 different areas of the conjunctiva from 8 separate donors. Highest grades of staining were observed in the medial canthal ($p < 0.01$)* together with inferior forniceal areas ($p < 0.01$)*. Error bars +/- 1SD.

3.6.8. Correlation between the Immunocytochemical Stains

In order to ascertain whether there was a correlation between the distribution patterns of staining with each SC marker from cultures across different anatomical areas of the conjunctiva, a Kendall's Tau correlation coefficient was employed. This showed significant correlations between each stain independently ($p < 0.01$ for each).

3.6.9. Immunocytochemical Staining and Donor Age

It was already established that there was a significant clustering of older donors for the tissue used for CFE and immunocytochemical studies, as demonstrated in Figure 63. Whole conjunctival immunocytochemical staining was determined as the average staining from all 8 individual areas for each donor and was compared to donor age. Significantly lower staining to ABCG2 and Hsp70 were noted with increasing donor age ($p < 0.01$ for each), as assessed using a generalised linear mixed model. No relationship was however evident between Δ Np63 staining and donor age ($p > 0.1$). By taking into account the pattern of staining values across the whole conjunctiva, statistical significance is achieved even though the linear trend lines of the average grades do not always appear to show a clear correlation. This data is shown in Figure 81.

3.6.10. Immunocytochemical Staining and Post Mortem Retrieval Time

Whole conjunctival immunocytochemical staining was similarly compared to PMRT. Longer PMRT was associated with significantly lower levels of ABCG2 staining ($p < 0.01$), but no relationship was evident between staining intensity of Δ Np63 ($p = 0.45$) or Hsp70 ($p > 0.1$), as also assessed using a generalised linear mixed model. This data is shown in Figure 82.

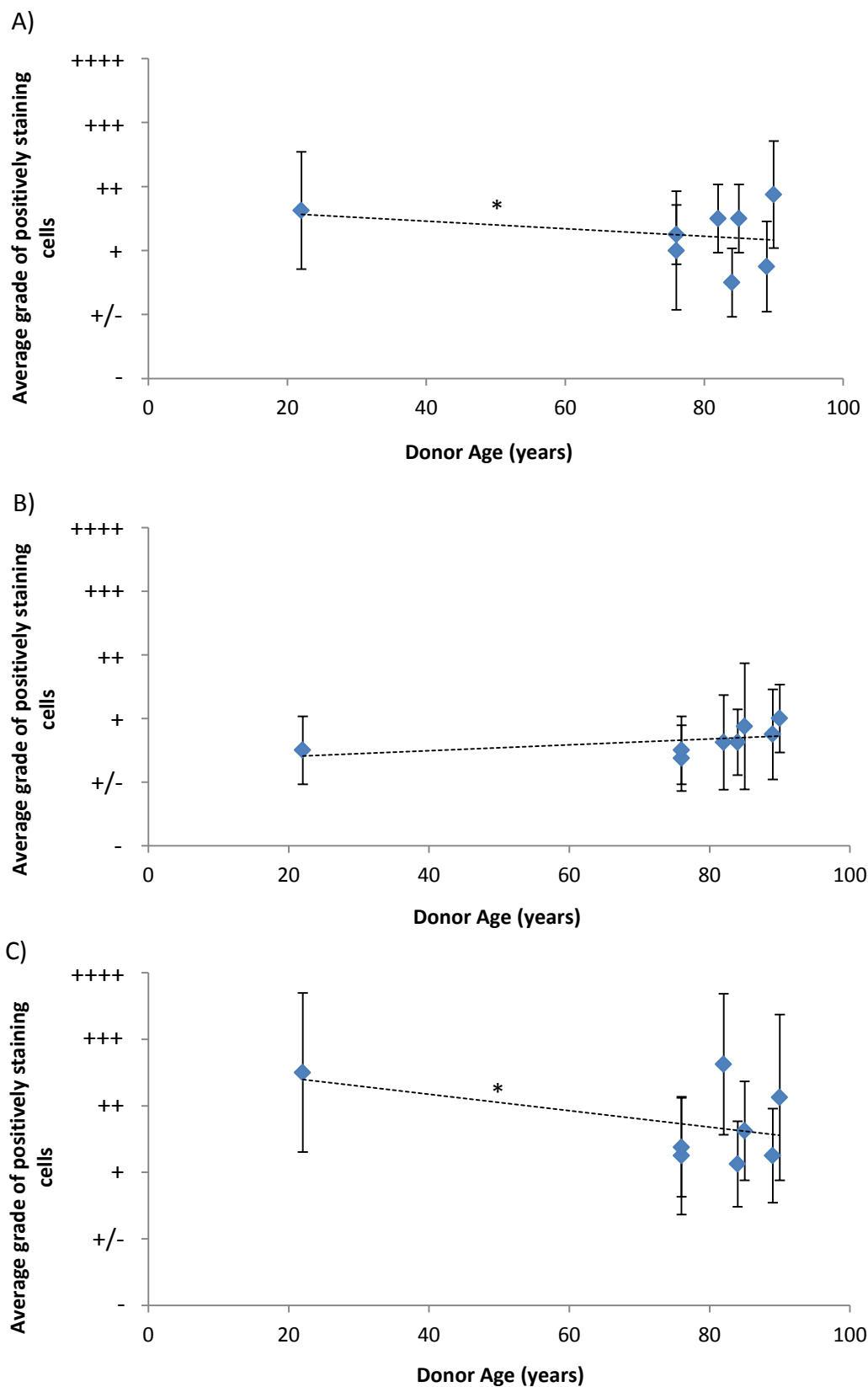


Figure 81: Line graphs showing the variance in conjunctival cell culture staining for A) ABCG2, B) Δ Np63 and C) Hsp70 with donor age. A reduction in both ABCG2 and Hsp70 staining is observed with increasing donor age ($p < 0.01$ for each)*, but no relationship was evident between Δ Np63 staining and donor age. Error bars +/-1SD, ---- linear trend lines.

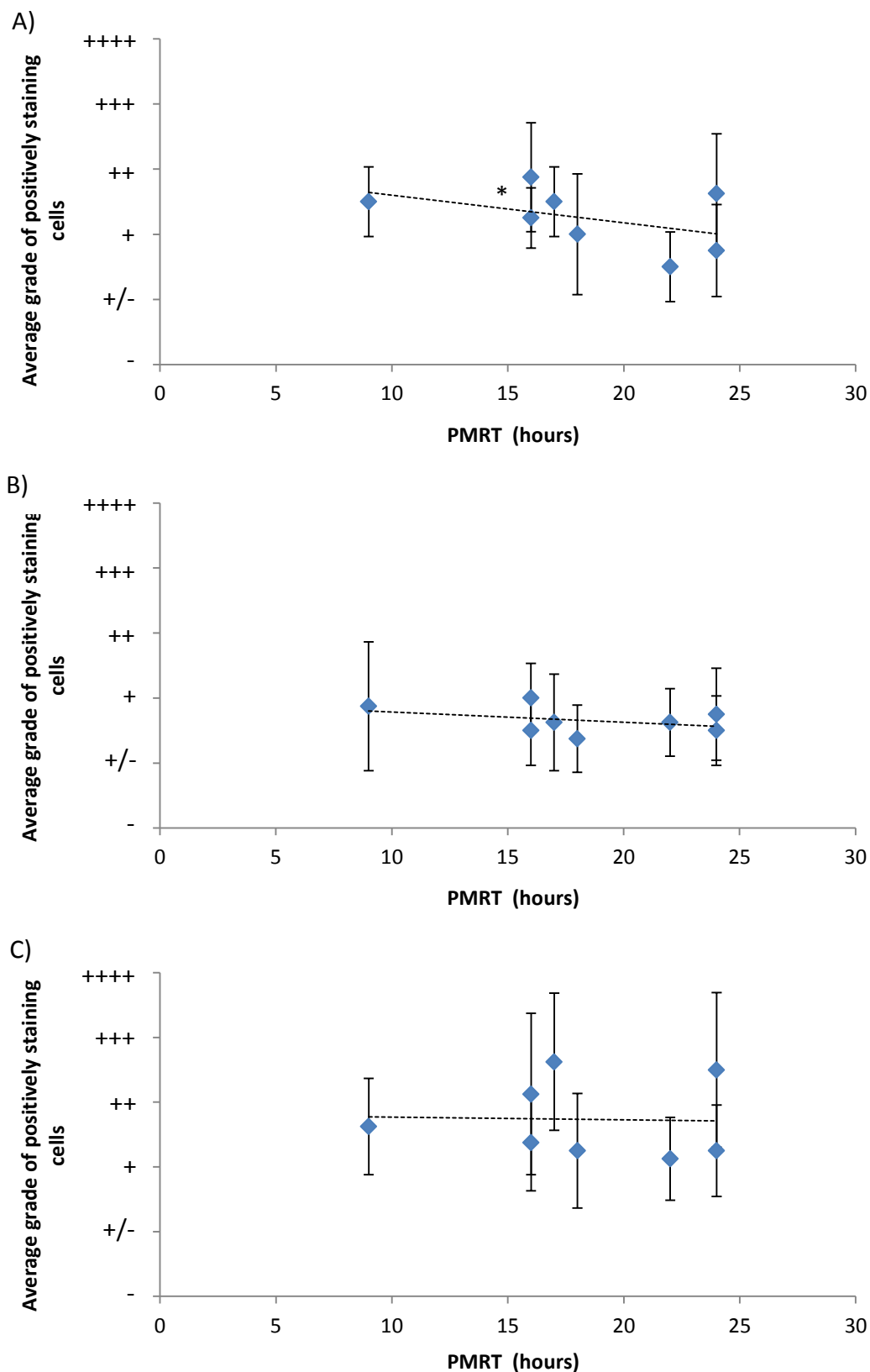


Figure 82: Line graphs showing the variance in conjunctival cell culture staining for A) ABCG2, B) Δ Np63 and C) Hsp70 with PMRT. A reduction in ABCG2 staining is observed with increasing PMRT ($p < 0.01$)*, but no relationship was evident between Δ Np63 or Hsp70 staining and PMRT. Error bars +/-1SD, ---- linear trend lines.

3.7. Stem Cell Marker Staining and Colony Forming Efficiency

A Kendall's Tau correlation coefficient using all eight tissue areas was employed to assess the correlation between the different putative SC marker staining by immunocytochemistry and CFE. Significant associations were noted between each marker independently ($p < 0.01$ for each).

Similarly, the immunohistochemical staining for ABCG2 was also correlated to both CFE, and to the immunocytochemical staining for each SC marker using a Kendall's Tau correlation. These analyses only included data from 5 donors which were used in both assessments. Significant associations were noted between ABCG2 immunohistochemical staining and CFE ($p < 0.01$), and between ABCG2 immunohistochemical staining and each SC marker immunocytochemical staining independently ($p < 0.01$ for each).

3.8. Conjunctival Cell Growth on Extracellular Matrix Proteins

Conjunctival epithelial cells grew on all three extracellular matrix proteins showing similar morphology on each to those control cultures on 3T3 feeder layer (Figure 83). However growth rates varied.

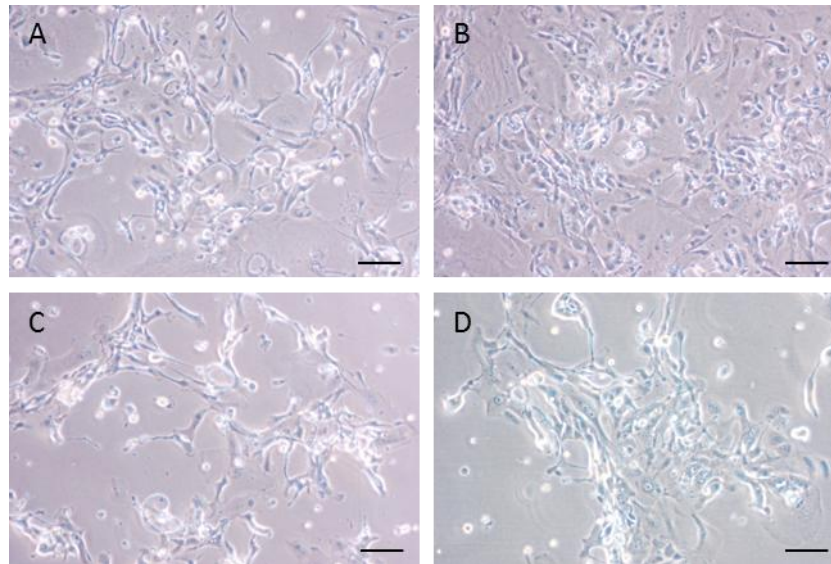


Figure 83: Phase contrast micrographs of conjunctival epithelial cell growth on A) collagen IV, B) fibronectin, C) laminin 1 and D) 3T3 feeder layer at day 10. Similar cell morphology is observed on each extracellular matrix protein but with greater number of cells evident on B) fibronectin. Scale bars 100 μ m.

Higher growth rates were demonstrated on fibronectin than on collagen IV than on laminin 1. This was statistically significant with one-way ANOVA testing at day 7 ($p < 0.01$) but not at day 10 ($p > 0.06$). Indeed, the difference in growth rates between fibronectin and laminin 1 alone at day 10 by Student's paired t -test were not significant ($p > 0.05$). This data is demonstrated in Figure 84.

Despite staining the conjunctival cells grown on the 3T3 feeder layer with CK19 it proved impossible in practice to differentiate the conjunctival nuclei from the 3T3 nuclei. Conjunctival epithelial cell culture was previously shown not to be supported by tissue culture plastic alone. Thus a control growth curve was not obtainable for comparative growth in this experiment.

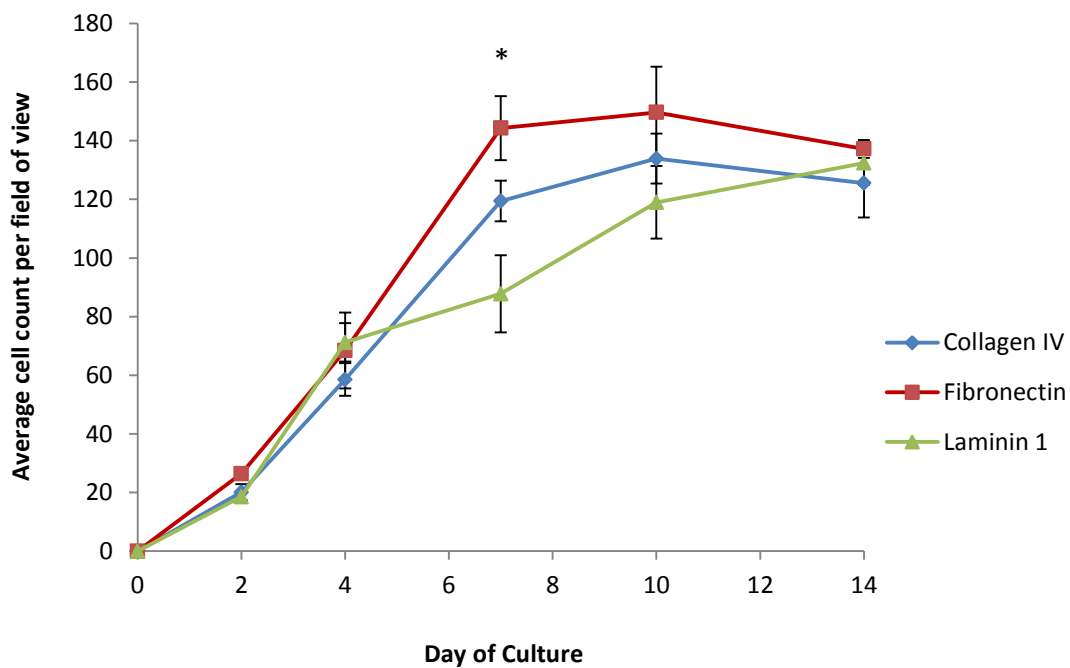


Figure 84: Line graph showing conjunctival epithelial cell growth curves on various extracellular matrix protein coatings. Highest growth rates were observed on fibronectin, with significant differences seen at day 7 ($p < 0.01$)*, but there was no significant difference between growth on any extracellular matrix protein by day 10. Error bars +/- 1 SD.

3.9. Summary of Key Findings

Development of a technique to retrieve whole human cadaveric conjunctiva has enabled an assessment of expression of a SC (ABCG2) and TAC (p63) marker in fixed tissue, clonogenic ability, and expression of several SC markers (ABCG2, Δ Np63 and Hsp70) in cell cultures, all across the tissue as a whole. Each component of this study demonstrates clear evidence that conjunctival PCs exist throughout the tissue but with significantly higher levels in a region comprising the medial canthal and inferior forniceal areas. Given the CFE and SC marker expression in cell cultures were undertaken on cultures from the same 8 donors, this data can be clearly summarised in an overall comparative chart (**Figure 85**).

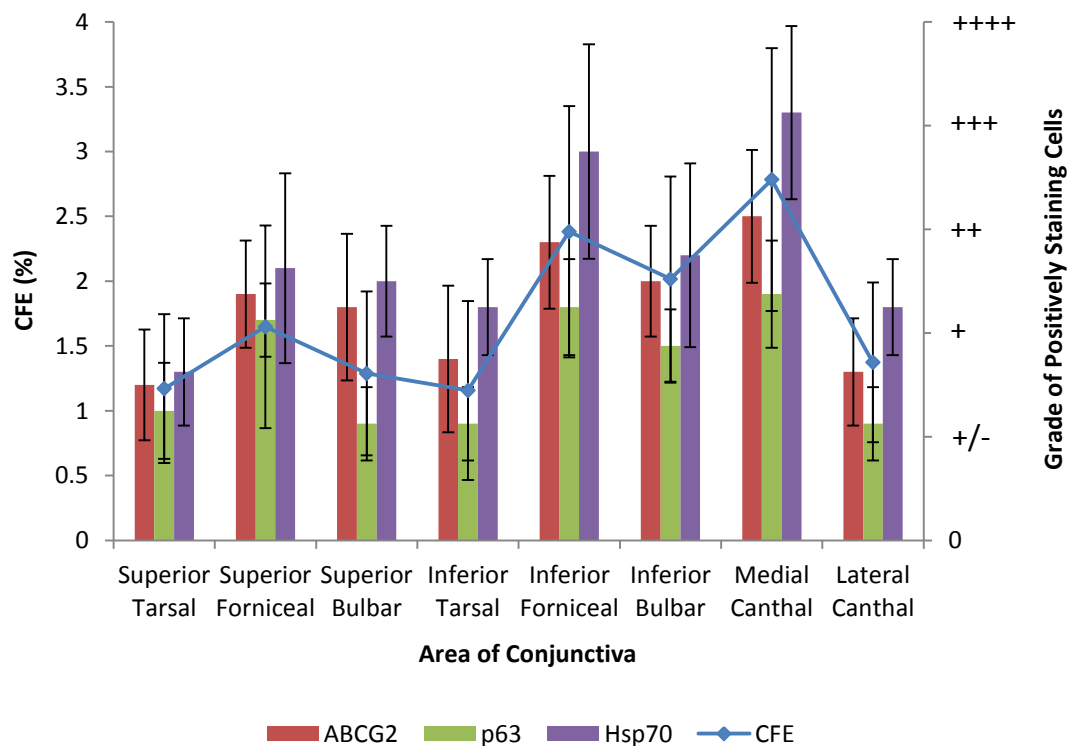


Figure 85: Overall graph showing both CFE and expression of the SC markers ABCG2, Δ Np63 and Hsp70 in cell cultures from 8 donors across 8 different areas of the human conjunctiva. Error bars +/- 1SD.

The significant correlations between each of the patterns of distribution of ABCG2 in fixed tissue, CFE, and expression of each SC marker in cell cultures adds further credence to this pattern of human conjunctival PC distribution.

Evidence is also presented that both increasing age and PMRT are associated with a reduction in ABCG2 expression in both fixed tissue and cell cultures, CFE.

4. Discussion

The conjunctiva is a mucous membrane that forms the majority of the ocular surface. It is of integral importance both to provide immunological defence and also to sustain a healthy tear film containing mucins. The tear film is essential; not only to maintain and prevent desiccation of a healthy corneal epithelium thus preserving vision, but the antimicrobial proteins and scaffold of mucins within bind and trap bacterial pathogens thus also preventing ocular infection (Gipson, 2004).

The conjunctiva is susceptible to a wide spectrum of diseases causing a considerable burden to society. This includes a significant cohort such as trachoma, chemical and thermal burns, mucous membrane pemphigoid and Stevens-Johnson syndrome, which may result in cicatrization, chronically painful eyes and blindness (Burton and Mabey, 2009, Radford *et al.*, 2012). Treatment modalities for these severe inflammatory disorders are presently very limited and primarily aimed at alleviation of symptoms and prevention of disease progression. Transplantation of a conjunctival epithelium offers potential to restore a healthy ocular surface in cases of extensive conjunctival scarring. *Ex vivo* expansion of cells enables large autografts to be generated, but both goblet cells and SCs must be present, both to produce a functioning conjunctival epithelium and to facilitate long-term success (Holland, 1996, Pellegrini *et al.*, 1999). To achieve this goal the conjunctival SCs must first be localised and characterised (Mason *et al.*, 2011). This is the first study to comprehensively assess the distribution of PCs across the whole human conjunctiva.

Conjunctival Tissue for Research

There has been a relative paucity of research into the pathophysiology of and potential treatments for conjunctival diseases compared to diseases affecting other structures in the eye. This may in part be explained by the comparative rarity of

blinding conjunctival disease in the Western world, but may also be attributable to a lack of human tissue for research.

Although animal models are available for research they often do not accurately reflect the anatomical or pathophysiological state of the human being, may not be susceptible to the same diseases, and knockout models of specific diseases may not be available. Human conjunctival cells may be obtained for research by impression and brush cytology techniques but these only enable collection of the superficial epithelial layers and disturb the normal anatomy (Calonge *et al.*, 2004, Tsubota *et al.*, 1990). Small samples of full thickness conjunctiva may be obtained from surgical specimens (Ang *et al.*, 2004a) or cadaveric donors (Cook *et al.*, 1998), but many studies would benefit from assessment of larger sheets of tissue or indeed the tissue as a whole, enabling comparison of different areas.

The technique I have developed to retrieve whole cadaveric conjunctiva (as described in Figure 17 and Figure 18) is relatively simple, yet innovative. Great care is required to preserve the integrity of the tarsal epithelium as initial samples revealed damage likely attributable to instrument handling (Figure 19), but this technique could easily be performed by those with basic surgical training or researchers with experience of tissue dissection. Single-use disposable instruments were used for all retrievals in this study to comply with the standards for eye retrieval for transplantation and research (The Royal College of Ophthalmologists, 2008, UK Blood Transfusion and Tissue Transplantation Services, 2013) and in order to minimise the risk of transmission of variant Creutzfeldt-Jakob Disease (vCJD) (National Institute for Health and Clinical Excellence, 2006), as consent had also been obtained for the eyes to be used for transplantation. Despite splitting of the eyelids antero-posteriorly to obtain the tarsal conjunctiva, good aesthetic results were still achieved (Figure 17J), with final donor cosmesis equal to that of standard eye retrieval. This is of utmost importance, both in respect for the donor and as relatives and friends may wish to view the body after retrieval (The Royal College of Ophthalmologists, 2008).

This novel technique to retrieve whole human cadaveric conjunctiva has not only enabled completion of this research project but will benefit much future *ex vivo* conjunctival research. This is of particular benefit to those studies requiring a continuum of conjunctival tissue such as anatomical research of the conjunctival vasculature and the distribution of immune cells.

Human Conjunctival Tissue Retrieved

Sufficient donor tissue was available for this project thanks to a dedicated eye retrieval consortium and established telephone consent process at NHSBT. Conjunctiva was retrieved from 18 donors (36 eyes) in total. All donors were Caucasian, reflecting that of the majority of the local population. The causes of death (Table 4) similarly reflect those commonly observed in the developed world, excluding conditions such as haematological malignancies, septicaemia, viral hepatitis and multiple sclerosis; all of which are contraindications for eye donation for transplantation (The Royal College of Ophthalmologists, 2008, UK Blood Transfusion and Tissue Transplantation Services, 2013).

Although donor age ranged from 22-93 years, the ages were heavily skewed, with the median age being 80.5 years (Table 4). Given a significant proportion of deaths at younger ages in the developed world may be attributable to the contraindicated conditions mentioned above, which have been excluded from this study, this age spectrum was not unexpected. In order to obtain a wider distribution of donor ages specific attempts were made to recruit younger donors from deaths on the intensive care unit but unfortunately these were not successful. The donor age range of the limbal tissue used was lower (57-74 years). This tissue was obtained post corneal graft surgery and thus reflects the age of donor eyes used for transplantation rather than simply retrieved. Currently there is no age limit on corneas used for transplantation in the United Kingdom, but they must meet certain criteria including an endothelial cell count of greater than 2200 cells/mm² (UK Corneal Transplant Service Eye Banks); a measure which decreases with age

(Laule *et al.*, 1978). The current (2012-2013) average donor age for corneal transplantation in the United Kingdom is 71.4 years (NHSBT data).

Ideally tissue should be retrieved as soon as possible. The ocular surface microbial flora increases post mortem even under closed eyelids and with refrigeration (Berry and Radburn-Smith, 2005) rendering culture infection more likely. There is also some evidence that proliferative potential of the limbal epithelium reduces with increased PMRT (Kim *et al.*, 2004, Shanmuganathan *et al.*, 2006). The Royal College of Ophthalmologists recommend that enucleation should take place up to (preferably not longer than) 24 hours post mortem (The Royal College of Ophthalmologists, 2008). In practice, extensions post 24 hours have been not infrequently permitted. Indeed in this study, tissue was retrieved up to 27.5 hours post mortem. Likewise to donor ages, PMRTs were similarly skewed: ranging from 8.5 to 27.5 hours but with a median time of 22 hours (Table 4). More recent recommendations from the Department of Health demand that ocular tissue is retrieved within 24 hours post mortem provided the body has been refrigerated within 6 hours (The Advisory Committee on the Safety of Blood Tissues and Organs, 2011). Even with a dedicated eye retrieval consortium and telephone consent, significant time delays were often experienced in contacting and interviewing the donor's family during a time of intense grieving. Reducing tissue retrieval times remains to be a significant challenge.

Confirmation of Conjunctival Tissue Origin

The tissue retrieved was confirmed to be conjunctival in origin by both histology (Figure 21) and immunohistochemical staining for CK19 (Figure 24). Similarly all the cells cultured from the tissue were also confirmed to be of conjunctival phenotype by immunocytochemical staining for CK19 (Figure 68). Cytokeratin 19 has long been recognised as a marker of conjunctival epithelial phenotype, being expressed intensely throughout all layers of the bulbar and tarsal conjunctiva (Kasper *et al.*, 1988, Elder *et al.*, 1997). Equivalent results were demonstrated in this study with deep staining throughout all layers of the epithelium in all areas, confirming that it

was conjunctival in origin (Figure 24). Given that CK19 expression is usually confined to the basal cells of stratified epithelia, it has been postulated that the distribution in the conjunctiva may be attributed to either high proliferative activity (Pitz and Moll, 2002) or a close relationship with simple epithelia (Kasper *et al.*, 1988).

CK19 is also recognised as a limbal SC marker (Barnard *et al.*, 2001, Chen *et al.*, 2004) and is not expressed in the central adult corneal epithelium (Lauweryns *et al.*, 1993, Elder *et al.*, 1997). Indeed CK3 negative, CK19 positive cells are considered evidence of conjunctivalisation of the cornea in limbal SC deficiency (Donisi *et al.*, 2003, Sacchetti *et al.*, 2005). Some recent studies have however, demonstrated CK19 positive cells within the superficial layers of both the central and peripheral cornea, and proposed CK13 (Ramirez-Miranda *et al.*, 2011) or CK7 (Jirsova *et al.*, 2011) as more specific markers of conjunctival epithelium; but conversely, there is also evidence of CK7 positivity in the basal and suprabasal layers of the cornea (Elder *et al.*, 1997). Thus there remains to be some controversy over the most specific conjunctival cytokeratin marker and the diagnosis of limbal SC deficiency by cytokeratin expression.

Immunohistochemical Stem Cell Marker Expression

Specimens of the superior and inferior tissue were sectioned for immunohistochemical studies to incorporate the full length of tissue from eyelid margin to limbus, thus facilitating optimal visualisation of the normal histology (Figure 21) and subsequent anatomical localisation of staining.

Specimens were fixated with NBF and paraffin-embedded as this better preserves tissue morphology than cryosectioning and enabled long-term storage of samples whilst both more tissue was being retrieved and immunohistochemical techniques and protocols were being optimised. Chemical fixation however cross-links proteins which often renders target antigen epitopes inaccessible to larger antibody molecules, thus antigen retrieval techniques are frequently required. These

techniques may cause tissue degradation, loss of morphology, and high levels of background staining (Shi *et al.*, 2001, Leong, 2004). Although paraformaldehyde is reported to have less effect on concealment of epitopes, it has a short shelf life and NBF remains the most favoured fixative in practice. Great difficulty was encountered in this study in preventing tissue degradation and maintaining the samples on the slides. This was most problematic during heat-induced antigen retrieval but evident even during initial de-waxing with xylene. The tarsal plate is renowned for its poor adhesion to slides (personal communication with Mr S. Biddolph, Dept. of Pathology, Royal Liverpool University Hospital). APES coating of slides was of little benefit and tissue adherence was only greatly improved by the use of pre-prepared adhesive slides. Cryopreservation and sectioning may have been preferential in avoiding the need for antigen retrieval and would also have enabled a greater array of suitable SC marker antibodies to be employed.

There is a wealth of reported putative SC markers. Given the proximity and many similarities of the conjunctival epithelium to the corneal epithelium I examined recognised markers of limbal SCs, as have previous authors (Budak *et al.*, 2005, Tanioka *et al.*, 2006, Vascotto and Griffith, 2006). Indeed, many of these have been proposed as markers of conjunctival SCs (Budak *et al.*, 2005, Vascotto and Griffith, 2006, Qi *et al.*, 2010, Pauklin *et al.*, 2011).

Although a number of markers were investigated for immunohistochemical analysis, similarly none had previously been optimised in our laboratories and only a few were optimised sufficiently for use in this study (Table 5). This included only one recognized SC marker (ABCG2) (Zhou *et al.*, 2001) and one recognized TAC marker (p63) (Parsa *et al.*, 1999). Ideally multiple markers would have been studied to provide confirmatory immunohistochemical evidence of SC distribution. Future work should endeavor to optimize additional SC marker antibodies to this aim.

Moderate degrees of background staining remained in the immunohistochemical images (Figure 25 to Figure 39), even despite additional blocking with 3% hydrogen peroxide for 5-10 minutes. This may be attributable to the antigen retrieval

techniques employed, but is also a recognised weakness of the Envision™ system, thought to be attributable to the larger reaction product (Leong, 2004).

Quantitative image analysis software, such as the Aequitas™ Image Analysis Software (Dynamic Data Links Ltd) is available and has been successfully employed in immunohistochemical studies (Howard *et al.*, 2010); but this relies on a grey-scale value of staining and is thus not possible in the presence of haematoxylin counterstaining. The latter was employed to enable accurate localisation of antibody staining within the epithelium. Various semi-quantitative grading methods have been advocated, usually incorporating both intensity of staining and/or proportion of positively staining cells (Adams *et al.*, 1999, Leong, 2004). I thus devised two similar grading scales (see Section 2.4.4, **Figure 23** and Table 6) for use in this study. The first scale employing solely proportion of positively staining cells was used throughout the analysis. The second scale which additionally employed a qualitative assessment of staining intensity demonstrated equivalent statistical significance in the variation across the tissue, but was useful to identify a smaller region of highest immunoreactivity.

As loss of tarsal epithelium was noted in some early embedded specimens (Figure 19) and trauma to the eyelid margin in others, conjunctival tissues were selected for immunohistochemical analysis on the basis of the most complete intact epithelium demonstrated on H&E histology. The selection of tissues used did not therefore replicate those used for immunocytochemical and CFE studies, although there was considerable overlap. Likewise, assessment of SC marker expression at the eyelid margin was not feasible within this study, as later described.

Expression of ABCG2 was demonstrated in the basal layers of the epithelium throughout all areas of all conjunctival specimens (Figure 26 to Figure 29). The presence of staining not solely restricted to the cell membranes but additionally often seen throughout the cytoplasm has been previously reported in both human limbal (Chen *et al.*, 2004, Dua *et al.*, 2005) and conjunctival cells (Budak *et al.*, 2005); and likely represents cytoplasmic processing of the protein and/or non-

specificity of the antibodies. In areas in the conjunctiva with highest levels of staining, intense membrane and cytoplasmic staining was demonstrated basally but also to some degree throughout the majority of epithelial cells, thus sparing only the superficial layers (Figure 26). This pattern of staining replicates that previously noted in immunohistochemical studies of the limbal and conjunctival epithelium (Dua *et al.*, 2005, Budak *et al.*, 2005), although particularly high levels of staining were demonstrated in the limbal crypts and basal cells (Dua *et al.*, 2005). Although these immunohistochemical staining patterns would perhaps support 'the notion' that ABCG2 is better considered a PC marker rather than a pure SC marker, this is not consistent with either the level of staining demonstrated in cell cultures in this or other human studies (Tanioka *et al.*, 2006, Schrader *et al.*, 2009a, Eidet *et al.*, 2012b), or the intense immunofluorescent staining noted in the basal layer alone of the bulbar conjunctiva in another study (Qi *et al.*, 2010).

A clear pattern of varying levels of ABCG2 staining was consistently demonstrated across the whole conjunctival tissue, but more intense in some areas than others. Statistically significantly higher levels were demonstrated in a region comprising the medial canthal area and inferior medial and inferior central fornices (Figure 29). Higher levels of staining in the forniceal than in bulbar than in tarsal areas was demonstrated (Figure 26). This reflects the findings of a previous study where higher expression was noted in the palpebral-forniceal zone than in the palpebral area of the conjunctiva (Budak *et al.*, 2005).

Although only two conjunctival specimens were stained immunohistochemically for p63, a consistent pattern was demonstrated between them. As expected for a nuclear TAC marker, staining was solely nuclear in origin, and in areas of most intense staining it incorporated not only the basal layers but also the intermediate layers of the epithelium (Figure 31). Similar expression of p63 has been demonstrated throughout the layers of the human limbal epithelium (Chen *et al.*, 2004), and to a lesser degree (with marked basal but only mild suprabasal staining) in the bulbar conjunctiva (Qi *et al.*, 2010). More so, the pattern across the tissue, which has not been previously assessed, replicated that of the distribution of

ABCG2 staining (Figure 29), but with greater distinction (Figure 32, Figure 34). Statistically significant highest staining levels were similarly demonstrated in the area comprising the medial canthal and the inferior medial and inferior central forniceal areas.

Highest levels of both ABCG2 and p63 immunohistochemical staining were predominantly detected in the basal layer throughout the conjunctival epithelium. This distribution pattern supports the hypothesis that the conjunctival epithelium is maintained by PCs within its basal layer (Vascotto and Griffith, 2006, Qi *et al.*, 2010); a pattern that is replicated in other stratified epithelia (Alonso and Fuchs, 2003, Daniels *et al.*, 2001).

The Search for a Cytokeratin Stem Cell Marker

While there is evidence that the human basal conjunctival epithelial cells express a similar pattern of SC markers to that of the basal limbal epithelium (Budak *et al.*, 2005, Vascotto and Griffith, 2006, Qi *et al.*, 2010, Pauklin *et al.*, 2011), the expression of cytokeratins are unique (Kasper *et al.*, 1988, Elder *et al.*, 1997, Qi *et al.*, 2010), and none had been clearly identified as markers of conjunctival SCs.

Thus, with the aim of identifying prospective negative conjunctival SC markers, I therefore employed a number of pan-cytokeratin antibodies which each detected differing incomplete but overlapping arrays of the spectrum of cytokeratins. Comparative studies of these may have elucidated a smaller number of potential negative CK candidate SC markers to further investigate. Indeed a collection of basal non-AE1/AE3 staining cells were demonstrated (Figure 38) which may represent a collection of basal SCs. Unfortunately, adjacent tissue sections were no longer available to further investigate the nature of these cells and their CK or other SC marker expression, or to exclude melanocytic or immunological cell origin. No further collections of non-staining cells were noted on pan-cytokeratin staining. Since the commencement of this study CK8, 14 and 15 have been reported in the

basal layers of the bulbar conjunctival epithelium in other studies (Merjava *et al.*, 2011b, Qi *et al.*, 2010) and may represent positive conjunctival SC markers.

The Eyelid Margin

The eyelid margin is a transitional zone between two epithelial phenotypes: the mucous membrane of the conjunctiva and the keratinized epithelium of the skin. This mucocutaneous junction has been proposed as a source of palpebral conjunctival epithelial SCs in several animal label retention studies (Pe'er *et al.*, 1996, Wirtschafter *et al.*, 1999, Su *et al.*, 2011). However, the validity of such studies in the detection of SCs has been questioned (Pellegrini *et al.*, 1999, Kiel *et al.*, 2007, Snippert and Clevers, 2011). Liu *et al.* recently detected CK14 positive cells in the basal layers of the mucocutaneous junction of the monkey conjunctiva, and also concluded that this may represent a conjunctival SC niche (Liu *et al.*, 2007); yet CK14 is widely expressed in all epithelial layers of the human bulbar conjunctiva, limbus and the central cornea (Merjava *et al.*, 2011b), and is unlikely to be a marker of SCs. A more comprehensive study of the expression of a battery of cytokeratin, mucin and SC markers at the mucocutaneous junction in the human eyelid demonstrated no expression of CK15, ABCG2 or integrin- β 1 there but significant expression of N-Cadherin. Conversely CK15, integrin- β 1 and N-Cadherin were expressed in the ductal epithelium of the meibomian glands, and CK15 in the bulge region of the eyelid hair follicle. The authors conclude that these two latter regions may represent sites for conjunctival SCs (Tektaş *et al.*, 2012).

An area of high epithelial turnover known as Marx's line is described clinically in humans with lissamine green staining. It lies directly posterior to the mucocutaneous junction in healthy eyelids (Hughes *et al.*, 2003, Bron *et al.*, 2011). It is speculated that this is caused by both mechanical stress and hyperosmolar physiological stress secondary to evaporative water loss from the tear meniscus at the eyelid margin (Bron *et al.*, 2011). It is not clear whether the sparse evidence above for the proliferative cells at the eyelid margin represents this proliferative zone or SCs to support this region or the palpebral conjunctiva.

Human conjunctival specimens in this study were obtained by surgically excising down the grey line, hence anterior to the tarsal plate (Figure 17, Figure 18). All specimens should therefore have incorporated the mucocutaneous junction, but in reality it was often not evident. This may be due to loss of eyelid margin epithelium (attributable to surgical trauma or sloughing off of the superficial layers post mortem); the increasing irregularity of the anatomical junction that is noted with increasing age (Bron *et al.*, 2011); or anterior migration of the mucocutaneous junction which is often secondary to chronic blepharitis (Bron *et al.*, 2011). Given the older age distribution of donors enlisted in this study, the latter two explanations may well be responsible. This inability to delineate the mucocutaneous junction in many specimens meant that SC localisation by immunohistochemical analysis at the eyelid margin was not possible in this study.

Whether there is indeed a focal concentration of SCs supplying the conjunctiva at the eyelid margin, and the exact origin of these cells remains to be determined. It is perhaps also interesting to note that the basal epithelial layers of the marginal zone of the human conjunctiva feature papillae (Bron *et al.*, 1997); a characteristic not observed in the remaining conjunctiva, but well described in the human limbal epithelium (Dua *et al.*, 2005). Certainly further studies to investigate the clonogenic ability of these cells are required (Liu *et al.*, 2007).

Conjunctival Epithelial Cell Culture

Development of a technique to harvest and culture conjunctival epithelial cells proved to be challenging. Primary cell cultures are more liable to infection, and many other factors such as donor age and PMRT may contribute to culture success or failure (Baylis *et al.*, 2013, James *et al.*, 2001). Cultures from two specimens in this study became infected, after which the additional step of washing out the donor fornices with povidone iodine prior to tissue retrieval was introduced with good effect. This gave an overall contamination rate of 11.1%. Given the small sample size and nature of the tissue retrieved (the eyelid margins being exposed, and the folds of tissue in the fornices being difficult to clean) this does not compare

unfavourably with a reported microbial contamination rate of 5% of human corneas in culture (Armitage and Easty, 1997). Although no association between donor factors and infection in culture was noted in this study, significantly higher contamination rates have been previously reported in those with infectious causes of death and longer PMRTs (Armitage and Easty, 1997). The latter is presumably due to an increasing microbial load developing on the ocular surface with lack of tears and blinking post mortem (Berry and Radburn-Smith, 2005). The use of povidone iodine is recommended practice for eye retrieval in Australia and the USA (Eye Bank Association of America, 2011, Eye Bank of South Australia, 2012), and it would seem reasonable to also adopt this practice in the UK.

Several other specimens failed to culture colonies for no apparent reason despite using previously successful techniques. Similarly there was no apparent correlation of this to donor age, cause of death or PMRT. It is for this reason that the CFE and immunocytochemistry results are not from complete chronological specimens. Indeed, despite the more established techniques, fresh human cadaveric limbal epithelial biopsies may have culture success rates as low as 60% (James *et al.*, 2001).

Conjunctival epithelial cell harvesting with cloning rings proved unsuccessful, but the more established technique of trypsinisation of whole chopped tissue resulted in colony growth on a 3T3 feeder layer (Figure 44). The use of a 3T3 feeder layer for culture of epithelial cells was first proposed by Rheinwald and Green in 1975 (Rheinwald and Green, 1975a, Rheinwald and Green, 1975b). Fibroblasts are required for both epithelial cell colony formation and subsequent growth, but the fibroblasts usually take over the culture unless inactivated. It is believed that fibroblasts secrete factors into the media which aid growth but their presence is also required as epithelial growth is not supported in 3T3 conditioned media alone (Rheinwald and Green, 1975a, Rheinwald and Green, 1975b). Traditionally inactivation was achieved with irradiation, but it can equally be achieved chemically with mitomycin C. It was therefore not unexpected that conjunctival epithelial cells growth was not supported by tissue culture plastic alone (Figure 44).

Matrigel™ basement membrane matrix is a commercially available substrate comprised of 56% laminin, 31% collagen IV, heparan sulphate, 8% nidogen and an array of growth factors. It supports the attachment and growth of a variety of cells including rabbit conjunctival epithelial cells (Tsai and Tseng, 1988), and has been reported to maintain feeder-free growth of human embryonic SCs (Xu *et al.*, 2001, Ludwig *et al.*, 2006) and induced pluripotent SCs (Takahashi *et al.*, 2007). The normal human conjunctival basement membrane contains laminins $\alpha 1$, $\alpha 3$, $\gamma 1$ and 5, in addition to integrin- $\beta 4$ and collagens IV and VII (Messmer *et al.*, 2012). It is therefore perhaps surprising that Matrigel™ basement membrane matrix did not support the growth of conjunctival epithelial cells either seeded post enzymatic digestion (Figure 44) or by explant culture (Figure 45) in this study, especially considering that both laminin 1 and collagen IV alone supported conjunctival epithelial growth (Figure 83). However this experiment was not performed on repeated occasions and is thus worth repeating before definitive conclusions are drawn.

Although I was unable to establish conjunctival epithelial growth from explants (Figure 45), similarly this experiment was only performed on two occasions and there was a sparsity of feeder layer cells in proximity to them. This likely represents the mechanical removal of 3T3 cells during placement of the explants. To alleviate this problem the 3T3 feeder layer may be added to the culture dish after attachment of the explants (James *et al.*, 2001); but even when using this technique trypsinisation has been shown to be more reliable in producing limbal epithelial cultures than explant outgrowths (James *et al.*, 2001). In addition, given that by their very nature SCs remain in their niche and have been suggested not to migrate out of explants (Selver *et al.*, 2011), the outgrowths may not incorporate as higher concentration of SCs as compared to cultures post-enzymatic digestion. For these reasons, I therefore continued to culture cells post enzymatic digestion of whole chopped epithelial tissue.

Human conjunctival epithelial cells can be successfully grown without a feeder layer, either by using an alternative substrate such as amniotic membrane (Ang *et*

al., 2004a, Tanioka *et al.*, 2006), acellular dermis (Yoshizawa *et al.*, 2004) or gelatin (Vascotto and Griffith, 2006); or in the presence of specialised keratinocyte serum-free media (Ang *et al.*, 2004b). But there is no evidence that SCs are supported in these systems, and indeed cells cultured in serum-free media demonstrate lower colony forming capacity compared to those cultured in the presence of a 3T3 feeder layer (Ang *et al.*, 2004b). Thus in order to maintain optimal proliferative potential for comparative studies across different areas of the conjunctiva, media containing FCS in conjunction with a 3T3 feeder layer was used in this study. The epithelial media was prepared according to compositions used in previously established laboratories (Pellegrini *et al.*, 1999, Kolli *et al.*, 2008).

Cultured human conjunctival cells demonstrated typical epithelioid morphology and growth patterns as previously described under these culture conditions in other studies (Pellegrini *et al.*, 1999, Ang *et al.*, 2004b, Vascotto and Griffith, 2006, Schrader *et al.*, 2009a). Colonies are the progeny of a single cell (Rheinwald and Green, 1975b, Lindberg *et al.*, 1993). Thus the development of colonies from all areas of the conjunctiva (Figure 46) implies the presence of PCs throughout the tissue. Indeed epithelial cells from the central and paracentral cornea do not produce colonies in culture and cannot be serially cultivated (Lindberg *et al.*, 1993, Pellegrini *et al.*, 1999); being solely differentiated cells, as consistent with the XYZ model of maintenance of the corneal epithelium by limbal SCs (Thoft and Friend, 1983).

Although goblet cells were not noted to be present in human conjunctival cell cultures in this study, no specific attempts were made to identify them. Appropriate methods to achieve this are Periodic Acid Schiff (PAS) staining or immunocytochemical staining to MUC5AC or UEA-1 lectin; these markers to the cells secretory product will not however detect immature, migrating or proliferating cells which lose their secretory products (Fostad *et al.*, 2012). More accurate identification may thus be achieved using the RCK105 clone of CK7 (Shatos *et al.*, 2003). Early human conjunctival epithelial culture studies similarly reported no evidence of goblet cells in cultures (Diebold and Calonge, 1997, Risse Marsh *et al.*,

2002), but concluded that they were not necessarily absent but perhaps required different culture conditions or time to develop (Diebold and Calonge, 1997). Indeed, human goblet cells have been successfully isolated and cultured in RPMI-1640 media, and the addition of EGF has been shown to stimulate their proliferation (Shatos *et al.*, 2003). Goblet cells have also been reported in conjunctival co-cultures with a 3T3 feeder layer (Pellegrini *et al.*, 1999, Ang *et al.*, 2004b, Berry and Radburn-Smith, 2005). They are observed with much greater frequency in confluent cultures; and occur singly, as doublets or in clusters of up to 10 cells (Pellegrini *et al.*, 1999, Ang *et al.*, 2005b, Berry and Radburn-Smith, 2005). Most reports relating to human conjunctival epithelial culture do not however mention their presence or absence (Yoshizawa *et al.*, 2004, Tanioka *et al.*, 2006, Schrader *et al.*, 2009a, Ang *et al.*, 2011, Schrader *et al.*, 2012).

All primary cells have a limited life-span in culture. *In vitro* conditions cannot exactly replicate those *in vivo*, and with increasing subculture in non-optimal conditions, cells typically become increasingly more differentiated in appearance until cellular senescence ensues. The changing morphology of conjunctival cells during serial cultivation (figure 31) and the attainment of senescence by passage 4 are consistent with that demonstrated in primary conjunctival epithelial cell cultures in other studies (Schrader *et al.*, 2009a).

Cellular Growth, Clonogenic Ability and Proliferative Capacity

Cellular growth, clonogenic ability and proliferative capacity may be assessed by a number of different measures. The former may easily be measured by outgrowth measurements from explant cultures (Ang *et al.*, 2004b, Eidet *et al.*, 2012a), but is difficult to quantify in dissociated cells seeded in co-culture. Clonogenic ability indicates the capacity of a single cell to generate a colony and is typically measured by the CFE assay (Pellegrini *et al.*, 1999). In contrast, proliferative potential is a measure of the capacity of a cell to self-renew and produce subsequent generations (Pellegrini *et al.*, 1999). This may be assessed by the number of cell generations maintained until senescence (Ang *et al.*, 2005b), the cell population doublings

(Schrader *et al.*, 2009a) or a BrdU ELISA cell proliferation assay (Ang *et al.*, 2004a, Ang *et al.*, 2005b).

As this study aimed to assess the distribution of SCs across the conjunctiva, I performed CFE assays. Isolation of single cells in order to assess true holoclone growth was however beyond the scope of this study. Given no differentiation to clone type (Barrandon and Green, 1987) was made, as indeed most previous studies have not, this should strictly be considered a measure of PCs rather than SCs. Culture wells were seeded with variable number of cells. Those seeded with 5000 or 10000 cells demonstrated proportionally fewer colonies and lower CFE (Figure 50 and Figure 51). An observation likely due to increased demand for nutrients, growth factors and oxygen in the media, increased accumulation of toxic metabolic by-products and cell contact inhibition. In addition, colony counts were often unobtainable in these wells due to overcrowding (Figure 49), thus these wells were excluded from the analysis.

Clonogenic ability was consistently demonstrated across all areas of the conjunctiva but with uneven distribution and with a replicable pattern across all 8 donors (Figure 55 to Figure 62); indicating again that although there are PCs throughout the human conjunctiva, some areas are richer in PCs than others. These regions were namely foremost the medial canthal area and then the inferior fornix, where significantly higher CFE was noted. Consistent patterns of higher CFE in the fornices than bulbar than tarsal conjunctiva, and in the inferior than superior conjunctiva were again apparent.

Two analogous studies comparing growth and CFE across the whole rabbit and rat conjunctiva have been recently reported. Su *et al.* examined the cellular growth, proliferative potential and CFE from the palpebral, forniceal and bulbar areas of New Zealand white rabbits. They report palpebral and forniceal cells reached confluence faster and were maintained through significantly more cell generations than bulbar cells; and that CFE was higher in the palpebral than forniceal than bulbar cells. It is not however clear how many subjects were included, and no

distinction was made between the superior and inferior regions of the conjunctiva (Su *et al.*, 2011). Eidet *et al.* similarly report cellular growth from explant cultures and CFE from 6 regions across the rat conjunctiva in 6 subjects. Significantly larger outgrowth was demonstrated from the superior and inferior forniceal explants, and more so in the superior tarsal than superior bulbar epithelium. Markedly higher CFE was noted in the superior fornix than all other areas. The canthal regions were not specifically assessed (Eidet *et al.*, 2012a).

Only one previous study has assessed the clonogenic ability across the human conjunctival epithelium (Pellegrini *et al.*, 1999). Although in contrast the authors noted comparable rates across the four bulbar and two forniceal areas, assays were only compared from cells obtained from single 1-2mm² biopsies from a single donor, and did not include assessment of the tarsal regions. Thus this present study is the first study that has comprehensively examined the clonogenic ability of the human conjunctival epithelium as a whole.

Although not a formal assessment, the observation of colonies at earlier time points and of larger colony size at equivalent time points in cultures from the medial canthal area, fornices and inferior bulbar conjunctiva (Figure 46) suggests that these areas which demonstrate higher clonogenic ability also show greater rates of cellular growth. Proliferative potential of cultures from different areas across the conjunctiva, as measured by passage number achieved, was not formally assessed in this study.

Higher clonogenic ability and greater cellular growth rates were demonstrated from limbal than from conjunctival cell cultures (Figure 65 and Figure 48). This effect was noticeable to both the overall conjunctival CFE and that from the medial canthal area alone, although statistical analysis was not possible due to the small sample size. Given the significant decline noted in conjunctival CFE with increasing donor age (Figure 63), this may be in part be attributable to younger donor age of the limbal tissue (median 68 years versus median 80.5 years). It is also worth noting that the limbal tissue had been maintained in organ culture for a period of time

prior to cell culture. Pellegrini *et al.* performed similar comparative CFE assays from 4 limbal and 6 bulbar/forniceal human conjunctival biopsies noting equivalent values throughout, but samples were only assessed from biopsies from a single donor (Pellegrini *et al.*, 1999). In contrast, Lindberg *et al.* demonstrated higher proliferative potential (as measured by population doublings) in limbal compared to bulbar conjunctival cells from 6 human donors (Lindberg *et al.*, 1993). It is well recognised that the limbus acts as a SC niche to maintain the corneal epithelium which is devoid of SCs (Daniels *et al.*, 2001, Dua *et al.*, 2005, Stepp and Zieske, 2005, Tseng, 1996). Given that I have demonstrated clonogenic ability throughout the human conjunctiva in this study, it is plausible that equivalent areas as enriched in SCs as the limbus are not required, as they are not supplying other areas devoid of SCs such as the limbus does to the cornea. Comparative data from a greater number of donors would enable statistical analysis to verify any difference.

Immunocytochemical Stem Cell Marker Expression

In order to complement studies assessing the immunohistochemical expression of ABCG2 and the clonogenic ability of cells across the human conjunctiva, I also performed comparative studies of SC marker expression in cell cultures. SC markers selected for immunohistochemical studies were similarly investigated with the addition of N-Cadherin and Hsp70.

SC marker expression in cultured conjunctival epithelial cells was assessed from the same cultures (same tissue divisions from the same donor tissues) as for CFE assays, thus enabling direct comparisons.

Cultured cells for immunocytochemical staining were fixed with methanol as this enabled long-term storage whilst a range of antibodies were being optimised. Alcohol fixation has however been reported to produce less reproducible staining and false-negative staining for antibodies to nuclear antigens (Gong *et al.*, 2004, Skoog and Tani, 2011). NBF offers an alternative fixation agent. Immunocytochemistry is a complex technique with numerous stages that require

optimisation to provide maximal specificity and sensitivity of staining. None of the antibodies included in this study had been previously optimised in our laboratories. Optimisation is often time-consuming and satisfactory staining is not always achieved. Indeed a number of antibodies such as N-Cadherin and CD168 were not sufficiently optimised for inclusion in the final comparative staining.

Cells expressing ABCG2, Δ Np63 and Hsp70 were demonstrated in cultures from all regions of the conjunctiva from all 8 donors. Significant variation was shown across the regions with a consistent pattern for each marker of significantly higher staining both in the medial canthal region alone and in the medial canthal and inferior forniceal regions together (Figure 70 to Figure 72, Figure 74 to Figure 76, and Figure 78 to Figure 80). The pattern demonstrated for CFE levels across the tissue was replicated; with the same regions that demonstrated highest CFE also showing highest SC marker expression. Similarly, greater levels of staining in inferior compared to superior areas of the tissue, and greater levels in the forniceal than bulbar than tarsal areas were noted. There was highly significant positive correlation in this distribution pattern not only between each marker but also between each marker and CFE levels.

Expression of both ABCG2 and p63 α (Schrader *et al.*, 2009a) or Δ Np63 α (Eidet *et al.*, 2012b) have been previously demonstrated in human conjunctival epithelial cultures, but not compared in cultures from across different areas of the tissue. Although attempts have been made to compare ABCG2 and p63 gene expression using PCR from human conjunctival cells from across the tissue, there has been no complete study. Harun *et al.* compared expression of a number of SC marker genes including ABCG2 from passage 2 cells cultured from small biopsies from only the inferior bulbar, forniceal and palpebral areas. No ABCG2 genes were detected in cells from any area (Harun *et al.*, 2013). While Pauklin *et al.* demonstrated higher levels of ABCG2 genes in cells from forniceal than from bulbar conjunctiva from 4 donors; they conversely showed higher levels of Δ Np63 α genes in the bulbar conjunctiva. They did not assess the tarsal conjunctival cells, nor was there a comparison between superior and inferior areas (Pauklin *et al.*, 2011). Expression

of the translated proteins is perhaps of greater physiological relevance. This is the first study not only to compare degree of ABCG2 and Δ Np63 protein expression across cultures from differing regions of the human conjunctiva, but also to assess the whole tissue.

ABCG2 and p63 α expression and CFE have been concurrently assessed in other studies of human conjunctival cell cultures. It is observed that all factors reduce together with serial passage (Schrader *et al.*, 2009a) and when cultured in a xenobiotic-free culture system (Schrader *et al.*, 2012). The positive correlation between both ABCG2 and Δ Np63 marker expression; and between each of them and CFE is also confirmed in their distribution across the different areas of the human conjunctiva in this study, at a highly statistically significant level. This supports the proposal of both of these markers as putative conjunctival SC markers (Budak *et al.*, 2005, Vascotto and Griffith, 2006, Qi *et al.*, 2010, Pauklin *et al.*, 2011).

Hsp70 has been proposed as a possible limbal SC marker and is also reported to be widely expressed in the basal layer of the bulbar conjunctiva (Lyngholm *et al.*, 2008). The significant positive correlations of the distribution of Hsp70 staining compared to both ABCG2 and Δ Np63 staining and to CFE in this study suggests that it may also be considered as a putative conjunctival SC marker; but without data to demonstrate co-localisation of staining to specific cells this cannot be confirmed. Higher levels of staining were demonstrated for Hsp70 (Figure 80) than for the other SC markers in conjunctival cultures in this study (Figure 72, Figure 76). This is perhaps to be expected given Hsp70 expression has been demonstrated in all ocular surface cells with proliferative properties including to a minor extent even in the central corneal epithelium (Lyngholm *et al.*, 2008). It is perhaps more appropriate that it is therefore considered a PC or TAC marker.

The significant correlations both between immunocytochemical SC marker expression and between them and CFE demonstrated in this study (see Section 3.7 and **Figure 85**) also reflects the pattern of the PC distribution across the human conjunctiva indicated by ABCG2 immunohistochemical analysis; with PCs present

throughout the tissue but with highest levels in the medial canthal and inferior forniceal areas.

Summary of Human Conjunctival Progenitor Cell Distribution

There has been much conflicting evidence as to the location of both animal (Wei *et al.*, 1993, Pe'er *et al.*, 1996, Wirtschafter *et al.*, 1997, Lavker *et al.*, 1998, Wirtschafter *et al.*, 1999, Chen *et al.*, 2003, Su *et al.*, 2011, Eidet *et al.*, 2012a) and human (Pellegrini *et al.*, 1999, Budak *et al.*, 2005, Vascotto and Griffith, 2006, Pauklin *et al.*, 2011, Harun *et al.*, 2013, Tektaş *et al.*, 2012) conjunctival SCs. The lack of a single definitive SC marker, the interspecies variation and doubt regarding the strength of label-retaining studies, and the limited access to whole human conjunctival tissue for research purposes have substantially hindered progress in this field.

This is the first study to comprehensively assess the whole human conjunctival tissue, and to localise PCs by both clonogenic ability and SC marker expression. Although some previous studies have utilized sections of human conjunctiva, only the bulbar or bulbar and forniceal areas have been examined (Vascotto and Griffith, 2006, Qi *et al.*, 2010, Pauklin *et al.*, 2011); or it is not clear whether the whole tissue has been assessed (Budak *et al.*, 2005). Other authors have sampled small biopsies of tissue from various regions (Pellegrini *et al.*, 1999, Harun *et al.*, 2013); but if indeed SCs are scattered throughout the epithelium such as is proposed in the skin (Alonso and Fuchs, 2003), assuming their distribution is not uniform, this latter method risks sampling areas with inaccurate representations of SC concentration. Although some other studies have examined the expression of a more complete battery of SC markers (Vascotto and Griffith, 2006, Qi *et al.*, 2010, Pauklin *et al.*, 2011), none of these studies examined the whole tissue. More so, this present study assesses tissue from a greater number of donors than any of the aforementioned studies, and attempts to localize the PCs by both clonogenic ability and SC marker expression in both fixed tissue and cultured cells from the same donors.

Substantial evidence from each aspect of this study indicates the presence of PCs throughout the human conjunctival epithelium, but with significantly highest concentrations in the medial canthal and inferior forniceal areas. The significant positive correlations between clonogenic ability and SC marker expression in both cultured cells and fixed tissue adds further credence to these conclusions. Thus my hypothesis that PCs are located in specific areas of the human conjunctiva, and can be identified by such methods can be accepted.

These findings are in keeping with other reports suggesting that human conjunctival epithelial SCs are located predominantly in the fornix (Budak *et al.*, 2005, Pauklin *et al.*, 2011), but are also present in other areas (Pellegrini *et al.*, 1999, Budak *et al.*, 2005, Vascotto and Griffith, 2006, Qi *et al.*, 2010, Pauklin *et al.*, 2011).

It is likely that the SCs are scattered across the basal layer of the whole human conjunctival epithelium. Immunohistochemical staining of tissue sections demonstrated predominantly basal ABCG2 and p63 staining throughout the tissue, a finding confirmed in areas of the conjunctiva in other studies (Budak *et al.*, 2005, Vascotto and Griffith, 2006, Qi *et al.*, 2010).

This theory of scattered human conjunctival SCs would also explain why the conjunctival cells, in comparison to the SC-rich cells of the limbus, exhibit lower CFE values as demonstrated in this study (Figure 65), lower proliferative potential (Lindberg *et al.*, 1993), and a lower expression of pluripotency/multipotency molecules (Pauklin *et al.*, 2011). However these findings are in discrepancy to those reported in other studies by comparative CFE (Pellegrini *et al.*, 1999), and expression of ABCG2 (Budak *et al.*, 2005, Pauklin *et al.*, 2011). It also contradicts the assumption that CK19 expression throughout all layers of the conjunctiva may be attributed to a particularly high proliferative activity (Pitz and Moll, 2002).

Proposed Model of Conjunctival Epithelial Renewal

Aside from the single collection of AE1/AE3 negative basal cells (Figure 38), histological and immunohistochemical examination revealed no distinct defined collections of SCs or TACs, and no obvious morphologically distinct region or niche for the conjunctival SC, such as are seen in the limbus as the source of corneal epithelial cells. It has been proposed that there are pockets of SCs throughout the basal layer of the human conjunctival epithelium (Qi *et al.*, 2010). Certainly, the widespread expression of SC markers in the basal conjunctival epithelium noted both in this study (Figure 26, Figure 27) and in other studies (Budak *et al.*, 2005, Vascotto and Griffith, 2006, Liu *et al.*, 2007, Qi *et al.*, 2010) would be in keeping with this. The co-localization of SC and TAC markers within the same layer (Figure 26, Figure 31) suggests a heterogeneous distribution of both cell types, which has also been reported by other authors (Vascotto and Griffith, 2006).

It is therefore plausible that a similar renewal model to the inter-follicular SC model proposed in the skin (Alonso and Fuchs, 2003) is also true of the conjunctival epithelium; whereby in addition to the stem cells of the bulge of the hair follicle, scattered single basal epithelial SCs give rise to single maturing columns of TACs and differentiated cells through the layers of the epithelium (Alonso and Fuchs, 2003). Scattered Δ Np63 and CK19 expression has been detected in the superficial layers of the conjunctival epithelium (Vascotto and Griffith, 2006). However the Δ Np63 antibody used in this study was not specific to the α isoform which is recognized as a SC marker (Di Iorio *et al.*, 2005, Kawasaki *et al.*, 2006). These cells may thus represent a collection of TACs or even less terminally differentiated cells that form part of a maturing SC column. Indeed, the petalloid arrangement of surface human conjunctival epithelial cells described around a central core of cells (Pfister, 1975), and the general immobility of bulbar conjunctival cells in transgenic mice (Nagasaki and Zhao, 2005) may also be consistent with this theory.

Until a pure conjunctival SC marker or clear measure of slow-cycling and proliferation potential within human tissue is identified, one can only speculate on the nature of conjunctival epithelial renewal.

The Relation of Progenitor Cell to Goblet Cell Distribution

This widespread distribution of conjunctival PCs across the tissue but with highest levels in the medial canthal and inferior forniceal areas mimics that of the distribution of human goblet cells and intra-epithelial mucous crypts as shown in Figure 4 (Kessing, 1968). Indeed more intense ABCG2 staining has been previously correlated to the goblet cell-rich areas of the conjunctiva (Budak *et al.*, 2005). There was not however, an apparent direct relationship in immediate co-localisation of these cells within the epithelium in immunohistochemical studies; with very variable levels of both ABCG2 and p63 positive cells noted adjacent to clusters of goblet cells (Figure 30, Figure 35). Similarly, the crypt SCs in the colonic epithelium are not noted in immediate proximity to goblet cells (Moore and Lemischka, 2006). Assessment of the co-localisation of PCs and goblet cells in culture was not possible in this study, given the culture conditions used did not favour the growth of goblet cells as previously discussed. This distribution pattern may simply reflect the pattern of epithelial renewal in the conjunctival epithelium: as goblet cells arise from a common conjunctival bipotent SC or TAC (Pellegrini *et al.*, 1999), thus greater concentrations would perhaps be expected in proximity to them. However, their co-existence may alternatively be essential to the conjunctival SC niche; and it is perhaps not coincidental that the bulge SCs of the skin epidermal hair follicle also reside in close proximity to sebaceous glands (Alonso and Fuchs, 2003, Mitsiadis *et al.*, 2007).

The Medial Canthal and Inferior Forniceal Areas

As the richest source of human conjunctival PCs, the medial canthal and inferior forniceal areas may offer greater physical protection to the PC niches. But perhaps more importantly, these regions, and in particular the plica semilunaris and caruncle, are also densely vascularised, and especially rich in goblet cells, intra-epithelial mucous crypts and the accessory lacrimal glands (Kessing, 1968, Bron *et al.*, 1997, Arends and Schramm, 2004); although the nature and significance of these relationships remains to be established. These areas are additionally noted to contain melanocytes (Bron *et al.*, 1997, Arends and Schramm, 2004), and the

plica semilunaris to be abundantly infiltrated with both specific and non-specific immune cells (Arends and Schramm, 2004). These features are common to other SC niches such as the limbus (Li *et al.*, 2007). Rich vascularisation provides a plentiful supply of nutrients, blood-borne growth and survival factors (Tseng, 1996). Melanin offers protection against the carcinogenic insult from ultraviolet light and subsequent formation of reactive oxygen species (Boulton and Albon, 2004). It is interesting to note, that whereas the limbal SCs are predominantly located superiorly and inferiorly (Shortt *et al.*, 2007a), the conjunctival PCs reside predominantly close to the midline. It has been suggested that the plica semilunaris plays an important role as a specialised organ in ocular defence (Arends and Schramm, 2004), but perhaps its significance extends further than this, to also incorporate conjunctival epithelial renewal.

The Implications of Human Conjunctival Progenitor Cell Distribution

The implications of the distribution of conjunctival PCs are numerous. Firstly, knowledge of the PC-rich areas enables avoidance or minimisation of damage to them during conjunctival or other ocular surgery. Conversely, biopsies taken with a view to *ex vivo* expansion for conjunctival epithelial replacement should be taken from these PC-rich areas to provide optimal success (Holland, 1996, De Luca *et al.*, 2006, Shortt *et al.*, 2007a). Additionally, the medial canthal and inferior forniceal areas are possibly the sites where any topically administered eye medications will naturally accumulate, and are thus most exposed to toxicity from the preservatives within. It is therefore perhaps imperative that preservative-free topical ophthalmic medications are considered in any patient with significant conjunctival disease. It is also noteworthy that this PC-rich zone is an area which is often more severely affected in inflammatory disorders such as mucous membrane pemphigoid.

The Effect of Donor Age on Human Conjunctival Progenitor Cells

SC niche microenvironments of a variety of tissues are known to deteriorate with age, with a subsequent critical effect on SC number, phenotype and clonogenic ability (Wagner *et al.*, 2008, Gago *et al.*, 2009, Zhao *et al.*, 2008, Zheng *et al.*, 2009).

Indeed, increasing donor age was associated with significantly lower CFE (Figure 63), significantly lower expression of ABCG2 in both tissue sections and cultured cells (Figure 41, Figure 81), and significantly lower expression of Hsp70 in cultured cells (Figure 81) in this study. These findings should however, be interpreted with caution given the skewed distribution of donor age. In a previous study comparing human conjunctival epithelial culture methods, the authors comment that no significant differences in cell proliferation were noted with varying donor age (Ang *et al.*, 2004a), but the data is not shown and the donor age distribution was similarly skewed. A significant reduction in CFE of human limbal cells with increasing donor age has been recently reported (Notara *et al.*, 2013), and a similar trend of reduction in limbal culture success rates previously noted (James *et al.*, 2001). Other studies have however demonstrated no association of donor age to limbal culture success rate (Kim *et al.*, 2004, Baylis *et al.*, 2013) or proliferative potential (Shanmuganathan *et al.*, 2006). It is interesting to note that equally no relationship between increasing donor age and cell culture success rate was noted in this study: there are many confounding factors to culture success, and perhaps CFE is a more accurate measure. These latter studies also compared tissue from corneo-scleral rims that had been stored in organ culture for up to 93 days prior to cell culture (Baylis *et al.*, 2013). It is not clear whether tissue used in Notara *et al.*'s study was also previously subjected to organ culture, and if so the duration of (Notara *et al.*, 2013). The effect of such storage on culture success rates and proliferative potential is however also debated (James *et al.*, 2001, Kim *et al.*, 2004, Shanmuganathan *et al.*, 2006, Baylis *et al.*, 2013).

Only one study has assessed the effect of donor age on SC marker expression of human ocular surface epithelial cultures. It is interesting, that despite noting changes in the limbal SC niche microstructures, together with a reduction of CFE with increasing donor age; no associated reduction in SC marker expression in cultures was noted (Notara *et al.*, 2013). In contrast, in this study such relationships were ascertained in conjunctival tissue sections and for some SC markers in cultures. Clearly further investigations to clarify any relationships are indicated.

The Effect of Post Mortem Retrieval Time on Human Conjunctival Progenitor Cells

Significant associations were detected between increasing PMRT and lower CFE (Figure 64), and lower expression of ABCG2 in both tissue sections and cultured cells (Figure 42, Figure 82). These results should however similarly be interpreted with some caution due to the skewed distribution of PMRTs in this study. Previous studies have shown longer death to enucleation time, but interestingly not enucleation to culture medium time is associated with reduced human limbal epithelial culture success, growth rates and proliferative potential (Kim *et al.*, 2004, Shanmuganathan *et al.*, 2006). This is likely related to poor SC survival during a period of lack of vascular perfusion of the niche after death before being placed in nutrient-rich culture medium (Baylis *et al.*, 2013). However, other studies report no adverse effects of such delays (Baylis *et al.*, 2013). No previous studies have assessed the effect of PMRT on conjunctival clonogenic ability or conjunctival or limbal SC marker expression.

It is interesting to note, that although significant correlations between ABCG2 expression and both increasing donor age and PMRT, and between Hsp70 expression and increasing donor age were detected, no correlation was detected between Δ Np63 expression and either factor (Figure 82). Although p63 is considered a TAC marker (Parsa *et al.*, 1999), the Δ Np63 antibody encompasses the Δ Np63 α isoform which is considered a relatively pure SC marker (Kawasaki *et al.*, 2006). The reduction of CFE is perhaps however more clinically significant (Notara *et al.*, 2013). Certainly this data indicates that conjunctival cultures generated from younger donors and those with shorter PMRTs have greater proliferative potential, a factor which is of great clinical significance in generating epithelial equivalents for ocular surface reconstruction.

The Clinical Need for Progenitor Cells and Goblet Cells in Epithelial Constructs for Transplantation

Goblet cell and mucin deficiency are implicated in a wide spectrum of disabling conjunctival diseases (Tseng *et al.*, 1984, Doughty, 2012), and it can be presumed

that there is also significant SC deficiency in widespread severe conjunctival disease. Furthermore, reconstruction of the ocular surface in these severe cases will often require transplantation of large epithelial constructs. The levels of SCs and goblet cells in small *ex vivo* cultured conjunctival constructs for transplantation into otherwise healthy eyes may not be critical, and indeed transplantation of present constructs is reported with some success (Tan *et al.*, 2004, Ang *et al.*, 2005a, Ang and Tan, 2005). However, it is paramount that optimal levels of SC and goblet cells are achieved for extensive transplantations in severe disease, both to produce a functioning epithelium and to facilitate long-term success (Holland, 1996, Pellegrini *et al.*, 1999). Indeed, limbal epithelial transplantation containing inadequate numbers of SCs are associated with poor clinical outcomes (Rama *et al.*, 2010), and MUC5AC deficiency causes functional and structural changes in the ocular surface (Floyd *et al.*, 2012).

The localisation of the PC rich areas of the human conjunctiva in this study enables optimal PC rich biopsies to be selected for *ex vivo* expansion (Holland, 1996). Given these biopsies will often be required from patients with extensive ocular surface damage and associated conjunctival SC loss, this even more pertinent. For those patients with particularly severe disease who are unable to provide an adequate biopsy, the significance of younger donor age and shorter PMRTs to increasing SC yield and clonogenic ability in culture, will enable optimal selection of allograft donor tissue.

Ultimately, further characterisation of the conjunctival PCs will enable their positive selection and enrichment of cultures, such as has been achieved for limbal SC cultures (Hayashi *et al.*, 2007, Arpitha *et al.*, 2008).

Both goblet cells and mucins have been demonstrated in human conjunctival cultures (Corfield *et al.*, 1991, Frescura *et al.*, 1993, Diebold and Calonge, 1997, Pellegrini *et al.*, 1999, Shatos *et al.*, 2003, Berry and Radburn-Smith, 2005, Ang *et al.*, 2005b), but this has been difficult to achieve (Ang *et al.*, 2004b). This is despite the recognition that commitment to goblet cell differentiation may arise from TACs

(Pellegrini *et al.*, 1999); perhaps as the factors or stimuli regulating their proliferation is poorly understood (Shatos *et al.*, 2003). Although goblet cell differentiation in culture has been aided by the addition of various growth factors (Shatos *et al.*, 2003, Ríos *et al.*, 2006, Li *et al.*, 2010), higher initial concentrations of PCs in culture can only further support their development. Indeed, rat forniceal biopsies have been shown to yield the greatest number of goblet cells (Fostad *et al.*, 2012).

More specific than the need for goblet cells in epithelial constructs is the need for a normal mucin profile, including not only secreted MUC5AC but also the relative expression of membrane-associated mucins MUC1, 4 and 16. Human conjunctival cells in culture have been demonstrated to both synthesise and secrete mucins (Corfield *et al.*, 1991, Frescura *et al.*, 1993), and limbal epithelial cells cultured on amniotic membrane to express MUC1, 4 and 16 but at altered levels to normal tissue (Pauklin *et al.*, 2009). Given that both over and underproduction of mucins may induce ocular surface disease (Dartt, 2004), culture conditions must be optimised to achieve normal mucin profiles.

The Requirement of a Suitable Substrate

As the nature of the underlying matrix plays a key role in determining cellular growth and differentiation (Lin *et al.*, 2000, Ma, 2008), this must be intimately involved in the pursuit to produce a conjunctival epithelial equivalent which is replicable of the physiological state.

Substrates for conjunctival epithelial replacement must ideally be flexible and elastic to accommodate eye movement, mechanically strong to maintain reconstructed fornices (Kearns *et al.*, 2012), provide good cellular attachment (Ang *et al.*, 2004a), and promote the development of normal conjunctival epithelial physiology including the regenerative capacity of SCs and goblet cells.

To date, no substrate fulfils these requirements adequately. Although amniotic membrane has been favoured and indeed used in clinical transplantation, it is variable in quality (Liu *et al.*, 2010), liable to shrinkage (Barabino and Rolando, 2003, Honavar *et al.*, 2000), and unpredictable in its rate of degradation (Vyas and Rathi, 2009). Stratified conjunctival epithelial constructs have also been cultured on collagen gels (Berry and Radburn-Smith, 2005), and the polymer ultrathin Poly(ϵ -Caprolactone) (Ang *et al.*, 2006). Although the latter is a synthetic product which offers consistency in quality and is disease free; both are bio-resorbable materials. Long-term success in maintaining reconstructed fornices may be more likely to be achieved with a synthetic non-degradable scaffold. Expanded-polytetrafluoroethylene (ePTFE) is one such material. It offers biostability, porosity and excellent mechanical properties including elasticity and high tensile strength. It has been successfully used as a 'stent' for short-term forniceal maintenance in anophthalmic patients (Demirci *et al.*, 2010), and as a substrate for the attachment and proliferation of retinal pigment epithelial cells (Williams *et al.*, 2005, Krishna *et al.*, 2011). Although it is opaque, given the conjunctiva is not within the visual axis as the corneal epithelium is, optical clarity of a substrate is not required here. However being hydrophobic, it requires surface modification to enhance cellular adhesion. Such modification should aim to mimic the normal extracellular matrix and may be achieved in a number of different ways, such as plasma polymer coating (Notara *et al.*, 2007) or coatings with extracellular matrix proteins.

With a view to developing suitable substrate(s) for conjunctival epithelial constructs, attachment and growth of conjunctival cells on various extracellular matrix proteins were assessed. Each could be further developed as a pure biological substrate or as a coating on a synthetic substrate such as ePTFE. Growth rates on collagen IV, fibronectin, and laminin 1 were compared with the aim of replicating features of the normal conjunctival basement membrane (Tuori *et al.*, 1996, Schlötzer-Schrehardt *et al.*, 2007, Messmer *et al.*, 2012).

Conjunctival epithelial cells maintained similar morphology on each coating and were equally comparable to the control cells cultured with a 3T3 feeder layer

(Figure 83, Figure 84). Although statistically fibronectin supported greater growth at day 7 in culture, the effects were no longer apparent by day 10. However, it must be noted that these results have not been replicated, and thus these findings can only be judged as preliminary data. Cell counts for the control cells cultured with a 3T3 feeder layer were also not possible.

Given the normal conjunctival basement membrane comprises a variety of extracellular matrix proteins (Tuori *et al.*, 1996, Schlötzer-Schrehardt *et al.*, 2007, Messmer *et al.*, 2012), it is likely that optimal epithelial growth would be maintained by a combination of these. As such it is surprising that conjunctival epithelial cells were not successfully cultured on Matrigel™ basement membrane matrix (Figure 44, Figure 45), which contains both laminin and collagen IV in addition to other proteins and growth factors. It would be interesting to further compare conjunctival epithelial cell growth on coatings of each of these extracellular matrix proteins in differing concentrations, and also in combination with differing proportions of each. Indeed, the understanding of niche environments and the complexities of basement membrane compositions is becoming increasingly apparent; and it is likely that the ideal biological substrate or coating would comprise a composite of not only specific isoforms of these extracellular matrix proteins but also others such as nidogen, perlecan and clusterin which are found in the physiological basement membrane (Schlötzer-Schrehardt *et al.*, 2007).

Time restraints to this study unfortunately limited any further work to develop stratified conjunctival epithelial cell cultures on these coatings, and to ascertain their similarities to retrieved donor conjunctival epithelium in terms of their histological structure, expression of SC markers, presence of goblet cells, and their mucin profiles.

Overall Summary and Implications

Severe conjunctival diseases cause significant chronic pain, predisposition to ocular surface infections and often secondary blindness. Their management remains to be a great challenge to ophthalmologists. The prospect of a functional cultured conjunctival epithelial equivalent to restore the ocular surface of these patients offers immense hope.

This study describes an innovative technique to successfully retrieve whole human cadaveric conjunctival tissue for research purposes. This will benefit a wide range of future research into human conjunctival anatomy, pathophysiology and potential therapeutic targets. Using this technique I have performed the first comprehensive assessment of PCs across the whole human conjunctiva. Substantial evidence is presented through both CFE and SC marker expression that human conjunctival PCs are scattered throughout the tissue in the basal layer of the epithelium, but are in highest concentrations in the medial canthal and inferior forniceal areas. These areas may provide greater physical protection. But perhaps more importantly, they and in particular the plica semilunaris, are noted to be especially rich in goblet cells, intra-epithelial mucous crypts and the accessory lacrimal glands, blood vessels, melanocytes and immune cells; features which are common to other SC niches and may constitute features of the human conjunctival SC niche. Clonogenic ability and SC marker expression were inversely proportional to both donor age and PMRT. Finally, preliminary studies demonstrated fibronectin, collagen IV and laminin 1 may all support conjunctival epithelial *ex vivo* expansion.

As in all research, there are limitations to this study. Firstly, CFE and SC marker expression on cultured cells were performed at passage 1 in culture; ideally with sufficient cells these would have both been performed at passage 0. Secondly, immunohistochemical analysis was taken comparatively of subjectively selected representative images from each defined zone. In addition, the loss of eyelid margin epithelium and inability to consistently identify the mucocutaneous junction on immunohistochemical specimens meant that specific assessment of SC marker expression at the eyelid margin was unobtainable. In common with all studies

assessing SC marker expression, given there is no single definitive SC marker, a wider range of putative markers would have ideally been employed. Furthermore, only preliminary data was obtained on growth on different extracellular matrix proteins towards the development of a suitable substrate. Finally, because the sample sizes were limited, there is a risk that the results considered non-significant may well have been significant (i.e. type II error).

Conjunctival biopsies for human *ex vivo* expansion should be taken from the PC-rich medial canthal or inferior forniceal areas. Ideally biopsies should be retrieved from young donors with short PMRTs. I now hypothesise that such tissue can be propagated *ex vivo* into PC-rich functional epithelial equivalents on suitable substrates. Future work should be directed to this aim, to offer optimal success in long-term restoration of the ocular surface.

5. Conclusions

- Whole human cadaveric conjunctiva can be successfully retrieved with good donor cosmesis.
- Both expression of the SC marker ABCG2 in fixed tissue, CFE and the expression of the SC markers ABCG2, Δ Np63 and Hsp70 in cell cultures, indicate that conjunctival PCs are distributed throughout the human conjunctiva, but with significantly highest levels in the medial canthal and inferior forniceal areas.
- Increasing donor age is associated with a significant reduction in both ABCG2 expression in fixed tissue, CFE and ABCG2 and Hsp70 expression in cell cultures. Similarly, increasing PMRT is associated with a significant reduction in both ABCG2 expression in fixed tissue, CFE and ABCG2 expression in cell cultures.
- Preliminary results demonstrate that primary human conjunctival epithelial cell growth is supported by fibronectin, collagen IV and laminin 1 coatings.

6. Future Work

Future research should aim to further investigate the distribution of conjunctival PCs, in particular at the eyelid margin and in their relation to goblet cells. Although the technique employed in this study to retrieve whole conjunctival research specimens is notable, obtaining full thickness eyelid specimens from surgical procedures would enable better analysis of the distribution of PCs at the eyelid margin. Studies should seek to assess the expression of further putative SC markers across the tissue, such as connexin 43 (Wolosin *et al.*, 2000), integrin- β 1 (Pajoohesh-Ganji *et al.*, 2006), CK15 (Qi *et al.*, 2010, Pauklin *et al.*, 2011) and TrkA (Qi *et al.*, 2008, Qi *et al.*, 2010). Molecules associated with pluripotency/multipotency such as NANOG, OCT4 and SOX2 (Nichols *et al.*, 1998, Mitsui *et al.*, 2003, Chambers *et al.*, 2003) have also been detected in the human conjunctiva (Pauklin *et al.*, 2011); and an assessment into their expression across the whole tissue would also be warranted. Employing molecular techniques such as PCR would enable quantifiable assessment of SC marker gene expression, although this does not necessarily directly correlate with protein expression.

The conjunctival SC niche may then be characterised in terms of the relations to the immediately adjacent cells, the preferential expression of basement membrane proteins and proteoglycans, the signalling pathways controlling its regulation, and age-related effects. In order to further understand the mechanisms of conjunctival epithelial renewal, the effect of donor age and PMRT should be further clarified by the addition of fresh surgical samples and tissue from younger donors; and the development of goblet cells and regulation thereof should be investigated.

Using PC-rich biopsies from the medial canthal and inferior forniceal conjunctiva, culture conditions should be optimised to maintain the PCs *in vitro* and replicate the conjunctival SC niche to develop a stratified, functional and self-renewing epithelium for transplantation. In particular, optimal levels of functional goblet

cells must be obtained. Specific substrates should be developed to support such constructs, with properties that are suitable for ocular surface transplantation and in particular to maintain forniceal reconstruction. This offers the prospect of a long-awaited successful treatment for a multitude of severely disabling ocular surface disorders.

7. References

- ADAMS, E. J., GREEN, J. A., CLARK, A. H. & YOUNGSON, J. H. 1999. Comparison of different scoring systems for immunohistochemical staining. *Journal of Clinical Pathology*, 52, 75-77.
- AHMAD, S., FIGUEIREDO, F. & LAKO, M. 2006. Corneal epithelial stem cells: characterization, culture and transplantation. *Regenerative Medicine*, 1, 29-44.
- AHMAD, S., KOLLI, S., LI, D. Q., DE PAIVA, C. S., PRYZBORSKI, S., DIMMICK, I., ARMSTRONG, L., FIGUEIREDO, F. C. & LAKO, M. 2008. A putative role for RHAMM/HMMR as a negative marker of stem cell-containing population of human limbal epithelial cells. *Stem Cells*, 26, 1609-1619.
- AKNIN, M. L. R., BERRY, M., DICK, A. D. & KHAN-LIM, D. 2004. Normal but not altered mucins activate neutrophils. *Cell and Tissue Research*, 318, 545-551.
- AKNIN, M. R., KHAN-LIM, D., DICK, A. D. & BERRY, M. 2003. Mucins Recruit Leucocytes Selectively. *Investigative Ophthalmology and Visual Science*, 44, 2503-.
- ALBERTS, E. J., JOHNSON, A., LEWIS, J., RAFF, M., ROBERTS, K. & WATTS, P. 2008. *Molecular biology of the cell*, New York, Garland Science.
- ALONSO, L. & FUCHS, E. 2003. Stem cells of the skin epithelium. *Proceedings of the National Academy of Sciences of the United States of America*, 100, 11830-11835.
- ANDERSEN, H., EHLERS, N. & MATTHIESSEN, M. E. 1965. Histochemistry and development of the human eyelids. *Acta Ophthalmologica*, 43, 642-668.
- ANG, L. P. K., DO, T. P., THEIN, Z. M., REZA, H. M., TAN, X. W., YAP, C., TAN, D. T. H. & BEUERMAN, R. W. 2011. Ex vivo expansion of conjunctival and limbal epithelial cells using cord blood serum-supplemented culture medium. *Investigative Ophthalmology and Visual Science*, 52, 6138-6147.
- ANG, L. P. K., TAN, D. T., CAJUCOM-UY, H. & BEUERMAN, R. W. 2005a. Autologous cultivated conjunctival transplantation for pterygium surgery. *American Journal of Ophthalmology*, 139, 611-619.
- ANG, L. P. K. & TAN, D. T. H. 2005. Autologous cultivated conjunctival transplantation for recurrent viral papillomata. *American Journal of Ophthalmology*, 140, 136-138.
- ANG, L. P. K., TAN, D. T. H., BEUERMAN, R. W. & LAVKER, R. M. 2004a. Development of a conjunctival epithelial equivalent with improved proliferative properties using a multistep serum-free culture system. *Investigative Ophthalmology and Visual Science*, 45, 1789-1795.

- ANG, L. P. K., TAN, D. T. H., PHAN, T. T., LI, J., BEUERMAN, R. & LAVKER, R. M. 2004b. The in vitro and in vivo proliferative capacity of serum-free cultivated human conjunctival epithelial cells. *Current Eye Research*, 28, 307-317.
- ANG, L. P. K., TAN, D. T. H., SEAH, C. J. Y. & BEUERMAN, R. W. 2005b. The use of human serum in supporting the in vitro and in vivo proliferation of human conjunctival epithelial cells. *British Journal of Ophthalmology*, 89, 748-752.
- ANG, L. P. K., ZI, Y. C., BEUERMAN, R. W., SWEE, H. T., ZHU, X. & TAN, D. T. H. 2006. The development of a serum-free derived bioengineered conjunctival epithelial equivalent using an ultrathin poly(ϵ -caprolactone) membrane substrate. *Investigative Ophthalmology and Visual Science*, 47, 105-112.
- ARENDS, G. & SCHRAMM, U. 2004. The structure of the human semilunar plica at different stages of its development - A morphological and morphometric study. *Annals of Anatomy*, 186, 195-207.
- ARGÜESO, P., SPURR-MICHAUD, S., RUSSO, C. L., TISDALE, A. & GIPSON, I. K. 2003a. MUC16 mucin is expressed by the human ocular surface epithelia and carries the H185 carbohydrate epitope. *Investigative Ophthalmology and Visual Science*, 44, 2487-2495.
- ARGÜESO, P., TISDALE, A., MANDEL, U., LETKO, E., FOSTER, C. S. & GIPSON, I. K. 2003b. The cell-layer- and cell-type-specific distribution of Ga1NAc-transferases in the ocular surface epithelia is altered during keratinization. *Investigative Ophthalmology and Visual Science*, 44, 86-92.
- ARI, A. B. 2006. Eye injuries on the battlefields of Iraq and Afghanistan: Public health implications. *Optometry - Journal of the American Optometric Association*, 77, 329-339.
- ARMITAGE, W. J. & EASTY, D. L. 1997. Factors influencing the suitability of organ-cultured corneas for transplantation. *Investigative Ophthalmology and Visual Science*, 38, 16-24.
- ARPITHA, P., PRAJNA, N. V., SRINIVASAN, M. & MUTHUKKARUPPAN, V. 2008. A method to isolate human limbal basal cells enriched for a subset of epithelial cells with a large nucleus/cytoplasm ratio expressing high levels of p63. *Microscopy Research and Technique*, 71, 469-476.
- BALASUBRAMANIAN, S., JASTY, S., SITALAKSHMI, G., MADHAVAN, H. N. & KRISHNAKUMAR, S. 2008. Influence of feeder layer on the expression of stem cell markers in cultured limbal corneal epithelial cells. *Indian Journal of Medical Research*, 128, 616-622.
- BARABINO, S. & ROLANDO, M. 2003. Amniotic membrane transplantation elicits goblet cell repopulation after conjunctival reconstruction in a case of severe ocular cicatricial pemphigoid. *Acta Ophthalmologica Scandinavica*, 81, 68-71.
- BARNARD, Z., APEL, A. J. G. & HARKIN, D. G. 2001. Phenotypic analyses of limbal epithelial cell cultures derived from donor corneoscleral rims. *Clinical and Experimental Ophthalmology*, 29, 138-142.

- BARRANDON, Y. 1993. The epidermal stem cell: an overview. *Seminars in Developmental Biology*, 4, 209-215.
- BARRANDON, Y. 2007. Crossing boundaries: Stem cells, holoclones, and the fundamentals of squamous epithelial renewal. *Cornea*, 26, S10-S12.
- BARRANDON, Y. & GREEN, H. 1987. Three clonal types of keratinocyte with different capacities for multiplication. *Proceedings of the National Academy of Sciences of the United States of America*, 84, 2302-2306.
- BAYLIS, O., FIGUEIREDO, F., HENEIN, C., LAKO, M. & AHMAD, S. 2011. 13 Years of cultured limbal epithelial cell therapy: A review of the outcomes. *Journal of Cellular Biochemistry*, 112, 993-1002.
- BAYLIS, O., ROONEY, P., FIGUEIREDO, F., LAKO, M. & AHMAD, S. 2013. An investigation of donor and culture parameters which influence epithelial outgrowths from cultured human cadaveric limbal explants. *Journal of Cellular Physiology*, 228, 1025-1030.
- BELKIN, A. M. & STEPP, M. A. 2000. Integrins as receptors for laminins. *Microscopy Research and Technique*, 51, 280-301.
- BERNAUER, W., ELDER, M. J. & DART, J. K. 1997. Introduction to cicatrising conjunctivitis. *Developments in Ophthalmology*, 28, 1-10.
- BERRY, M. & RADBURN-SMITH, M. 2005. Conjunctiva organ and cell culture. *Methods in Molecular Medicine*, 107, 325-341.
- BLACK, B. L. & MOOG, F. 1977. Goblet cells in embryonic intestine: Accelerated differentiation in culture. *Science*, 197, 368-370.
- BOULTON, M. & ALBON, J. 2004. Stem cells in the eye. *International Journal of Biochemistry and Cell Biology*, 36, 643-657.
- BRON, A. J., TRIPATHI, R. C. & TRIPATHI, B. J. 1997. *Wolff's Anatomy of the Eye and Orbit*, London, Chapman and Hall.
- BRON, A. J., YOKOI, N., GAFFNEY, E. A. & TIFFANY, J. M. 2011. A solute gradient in the tear meniscus. i. a hypothesis to explain Marx's line. *Ocular Surface*, 9, 70-91.
- BUDAK, M. T., ALPDOGAN, O. S., ZHOU, M., LAVKER, R. M., AKINCI, M. A. M. & WOLOSIN, J. M. 2005. Ocular surface epithelia contain ABCG2-dependent side population cells exhibiting features associated with stem cells. *Journal of Cell Science*, 118, 1715-1724.
- BURTON, M. J. & MABEY, D. C. W. 2009. The global burden of trachoma: A review. *PLoS Neglected Tropical Diseases*, 3.
- BUTOVICH, I. A., MILLAR, T. J. & HAM, B. M. 2008. Understanding and analyzing meibomian lipids - A review. *Current Eye Research*, 33, 405-420.

- CALONGE, M., DIEBOLD, Y., SÁEZ, V., DE SALAMANCA, A. E., GARCÍA-VÁZQUEZ, C., CORRALES, R. M. & HERRERAS, J. M. 2004. Impression cytology of the ocular surface: A review. *Experimental Eye Research*, 78, 457-472.
- CALVI, L. M., ADAMS, G. B., WEIBRECHT, K. W., WEBER, J. M., OLSON, D. P., KNIGHT, M. C., MARTIN, R. P., SCHIPANI, E., DIVIETI, P., BRINGHURST, F. R., MILNER, L. A., KRONENBERG, H. M. & SCADDEN, D. T. 2003. Osteoblastic cells regulate the haematopoietic stem cell niche. *Nature*, 425, 841-846.
- CHAKRABORTY, A., DUTTA, J., DAS, S. & DATTA, H. 2013. Comparison of ex vivo cultivated human limbal epithelial stem cell viability and proliferation on different substrates. *International Ophthalmology*, 1-6.
- CHALLEN, G. A. & LITTLE, M. H. 2006. A side order of stem cells: The SP phenotype. *Stem Cells*, 24, 3-12.
- CHAMBERS, I., COLBY, D., ROBERTSON, M., NICHOLS, J., LEE, S., TWEEDIE, S. & SMITH, A. 2003. Functional expression cloning of Nanog, a pluripotency sustaining factor in embryonic stem cells. *Cell*, 113, 643-655.
- CHAN, L. S., RAZZAQUE AHMED, A., ANHALT, G. J., BERNAUER, W., COOPER, K. D., ELDER, M. J., FINE, J. D., STEPHEN FOSTER, C., GHOHESTANI, R., HASHIMOTO, T., HOANG-XUAN, T., KIRTSCHIG, G., KORMAN, N. J., LIGHTMAN, S., LOZADA-NUR, F., PETER MARINKOVICH, M., MONDINO, B. J., PROST-SQUARCIONI, C., ROGERS III, R. S., SETTERFIELD, J. F., WEST, D. P., WOJNAROWSKA, F., WOODLEY, D. T., YANCEY, K. B., ZILLIKENS, D. & ZONE, J. J. 2002. The first international consensus on mucous membrane pemphigoid: Definition, diagnostic criteria, pathogenic factors, medical treatment and prognostic indicators. *Archives of Dermatology*, 138, 370-379.
- CHEN, B., MI, S., WRIGHT, B. & CONNON, C. J. 2010. Differentiation status of limbal epithelial cells cultured on intact and denuded amniotic membrane before and after air-lifting. *Tissue Engineering - Part A*, 16, 2721-2729.
- CHEN, J. J. Y. & TSENG, S. C. G. 1991. Abnormal corneal epithelial wound healing in partial-thickness removal of limbal epithelium. *Investigative Ophthalmology and Visual Science*, 32, 2219-2233.
- CHEN, W., ISHIKAWA, M., YAMAKI, K. & SAKURAGI, S. 2003. Wistar rat palpebral conjunctiva contains more slow-cycling stem cells that have larger proliferative capacity: Implication for conjunctival epithelial homeostasis. *Japanese Journal of Ophthalmology*, 47, 119-128.
- CHEN, Y. T., LI, W., HAYASHIDA, Y., HE, H., CHEN, S. Y., TSENG, D. Y., KHEIRKHAH, A. & TSENG, S. C. G. 2007. Human amniotic epithelial cells as novel feeder layers for promoting ex vivo expansion of limbal epithelial progenitor cells. *Stem Cells*, 25, 1995-2005.
- CHEN, Z., DE PAIVA, C. S., LUO, L., KRETZER, F. L., PFLUGFELDER, S. C. & LI, D. Q. 2004. Characterization of putative stem cell phenotype in human limbal epithelia. *Stem Cells*, 22, 355-366.

- CIRALSKY, J. B., SIPPEL, K. C. & GREGORY, D. G. 2013. Current ophthalmologic treatment strategies for acute and chronic Stevens-Johnson syndrome and toxic epidermal necrolysis. *Current Opinion in Ophthalmology*, 24, 321-328.
- COOK, E. B., STAHL, J. L., MILLER, S. T., GERN, J. E., SUKOW, K. A., GRAZIANO, F. M. & BARNEY, N. P. 1998. Isolation of human conjunctival mast cells and epithelial cells: Tumor necrosis factor- α from mast cells affects intercellular adhesion molecule 1 expression on epithelial cells. *Investigative Ophthalmology and Visual Science*, 39, 336-343.
- CORFIELD, A. P., MYERSCOUGH, N., BERRY, M., CLAMP, J. R. & EASTY, D. L. 1991. Mucins synthesized in organ culture of human conjunctival tissue. *Biochemical Society Transactions*, 19.
- COTSARELIS, G., CHENG, S. Z., DONG, G., SUN, T. T. & LAVKER, R. M. 1989. Existence of slow-cycling limbal epithelial basal cells that can be preferentially stimulated to proliferate: Implications on epithelial stem cells. *Cell*, 57, 201-209.
- COTSARELIS, G., SUN, T. T. & LAVKER, R. M. 1990. Label-retaining cells reside in the bulge area of pilosebaceous unit: Implications for follicular stem cells, hair cycle, and skin carcinogenesis. *Cell*, 61, 1329-1337.
- DANIELS, J. T., DART, J. K. G., TUFT, S. J. & KHAW, P. T. 2001. Corneal stem cells in review. *Wound Repair and Regeneration*, 9, 483-494.
- DARTT, D. A. 2004. Control of mucin production by ocular surface epithelial cells. *Experimental Eye Research*, 78, 173-185.
- DARTT, D. A. 2011. Formation and function of the tear film. In: LEVIN, L. A., NILSSON, S. F. E., VER HOEVE, J. & WU, S. M. (eds.) *Adler's Physiology of the Eye*. 11 ed. Edinburgh: Saunders.
- DATA PROTECTION ACT 1998. United Kingdom:
<http://www.legislation.gov.uk/ukpga/1998/29/contents>.
- DAVANGER, M. & EVENSEN, A. 1971. Role of the pericorneal papillary structure in renewal of corneal epithelium. *Nature*, 229, 560-561.
- DAWSON, D. G., UBELS, J. L. & F., E. H. 2011. Cornea and sclera. In: LEVIN, L. A., NILSSON, S. F. E., VER HOEVE, J. & WU, S. M. (eds.) *Adler's Physiology of the Eye*. 11 ed. Edinburgh: Saunders.
- DAYA, S. M., WATSON, A., SHARPE, J. R., GILEDI, O., ROWE, A., MARTIN, R. & JAMES, S. E. 2005. Outcomes and DNA analysis of ex vivo expanded stem cell allograft for ocular surface reconstruction. *Ophthalmology*, 112, 470-477.
- DE LUCA, M., PELLEGRINI, G. & GREEN, H. 2006. Regeneration of squamous epithelia from stem cells of cultured grafts. *Regenerative Medicine*, 1, 45-57.
- DEMIRCI, H., ELNER, S. G. & ELNER, V. M. 2010. Rigid nylon foil-anchored polytetrafluoroethylene (Gore-Tex) sheet stenting for conjunctival fornix reconstruction. *Ophthalmology*, 117, 1736-1742.

- DI IORIO, E., BARBARO, V., RUZZA, A., PONZIN, D., PELLEGRINI, G. & DE LUCA, M. 2005. Isoforms of Δ Np63 and the migration of ocular limbal cells in human corneal regeneration. *Proceedings of the National Academy of Sciences of the United States of America*, 102, 9523-9528.
- DI IORIO, E., FERRARI, S., FASOLO, A., BÖHM, E., PONZIN, D. & BARBARO, V. 2010. Techniques for culture and assessment of limbal stem cell grafts. *Ocular Surface*, 8, 146-153.
- DIEBOLD, Y. & CALONGE, M. 1997. Characterization of epithelial primary cultures from human conjunctiva. *Graefe's Archive for Clinical and Experimental Ophthalmology*, 235, 268-276.
- DIEBOLD, Y., CALONGE, M., CALLEJO, S., LÁZARO, M. C., BRINGAS, R. & HERRERAS, J. M. 1999. Ultrastructural evidence of mucus in human conjunctival epithelial cultures. *Current Eye Research*, 19, 95-105.
- DING, X. W., WU, J. H. & JIANG, C. P. 2010. ABCG2: A potential marker of stem cells and novel target in stem cell and cancer therapy. *Life Sciences*, 86, 631-637.
- DONISI, P. M., RAMA, P., FASOLO, A. & PONZIN, D. 2003. Analysis of limbal stem cell deficiency by corneal impression cytology. *Cornea*, 22, 533-538.
- DOUGHTY, M. J. 2012. Goblet cells of the normal human bulbar conjunctiva and their assessment by impression cytology sampling. *Ocular Surface*, 10, 149-169.
- DUA, H. S., SHANMUGANATHAN, V. A., POWELL-RICHARDS, A. O., TIGHE, P. J. & JOSEPH, A. 2005. Limbal epithelial crypts: A novel anatomical structure and a putative limbal stem cell niche. *British Journal of Ophthalmology*, 89, 529-532.
- DUKE-ELDER, S. & COOK, C. 1963. *System of ophthalmology: Normal and abnormal development* London, Kimpton.
- EBATO, B., FRIEND, J. & THOFT, R. A. 1988. Comparison of limbal and peripheral human corneal epithelium in tissue culture. *Investigative Ophthalmology and Visual Science*, 29, 1533-1537.
- EIDET, J. R., FOSTAD, I. G., SHATOS, M. A., UTHEIM, T. P., UTHEIM, Ø. A., RAEDER, S. & DARTT, D. A. 2012a. Effect of biopsy location and size on proliferative capacity of ex vivo expanded conjunctival tissue. *Investigative Ophthalmology and Visual Science*, 53, 2897-2903.
- EIDET, J. R., UTHEIM, O. A., RAEDER, S., DARTT, D. A., LYBERG, T., CARRERAS, E., HUYNH, T. T., MESSELT, E. B., LOUCH, W. E., ROALD, B. & UTHEIM, T. P. 2012b. Effects of serum-free storage on morphology, phenotype, and viability of ex vivo cultured human conjunctival epithelium. *Experimental Eye Research*, 94, 109-116.
- ELDER, M. J., HISCOTT, P. & DART, J. K. G. 1997. Intermediate filament expression by normal and diseased human corneal epithelium. *Human Pathology*, 28, 1348-1354.

- EYE BANK ASSOCIATION OF AMERICA 2011. Medical Standards.
<http://www.restoresight.org/wp-content/uploads/2011/11/Medical-Standards-October-2011.pdf>.
- EYE BANK OF SOUTH AUSTRALIA 2012. Eye bank procedure manual.
- FENTEANY, G. & GLOGAUER, M. 2004. Cytoskeletal remodeling in leukocyte function. *Current Opinion in Hematology*, 11, 15-24.
- FISH, R. & DAVIDSON, R. S. 2010. Management of ocular thermal and chemical injuries, including amniotic membrane therapy. *Current Opinion in Ophthalmology*, 21, 317-321.
- FLOYD, A. M., ZHOU, X., EVANS, C., ROMPALA, O. J., ZHU, L., WANG, M. & CHEN, Y. 2012. Mucin Deficiency Causes Functional and Structural Changes of the Ocular Surface. *PLoS ONE*, 7.
- FOSTAD, I. G., EIDET, J. R., SHATOS, M. A., UTHEIM, T. P., UTHEIM, O. A., RAEDER, S. & DARTT, D. A. 2012. Biopsy harvesting site and distance from the explant affect conjunctival epithelial phenotype ex vivo. *Experimental Eye Research*, 104, 15-25.
- FRESCURA, M., CORFIELD, A. P. & BERRY, M. 1993. Cultured human conjunctival cells secrete mucins. *Biochemical Society Transactions*, 21.
- FRITSCH, P. 2008. European Dermatology Forum: Skin diseases in Europe. Skin diseases with a high public health impact: toxic epidermal necrolysis and Stevens-Johnson syndrome. *European Journal of Dermatology*, 18, 216-217.
- FUCHS, E. & CHEN, T. 2013. A matter of life and death: Self-renewal in stem cells. *EMBO Reports*, 14, 39-48.
- FUKUDA, K., CHIKAMA, T. I., NAKAMURA, M. & NISHIDA, T. 1999. Differential distribution of subchains of the basement membrane components type IV collagen and laminin among the amniotic membrane, cornea, and conjunctiva. *Cornea*, 18, 73-79.
- GAGO, N., PÉREZ-LÓPEZ, V., SANZ-JAKA, J. P., CORMENZANA, P., EIZAGUIRRE, I., BERNAD, A. & IZETA, A. 2009. Age-dependent depletion of human skin-derived progenitor cells. *Stem Cells*, 27, 1164-1172.
- GARRIDO, C., GURBUXANI, S., RAVAGNAN, L. & KROEMER, G. 2001. Heat shock proteins: Endogenous modulators of apoptotic cell death. *Biochemical and Biophysical Research Communications*, 286, 433-442.
- GIPSON, I. K. 2004. Distribution of mucins at the ocular surface. *Experimental Eye Research*, 78, 379-388.
- GIPSON, I. K., SPURR-MICHAUD, S., ARGÜESO, P., TISDALE, A., NG, T. F. & RUSSO, C. L. 2003. Mucin gene expression in immortalized human corneal-limbal and conjunctival epithelial cell lines. *Investigative Ophthalmology and Visual Science*, 44, 2496-2506.

- GOLDBERG, M. F. & BRON, A. J. 1982. Limbal palisades of Vogt. *Transactions of the American Ophthalmological Society*, Vol. 80, 155-171.
- GONG, Y., SYMMANS, W. F., KRISHNAMURTHY, S., PATEL, S. & SNEIGE, N. 2004. Optimal Fixation Conditions for Immunocytochemical Analysis of Estrogen Receptor in Cytologic Specimens of Breast Carcinoma. *Cancer*, 102, 34-40.
- GRUETERICH, M., ESPANA, E. M., TOUHAMI, A., TI, S. E. & TSENG, S. C. G. 2002. Phenotypic study of a case with successful transplantation of ex vivo expanded human limbal epithelium for unilateral total limbal stem cell deficiency. *Ophthalmology*, 109, 1547-1552.
- GRUETERICH, M., ESPANA, E. M. & TSENG, S. C. G. 2003. Ex vivo expansion of limbal epithelial stem cells: Amniotic membrane serving as a stem cell niche. *Survey of Ophthalmology*, 48, 631-646.
- HAN, B., SCHWAB, I. R., MADSEN, T. K. & ISSEROFF, R. R. 2002. A fibrin-based bioengineered ocular surface with human corneal epithelial stem cells. *Cornea*, 21, 505-510.
- HANNA, C., BICKNELL, D. S. & O'BRIEN, J. E. 1961. Cell turnover in the adult human eye. *Archives of Ophthalmology*, 65, 695-698.
- HARUN, M. H. N., SEPIAN, S. N., CHUA, K. H., ROPILAH, A. R., ABD GHAFAR, N., CHE-HAMZAH, J., BT HJ IDRUS, R. & ANNUAR, F. H. 2013. Human fornical region is the stem cell-rich zone of the conjunctival epithelium. *Human Cell*, 26, 35-40.
- HAYASHI, I., LARNER, J. & SATO, G. 1978. Hormonal growth control of cells in culture. *In Vitro*, 14, 23-30.
- HAYASHI, R., YAMATO, M., SUGIYAMA, H., SUMIDE, T., YANG, J., OKANO, T., TANO, Y. & NISHIDA, K. 2007. N-cadherin is expressed by putative stem/progenitor cells and melanocytes in the human limbal epithelial stem cell niche. *Stem Cells*, 25, 289-296.
- HAYNES, R. J., TIGHE, P. J. & DUA, H. S. 1999. Antimicrobial defensin peptides of the human ocular surface. *British Journal of Ophthalmology*, 83, 737-741.
- HERMAN, W. K., DOUGHMAN, D. J. & LINDSTROM, R. L. 1983. Conjunctival autograft transplantation for unilateral ocular surface diseases. *Ophthalmology*, 90, 1121-1126.
- HERNANDEZ GALINDO, E. E., THEISS, C., STEUHL, K. P. & MELLER, D. 2003. Expression of Δ Np63 in response to phorbol ester in human limbal epithelial cells expanded on intact human amniotic membrane. *Investigative Ophthalmology and Visual Science*, 44, 2959-2965.
- HIGA, K., SHIMMURA, S., MIYASHITA, H., KATO, N., OGAWA, Y., KAWAKITA, T., SHIMAZAKI, J. & TSUBOTA, K. 2009. N-Cadherin in the maintenance of human corneal limbal epithelial progenitor cells in vitro. *Investigative Ophthalmology and Visual Science*, 50, 4640-4645.

- HOFFMAN, M. P., NOMIZU, M., ROQUE, E., LEE, S., JUNG, D. W., YAMADA, Y. & KLEINMAN, H. K. 1998. Laminin-1 and laminin-2 G-domain synthetic peptides bind syndecan-1 and are involved in acinar formation of a human submandibular gland cell line. *Journal of Biological Chemistry*, 273, 28633-28641.
- HOLLAND, E. J. 1996. Epithelial transplantation for the management of severe ocular surface disease. *Transactions of the American Ophthalmological Society*, 94, 677-743.
- HONAVAR, S. G., BANSAL, A. K., SANGWAN, V. S. & RAO, G. N. 2000. Amniotic membrane transplantation for ocular surface reconstruction Stevens-Johnson syndrome. *Ophthalmology*, 107, 975-979.
- HOWARD, C., GARCIA-FIÑANA, M., YAN, Q. & HISCOTT, P. 2010. Human retinal pigment epithelial SPARC expression and age: An immunohistochemical study. *Histology and Histopathology*, 25, 1163-1169.
- HUANG, A. J. W. & TSENG, S. C. G. 1991. Corneal epithelial wound healing in the absence of limbal epithelium. *Investigative Ophthalmology and Visual Science*, 32, 96-105.
- HUGHES, C., HAMILTON, L. & DOUGHTY, M. J. 2003. A quantitative assessment of the location and width of Marx's line along the marginal zone of the human eyelid. *Optometry and Vision Science*, 80, 564-572.
- HUMAN TISSUE ACT 2004. United Kingdom:
<http://www.legislation.gov.uk/ukpga/2004/30/contents>.
- INATOMI, T., SPURR-MICHAUD, S., TISDALE, A. S. & GIPSON, I. K. 1995. Human corneal and conjunctival epithelia express MUC1 mucin. *Investigative Ophthalmology and Visual Science*, 36, 1818-1827.
- INATOMI, T., SPURR-MICHAUD, S., TISDALE, A. S., ZHAN, Q., FELDMAN, S. T. & GIPSON, I. K. 1996. Expression of secretory mucin genes by human conjunctival epithelia. *Investigative Ophthalmology and Visual Science*, 37, 1684-1692.
- IVANOVA, N. B., DIMOS, J. T., SCHANIEL, C., HACKNEY, J. A., MOORE, K. A. & LEMISCHKA, I. R. 2002. A stem cell molecular signature. *Science*, 298, 601-604.
- IWATA, T., OHKAWA, K. & UYAMA, M. 1976. The fine structural localization of peroxidase activity in goblet cells of the conjunctival epithelium of rats. *Investigative Ophthalmology*, 15, 40-44.
- JAMES, S. E., ROWE, A., ILARI, L., DAYA, S. & MARTIN, R. 2001. The potential for eye bank limbal rings to generate cultured corneal epithelial allografts. *Cornea*, 20, 488-494.
- JIRSOVA, K., DUDAKOVA, L., KALASOVA, S., VESELA, V. & MERJAVA, S. 2011. The OV-TL 12/30 clone of anti-cytokeratin 7 antibody as a new marker of corneal conjunctivalization in patients with limbal stem cell deficiency. *Investigative Ophthalmology and Visual Science*, 52, 5892-5898.

- JOYCE, N. C., MEKLIR, B., JOYCE, S. J. & ZIESKE, J. D. 1996. Cell cycle protein expression and proliferative status in human corneal cells. *Investigative Ophthalmology and Visual Science*, 37, 645-655.
- KALASKAR, D. M., DOWNES, J. E., MURRAY, P., EDGAR, D. H. & WILLIAMS, R. L. 2013. Characterization of the interface between adsorbed fibronectin and human embryonic stem cells. *Journal of the Royal Society Interface*, 10.
- KASPER, M., MOLL, R., STOSIEK, P. & KARSTEN, U. 1988. Patterns of cytokeratin and vimentin expression in the human eye. *Histochemistry*, 89, 369-377.
- KAWASAKI, S., TANIOKA, H., YAMASAKI, K., CONNON, C. J. & KINOSHITA, S. 2006. Expression and tissue distribution of p63 isoforms in human ocular surface epithelia. *Experimental Eye Research*, 82, 293-299.
- KEARNS, V., STEWART, R., MASON, S., SHERIDAN, C. & WILLIAMS, R. 2012. Ophthalmic applications of biomaterials in regenerative medicine. In: RAMALINGHAM, M., RAMAKRISHNA, S. & BEST, S. (eds.) *Biomaterials and Stem Cells in Regenerative Medicine*. London: CRC Press.
- KENYON, K. R. & TSENG, S. C. G. 1989. Limbal autograft transplantation for ocular surface disorders. *Ophthalmology*, 96, 709-723.
- KESIMER, M., EHRE, C., BURNS, K. A., DAVIS, C. W., SHEEHAN, J. K. & PICKLES, R. J. 2013. Molecular organization of the mucins and glycocalyx underlying mucus transport over mucosal surfaces of the airways. *Mucosal Immunology*, 6, 379-392.
- KESSING, S. V. 1968. Mucous gland system of the conjunctiva. A quantitative normal anatomical study. *Acta Ophthalmologica*, Suppl 95, 1+.
- KHOSHNOODI, J., PEDCHENKO, V. & HUDSON, B. G. 2008. Mammalian collagen IV. *Microscopy Research and Technique*, 71, 357-370.
- KIEL, M. J., HE, S., ASHKENAZI, R., GENTRY, S. N., TETA, M., KUSHNER, J. A., JACKSON, T. L. & MORRISON, S. J. 2007. Haematopoietic stem cells do not asymmetrically segregate chromosomes or retain BrdU. *Nature*, 449, 238-242.
- KIM, H. S., SONG, X. J., DE PAIVA, C. S., CHEN, Z., PFLUGFELDER, S. C. & LI, D. Q. 2004. Phenotypic characterization of human corneal epithelial cells expanded ex vivo from limbal explant and single cell cultures. *Experimental Eye Research*, 79, 41-49.
- KNOP, E. & KNOP, N. 2007. Anatomy and immunology of the ocular surface. *Chemical Immunology and Allergy*, 92, 36-49.
- KOIZUMI, N., INATOMI, T., SUZUKI, T., SOTOZONO, C. & KINOSHITA, S. 2001. Cultivated corneal epithelial stem cell transplantation in ocular surface disorders. *Ophthalmology*, 108, 1569-1574.
- KOIZUMI, N., RIGBY, H., FULLWOOD, N. J., KAWASAKI, S., TANIOKA, H., KOIZUMI, K., KOCIOK, N., JOUSSEN, A. M. & KINOSHITA, S. 2007. Comparison of intact and denuded amniotic membrane as a substrate for cell-suspension culture of

- human limbal epithelial cells. *Graefe's Archive for Clinical and Experimental Ophthalmology*, 245, 123-134.
- KOLLI, S., LAKO, M., FIGUEIREDO, F., MUDHAR, H. & AHMAD, S. 2008. Loss of corneal epithelial stem cell properties in outgrowths from human limbal explants cultured on intact amniotic membrane. *Regenerative Medicine*, 3, 329-342.
- KOLLI, S. A. I., AHMAD, S., LAKO, M. & FIGUEIREDO, F. 2010. Successful clinical implementation of corneal epithelial stem cell therapy for treatment of unilateral limbal stem cell deficiency. *Stem Cells*, 28, 597-610.
- KOROMA, B. M., YANG, J. M. & SUNDIN, O. H. 1997. The Pax-6 homeobox gene is expressed throughout the corneal and conjunctival epithelia. *Investigative Ophthalmology and Visual Science*, 38, 108-120.
- KRENZER, K. L. & FREDDO, T. F. 1994. Patterns of cytokeratin expression in impression cytology specimens from normal human conjunctival epithelium. *Advances in Experimental Medicine and Biology*, 350, 289-292.
- KRISHNA, Y., SHERIDAN, C., KENT, D., KEARNS, V., GRIERSON, I. & WILLIAMS, R. 2011. Expanded polytetrafluoroethylene as a substrate for retinal pigment epithelial cell growth and transplantation in age-related macular degeneration. *British Journal of Ophthalmology*, 95, 569-573.
- KRUSE, F. E., CHEN, J. J. Y., TSAI, R. J. F. & TSENG, S. C. G. 1990. Conjunctival transdifferentiation is due to the incomplete removal of limbal basal epithelium. *Investigative Ophthalmology and Visual Science*, 31, 1903-1913.
- KUCKELKORN, R., SCHRAGE, N., KELLER, G. & REDBRAKE, C. 2002. Emergency treatment of chemical and thermal eye burns. *Acta Ophthalmologica Scandinavica*, 80, 4-10.
- LAJTHA, L. G. & HOLTZER, H. 1979. Stem cell concepts. *Differentiation*, 14, 23-34.
- LANGER, G., JAGLA, W., BEHRENS-BAUMANN, W., WALTER, S. & HOFFMANN, W. 1999. Secretory peptides TFF1 and TFF3 synthesized in human conjunctival goblet cells. *Investigative Ophthalmology and Visual Science*, 40, 2220-2224.
- LAULE, A., CABLE, M. K., HOFFMAN, C. E. & HANNA, C. 1978. Endothelial cell population changes of human cornea during life. *Archives of Ophthalmology*, 96, 2031-2035.
- LAUWERYNS, B., VAN DEN OORD, J. J., DE VOS, R. & MISSOTTEN, L. 1993. A new epithelial cell type in the human cornea. *Investigative Ophthalmology and Visual Science*, 34, 1983-1990.
- LAVKER, R. M., TSENG, S. C. G. & SUN, T. T. 2004. Corneal epithelial stem cells at the limbus: Looking at some old problems from a new angle. *Experimental Eye Research*, 78, 433-446.
- LAVKER, R. M., WEI, Z. G. & SUN, T. T. 1998. Phorbol ester preferentially stimulates mouse fornical conjunctival and limbal epithelial cells to proliferate in vivo. *Investigative Ophthalmology and Visual Science*, 39, 301-307.

- LEMP, M. A. & MARQUARDT, R. 1992. *The dry eye: A comprehensive guide*, Berlin, Springer-Verlag.
- LEONG, A. S. 2004. Pitfalls in diagnostic immunohistology. *Advances in anatomic pathology*, 11, 86-93.
- LEVIS, H. J., BROWN, R. A. & DANIELS, J. T. 2010. Plastic compressed collagen as a biomimetic substrate for human limbal epithelial cell culture. *Biomaterials*, 31, 7726-7737.
- LI, D. Q., CHEN, Z., SONG, X. J., DE PAIVA, C. S., KIM, H. S. & PFLUGFELDER, S. C. 2005. Partial enrichment of a population of human limbal epithelial cells with putative stem cell properties based on collagen type IV adhesiveness. *Experimental Eye Research*, 80, 581-590.
- LI, W., HAYASHIDA, Y., CHEN, Y. T. & TSENG, S. C. G. 2007. Niche regulation of corneal epithelial stem cells at the limbus. *Cell Research*, 17, 26-36.
- LI, W., SUN, X., WANG, Z., LI, R. & LI, L. 2010. The effect of nerve growth factor on differentiation of corneal limbal epithelial cells to conjunctival goblet cells in vitro. *Molecular Vision*, 16, 2739-2744.
- LIN, L., DANESHVAR, C. & KURPAKUS-WHEATER, M. 2000. Evidence for differential signaling in human conjunctival epithelial cells adherent to laminin isoforms. *Experimental Eye Research*, 70, 537-546.
- LINDBERG, K., BROWN, M. E., CHAVES, H. V., KENYON, K. R. & RHEINWALD, J. G. 1993. In vitro propagation of human ocular surface epithelial cells for transplantation. *Investigative Ophthalmology and Visual Science*, 34, 2672-2679.
- LIU, J., LAWRENCE, B. D., LIU, A., SCHWAB, I. R., OLIVEIRA, L. A. & ROSENBLATT, M. I. 2012a. Silk fibroin as a biomaterial substrate for corneal epithelial cell sheet generation. *Investigative Ophthalmology and Visual Science*, 53, 4130-4138.
- LIU, J., SHEHA, H., FU, Y., LIANG, L. & TSENG, S. C. G. 2010. Update on amniotic membrane transplantation. *Expert Review of Ophthalmology*, 5, 645-661.
- LIU, S., LI, J., TAN, D. T. H. & BEUERMAN, R. W. 2007. The eyelid margin: A transitional zone for 2 epithelial phenotypes. *Archives of Ophthalmology*, 125, 523-532.
- LIU, T., ZHAI, H., XU, Y., DONG, Y., SUN, Y., ZANG, X. & ZHAO, J. 2012b. Amniotic membrane traps and induces apoptosis of inflammatory cells in ocular surface chemical burn. *Molecular Vision*, 18, 2137-2146.
- LUDWIG, T. E., BERGENDAHL, V., LEVENSTEIN, M. E., YU, J., PROBASCO, M. D. & THOMSON, J. A. 2006. Feeder-independent culture of human embryonic stem cells. *Nature Methods*, 3, 637-646.
- LYNGHOLM, M., VORUM, H., NIELSEN, K., ØSTERGAARD, M., HONORÉ, B. & EHLERS, N. 2008. Differences in the protein expression in limbal versus central human corneal epithelium - a search for stem cell markers. *Experimental Eye Research*, 87, 96-105.

- MA, D. H. K., LAI, J. Y., YU, S. T., LIU, J. Y., YANG, U., CHEN, H. C. J., YEH, L. K., HO, Y. J., CHANG, G., WANG, S. F., CHEN, J. K. & LIN, K. K. 2012. Up-regulation of heat shock protein 70-1 (Hsp70-1) in human limbo-corneal epithelial cells cultivated on amniotic membrane: A proteomic study. *Journal of Cellular Physiology*, 227, 2030-2039.
- MA, P. X. 2008. Biomimetic materials for tissue engineering. *Advanced Drug Delivery Reviews*, 60, 184-198.
- MALINDA, K. M. & KLEINMAN, H. K. 1996. The laminins. *International Journal of Biochemistry and Cell Biology*, 28, 957-959.
- MANTELLI, F. & ARGÜESO, P. 2008. Functions of ocular surface mucins in health and disease. *Current Opinion in Allergy and Clinical Immunology*, 8, 477-483.
- MARIAPPAN, I., MADDILETI, S., SAVY, S., TIWARI, S., GADDIPATI, S., FATIMA, A., SANGWAN, V. S., BALASUBRAMANIAN, D. & VEMUGANTI, G. K. 2010. In vitro culture and expansion of human limbal epithelial cells. *Nature Protocols*, 5, 1470-1479.
- MARTÍNEZ-OSORIO, H., CALONGE, M., CORELL, A., REINOSO, R., LÓPEZ, A., FERNÁNDEZ, I., SAN JOSÉ, E. G. & DIEBOLD, Y. 2009. Characterization and short-term culture of cells recovered from human conjunctival epithelium by minimally invasive means. *Molecular Vision*, 15, 2185-2195.
- MASON, S. L., STEWART, R. M., KEARNS, V. R., WILLIAMS, R. L. & SHERIDAN, C. M. 2011. Ocular epithelial transplantation: Current uses and future potential. *Regenerative Medicine*, 6, 767-782.
- MAYHALL, E. A., PAFFETT-LUGASSY, N. & ZON, L. I. 2004. The clinical potential of stem cells. *Current Opinion in Cell Biology*, 16, 713-720.
- MCKENZIE, R. W., JUMBLATT, J. E. & JUMBLATT, M. M. 2000. Quantification of MUC2 and MUC5AC transcripts in human conjunctiva. *Investigative Ophthalmology and Visual Science*, 41, 703-708.
- MCNAMARA, N. A., VAN, R., TUCHIN, O. S. & FLEISZIG, S. M. J. 1999. Ocular surface epithelia express mRNA for human beta defensin-2. *Experimental Eye Research*, 69, 483-490.
- MELLER, D., DABUL, V. & TSENG, S. C. G. 2002. Expansion of conjunctival epithelial progenitor cells on amniotic membrane. *Experimental Eye Research*, 74, 537-545.
- MELLER, D. & TSENG, S. C. G. 1999. Conjunctival epithelial cell differentiation on amniotic membrane. *Investigative Ophthalmology and Visual Science*, 40, 878-886.
- MERJAVA, S., BREJCHOVA, K., VERNON, A., DANIELS, J. T. & JIRSOVA, K. 2011a. Cytokeratin 8 is expressed in human corneconjunctival epithelium, particularly in limbal epithelial cells. *Investigative Ophthalmology and Visual Science*, 52, 787-794.

- MERJAVA, S., NEUWIRTH, A., TANZEROVA, M. & JIRSOVA, K. 2011b. The spectrum of cytokeratins expressed in the adult human cornea, limbus and perilimbal conjunctiva. *Histology and Histopathology*, 26, 323-331.
- MERLE, H., GÉRARD, M. & SCHRAGE, N. 2008. Ocular burns. *Journal Français d'Ophthalmologie*, 31, 723-734.
- MESSMER, E. M., VALET, V. M. & KAMPIK, A. 2012. Differences in basement membrane zone components of normal conjunctiva, conjunctiva in glaucoma and normal skin. *Acta Ophthalmologica*, 90, e476-e481.
- MI, S., CHEN, B., WRIGHT, B. & CONNON, C. J. 2010. Plastic compression of a collagen gel forms a much improved scaffold for ocular surface tissue engineering over conventional collagen gels. *Journal of Biomedical Materials Research Part A*, 95A, 447-453.
- MIKKERS, H. & FRISÉN, J. 2005. Deconstructing stemness. *EMBO Journal*, 24, 2715-2719.
- MITSIADIS, T. A., BARRANDON, O., ROCHAT, A., BARRANDON, Y. & DE BARI, C. 2007. Stem cell niches in mammals. *Experimental Cell Research*, 313, 3377-3385.
- MITSUI, K., TOKUZAWA, Y., ITOH, H., SEGAWA, K., MURAKAMI, M., TAKAHASHI, K., MARUYAMA, M., MAEDA, M. & YAMANAKA, S. 2003. The homeoprotein nanog is required for maintenance of pluripotency in mouse epiblast and ES cells. *Cell*, 113, 631-642.
- MIYASHITA, K., AZUMA, N. & HIDA, T. 1992. Morphological and histochemical studies of goblet cells in developing human conjunctiva. *Japanese Journal of Ophthalmology*, 36, 169-174.
- MOLL, R., FRANKE, W. W., SCHILLER, D. L., GEIGER, B. & KREPLER, R. 1982. The catalog of human cytokeratins: Patterns of expression in normal epithelia, tumors and cultured cells. *Cell*, 31, 11-24.
- MOORE, K. A. & LEMISCHKA, I. R. 2006. Stem cells and their niches. *Science*, 311, 1880-1885.
- MUSHTAQ, S., NAQVI, Z. A., SIDDIQUI, A. A., PALMBERG, C., SHAFQAT, J. & AHMED, N. 2007. Changes in albumin precursor and heat shock protein 70 expression and their potential role in response to corneal epithelial wound repair. *Proteomics*, 7, 463-468.
- NAGASAKI, T. & ZHAO, J. 2005. Uniform distribution of epithelial stem cells in the bulbar conjunctiva. *Investigative Ophthalmology and Visual Science*, 46, 126-132.
- NAKAMURA, T., ANG, L. P. K., RIGBY, H., SEKIYAMA, E., INATOMI, T., SOTOZONO, C., FULLWOOD, N. J. & KINOSHITA, S. 2006. The use of autologous serum in the development of corneal and oral epithelial equivalents in patients with Stevens-Johnson syndrome. *Investigative Ophthalmology and Visual Science*, 47, 909-916.

- NATIONAL INSTITUTE FOR HEALTH AND CLINICAL EXCELLENCE 2006. Patient safety and reduction of risk of transmission of Creutzfeldt-Jakob disease (CJD) via interventional procedures (IPG 196). <http://www.nice.org.uk/IPG196>.
- NICHOLS, J., ZEVIK, B., ANASTASSIADIS, K., NIWA, H., KLEWE-NEBENIUS, D., CHAMBERS, I., SCHÖLER, H. & SMITH, A. 1998. Formation of pluripotent stem cells in the mammalian embryo depends on the POU transcription factor Oct4. *Cell*, 95, 379-391.
- NISHINA, S., KOHSAKA, S., YAMAGUCHI, Y., HANDA, H., KAWAKAMI, A., FUJISAWA, H. & AZUMA, N. 1999. PAX6 expression in the developing human eye. *British Journal of Ophthalmology*, 83, 723-727.
- NOSKE, W., FROMM, M., LEVARLET, B., KREUSEL, K. M. & HIRSCH, M. 1994. Tight junctions of the human corneal endothelium: morphological and electrophysiological features. *German journal of ophthalmology*, 3, 253-257.
- NOTARA, M., BULLETT, N. A., DESHPANDE, P., HADDOW, D. B., MACNEIL, S. & DANIELS, J. T. 2007. Plasma polymer coated surfaces for serum-free culture of limbal epithelium for ocular surface disease. *Journal of Materials Science: Materials in Medicine*, 18, 329-338.
- NOTARA, M., SHORTT, A. J., O'CALLAGHAN, A. R. & DANIELS, J. T. 2013. The impact of age on the physical and cellular properties of the human limbal stem cell niche. *Age*, 35, 289-300.
- OHLSTEIN, B., KAI, T., DECOTTO, E. & SPRADLING, A. 2004. The stem cell niche: Theme and variations. *Current Opinion in Cell Biology*, 16, 693-699.
- OMOTO, M., MIYASHITA, H., SHIMMURA, S., HIGA, K., KAWAKITA, T., YOSHIDA, S., MCGROGAN, M., SHIMAZAKI, J. & TSUBOTA, K. 2009. The use of human mesenchymal stem cell-derived feeder cells for the cultivation of transplantable epithelial sheets. *Investigative Ophthalmology and Visual Science*, 50, 2109-2115.
- OSEI-BEMPONG, C., HENEIN, C. & AHMAD, S. 2009. Culture conditions for primary human limbal epithelial cells. *Regenerative Medicine*, 4, 461-470.
- PAJOOHESH-GANJI, A., PAL-GHOSH, S., SIMMENS, S. J. & STEPP, M. A. 2006. Integrins in Slow-Cycling Corneal Epithelial Cells at the Limbus in the Mouse. *Stem Cells*, 24, 1075-1086.
- PANKOV, R. & YAMADA, K. M. 2002. Fibronectin at a glance. *Journal of Cell Science*, 115, 3861-3863.
- PAPINI, S., ROSELLINI, A., NARDI, M., GIANNARINI, C. & REVOLTELLA, R. P. 2005. Selective growth and expansion of human corneal epithelial basal stem cells in a three-dimensional-organ culture. *Differentiation*, 73, 61-68.
- PARSA, R., YANG, A., MCKEON, F. & GREEN, H. 1999. Association of p63 with proliferative potential in normal and neoplastic human keratinocytes. *Journal of Investigative Dermatology*, 113, 1099-1105.

- PAUKLIN, M., FUCHSLUGER, T. A., WESTEKEMPER, H., STEUHL, K. P. & MELLER, D. 2010. Midterm results of cultivated autologous and allogeneic limbal epithelial transplantation in limbal stem cell deficiency. *Developments in Ophthalmology*, 45, 57-70.
- PAUKLIN, M., KAKKASSERY, V., STEUHL, K. P. & MELLER, D. 2009. Expression of membrane-associated mucins in limbal stem cell deficiency and after transplantation of cultivated limbal epithelium. *Current Eye Research*, 34, 221-230.
- PAUKLIN, M., THOMASEN, H., PESTER, A., STEUHL, K. P. & MELLER, D. 2011. Expression of pluripotency and multipotency factors in human ocular surface tissues. *Current Eye Research*, 36, 1086-1097.
- PAULSEN, F. P. & BERRY, M. S. 2006. Mucins and TFF peptides of the tear film and lacrimal apparatus. *Progress in Histochemistry and Cytochemistry*, 41, 1-53.
- PE'ER, J., ZAJICEK, G., GREIFNER, H. & KOGAN, M. 1996. Streaming conjunctiva. *Anatomical Record*, 245, 36-40.
- PELLEGRINI, G., DELLAMBRA, E., GOLISANO, O., MARTINELLI, E., FANTOZZI, I., BONDANZA, S., PONZIN, D., MCKEON, F. & DE LUCA, M. 2001. p63 identifies keratinocyte stem cells. *Proceedings of the National Academy of Sciences of the United States of America*, 98, 3156-3161.
- PELLEGRINI, G., GOLISANO, O., PATERNA, P., LAMBIASE, A., BONINI, S., RAMA, P. & DE LUCA, M. 1999. Location and clonal analysis of stem cells and their differentiated progeny in the human ocular surface. *Journal of Cell Biology*, 145, 769-782.
- PELLEGRINI, G., TRAVERSO, C. E., FRANZI, A. T., ZINGIRIAN, M., CANCEDDA, R. & DE LUCA, M. 1997. Long-term restoration of damaged corneal surfaces with autologous cultivated corneal epithelium. *Lancet*, 349, 990-993.
- PEPPERL, J. E. 2007. Conjunctiva. In: TASMAN, W. & A., J. E. (eds.) *Duane's Foundations of Clinical Ophthalmology*. Lippincott.
- PFISTER, R. R. 1975. The normal surface of conjunctiva epithelium. A scanning electron microscopic study. *Investigative Ophthalmology*, 14, 267-279.
- PFLUGFELDER, S. C., LIU, Z., MONROY, D., LI, D. Q., CARVAJAL, M. E., PRICE-SCHIAVI, S. A., IDRIS, N., SOLOMON, A., PEREZ, A. & CARRAWAY, K. L. 2000. Detection of sialomucin complex (MUC4) in human ocular surface epithelium and tear fluid. *Investigative Ophthalmology and Visual Science*, 41, 1316-1326.
- PILARSKI, L. M., PRUSKI, E., WIZNIAK, J., PAINE, D., SEEBERGER, K., MANT, M. J., BROWN, C. B. & BELCH, A. R. 1999. Potential role for hyaluronan and the hyaluronan receptor RHAMM in mobilization and trafficking of hematopoietic progenitor cells. *Blood*, 93, 2918-2927.
- PITZ, S. & MOLL, R. 2002. Intermediate-filament expression in ocular tissue. *Progress in Retinal and Eye Research*, 21, 241-262.

- POTTEN, C. S. & LOEFFLER, M. 1990. Stem cells: Attributes, cycles, spirals, pitfalls and uncertainties. Lessons for and from the crypt. *Development*, 110, 1001-1020.
- QI, H., LI, D. Q., SHINE, H. D., CHEN, Z., YOON, K. C., JONES, D. B. & PFLUGFELDER, S. C. 2008. Nerve growth factor and its receptor TrkA serve as potential markers for human corneal epithelial progenitor cells. *Experimental Eye Research*, 86, 34-40.
- QI, H., ZHENG, X., YUAN, X., PFLUGFELDER, S. C. & LI, D. Q. 2010. Potential localization of putative stem/progenitor cells in human bulbar conjunctival epithelium. *Journal of Cellular Physiology*, 225, 180-185.
- RADFORD, C. F., RAUZ, S., WILLIAMS, G. P., SAW, V. P. J. & DART, J. K. G. 2012. Incidence, presenting features, and diagnosis of cicatrising conjunctivitis in the United Kingdom. *Eye (Basingstoke)*, 26, 1199-1208.
- RAMA, P., MATUSKA, S., PAGANONI, G., SPINELLI, A., DE LUCA, M. & PELLEGRINI, G. 2010. Limbal stem-cell therapy and long-term corneal regeneration. *New England Journal of Medicine*, 363, 147-155.
- RAMAESH, K. & DHILLON, B. 2003. Ex vivo expansion of corneal limbal epithelial/stem cells for corneal surface reconstruction. *European Journal of Ophthalmology*, 13, 515-524.
- RAMALHO-SANTOS, M., YOON, S., MATSUZAKI, Y., MULLIGAN, R. C. & MELTON, D. A. 2002. "Stemness": Transcriptional profiling of embryonic and adult stem cells. *Science*, 298, 597-600.
- RAMIREZ-MIRANDA, A., NAKATSU, M. N., ZAREI-GHANAVATI, S., NGUYEN, C. V. & DENG, S. X. 2011. Keratin 13 is a more specific marker of conjunctival epithelium than keratin 19. *Molecular Vision*, 17, 1652-1661.
- RHEINWALD, J. G. & GREEN, H. 1975a. Formation of a keratinizing epithelium in culture by a cloned cell line derived from a teratoma. *Cell*, 6, 317-330.
- RHEINWALD, J. G. & GREEN, H. 1975b. Serial cultivation of strains of human epidermal keratinocytes: the formation of keratinizing colonies from single cells. *Cell*, 6, 331-334.
- RINNE, T., HAMEL, B., VAN BOKHOVEN, H. & BRUNNER, H. G. 2006. Pattern of p63 mutations and their phenotypes - Update. *American Journal of Medical Genetics, Part A*, 140, 1396-1406.
- RÍOS, J. D., SHATOS, M., URASHIMA, H., TRAN, H. & DARTT, D. A. 2006. OPC-12759 increases proliferation of cultured rat conjunctival goblet cells. *Cornea*, 25, 573-581.
- RISSE MARSH, B. C., MASSARO-GIORDANO, M., MARSHALL, C. M., LAVKER, R. M. & JENSEN, P. J. 2002. Initiation and characterization of keratinocyte cultures from biopsies of normal human conjunctiva. *Experimental Eye Research*, 74, 61-69.
- SACCHETTI, M., LAMBIASE, A., CORTES, M., SGRULLETTA, R., BONINI, S., MERLO, D. & BONINI, S. 2005. Clinical and cytological findings in limbal stem cell deficiency. *Graefes's Archive for Clinical and Experimental Ophthalmology*, 243, 870-876.

- SANGWAN, V. S., MATALIA, H. P., VEMUGANTI, G. K., FATIMA, A., IFTHEKAR, G., SINGH, S., NUTHETI, R. & RAO, G. N. 2006. Clinical outcome of autologous cultivated limbal epithelium transplantation. *Indian Journal of Ophthalmology*, 54, 29-34.
- SCHLÖTZER-SCHREHARDT, U., DIETRICH, T., SAITO, K., SOROKIN, L., SASAKI, T., PAULSSON, M. & KRUSE, F. E. 2007. Characterization of extracellular matrix components in the limbal epithelial stem cell compartment. *Experimental Eye Research*, 85, 845-860.
- SCHRADER, S., NOTARA, M., BEACONSFIELD, M., TUFT, S., GEERLING, G. & DANIELS, J. T. 2009a. Conjunctival epithelial cells maintain stem cell properties after long-term culture and cryopreservation. *Regenerative Medicine*, 4, 677-687.
- SCHRADER, S., NOTARA, M., BEACONSFIELD, M., TUFT, S. J., DANIELS, J. T. & GEERLING, G. 2009b. Tissue engineering for conjunctival reconstruction: Established methods and future outlooks. *Current Eye Research*, 34, 913-924.
- SCHRADER, S., NOTARA, M., TUFT, S. J., BEACONSFIELD, M., GEERLING, G. & DANIELS, J. T. 2010. Simulation of an in vitro niche environment that preserves conjunctival progenitor cells. *Regenerative Medicine*, 5, 877-889.
- SCHRADER, S., TUFT, S. J., BEACONSFIELD, M., BORRELLI, M., GEERLING, G. & DANIELS, J. T. 2012. Evaluation of human MRC-5 cells as a feeder layer in a xenobiotic-free culture system for conjunctival epithelial progenitor cells. *Current Eye Research*, 37, 1067-1074.
- SCHWAB, I. R. 1999. Cultured corneal epithelia for ocular surface disease. *Transactions of the American Ophthalmological Society*, 97, 891-986.
- SELLHEYER, K. & SPITZNAS, M. 1988. Ultrastructural observations on the development of the human conjunctival epithelium. *Graefes Archive for Clinical and Experimental Ophthalmology*, 226, 489-499.
- SELVER, O. B., BARASH, A., AHMED, M. & MARIO WOLOSIN, J. 2011. ABCG2-dependent dye exclusion activity and clonal potential in epithelial cells continuously growing for 1 month from limbal explants. *Investigative Ophthalmology and Visual Science*, 52, 4330-4337.
- SHAHDAFAR, A., HAUG, K., PATHAK, M., DROLSUM, L., OLSTAD, O. K., JOHNSEN, E. O., PETROVSKI, G., MOE, M. C. & NICOLAISSEN, B. 2012. Ex vivo expanded autologous limbal epithelial cells on amniotic membrane using a culture medium with human serum as single supplement. *Experimental Eye Research*, 97, 1-9.
- SHANMUGANATHAN, V. A., FOSTER, T., KULKARNI, B. B., HOPKINSON, A., GRAY, T., POWE, D. G., LOWE, J. & DUA, H. S. 2007. Morphological characteristics of the limbal epithelial crypt. *British Journal of Ophthalmology*, 91, 514-519.
- SHANMUGANATHAN, V. A., ROTCHFORD, A. P., TULLO, A. B., JOSEPH, A., ZAMBRANO, I. & DUA, H. S. 2006. Epithelial proliferative potential of organ cultured corneoscleral rims; implications for allo-limbal transplantation and eye banking. *British Journal of Ophthalmology*, 90, 55-58.

- SHAPIRO, M. S., FRIEND, J. & THOFT, R. A. 1981. Corneal re-epithelialization from the conjunctiva. *Investigative Ophthalmology and Visual Science*, 21, 135-142.
- SHARMA, S. M., FUCHSLUGER, T., AHMAD, S., KATIKIREDDY, K. R., ARMANT, M., DANA, R. & JURKUNAS, U. V. 2012. Comparative Analysis of Human-Derived Feeder Layers with 3T3 Fibroblasts for the Ex Vivo Expansion of Human Limbal and Oral Epithelium. *Stem Cell Reviews and Reports*, 8, 696-705.
- SHATOS, M. A., RÍOS, J. D., HORIKAWA, Y., HODGES, R. R., CHANG, E. L., BERNARDINO, C. R., RUBIN, P. A. D. & DARTT, D. A. 2003. Isolation and characterization of cultured human conjunctival goblet cells. *Investigative Ophthalmology and Visual Science*, 44, 2477-2486.
- SHI, S. R., COTE, R. J. & TAYLOR, C. R. 2001. Antigen retrieval techniques: Current perspectives. *Journal of Histochemistry and Cytochemistry*, 49, 931-937.
- SHORE, J. W., FOSTER, C. S., WESTFALL, C. T. & RUBIN, P. A. D. 1992. Results of buccal mucosal grafting for patients with medically controlled ocular cicatricial pemphigoid. *Ophthalmology*, 99, 383-395.
- SHORTT, A. J., SECKER, G. A., LOMAS, R. J., WILSHAW, S. P., KEARNEY, J. N., TUFT, S. J. & DANIELS, J. T. 2009. The effect of amniotic membrane preparation method on its ability to serve as a substrate for the ex-vivo expansion of limbal epithelial cells. *Biomaterials*, 30, 1056-1065.
- SHORTT, A. J., SECKER, G. A., MUNRO, P. M., KHAW, P. T., TUFT, S. J. & DANIELS, J. T. 2007a. Characterization of the limbal epithelial stem cell niche: Novel imaging techniques permit in vivo observation and targeted biopsy of limbal epithelial stem cells. *Stem Cells*, 25, 1402-1409.
- SHORTT, A. J., SECKER, G. A., NOTARA, M. D., LIMB, G. A., KHAW, P. T., TUFT, S. J. & DANIELS, J. T. 2007b. Transplantation of Ex Vivo Cultured Limbal Epithelial Stem Cells: A Review of Techniques and Clinical Results. *Survey of Ophthalmology*, 52, 483-502.
- SHORTT, A. J. & TUFT, S. J. 2011. Ocular surface reconstruction. *British Journal of Ophthalmology*, 95, 901-902.
- SKOOG, L. & TANI, E. 2011. Immunocytochemistry: An indispensable technique in routine cytology. *Cytopathology*, 22, 215-229.
- SMITH, A. 2006. A glossary for stem-cell biology. *Nature*, 441, 1060-1060.
- SNIPPERT, H. J. & CLEVERS, H. 2011. Tracking adult stem cells. *EMBO Reports*, 12, 113-122.
- SOLOMON, A., ESPANA, E. M. & TSENG, S. C. G. 2003. Amniotic membrane transplantation for reconstruction of the conjunctival fornices. *Ophthalmology*, 110, 93-100.
- SPRADLING, A., DRUMMOND-BARBOSA, D. & KAI, T. 2001. Stem cells find their niche. *Nature*, 414, 98-104.

- STEPP, M. A., ZHU, L., SHEPPARD, D. & CRANFILL, R. L. 1995. Localized distribution of $\alpha 9$ integrin in the cornea and changes in expression during corneal epithelial cell differentiation. *Journal of Histochemistry and Cytochemistry*, 43, 353-362.
- STEPP, M. A. & ZIESKE, J. D. 2005. The corneal epithelial stem cell niche. *Ocular Surface*, 3, 15-26.
- SU, L., CUI, H., XU, C., XIE, X., CHEN, Q. & GAO, X. 2011. Putative rabbit conjunctival epithelial stem/progenitor cells preferentially reside in palpebral conjunctiva. *Current Eye Research*, 36, 797-803.
- TAKAHASHI, K., TANABE, K., OHNUKI, M., NARITA, M., ICHISAKA, T., TOMODA, K. & YAMANAKA, S. 2007. Induction of Pluripotent Stem Cells from Adult Human Fibroblasts by Defined Factors. *Cell*, 131, 861-872.
- TAN, D. T. H., ANG, L. P. K. & BEUERMAN, R. W. 2004. Reconstruction of the ocular surface by transplantation of a serum-free derived cultivated conjunctival epithelial equivalent. *Transplantation*, 77, 1729-1734.
- TANIOKA, H., KAWASAKI, S., YAMASAKI, K., ANG, L. P. K., KOIZUMI, N., NAKAMURA, T., YOKOI, N., KOMURO, A., INATOMI, T. & KINOSHITA, S. 2006. Establishment of a cultivated human conjunctival epithelium as an alternative tissue source for autologous corneal epithelial transplantation. *Investigative Ophthalmology and Visual Science*, 47, 3820-3827.
- TEKTAŞ, O. Y., YADAV, A., GARREIS, F., SCHLÖTZER-SCHREHARDT, U., SCHICHT, M., HAMPEL, U., BRÄUER, L. & PAULSEN, F. 2012. Characterization of the mucocutaneous junction of the human eyelid margin and meibomian glands with different biomarkers. *Annals of Anatomy*, 194, 436-445.
- THE ADVISORY COMMITTEE ON THE SAFETY OF BLOOD TISSUES AND ORGANS 2011. Guidance on the microbiological safety of human organs, tissues and cells used in transplantation *In: HEALTH, D. O. (ed.)*. http://www.dh.gov.uk/en/Publicationsandstatistics/Publications/PublicationsPolicyAndGuidance/DH_121497.
- THE ROYAL COLLEGE OF OPHTHALMOLOGISTS 2008. Standards for the retrieval of human ocular tissue used in transplantation, research and training. <http://www.rcophth.ac.uk/page.asp?section=451§ionTitle=Clinical+Guidelines>.
- THOFT, R. A. 1977. Conjunctival transplantation. *Archives of Ophthalmology*, 95, 1425-1427.
- THOFT, R. A. 1984. Keratoepithelioplasty. *American Journal of Ophthalmology*, 97, 1-6.
- THOFT, R. A. & FRIEND, J. 1983. The X, Y, Z hypothesis of corneal epithelial maintenance. *Investigative Ophthalmology and Visual Science*, 24, 1442-1443.
- TISSUES AND CELLS DIRECTIVE 2004. European Union: <http://eur-lex.europa.eu/LexUriServ/LexUriServ.do?uri=OJ:L:2004:102:0048:0058:EN:PDF>.

- TSAI, R. J. F., LI, L. M. & CHEN, J. K. 2000. Reconstruction of damaged corneas by transplantation of autologous limbal epithelial cells. *New England Journal of Medicine*, 343, 86-93.
- TSAI, R. J. F. & TSENG, S. C. G. 1988. Substrate modulation of cultured rabbit conjunctival epithelial cell differentiation and morphology. *Investigative Ophthalmology and Visual Science*, 29, 1565-1576.
- TSENG, S. C. G. 1996. Regulation and clinical implications of corneal epithelial stem cells. *Molecular Biology Reports*, 23, 47-58.
- TSENG, S. C. G., DI PASCUALE, M. A., LIU, D. T. S., YING, Y. G. & BARADARAN-RAFII, A. 2005. Intraoperative mitomycin C and amniotic membrane transplantation for fornix reconstruction in severe cicatricial ocular surface diseases. *Ophthalmology*, 112, 896-903.
- TSENG, S. C. G., HIRST, L. W. & MAUMENEE, A. E. 1984. Possible mechanisms for the loss of goblet cells in mucin-deficient disorders. *Ophthalmology*, 91, 545-552.
- TSUBOTA, K., KAJIWARA, K., UGAJIN, S. & HASEGAWA, T. 1990. Conjunctival brush cytology. *Acta Cytologica*, 34, 233-235.
- TUMBAR, T., GUASCH, G., GRECO, V., BLANPAIN, C., LOWRY, W. E., RENDL, M. & FUCHS, R. 2004. Defining the Epithelial Stem Cell Niche in Skin. *Science*, 303, 359-363.
- TUORI, A., UUSITALO, H., BURGESSON, R. E., TERTTUNEN, J. & VIRTANEN, I. 1996. The immunohistochemical composition of the human corneal basement membrane. *Cornea*, 15, 286-294.
- TURLEY, E. A., NOBLE, P. W. & BOURGUIGNON, L. Y. W. 2002. Signaling properties of hyaluronan receptors. *Journal of Biological Chemistry*, 277, 4589-4592.
- TURNER, H. C., BUDAK, M. T., AKINCI, M. A. M. & WOLOSIN, J. M. 2007. Comparative analysis of human conjunctival and corneal epithelial gene expression with oligonucleotide microarrays. *Investigative Ophthalmology and Visual Science*, 48, 2050-2061.
- UK BLOOD TRANSFUSION AND TISSUE TRANSPLANTATION SERVICES 2013. Guidelines for the Blood Transfusion Services in the United Kingdom. <http://www.transfusionguidelines.org.uk/index.aspx?Publication=RB>.
- VASCOTTO, S. G. & GRIFFITH, M. 2006. Localization of candidate stem and progenitor cell markers within the human cornea, limbus, and bulbar conjunctiva in vivo and in cell culture. *Anatomical Record - Part A Discoveries in Molecular, Cellular, and Evolutionary Biology*, 288, 921-931.
- VASTINE, D. W., STEWART, W. B. & SCHWAB, I. R. 1982. Reconstruction of the periocular mucous membrane by autologous conjunctival transplantation. *Ophthalmology*, 89, 1072-1081.
- VYAS, S. & RATHI, V. 2009. Combined phototherapeutic keratectomy and amniotic membrane grafts for symptomatic bullous keratopathy. *Cornea*, 28, 1028-1031.

- WAGNER, W., HORN, P., BORK, S. & HO, A. D. 2008. Aging of hematopoietic stem cells is regulated by the stem cell niche. *Experimental Gerontology*, 43, 974-980.
- WATANABE, K., NISHIDA, K., YAMATO, M., UMEMOTO, T., SUMIDE, T., YAMAMOTO, K., MAEDA, N., WATANABE, H., OKANO, T. & TANO, Y. 2004. Human limbal epithelium contains side population cells expressing the ATP-binding cassette transporter ABCG2. *FEBS Letters*, 565, 6-10.
- WEI, Z. G., COTSARELIS, G., SUN, T. T. & LAVKER, R. M. 1995. Label-retaining cells are preferentially located in fornical epithelium: Implications on conjunctival epithelial homeostasis. *Investigative Ophthalmology and Visual Science*, 36, 236-246.
- WEI, Z. G., LIN, T., SUN, T. T. & LAVKER, R. M. 1997. Clonal analysis of the in vivo differentiation potential of keratinocytes. *Investigative Ophthalmology and Visual Science*, 38, 753-761.
- WEI, Z. G., SUN, T. T. & LAVKER, R. M. 1996. Rabbit conjunctival and corneal epithelial cells belong to two separate lineages. *Investigative Ophthalmology and Visual Science*, 37, 523-533.
- WEI, Z. G., WU, R. L., LAVKER, R. M. & SUN, T. T. 1993. In vitro growth and differentiation of rabbit bulbar, fornix, and palpebral conjunctival epithelia: Implications on conjunctival epithelial transdifferentiation and stem cells. *Investigative Ophthalmology and Visual Science*, 34, 1814-1828.
- WENKEL, H., RUMMELT, V. & NAUMANN, G. O. H. 2000. Long term results after autologous nasal mucosal transplantation in severe mucus deficiency syndromes. *British Journal of Ophthalmology*, 84, 279-284.
- WESTFALL, M. D., MAYS, D. J., SNIEZEK, J. C. & PIETENPOL, J. A. 2003. The Δ Np63 α phosphoprotein binds the p21 and 14-3-3 σ promoters in vivo and has transcriptional repressor activity that is reduced by Hay-Wells syndrome-derived mutations. *Molecular and Cellular Biology*, 23, 2264-2276.
- WILLIAMS, G. P., RADFORD, C., NIGHTINGALE, P., DART, J. K. G. & RAUZ, S. 2011. Evaluation of early and late presentation of patients with ocular mucous membrane pemphigoid to two major tertiary referral hospitals in the United Kingdom. *Eye*, 25, 1207-1218.
- WILLIAMS, R. L., KRISHNA, Y., DIXON, S., HARIDAS, A., GRIERSON, I. & SHERIDAN, C. 2005. Polyurethanes as potential substrates for sub-retinal retinal pigment epithelial cell transplantation. *Journal of Materials Science: Materials in Medicine*, 16, 1087-1092.
- WILSHAW, S. P., KEARNEY, J. N., FISHER, J. & INGHAM, E. 2006. Production of an acellular amniotic membrane matrix for use in tissue engineering. *Tissue Engineering*, 12, 2117-2129.
- WIRTSCHAFTER, J. D., KETCHAM, J. M., WEINSTOCK, R. J., TABESH, T. & MCLOON, L. K. 1999. Mucocutaneous junction as the major source of replacement palpebral conjunctival epithelial cells. *Investigative Ophthalmology and Visual Science*, 40, 3138-3146.

- WIRTSCHAFTER, J. D., MCLOON, L. K., KETCHAM, J. M., WEINSTOCK, R. J., CHEUNG, J. C. & JAKOBIEC, F. A. 1997. Palpebral conjunctival transient amplifying cells originate at the mucocutaneous junction and their progeny migrate toward the fornix. *Transactions of the American Ophthalmological Society*, 95, 417-432.
- WOLOSIN, J. M., BUDAK, M. T. & AKINCI, M. A. M. 2004. Ocular surface epithelial and stem cell development. *International Journal of Developmental Biology*, 48, 981-991.
- WOLOSIN, J. M., XIONG, X., SCHÜTTE, M., STEGMAN, Z. & TIENG, A. 2000. Stem cells and differentiation stages in the limbo-corneal epithelium. *Progress in Retinal and Eye Research*, 19, 223-255.
- WU, G., OSADA, M., GUO, Z., FOMENKOV, A., BEGUM, S., ZHAO, M., UPADHYAY, S., XING, M., WU, F., MOON, C., WESTRA, W. H., KOCH, W. M., MANTOVANI, R., CALIFANO, J. A., RATOVIJSKI, E., SIDRANSKY, D. & TRINK, B. 2005. $\Delta Np63\alpha$ up-regulates the Hsp70 gene in human cancer. *Cancer Research*, 65, 758-766.
- WU, H. & YI, E. S. 2006. Epigenetic regulation of stem cell differentiation. *Pediatric Research*, 59, 21R-25R.
- XU, C., INOKUMA, M. S., DENHAM, J., GOLDS, K., KUNDU, P., GOLD, J. D. & CARPENTER, M. K. 2001. Feeder-free growth of undifferentiated human embryonic stem cells. *Nature Biotechnology*, 19, 971-974.
- YANG, A. & MCKEON, F. 2000. p63 and p73: p53 mimics, menaces and more. *Nature Reviews Molecular Cell Biology*, 1, 199-207.
- YANG, A., SCHWEITZER, R., SUN, D., KAGHAD, M., WALKER, N., BRONSON, R. T., TABIN, C., SHARPE, A., CAPUT, D., CRUM, C. & MCKEON, F. 1999. p63 is essential for regenerative proliferation in limb, craniofacial and epithelial development. *Nature*, 398, 714-718.
- YOSHIDA, S., SHIMMURA, S., KAWAKITA, T., MIYASHITA, H., DEN, S., SHIMAZAKI, J. & TSUBOTA, K. 2006. Cytokeratin 15 can be used to identify the limbal phenotype in normal and diseased ocular surfaces. *Investigative Ophthalmology and Visual Science*, 47, 4780-4786.
- YOSHIZAWA, M., FEINBERG, S. E., MARCELO, C. L. & ELNER, V. M. 2004. Ex vivo produced human conjunctiva and oral mucosa equivalents grown in a serum-free culture system. *Journal of Oral and Maxillofacial Surgery*, 62, 980-988.
- ZHANG, J., NIU, C., YE, L., HUANG, H., HE, X., TONG, W. G., ROSS, J., HAUG, J., JOHNSON, T., FENG, J. Q., HARRIS, S., WIEDEMANN, L. M., MISHINA, Y. & LI, L. 2003. Identification of the haematopoietic stem cell niche and control of the niche size. *Nature*, 425, 836-841.
- ZHAO, R., XUAN, Y., LI, X. & XI, R. 2008. Age-related changes of germline stem cell activity, niche signaling activity and egg production in *Drosophila*. *Aging Cell*, 7, 344-354.
- ZHENG, W., WANG, S., MA, D., TANG, L., DUAN, Y. & JIN, Y. 2009. Loss of proliferation and differentiation capacity of aged human periodontal ligament stem cells and

rejuvenation by exposure to the young extrinsic environment. *Tissue engineering. Part A*, 15, 2363-2371.

ZHOU, S., SCHUETZ, J. D., BUNTING, K. D., COLAPIETRO, A. M., SAMPATH, J., MORRIS, J. J., LAGUTINA, I., GROSVELD, G. C., OSAWA, M., NAKAUCHI, H. & SORRENTINO, B. P. 2001. The ABC transporter Bcrp1/ABCG2 is expressed in a wide variety of stem cells and is a molecular determinant of the side-population phenotype. *Nature Medicine*, 7, 1028-1034.

ZIESKE, J. D., FRANCESCONI, C. M. & GUO, X. 2004. Cell cycle regulators at the ocular surface. *Experimental Eye Research*, 78, 447-456.

ZIESKE, J. D. & WASSON, M. 1993. Regional variation in distribution of EGF receptor in developing and adult corneal epithelium. *Journal of Cell Science*, 106, 145-152.